Title
AMPK Functions to Modulate Tissue and Organismal Aging in a Cell Non-Autonomous Manner

Author
Ulgherait, Matthew John

Publication Date
2014

Peer reviewed|Thesis/dissertation

UNIVERSITY OF CALIFORNIA

Los Angeles

AMPK Functions to Modulate Tissue and Organismal Aging in a Cell Non-Autonomous Manner

A dissertation submitted in partial satisfaction of the

requirements for the degree Doctor of Philosophy

in Biological Chemistry

by

Matthew John Ulgherait

2014

2014

ABSTRACT OF THE DISSERTATION:

AMPK Functions to Modulate Tissue and Organismal Aging

in a Cell Non-Autonomous Manner

by

Matthew Ulgherait

University of California Los Angeles, 2014

Professor Feng Guo, Co-Chair

Professor David W. Walker, Co-Chair

Understanding the biological mechanisms of aging represents an urgent biomedical challenge. AMP-activated protein kinase (AMPK) exhibits pro-longevity effects in diverse species. However, the tissue-specific mechanisms involved in AMPK regulation of aging are poorly understood. Here, we show that activation of AMPK in the adult *Drosophila* nervous system induces autophagy both in the brain and the intestinal epithelium. These cell autonomous and non-autonomous functions of AMPK are linked to improved intestinal homeostasis, muscle proteostasis and extended lifespan. Neuronal upregulation of the autophagy-specific protein kinase Atg1 is both necessary and sufficient to induce these inter-tissue effects during aging, resulting in prolonged lifespan. Furthermore, transgenic AMPK overexpression in neurons is sufficient to increase endogenous AMPK gene activity in distal tissues of the organism, including the intestine.

In a complementary approach, transgenic upregulation of AMPK specifically in the adult intestine induces autophagy both cell autonomously and non-autonomously in the brain, exhibiting slowed systemic aging and prolonged lifespan. Additionally, we show that the organism-wide response to tissue-specific AMPK/Atg1 activation is linked to suppressed *Drosophila* insulin-like peptide (DILP) signaling. Together, these results reveal that localized transgenic activation of AMPK can function to relay pro-longevity signals to distal tissues. AMPK may now represent part of a novel brain-to-gut and gut-to-brain signaling axis in *Drosophila*.

The dissertation of Matthew John Ulgherait is approved

Alison R. Frand

Alexander M. van der Bliek

Feng Guo, Committee Co-Chair

David W. Walker, Co-Chair

University of California

Los Angeles

DEDICATION:

To a longer and healthier life

CONTENTS:

ACKNOWLEGEMENTS:

Funding:

My work was supported by the Molecular Biology Institute (MBI), Cell and Molecular Biology (CMB) training grant—Ruth L. Kirschstein National Research Service Award (GM07185), the EUREKA Training Scholarship, and the Hyde Foundation Fellowship from University of California Los Angeles. I am grateful for all of my financial supporters at UCLA and external.

People:

First, I would like to thank my mentor David W. Walker for his support in all matters personal and professional. Without David's caring, motivation, and exceptional skill as a mentor none of the work presented here would have been possible. All of his help in focusing my interests, honing my skills, and critical thought contributed so greatly to my scientific career. I am very fortunate to have trained under such a remarkable and compassionate scientist.

Next, I would like to thank Michael Rera. Michael's talent, drive, and keen observational awareness led to some of the most interesting findings in our laboratory. Michael's contributions to this work include some of the initial lifespan screens found in Appendix I, and the truly thorough characterization of our "smurf" assay, along with Rebecca Clark. Also, thanks to Anil Rana. His outstanding skills as a researcher and colleague have made life in the Walker lab ideal for all. Much of this work would not have been possible without Anil's techniques, dissections, and discussion over findings. I am also grateful to Leanne Jones and all of her helpful dialogue

and recommendations for my research. Thanks to Jacqueline Graniel for all of her assistance in the very time-consuming feeding assays presented in this work.

Additionally, I want to thank all of the members of my committee. Alison Frand has offered only the best encouragement and support along every step of my graduate career. Even during the most difficult times over these last 6+ years, she has offered extremely helpful advice, reassurance, and inspiration at every step. I would also like to thank Feng Guo. As a mentor, Feng is one of the most positive, considerate, and skillful scientists imaginable. Thank you Feng for encouraging me to pursue my passions in the genetics of aging. Moreover, I would like to thank Alexander van der Bliek for all of his helpful discussion regarding my work, both for presentation and publication.

Outside of the sciences, I would like to my favorite ethnomusicologist and academic compatriot Lauren Flood. Our lengthy discussions on philosophy, music, and anthropology are an important part of my academic and personal life. Also, thank you to Soraya de Chadarevian for her encouragement and conversation over the history and philosophy of science. To my family, I am grateful to all of you for your support in my studies and graduate work.

Finally, thank you Cat Cohen. Without you, I never would have been able to complete this dissertation. Thank you for your encouragement, support, patience, friendship, and love.

VITA:

MATTHEW ULGHERAIT

PUBLICATIONS

Matthew Ulgherait, Anil Rana, Michael Rera, Jacqueline Graniel and David W. Walker AMPK modulates tissue and organismal aging in a cell non-autonomous manner. (In press) *Cell Reports*.

Jae H. Hur, Sepehr Bahadorani, Jacqueline Graniel, Christopher L. Koehler, **Matthew Ulgherait**, Michael Rera, D. Leanne Jones, and David W. Walker. Increased longevity mediated by yeast NDI1 expression in *Drosophila* intestinal stem and progenitor cells. *Aging.* (Albany, NY) 2013

Ming Gong, Yanqiu Chen, Rachel Senturia, **Matthew Ulgherait**, Michael Faller & Feng Guo. Caspases cleave and inhibit the microRNA processing protein DGCR8. *Protein Science.* 2012

Michael Rera, Sepehr Bahadorani, Jaehyoung Cho, Christopher L. Koehler, **Matthew Ulgherait**, Jae H. Hur, William S. Ansari, Thomas Lo Jr., D. Leanne Jones, David W. Walker. Modulation of longevity and tissue homeostasis by the *Drosophila* PGC-1 homolog**.** *Cell Metabolism.* 2011

ACKNOWLEDGMENTS

Michael Rera, Rebecca I. Clark, David W. Walker. Intestinal barrier dysfunction links metabolic and inflammatory markers of aging to death in *Drosophila.* PNAS. 2012

SPEAKING PRESENTATIONS

AMPK functions in a cell-non-autonomous manner to modulate tissue and organismal aging (Molecular, Cellular and Development Biology series UCLA, January 2014)

Regulation of microRNA processing through degradation of DGCR8 by the N-end rule pathway (Biological Chemistry annual retreat, May 2009)

TEACHING EXPERIENCE

Life Sciences Core Curriculum, UCLA

Teaching Assistant for Introduction to Molecular Biology, Spring 2009, Spring 2010

GRANTS / AWARDS

Hyde Foundation Fellowship, September 2013-June 2014

EUREKA Scholarship, September 2012-June 2013

UCLA Cellular and Molecular Biology Training Grant, June 2009 – June 2012

American Heart Association Western States Affiliates Predoctoral Fellowship, 2009
(Proposal accepted, declined funds - mutual exclusivity with above training grants)

Life Sciences, Outstanding Teaching Award, 2009-2010

Drexel University Relations Scholarship, 2006-2007

William Ebling Scholarship, 2003-2005

ORGANIZATION AND CONTRIBUTIONS:

Chapters II-VI represents a modified version of the following article:

Matthew Ulgherait, Anil Rana, Michael Rera, Jacqueline Graniel and David W. Walker**.** (2014) AMPK modulates tissue and organismal aging in a cell non-autonomous manner. (In press) *Cell Reports*

This dissertation is presented with additional data and discussion to that of the above paper. Of these chapters Michael Rera contributed to some of the initial lifespan data. Anil Rana performed numerous brain dissections for use in the immunofluorescence experiments and some Atg1 lifespans. Jacqueline Graniel performed the initial feeding quantification assays.

Appendix I contains our initial screens for lifespan-extending tissue-specific alterations of AMPK expression. Michael Rera and I contributed specifically to figures A1and A2 of this work. Moreover, this appendix contains additional evidence in support of AMPK regulation of autophagy not suitable for the previous chapters.

Notes on data presentation: All data presented in figures here are mean +/- standard error of the mean (SEM), unless otherwise noted. Statistical assessment (*ns = p>0.05, * = p<0.05, ** = p<0.01, *** = p<.001)*. All experimental gene-switch manipulations are graphs that have **black (-RU486),** and **red (+RU486)** presentation. All controls of W^{1118} backgrounds for RU486 effects are presented as grey/white (-RU486) and **black (+RU486)**.

Appendix II contains modified reproductions from two publications:

Hur, J. H., Bahadorani, S., Graniel, J., Koehler, C. L., Ulgherait, M., Rera, M., … Walker, D. W. (2013). Increased longevity mediated by yeast NDI1 expression in Drosophila intestinal stem and progenitor cells. *Aging*, *5*(9), 662–81.

Rera, M., Bahadorani, S., Cho, J., Koehler, C. L., Ulgherait, M., Hur, J. H., … Walker, D. W. (2011). Modulation of longevity and tissue homeostasis by the drosophila PGC-1 homolog. *Cell Metabolism*, *14*(5), 623–634.

My specific contributions to (Hur et al. 2013) are found in (Figure 2D) and (Figure S2A) of the above publication.

My contributions to (Rera et al. 2011) are found in the longevity experiments presented in (Fig 4) Dihydroethidium (DHE) staining presented in (Fig. 5E, F) (Fig. S5D, E) and initial characterization of smurf flies along with Michael Rera in (Fig. 7) of the above publication.

Appendix III contains a modified partial reproduction of the following article:

Gong, M., Chen, Y., Senturia, R., Ulgherait, M., Faller, M., & Guo, F. (2012). Caspases cleave and inhibit the microRNA processing protein DiGeorge Critical Region 8. *Protein Science*, *21*(6), 797–808.

My contribution to this paper is found in a small portion of the initial cloning and characterization of DGCR8 truncations. Additionally, I performed the analysis of DGCR8 cleavage upon apoptosis found in (Figure 2) of the above publication.

PREFACE:

AGING, LONGEVITY EXTENSION, IMMORTALITY: A BRIEF CONTEXTUAL HISTORY

Aging is the leading risk determinant for complex disease and mortality. This concept was first shown as an arithmetical law by the mathematician Benjamin Gompertz in the early 1800s [1]. Simply stated, a person's resistance to death decreases as the number of years spent living increases. Indeed, with aging comes increased risk of heart attack, cancer, neurodegeneration, and death [2]. While median lifespan has steadily increased since Gompertz' time, due to improved sanitation and medicine, we appear to be approaching an innate genetically-predetermined maximum lifespan plateau [3]. Therefore, the objective of the gerontologist is to study the biological processes governing this law, while trying to shift the Gompertz' equation in our favor. Delayed human aging, if not engineered biological immortality, seems a possibility. Although we are likely decades away from any life-extending genetic interventions in humans, a great deal of progress has been made towards achieving this goal with better understanding of the aging process as a whole.

Immortality is a concept with a cultural legacy that stretches much longer than that of modern experimental biology. Beyond the religious ideas of eternal life, the late 19th and early 20th century saw the possibility of life-extension as a truly corporeal and testable phenomenon in the laboratory. A lesser known, but sensational glimpse of immortal life came from the early cell culture experiments of French physician and Nobel Laureate Alexis Carrel. In his 1912 paper "On the permanent life of tissues outside of the organism," Carrel purported that his new tissue

culture techniques could maintain the cardiac tissue from embryonic chicken indefinitely [4]. Eventually he would go on to state that these cultures had been maintained for nearly 20 years (longer than the lifespan of a normal chicken) [5]. His papers, among others, established the hegemonic notion that normal tissue could be maintained outside the body forever.

It wasn't until decades later that Leonard Hayflick refuted Carrel's work and determined that normal primary cells in culture have a finite replicative capacity [6]. Although Carrel's initial findings of "normal" immortal tissues were later disproven, today we know that the lifespan of cells can be indefinite via the processes of tumorigenesis; the most famous cell-line of such infinite capacity being HeLa [7, 8]. While the distance between the immortal life of a cancerous cell to that of an immortal animal is vast, a new awareness of our biological nature had taken shape. From Carrel's ideas and techniques, we previewed the concept that extended life had a tangible and testable reality in science. No longer confined to philosophical ephemera, scientists began in earnest to study methods to delay the aging process.

Outside of the culture dish, the first report that normal animal lifespan could be extended in the laboratory came from the work of Clive McCay at Cornell in 1935 [9]. By restricting overall caloric intake of the rats, while not reducing essential nutrients and vitamins, McCay was able to extend the lifespan by over 30% [10]. Although it has been nearly 80 years since the publication of this study, these findings still remain relevant and repeatable today. Dietary Restriction (DR) in various forms continues to be one of the most reliably robust life-extending interventions for model organisms in the lab. Lifespan lengthening nutritional interventions have been well studied in *C. elegans*, *Drosophila*, mice, rats, and (with variable success) in primates [11, 12, 13]. The breadth and depth of nearly 80 years of research on nutritional/metabolic

control of lifespan, starting from McCay's initial report of extended longevity, set forth the possibility of genetic interventions to reprogram metabolic activity and alter the aging process.

From 1983-1988 Michael Klass and Tom Johnson began to independently describe the first mutations sufficient to extend lifespan in the worm *C. elegans* [14, 15]. The identification of the first gene known to extend lifespan, termed *age-1,* didn't come until 1988, from Tom Johnson's work [16]. Soon after, Cynthia Kenyon began to characterize definitively this genetic pathway capable of extending worm lifespan, with the discovery of *daf-2* mutation doubling lifespan of the worm, and this lifespan extension being dependent upon the gene *daf-16* [17]. In 1997 Gary Ruvkun's lab reported the identity of *daf-2*, uncovering that this gene belonged to the evolutionarily conserved insulin-like signaling pathway [18]. Later that year, both the Kenyon lab, and Ruvkun lab reported that *daf-16* encoded a transcription factor capable of mediating this suppressed insulin-like signaling response, and increased lifespan in the worm [19, 20]. These initial discoveries seemed counterintuitive to the medical and scientific communities in that dysregulated insulin signaling has been known to cause diabetic-like problems and increased mortality [21]. Contrary to this notion, years of research have confirmed that inhibition of the insulin-like signaling pathways is a particularly salient method of lifespan extension in many laboratory organisms [reviewed in 22, 23 and discussion in Chapter IV].

Since these early findings, multitudes of other mutations that regulate metabolism and nutritional response have been found to extend lifespan, particularly in the short-lived organisms *C. elegans* and *Drosophila*. At the crux of nutrition, metabolism, and aging lies an important set of genes capable of sensing intracellular energy: the AMP-activated protein kinase (AMPK) family. For the remainder of this dissertation I will discuss the evidence underlying AMPK involvement in nutrition, energy sensing, longevity, and age-related pathologies.

REFERENCES:

1. Gompertz, Benjamin (1825). "On the Nature of the Function Expressive of the Law of Human Mortality, and on a New Mode of Determining the Value of Life conntingencies". *Philosophical Transactions of the Royal Society of London* **115**: 513–585. doi:10.1098/rstl.1825.0026.

2. Christensen, K., Doblhammer, G., Rau, R., & Vaupel, J. W. (2009). Ageing populations: the challenges ahead. *Lancet, 374*(9696), 1196–208. doi:10.1016/S0140-6736(09)61460-4

3. Weon, B. M., & Je, J. H. (2009). Theoretical estimation of maximum human lifespan. *Biogerontology, 10*(1), 65–71. doi:10.1007/s10522-008-9156-4

4. Carrel, Alexis. (1912). On the permanent life of tissues outside of the organism. J Exp Med. May ; 15(5): 516–528.

5. Landecker,Hannah.(2007) Culturing Life: How Cells Became Technologies, Harvard University Press.

6. Hayflick, L., & Moorhead, P. S. (1961). The serial cultivation of human diploid cell strains. *Experimental Cell Research, 25*(3), 585–621.

7. Lucey, B. P., Nelson-Rees, W. A., & Hutchins, G. M. (2009). Henrietta Lacks, HeLa cells, and cell culture contamination. *Archives of Pathology and Laboratory Medicine*.

8. Skloot, Rebecca. (2010). The Immortal Life of Henrietta Lacks. Crown Publishers, New York.

9. McCay, C. M., Crowell, M. F., & Maynard, L. A. (1989). The effect of retarded growth upon the length of life span and upon the ultimate body size. 1935. *Nutrition (Burbank, Los Angeles County, Calif.), 5*(3), 155–171; discussion 172

10. McDonald, R. B., & Ramsey, J. J. (2010). Honoring Clive McCay and 75 years of calorie restriction research. *The Journal of Nutrition, 140*(7), 1205–10. doi:10.3945/jn.110.122804

11. Mair, W., & Dillin, A. (2008). Aging and survival: the genetics of life span extension by dietary restriction. *Annual Review of Biochemistry, 77*, 727–54. doi:10.1146/annurev.biochem.77.061206.171059

12. Mattison, J. A., Roth, G. S., Beasley, T. M., Tilmont, E. M., Handy, A. M., Herbert, R. L., … de Cabo, R. (2012). Impact of caloric restriction on health and survival in rhesus monkeys from the NIA study. *Nature, 489*(7415), 318–21. doi:10.1038/nature11432

13. Colman, R. J., Beasley, T. M., Kemnitz, J. W., Johnson, S. C., Weindruch, R., & Anderson, R. M. (2014). Caloric restriction reduces age-related and all-cause mortality in rhesus monkeys. *Nature Communications, 5*, 3557. doi:10.1038/ncomms4557

14. Johnson, T. E., & Wood, W. B. (1982). Genetic analysis of life-span in Caenorhabditis elegans. *Proceedings of the National Academy of Sciences of the United States of America*, *79*(21 I), 6603–6607.

15. Klass, M. R. (1983). A method for the isolation of longevity mutants in the nematode Caenorhabditis elegans and initial results. *Mechanisms of Ageing and Development*, *22*(3-4), 279–286.

16. Friedman, D. B., & Johnson, T. E. (1988). A mutation in the age-1 gene in Caenorhabditis elegans lengthens life and reduces hermaphrodite fertility. *Genetics*, *118*(1), 75–86.

17. Kenyon, C., Chang, J., Gensch, E., Rudner, A., & Tabtiang, R. (1993). A C. elegans mutant that lives twice as long as wild type. *Nature*, *366*(6454), 461–464.

18. Kimura, K. D. (1997). daf-2, an Insulin Receptor-Like Gene That Regulates Longevity and Diapause in Caenorhabditis elegans. *Science*, *277*(5328), 942–946. doi:10.1126/science.277.5328.942

19. Lin, K. (1997). daf-16: An HNF-3/forkhead Family Member That Can Function to Double the Life-Span of Caenorhabditis elegans. *Science*, *278*(5341), 1319–1322. doi:10.1126/science.278.5341.1319

20. Ogg, S., Paradis, S., Gottlieb, S., Patterson, G. I., Lee, L., Tissenbaum, H. A., & Ruvkun, G. (1997). The Fork head transcription factor DAF-16 transduces insulin-like metabolic and longevity signals in C. elegans. *Nature*, *389*(6654), 994–9. doi:10.1038/40194

21. Kenyon, C. (2011). The first long-lived mutants: discovery of the insulin/IGF-1 pathway for ageing. *Philosophical Transactions of the Royal Society of London. Series B, Biological Sciences*, *366*(1561), 9–16. doi:10.1098/rstb.2010.0276

22. Fontana, L., Partridge, L., & Longo, V. D. (2010). Extending healthy life span--from yeast to humans. *Science (New York, N.Y.)*, *328*(5976), 321–6. doi:10.1126/science.1172539

23. Kenyon, C. J. (2010). The genetics of ageing. *Nature*, *464*(7288), 504–12. doi:10.1038/nature08980

CHAPTER I:

AMPK, AGING AND CONTROL OF AUTOPHGY IN DROSOPHILA

AMP-activated protein kinase (AMPK) and aging

AMPK is a master regulator of energy homeostasis conserved from yeast to humans [1]. When energy status of the cell is low (limited ATP/high ADP-AMP concentration) AMPK becomes activated and influences a host of metabolic pathways. The ultimate response of AMPK activity is to shift cellular metabolism towards energy production via breakdown of energy stores, reduced ATP usage, and increased stress response. In mammals, AMPK is known to function as an obligate heterotrimeric complex consisting of an effector kinase subunit (AMPKα), a scaffolding regulatory subunit (AMPKβ), and a nucleotide binding regulatory subunit (AMPKγ) **(Fig. 1-1)** [2]. Phosphorylation of AMPK on Thr172 (in humans) or Thr184 (in *Drosophila*) is required for AMPK kinase function, increasing kinase activity by several orders of magnitude [3]. To date, only three kinases have been found to phosphorylate and activate AMPK. Liver Kinase B1 (LKB1) is the major kinase regulating AMPK phosphorylation under energetic stress [4, 5]. Although, calcium-dependent kinase kinase β (CaMKKβ) and transforming growth factor β activated kinase (Tak1) have also been shown to directly phosphorylate and activate AMPK [6,7].

AMPK activity is also regulated via nucleotide binding by the γ subunit of the complex. The AMPKγ subunit contains four putative nucleotide binding domains that are capable of directly binding AMP, ADP, and ATP in a competitive fashion [2]. Under energetic stress, cellular AMP and ADP concentrations can increase. Upon binding of ADP or AMP to the AMPK complex, a conformational change in the protein can occur, facilitating increased activating phosphorylation of the α-subunit of AMPK by upstream kinases [8]. Additionally, this conformational change appears to preserve phosphorylation of AMPK for extended time compared to unbound AMPKγ [8], resulting in prolonged AMPK activity.

Pharmacological pro-longevity AMPK agonists

Several drugs have been found to activate AMPK both directly and indirectly. The anti-diabetes compound metformin can activate AMPK *in vitro* and *in vivo* [9]. Although metformin is often used as a biochemical agonist of AMPK in cell culture experiments, the drug appears to function indirectly towards AMPK by lowering intracellular ATP production [10]. This altered ADP/AMP:ATP ratio can then activate AMPK by subsequent nucleotide binding [10]. While metformin is frequently prescribed as an anti-diabetic drug, it has the added benefit of being able to increase the lifespan of worms and mice [11, 12]. There is conflicting evidence suggesting that these benefits may not be due solely to AMPK activation. Metformin is known to influence a host of other intracellular processes, some of which may be beneficial or detrimental to organismal health [9]. In *Drosophila*, feeding of metformin is sufficient to increase AMPK phosphorylation and activation, but shortens lifespan of the animal at moderate to high concentrations [13].

The pro-longevity polyphenol resveratrol can extend lifespan and confer health benefits to many model organisms including *Drosophila* [14, 15]. It has been suggested that resveratrol extends lifespan by directly stimulating the NAD-dependent deacetylase Sir2 activity [16]. Although it has been recently suggested that, at least in *Drosophila* and *C. elegans*, increased Sir2 function is inadequate to explain these beneficial longevity effects [17]. Alternatively, AMPK has been known to be activated upon resveratrol administration in mammals for some time. Feeding AMPK-deficient mice resveratrol lessens the biochemical and health response to the drug [18]. In mammalian cells, AMPK has also been shown to activate Sir2p directly [19]. It is evident that AMPK plays a role in mediating the resveratrol response, but it is currently unclear as to how this relationship between AMPK and Sir2 can influence longevity.

5-amino-1-β-D-ribofuranosyl-imidazole-4-carboxamide (AICAR) is an AMP analog capable of binding the AMPK complex directly, stimulating kinase function [20]. While initially reported as an exercise mimetic drug [20], AICAR treatment has been found to ameliorate age-related deficits in cognition and exercise ability in aged mice [21]. These benefits are completely dependent upon AMPK function. Mice overexpressing a kinase-dead, dominant negative (DN) form of AMPK showed no health changes upon AICAR treatment regimen [21]. Although AICAR treatment has been shown to have many beneficial effects on mammalian health [22, 23], it is yet to be determined if AICAR is capable of extending lifespan. It may be partially due to the current prohibitively expensive cost of this drug. In the future, it will be interesting to see if AICAR can function as a pro-longevity compound, and if it is dependent upon AMPK activity. As AMPK activation has been implicated in many pro-longevity pharmacological interventions, it is important to highlight the downstream targets of AMPK in mediating these anti-aging effects.

AMPK controls multiple longevity-associated pathways

The importance of AMPK in the aging process is emphasized by its ability to regulate many genetic pathways implicated in lifespan extension. Most of the evidence for AMPK regulating these pathways comes from mammalian cell culture experiments. These interactions are summarized in **(Fig1-1, and Fig1-2)**. While AMPK is clearly involved in the following processes, not much work has been done to confirm the conservation of these findings in various invertebrate aging models, including *Drosophila*.

Lipid metabolism

Numerous life-extending interventions are associated with altered lipid homeostasis. In several organisms, including *Drosophila*, extended longevity is often accompanied by increased fat deposition, and subsequent lipolysis [24, 25, 26, 27, 28, 29]. In the fly, dietary restriction increases both triglyceride synthesis and lipolysis, allowing for improved stress resistance and lifespan [30]. Overexpression of the Lipase lipl-4 in *C. elegans* is able to extend lifespan by altering lipid composition and lipid cycling in the worm [25]. In mammals, AMPK can act as a core regulator of fat metabolism. Stimulated AMPK can directly phosphorylate and inhibit sterol regulatory element-binding protein (SREBP), suppressing lipogenesis [31]. Additionally, AMPK can inhibit sterol synthesis and lipogenesis by modifying targets including acetyl-CoA carboxylases (ACCs), and fatty acid synthase (FAS) [1]. AMPK has also been shown to regulate lipid homeostasis via *Drosophila* protein phosphatase V (PpV) inhibition [32]. PpV deletion leads to increased AMPK activity resulting in decreased lipid stores, reduced size and early developmental lethality [32]. The exact mechanism of how altered fat metabolism contributes to adult lifespan remains poorly understood. While AMPK is important in regulating fat accumulation and usage, it is currently unknown as to how AMPK activation influences lipid homeostasis in the context of an aging organism.

Mitochondrial biogenesis

Peroxisome proliferator-activated receptor-gamma coactivator 1 alpha (PGC-1α) is a transcription factor that plays a crucial role in the regulation of mitochondrial biogenesis [33]. Activation of PGC-1α leads to a coordinated gene expression cascade increasing the abundance of nuclear-encoded mitochondrial components, and the formation of new mitochondria [34]. Upregulation of PGC-1α has been linked to the improvement of various neurodegenerative and muscular diseases [35, 36]. Recently, our lab has shown that overexpression of the fly ortholog

of PGC-1α (*dPGC-1*) is capable of extending organismal lifespan while maintaining healthy tissue homeostasis during aging [37]. *dPGC-1* overexpression in the intestine leads to efficient maintenance of mitochondrial respiration with age, and a decrease in tissue-damaging reactive oxygen species (ROS) accumulation in late life [37]. Importantly, AMPK has been shown to directly phosphorylate PGC-1α in mouse skeletal muscle, activating gene expression of downstream targets [38]. As AMPK directly controls PGC-1 activity, it is probablethat AMPK could be involved in life-extending capacity of increased mitochondrial biogenesis.

TOR signaling

Target of rapamycin (TOR) signaling pathway suppression is necessary for a number of longevity extending interventions, including dietary restriction [39,40]. Furthermore, TOR pathway inhibition alone is sufficient to prolong lifespan in worms, flies, and mice [39]. At the molecular level, TOR signaling is a conserved genetic pathway that regulates general protein synthesis, cell growth and anabolism [40]. The TOR complex is known to act as an intracellular amino acid sensor. Under nutritionally abundant conditions TOR kinase activity is stimulated, allowing for phosphorylation of S6Kinase (S6K) [41]. Activation of S6K leads to phosphorylation of the S6 component of the ribosome, allowing for increased translation efficiency, subsequent protein synthesis, and cell growth [41]. Concurrently, TOR kinase inactivates the translational repressor 4E-BP, aiding in the amplified protein synthesis signal. Additionally, TOR can suppress the catabolic activity of autophagy via inhibition of the Autophagy-related-gene (Atg13/Atg1) complex [42]. Upon energetic stress/amino acid starvation, TOR kinase activity is suppressed, yielding decreased S6K phosphorylation, increased translational inhibition by 4E-BP, and increased autophagy induction via Atg1/Atg13 [42].

Nutrient availability antagonistically regulates AMPK and TOR function. As AMPK is activated by low energy availability, TOR is suppressed in part by AMPK. In mammals, AMPK has been shown to directly phosphorylate the mammalian TOR binding partner Raptor, thereby inhibiting TOR kinase activity [43]. Additionally, upstream of the TOR complex, AMPK has been known to activate the Tuberous Sclerosis protein 2 (TSC2), which can decrease TOR activity [44]. AMPK has also been known to induce autophagy [42]. It was originally assumed that AMPK activation induces autophagy indirectly via reduced TOR signaling [42]. However, more recently it has been shown that AMPK also mediates autophagy by direct phosphorylation of the protein kinase that initiates autophagy, Atg1 (ULK1 in mammals) [45, 46] **(Fig. 1-2)**.

Autophagy and AMPK

Autophagy describes many different cellular mechanisms used to deliver intracellular substrates to the lysosome for degradation and eventual recycling, with the ultimate goal of maintaining energy production and organelle homeostasis [42]. Macroautophagy (henceforth referred to as simply "autophagy") is the process in which large intracellular structures are engulfed by multi-membranous vesicles and ultimately degraded in the lysosome [42]. Under nutrient deprivation, organisms and cells utilize autophagy to break down intracellular components for energy production. During the aging process, damaged organelles and molecules accumulate, contributing to age-related pathologies. Autophagy is a crucial process in the removal of damaged intracellular organelles and misfolded proteins, serving as a component of intracellular quality control [42].

Generally, autophagy is a tightly regulated process at the molecular level, with numerous autophagy-related genes (Atgs) characterized thus far [42]. Autophagy begins with the formation of pre-autophagosome complexes (sometimes called phagophore membrane

complexes) to engulf cytoplasmic material. Next, the pre-autophagosome membrane elongates around the selected cargo, closing to form an autophagasome. Once the cargo is enclosed, the autophagosome can begin a fusion process with a lysosome. Upon fusion between lysosome and autophagosome (referred to as autolysosomes) materials and cargo in the lumen can then be degraded by lysosomal-associated acid hydrolases and other degradation enzymes [42] **(Fig 1-3).**

In mammals, initiation of autophagy is dependent upon two major protein complexes. Starting at the assembly of the pre-autophagosome sites, the Vps34 kinase complex and the Atg1/Atg13 complex can phosphorylate substrates involved in autophagosome formation [47]. In *Drosophila*, overexpression of Atg1 alone is sufficient to induce autophagosome formation in the fat body [48]. Elongation and autophagosome formation depends upon a series of reactions, resulting in the recruitment of ubiquitin-like protein Atg8 (LC3 in mammals) to the forming autophagosome [47]. There are two Atg8 genes in *Drosophila Atg8a/b*. Atg8 proteins are then conjugated to the autophagosome membrane by a lipid phosphatidylethanolamine (PE) linkage via the actions of other Atg proteins [42]. Post-conjugation, Atg8 is believed to aid in the traffic of the autophagosome to nearby lysosomes, where SNARE-dependent fusion occurs to form an autolysosome [47].

AMPK activity is able to induce autophagy via direct and indirect mechanisms. As stated previously, the TOR pathway suppresses Autophagy via inhibition of the Atg1 complex [42]. As AMPK is known to downregulate TOR signaling, it is able to promote autophagasome formation by derepression of Atg1. Additionally, AMPK has been found to directly activate Atg1 by phosphorylation, yielding increased autophagy initiation [45, 46]. AMPK also regulates the Vps34 complex in an autophagy-specific context. Upon pharmacological stimulation of AMPK, Vps34 in complex with pro-autophagy binding partners is activated by AMPK phosphorylation,

while the Vps34 protein in complex with non-autophagy functioning proteins is inhibited by AMPK phosphorylation [49]. In *C. elegans*, overexpression of a truncated, constitutively active form of AMPK is sufficient to activate autophagy, as marked by increased LGG (worm ortholog of Atg8) puncta [46]. It is clear that AMPK plays an important role in autophagy induction in mammals and worms. However, it is currently unknown as to whether AMPK activity is sufficient to induce autophagy in *Drosophila*.

The autophagic process can be actively monitored in the *Drosophila* intestine utilizing GFP-tagged Atg8a (under the control of its endogenous promoter), RFP-tagged LAMP1 (lysosome marker), or the acidophilic dye Lysotracker-Red **(Fig. 1-3B)**. In the *Drosophila* intestine under well-fed conditions (0 hours of starvation), very faint diffuse GFP-Atg8 and Lysotracker stain can be visualized. At 1 hour of starvation, a small increase in GFP-Atg8 and Lysotracker puncta can be visualized with almost no colocalization. Under longer starvation time (2-6 hours), a large increase in the number of both Lysotracker and GFP-Atg8 foci is observed, with an increased degree of colocalization, indicating an active increase in the amount of autolysomes found in the enterocytes of the intestine.

In support of autophagy regulating aging and lifespan, deletions of autophagy-related genes (Atgs) are frequently associated with premature aging phenotypes in mammals and invertebrates [42]. Multiple organisms show an age-related decline in the expression and function of autophagy genes as well [50]. Moreover, many interventions resulting in long-lived *C. elegans* and *Drosophila* (including DR and rapamycin treatment) require a properly functioning autophagy pathway to maintain extended lifespan [51, 52]. Specifically in *Drosophila*, the autophagy machinery is required to maintain improved muscle proteostasis via life extension by different insulin signaling pathway interventions [53]. Further highlighting the

importance of autophagy's role in combating age-related pathologies, upregulation of autophagy genes in the brain of *Drosophila* and mice is sufficient to increase organismal lifespan [54, 55]. It is yet to be determined whether AMPK plays an important role in aging-associated clearance of damaged intracellular components involving autophagy.

Genetic manipulation of AMPK in aging

As described previously, AMPK can regulate metabolic pathways essential for healthy aging. Along these lines, direct manipulation of AMPK gene activity has been shown to influence aging and lifespan [56, 57]. In *C. elegans*, increased gene dosage of the AMPK catalytic subunit, *aak-2*, increases lifespan [58, 59]. While some DR protocols require *aak-2* to promote lifespan extension [60], other dietary restriction methods do not appear completely dependent on worm AMPK expression [61, 62]. In *Drosophila*, deletion of the AMPK β (*Alicorn*), or γ (*Snf4aγ*) orthologs results in early lethality and "aging-like" neurodegeneration phenotypes [63, 64]. Supporting the role of AMPK in lifespan regulation, it was recently reported that muscle or fat body-specific upregulation of AMPKα (hereafter referred to as simply "AMPK") can extend lifespan in the fruit fly [65]. However, the driver lines used to upregulate AMPK in this study exhibit aberrant expression patterns [66] (to be discussed later in this chapter). Therefore, the tissue-specific requirements for AMPK-mediated lifespan extension remain unclear.

Biological markers of aging

As in humans, *Drosophila* aging progresses with the distinct accumulation of physiological pathologies associated with the aging process [67]. These pathological "markers of aging" can be used to help determine the health and biological age of an organism within the

context of chronological time. Upon extension of biological and chronological lifespan, it is expected that certain markers of aging will be delayed in their onset. We focus primarily on the age-related pathologies of two tissues in particular: the intestine and the muscle.

Intestinal barrier dysfunction as a marker of tissue and organismal aging

In mid-2011, I was performing feeding assays to measure the food intake of our long-lived flies that overexpress *dPGC-1* in the intestine [37]. To rule out the possibility these flies were restricted in their diet and feeding behavior (possibly contributing to the lifespan phenotype), I placed a large population of *dPGC-1* flies and control flies on media containing a high concentration of the food dye FD&C Blue No. 1 in order to quantify food intake. This blue dye is the same additive used in a number of candies and processed foods. Under normal circumstances this dye is non-absorbable, non-toxic, and remains confined to the intestinal lumen [37, 68]. Surprisingly, I observed a fraction of the population of the 30-day-old flies turned completely blue, indicating leakage of the dye from the intestine into the hemolymph. Moreover, Michael Rera and I found that this gut leakage phenotype was more prevalent in our shorter-lived control strain than in the long-lived transgenic *dPGC1*-expressing flies. This indicated to us that intestinal barrier dysfunction may be an important pathological marker of the aging process [37].

Michael Rera and Rebecca Clark went on to characterize further this age-related intestinal barrier dysfunction [68]. They were able to show that flies exhibiting blue dye leakage and intestinal barrier dysfunction (hereafter referred to as smurf-flies, or smurfs) were very short lived regardless of genotype or chronological age. This data indicates that turning smurf is an accurate predictor of imminent death and increased mortality at both the individual and population level. Conserved throughout fly genotypes and lifespan altering interventions, a

population of flies that exhibits higher proportions of smurfs to non-smurfs is always shorter-lived than a population of flies containing fewer smurfs. Likewise, flies under dietary yeast restriction are longer-lived, and exhibit smaller proportions of smurfs at a given chronological timepoint compared to well-fed controls [68]. Additionally, Rebecca Clark was able to determine that these flies suffer from a previously observed age-related phenotype: increased inflammation markers. While it is currently unknown as to how exactly intestinal barrier dysfunction can increase markers of inflammation and mortality, the smurf assay remains an effective means of estimating intestinal aging, as well as imminent death of individual flies and populations as a whole [68] **(Fig. 1-4).** In mammals, we know considerably less about intestinal aging. While there have been reports of intestinal aging in mice including increased intestinal permeability [69, 70], very little is understood. A number of human diseases are linked to intestinal dysfunction, including age-related pathologies [71], but it remains unclear if these can truly be considered markers of human aging.

Muscle proteostasis and muscle function during aging

Progressive muscle degeneration and loss of muscle strength is a conserved pathology of aging from worms to humans [72, 73]. The underlying molecular causes for this age-related decline in muscle function have been associated with decreased protein homeostasis in a variety of organisms [73]. In *Drosophila*, Fabio DeMontis and Norbert Perrimon have described this process as being the consequence of the accumulation of insoluble protein aggregates in muscle fibers of the fly over time [53]. During aging, insoluble aggregates rich in polyubiquitinated proteins accumulate in the thoracic flight muscle of *Drosophila* **(Fig. 1-5A).** They went on to show that overexpression of the insulin signaling pathway transcription factor *dFOXO* in the muscle can delay this accumulation of polyubiquitinated proteins, preserving climbing and flight

ability of the fly while extending lifespan [53]. In support of these findings, our laboratory has shown similarly delayed protein aggregate accumulation by overexpressing the ubiquitin E3-ligase Parkin, resulting in extended fly lifespan [74].

This accumulation of insoluble protein aggregates in the muscle tissue can be easily observed and quantified by immunofluorescence using anti-polyubiquitin antibodies **(Fig. 1-5B)**. In a similar approach, western blot analysis of triton X-100 insoluble thoracic lysates reveals an age-dependent increase in polyubiquitin-conjugated proteins **(Fig. 1-5C)**. As a physiological correlate to muscle pathology, climbing ability of the fly can be easily assayed [75, 76]. After gently tapping the flies to the bottom of a food vial, the number of individual flies that reach the top of the vial in a given period of time can be scored. Many labs (including ours) observe an age-related decline in climbing ability, correlated to decreased muscle proteostasis of the animal **(Fig. 1-5D).**

Tissue-specific genetic manipulation of *Drosophila* via the UAS-GAL4 system

In many model organisms, single gene manipulations have been shown to dramatically alter lifespan of the animal [77]. *Drosophila* is a powerful genetic model in which to study the aging process. Besides the short-lived nature of the fly, the UAS-GAL4 system offers a means to study tissue-specific alterations via expression of a single gene or multiple genes [78]. Pioneered in Norbert Perrimon's laboratory, the UAS-GAL4 system uses the yeast transcriptional activator GAL4 to drive transgene expression via GAL4-specific upstream activating sequence (UAS) [79]. GAL4 expression can be directed in a tissue-specific manner by a desired enhancer trap or promoter, thusly driving expression of a UAS-flanked transgene in the chosen tissue (e.g. neuronal tissue, intestinal tissue, muscle, etc…) **(Fig. 1-6)**. While this system is widely used and the number of publically available tissue-specific GAL4 driver flies

and UAS-transgene fly lines is extremely large, there are some caveats when this system is employed to study aging and life extension.

First, the standard UAS-GAL4 system does not allow complete temporal control of transgene expression. One can have some control over when a transgene is expressed, but this is completely determined by the enhancer trap or promoter used to drive GAL4 expression. In aging studies, it may be the case that lifespan-extending interventions are required at specific life stages (e.g. larval development only, or adult expression) only in a given tissue. Expressing a candidate protein at the wrong time in the life history of the fly, or in the wrong tissue set, could result in early mortality or no influence on lifespan.

Second, many of the publically available GAL4 driver lines and UAS-transgenes are of varying genetic background (*W^{1118}, Dahomey, Canton S., Yellow*). These distinct genetic backgrounds have a large degree of variation in median and maximum lifespan. Utilizing differing genetic lines makes lifespan determination due to specific genetic manipulations provided by the UAS-GAL4 system very difficult to assess [80]. It can never be assumed that a lifespan increase or decrease is solely due to UAS-GAL4 activation of a specific gene, as variation in lifespan is so largely disparate between organisms of different genetic background. In order to properly control for this genetic disparity, multiple rounds of back-crossing to a control line (e.g. *W^{1118}*) must be undertaken to help ensure genetic homogeneity. Even after careful fly husbandry, up to 8 months of time via 12 generations of backcrossing, there is no way to ensure that all lines used in subsequent lifespan experiments are genetically identical. A recent high-profile example of this problem described evidence that a gene thought to extend lifespan in worms and flies (*Sir2*) may simply be an aberrational phenotype due to improper genetic background, and not the activity of the *Sir2* gene alone [17, 80]. While we have

employed the use of outcrossed UAS-GAL4 lines for some experiments, the majority of our work has utilized a modified version of this system (gene-switch), which ensures genetic homogeneity for lifespan comparison.

Temporal and tissue-specific genetic manipulation of *Drosophila* via gene-switch

In order to have full control over where and when an exogenous gene is expressed in *Drosophila,* we have employed the use of the P-switch (henceforth referred to as gene-switch) system to activate transgene overexpression [81]. Gene-switch is an inducible modified version of the UAS-GAL4 system. The gene-switchconstruct is a chimeric GAL4 fused to the ligand binding domain of the human progesterone receptor and the transactivation domain of human P65 [81]. In the absence of the inducing molecule (progesterone-analog RU486), the GAL4 protein is inhibited and not able to bind the partner UAS-element, resulting in no transgene expression **(Fig. 1-7)**. When the flies are fed the drug, RU486 can bind the gene-switch GAL4 protein, inducing a conformational change that allows for UAS binding and subsequent transgene activation. Unlike standard UAS-GAL4, the gene-switch system permits complete temporal and spatial control over gene expression, as the animals can be dosed with RU486 at any time in development or adulthood.

Regarding the issue of genetic homogeneity in lifespan determination, gene-switch transgene induction allows us to study genetically identical populations of flies—the only difference being induction of the transgene via RU486 feeding, versus a control population fed the ethanol diluent vehicle. This system removes the variation in lifespan due to genetic background entirely. To note, more control experiments must be undertaken to ensure all the effects are due to transgene overexpression, and not simply due to the drug RU486 [81]. This is easily controlled for by using a genetic strain that harbors the gene-switch driver insertion

without the UAS-transgene insertion, to test the effects of RU486 and ethanol alone. Additionally, some gene-switch GAL4 lines have leaky expression outside of their previously characterized tissue-specificity [66]. This leaky expression may make some experiments more difficult to interpret. Likewise, this information calls into question the AMPK-lifespan data presented in [65], as the gene-switch muscle and fat body-specific drivers are known to be expressed in the intestine of the animal as well as the target tissues [66].

Summary and unanswered questions

While it is clear that AMPK is involved in many cellular aspects of aging, there are still many unanswered questions as to how AMPK functions to maintain or extend healthy lifespan, particularly in *Drosophila*. Although it has been shown that muscle and fat body-specific AMPK overexpression can extend lifespan, this does not address whether AMPK activity is required or sufficient to extend lifespan in other tissues or organ systems. Likewise, it is unknown which longevity-associated pathways (e.g. autophagy, lipid homeostasis) are required or sufficient to influence AMPK-mediated lifespan in the fly. These findings also do not address whether expression of AMPK in one tissue (e.g. neurons) can affect other organ systems (e.g. the intestine, muscle) to influence lifespan of the organism. Additionally, which age-associated pathologies are abrogated by targeted AMPK overexpression? Using the techniques, tools, and information provided in this introduction I will address these concerns in total.

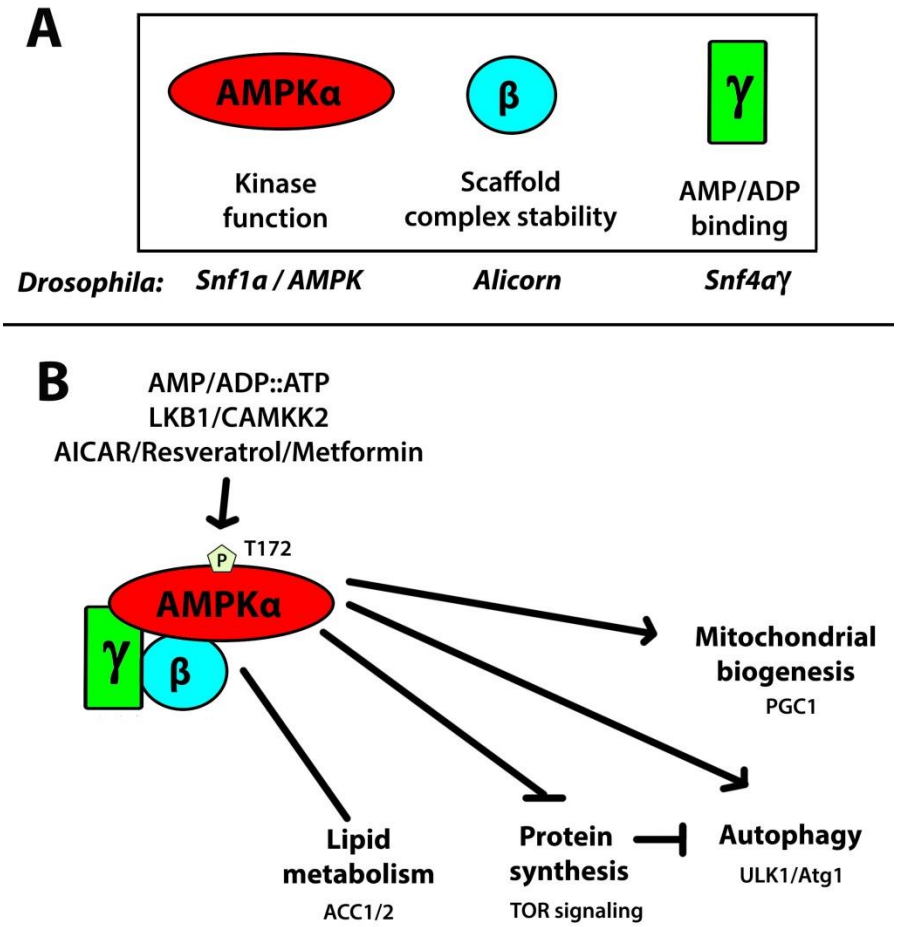

Figure 1-1. Schematic representation of AMPK complex and downstream pathways.

(A) AMPK complex subunits and *Drosophila* orthologs.

(B) Downstream target pathways of AMPK activity. In mammals, AMPK complex functions as an obligate heterotrimeric complex. AMPKα can become activated by phosphorylation on threonine 172 (184 in *Drosophila*) by LKB1, or CAMKK2 (β) kinases. This activation is also facilitated by the gamma subunit binding of AMP or ADP under low energy status, or activating drugs (e.g. AICAR) allowing for efficient phosphorylation of downstream substrates that control a host of metabolic processes. AMPK has been shown to regulate mitochondrial biogenesis via phosphorylation of PGC1α, autophagy and mitophagy via phosphorylation of ULK1 (Atg1 in *Drosophila*). AMPK has also been shown to downregulate TOR activity, repressing cell growth and protein synthesis, as well as lipid metabolism in various ways. (Arrows indicate upregulation/activation of the denoted process, bars indicate inhibition, lines indicate opposing/indeterminant effects).

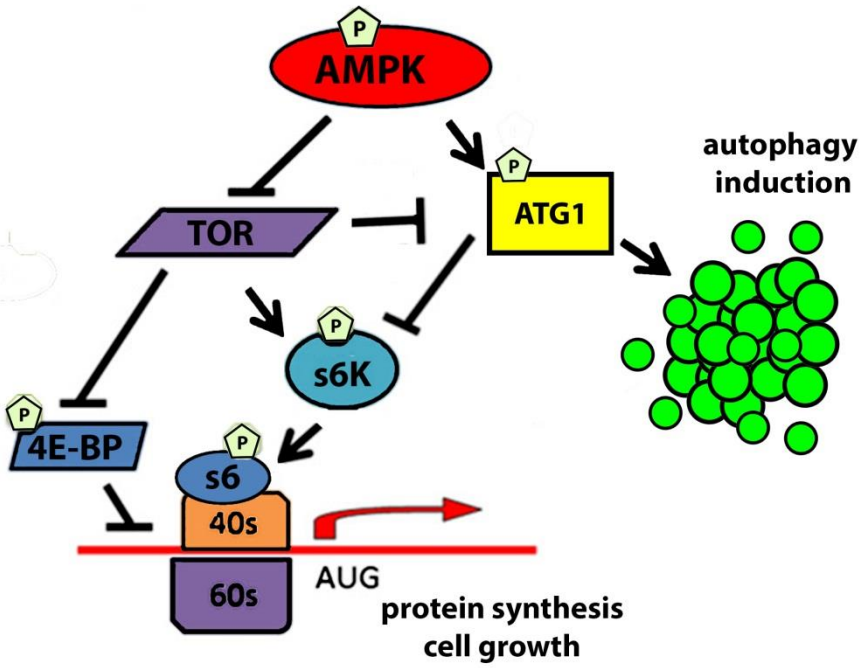

Figure 1-2. Schematic representation of AMPK influence on TOR signaling and autophagy.

Increased AMPK function allows for inhibition of TOR kinase, resulting in decreased S6K phosphorylation, increased 4E-BP inhibition of translation and decreased cell/organismal growth. AMPK activation also causes increased phosphorylation of Atg1, a major autophagy effector kinase. Phosphorylated Atg1 then functions to mediate autophagic vesicle formation and recycling of intracellular components.

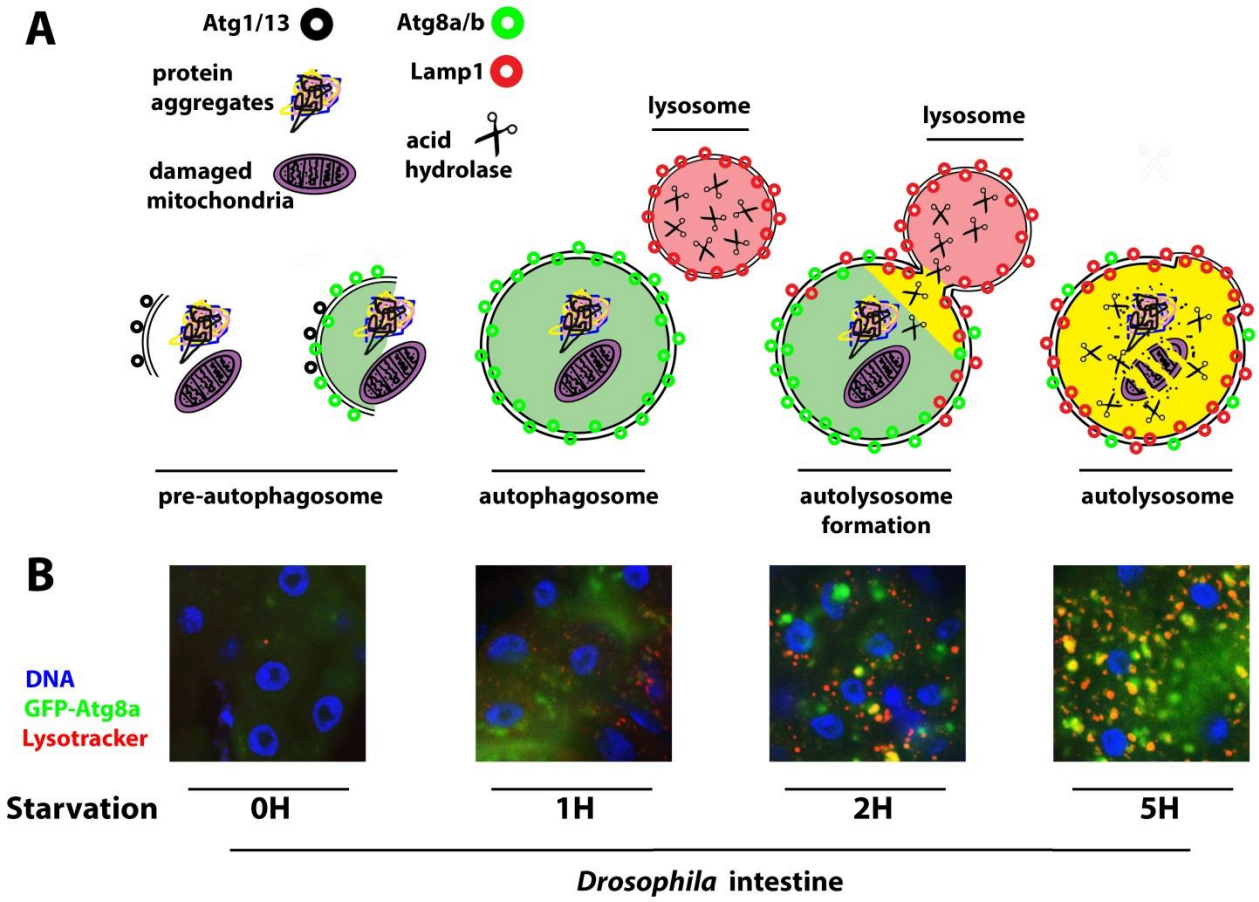

Figure 1-3. Autophagy promotes the clearance of damaged proteins and organelles.

(A) Damaged organelles, and aggregated proteins can be cleared by the macro-autophagic process. Activated Atg1/13 complex functions to promote membrane formation and organization, Atg8a/LC3 forms on the membrane post-lipidation to elongate membranes and engulf damaged proteins and organelles. Lysosomes containing acid hydrolases and proteases with Lamp1 on the membrane can fuse with the autophagosome, allowing for degradation and eventual recycling of vesicle contents.

(B) The autophagy process can be actively monitored in the *Drosophila* intestine by imaging flies expressing a GFP-tagged Atg8a under the control of its endogenous promoter, with simultaneous staining with the acidophilic dye Lysotracker Red. Colocalization of GFP-Atg8a foci, with acidophilic Lysotracker foci, can identify autolysomes (yellow vesicles).

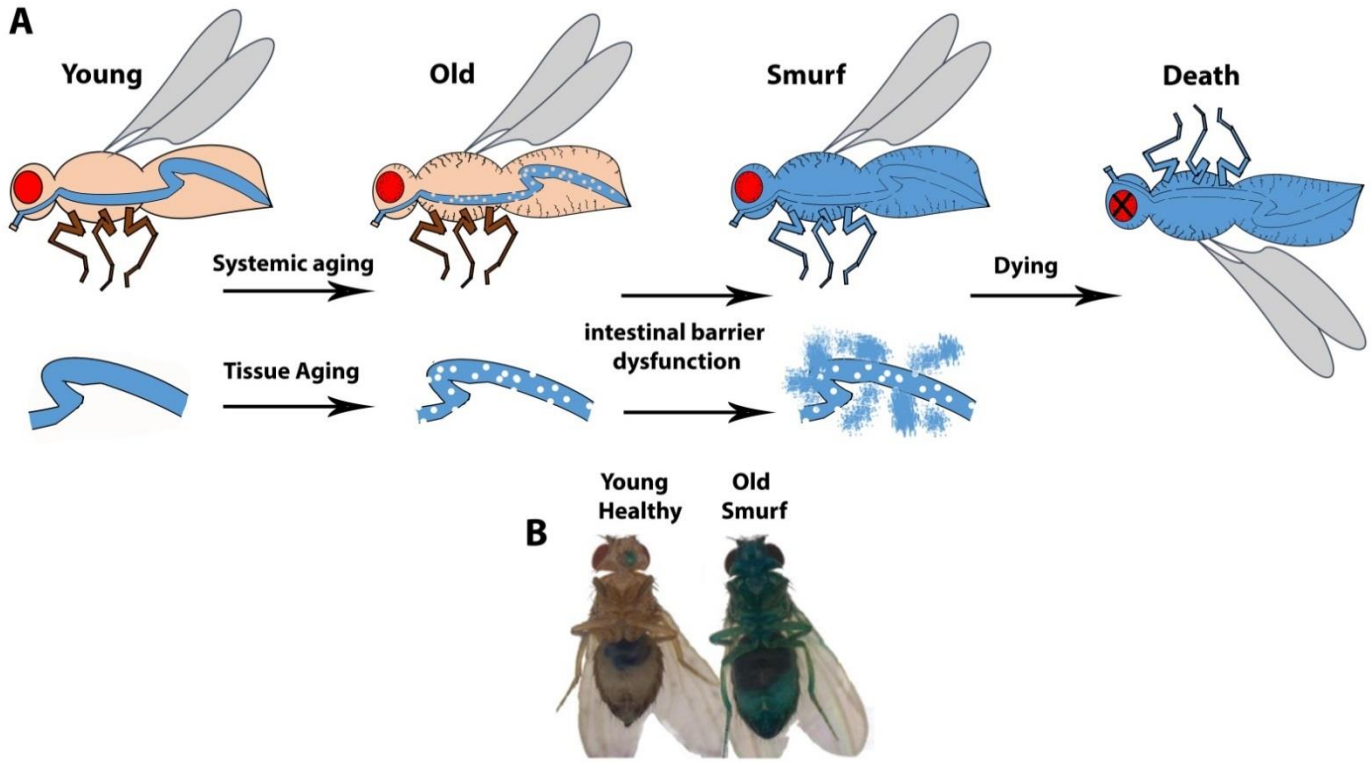

Figure 1-4. *Drosophila* smurf assay for age-related intestinal barrier dysfunction.

(A) As *Drosophila* aging progresses, intestinal barrier function decreases. By supplementing non-toxic, non-absorbable blue food dye into the *Drosophila* medium, gut barrier function can be actively monitored. Upon age-related intestinal barrier dysfunction, blue dye that is normally confined to the intestinal tract of the fly will leak into the hemolymph, producing a bright blue organism we have termed "smurfs." As a population of *Drosophila* ages, the proportion of smurfs to non-smurfs increases. Once the fly exhibits the smurf phenotype, it is followed by death within 2-12 days.

(B) Example of a biologically young fly alongside anintestinal barrier-compromised "smurf" fly (photo taken by Michael Rera).

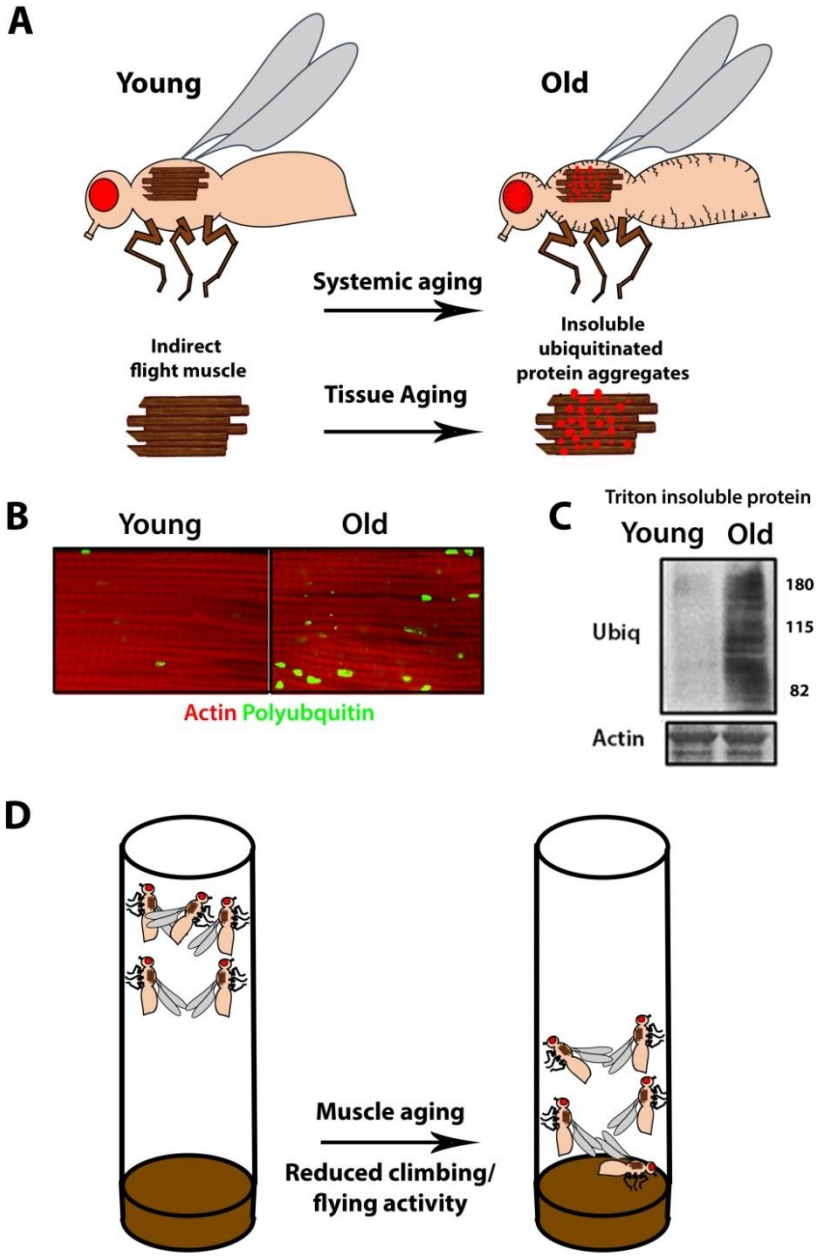

Figure 1-5. Markers of muscle aging in *Drosophila*.

(A) Schematic representation of muscle aging in *Drosophila*. As *Drosophila* age, the flight muscle accumulates large (polyubiquitin rich) insoluble protein aggregates that interfere with muscle function.

(B) Immunofluorescence images of young (left) and old (right) indirect flight muscle stained for poly-ubiquitin (green) and F-actin (Red). Older flies exhibit an increase in polyubiquitin aggregates.

(C) Representative western blot from Triton X-100 insoluble muscle lysates of young (left) and old (right) flies. Older flies accumulate more insoluble ubiquitin/actin staining.

(D) Schematic representation of climbing activity assay. Young flies (left) are able to climb to the top of a media vial faster and more frequently than older (right) *Drosophila*.

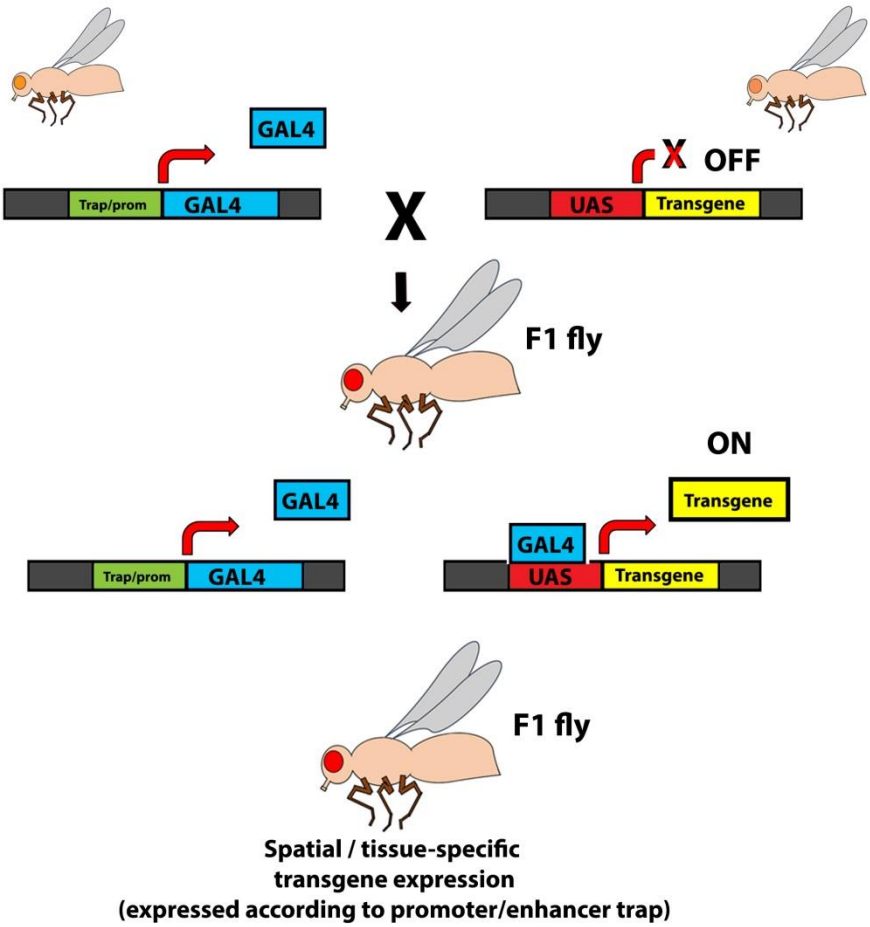

Figure 1-6. UAS-GAL4 system overview.

One parental fly strain containing the yeast GAL4 DNA binding domain under the control of tissue-specific enhancer trap or promoter is crossed to a fly strain containing a desired transgene under control of the GAL4-specific upstream activating sequence (UAS) element. Progeny from this cross can now express a desired UAS-transgene under control of the GAL4 transcription factor in a tissue-specific manner.

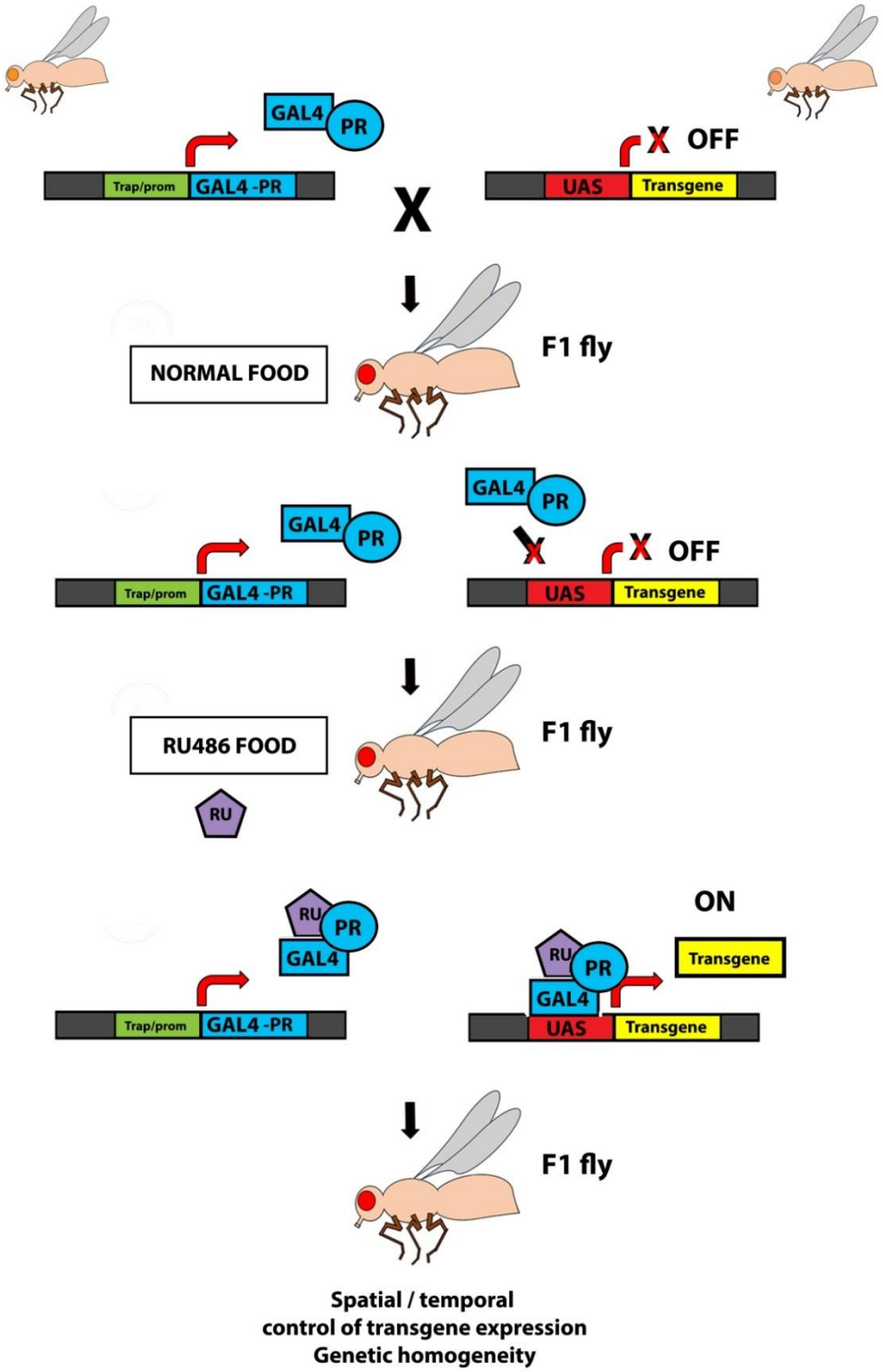

Figure1-7. Gene-Switch (p-switch) UAS-GAL4 system overview.

Using the specialized inducible gene-switch GAL4 system, flies placed on media containing NO RU486 will not express the desired UAS-transgene. Feeding flies media containing RU486 allows the drug to bind the modified progesterone receptor-GAL4 fusion protein, inducing a conformational change permitting UAS-transgene activation in a temporal and spatial manner.

REFERENCES:

1. Hardie, D. G., Ross, F. a, & Hawley, S. a. (2012). AMPK: a nutrient and energy sensor that maintains energy homeostasis. *Nature Reviews. Molecular Cell Biology*, *13*(4), 251–62. doi:10.1038/nrm3311

2. Xiao, B., Sanders, M. J., Underwood, E., Heath, R., Mayer, F. V, Carmena, D., … Gamblin, S. J. (2011). Structure of mammalian AMPK and its regulation by ADP. *Nature*, *472*(7342), 230–3. doi:10.1038/nature09932

3. Hawley, S. A., Davison, M., Woods, A., Davies, S. P., Beri, R. K., Carling, D., & Hardie, D. G. (1996). Characterization of the AMP-activated Protein Kinase Kinase from Rat Liver and Identification of Threonine 172 as the Major Site at Which It Phosphorylates AMP-activated Protein Kinase. *Journal of Biological Chemistry*, *271*(44), 27879–27887.

4. Hawley, S. A., Boudeau, J., Reid, J. L., Mustard, K. J., Udd, L., Mäkelä, T. P., … Hardie, D. G. (2003). Complexes between the LKB1 tumor suppressor, STRADα/β and MO25α/β are upstream kinases in the AMP-activated protein kinase cascade. *Journal of Biology*, *2*(4).

5. Shaw, R. J., Kosmatka, M., Bardeesy, N., Hurley, R. L., Witters, L. A., DePinho, R. A., & Cantley, L. C. (2004). The tumor suppressor LKB1 kinase directly activates AMP-activated kinase and regulates apoptosis in response to energy stress. *Proceedings of the National Academy of Sciences of the United States of America*, *101*(10), 3329–35. doi:10.1073/pnas.0308061100

6. Woods, A., Dickerson, K., Heath, R., Hong, S.-P., Momcilovic, M., Johnstone, S. R., … Carling, D. (2005). Ca2+/calmodulin-dependent protein kinase kinase-beta acts upstream of AMP-activated protein kinase in mammalian cells. *Cell Metabolism*, *2*(1), 21–33. doi:10.1016/j.cmet.2005.06.005

7. Momcilovic, M., Hong, S.-P., & Carlson, M. (2006). Mammalian TAK1 activates Snf1 protein kinase in yeast and phosphorylates AMP-activated protein kinase in vitro. *The Journal of Biological Chemistry*, *281*(35), 25336–43. doi:10.1074/jbc.M604399200

8. Gowans, G. J., Hawley, S. a, Ross, F. a, & Hardie, D. G. (2013). AMP is a true physiological regulator of AMP-activated protein kinase by both allosteric activation and enhancing net phosphorylation. *Cell Metabolism*, *18*(4), 556–66. doi:10.1016/j.cmet.2013.08.019

9. Gallagher, E. J., & LeRoith, D. (2011). Diabetes, cancer, and metformin: connections of metabolism and cell proliferation. *Annals of the New York Academy of Sciences*, *1243*(1), 54–68. doi:10.1111/j.1749-6632.2011.06285.

10. Hardie, D. G. (2006). Neither LKB1 nor AMPK are the direct targets of metformin. *Gastroenterology*, *131*(3), 973; author reply 974–5. doi:10.1053/j.gastro.2006.07.032

11. Anisimov, V. N., Berstein, L. M., Egormin, P. a, Piskunova, T. S., Popovich, I. G., Zabezhinski, M. a, … Franceschi, C. (2005). Effect of metformin on life span and on the development of spontaneous mammary tumors in HER-2/neu transgenic mice. *Experimental Gerontology*, *40*(8-9), 685–93. doi:10.1016/j.exger.2005.07.007

12. Cabreiro, F., Au, C., Leung, K.-Y., Vergara-Irigaray, N., Cochemé, H. M., Noori, T., … Gems, D. (2013). Metformin retards aging in C. elegans by altering microbial folate and methionine metabolism. *Cell*, *153*(1), 228–39. doi:10.1016/j.cell.2013.02.035

13. Slack, C., Foley, A., & Partridge, L. (2012). Activation of AMPK by the putative dietary restriction mimetic metformin is insufficient to extend lifespan in Drosophila. *PloS One*, *7*(10), e47699. doi:10.1371/journal.pone.0047699

14. Bass, T. M., Weinkove, D., Houthoofd, K., Gems, D., & Partridge, L. (2007). Effects of resveratrol on lifespan in Drosophila melanogaster and Caenorhabditis elegans. *Mechanisms of Ageing and Development*, *128*(10), 546–52. doi:10.1016/j.mad.2007.07.007

15. Baur, J. a, Pearson, K. J., Price, N. L., Jamieson, H. a, Lerin, C., Kalra, A., … Sinclair, D. a. (2006). Resveratrol improves health and survival of mice on a high-calorie diet. *Nature*, *444*(7117), 337–42. doi:10.1038/nature05354

16. Kaeberlein, M., McDonagh, T., Heltweg, B., Hixon, J., Westman, E. A., Caldwell, S. D., … Kennedy, B. K. (2005). Substrate-specific activation of sirtuins by resveratrol. *The Journal of Biological Chemistry*, *280*(17), 17038–45. doi:10.1074/jbc.M500655200

17. Burnett, C., Valentini, S., Cabreiro, F., Goss, M., Somogyvári, M., Piper, M. D., … Gems, D. (2011). Absence of effects of Sir2 overexpression on lifespan in C. elegans and Drosophila. *Nature*, *477*(7365), 482–5. doi:10.1038/nature10296

18. Um, J., Park, S., Kang, H., Yang, S., Foretz, M., Mcburney, M. W., … Chung, J. H. (2010). AMP-Activated Protein Kinase – Deficient Mice Are Resistant to the Metabolic Effects of Resveratrol, *59*(March). doi:10.2337/db09-0482.J.-H.U.

19. Cantó, C., Gerhart-Hines, Z., Feige, J. N., Lagouge, M., Noriega, L., Milne, J. C., … Auwerx, J. (2009). AMPK regulates energy expenditure by modulating NAD+ metabolism and SIRT1 activity. *Nature*, *458*(7241), 1056–60. doi:10.1038/nature07813

20. Narkar, V. A., Downes, M., Yu, R. T., Embler, E., Wang, Y.-X., Banayo, E., … Evans, R. M. (2008). AMPK and PPARdelta agonists are exercise mimetics. *Cell*, *134*(3), 405–15. doi:10.1016/j.cell.2008.06.051

21. Kobilo, T., Guerrieri, D., Zhang, Y., Collica, S. C., Becker, K. G., & van Praag, H. (2014). AMPK agonist AICAR improves cognition and motor coordination in young and aged mice. *Learning & Memory (Cold Spring Harbor, N.Y.)*, *21*(2), 119–26. doi:10.1101/lm.033332.113

22. Mullane, K. (1993). Acadesine: The prototype adenosine regulating agent for reducing myocardial ischaemic injury. *Cardiovascular Research*.

23. Cuthbertson, D. J., Babraj, J. A., Mustard, K. J. W., Towler, M. C., Green, K. A., Wackerhage, H., … Rennie, M. J. (2007). 5-aminoimidazole-4-carboxamide 1-beta-D-ribofuranoside acutely stimulates skeletal muscle 2-deoxyglucose uptake in healthy men. *Diabetes*, *56*(8), 2078–84. doi:10.2337/db06-1716

24. Lapierre, L. R., Gelino, S., Meléndez, A., & Hansen, M. (2011). Autophagy and lipid metabolism coordinately modulate life span in germline-less C. elegans. *Current Biology : CB*, *21*(18), 1507–14. doi:10.1016/j.cub.2011.07.042

25. Lapierre, L. R., Meléndez, A., & Hansen, M. (2012). Autophagy links lipid metabolism to longevity in C. elegans. *Autophagy*, *8*(1), 144–6. doi:10.4161/auto.8.1.18722

26. O'Rourke, E. J., Kuballa, P., Xavier, R., & Ruvkun, G. (2013). ω-6 Polyunsaturated fatty acids extend life span through the activation of autophagy. *Genes & Development*, *27*(4), 429–40. doi:10.1101/gad.205294.112

27. O'Rourke, E. J., & Ruvkun, G. (2013). MXL-3 and HLH-30 transcriptionally link lipolysis and autophagy to nutrient availability. *Nature Cell Biology*, *15*(6), 668–76. doi:10.1038/ncb2741

28. Wang, M. C., O'Rourke, E. J., & Ruvkun, G. (2008). Fat metabolism links germline stem cells and longevity in C. elegans. *Science (New York, N.Y.)*, *322*(5903), 957–60. doi:10.1126/science.1162011

29. Hansen, M., Flatt, T., & Aguilaniu, H. (2013). Reproduction, fat metabolism, and life span: what is the connection? *Cell Metabolism*, *17*(1), 10–9. doi:10.1016/j.cmet.2012.12.003

30. Katewa, S. D., Demontis, F., Kolipinski, M., Hubbard, A., Gill, M. S., Perrimon, N., … Kapahi, P. (2012). Intramyocellular fatty-acid metabolism plays a critical role in mediating responses to dietary restriction in Drosophila melanogaster. *Cell Metabolism*, *16*(1), 97–103. doi:10.1016/j.cmet.2012.06.005

31. Li, Y., Xu, S., Mihaylova, M. M., Zheng, B., Hou, X., Jiang, B., … Zang, M. (2011). AMPK phosphorylates and inhibits SREBP activity to attenuate hepatic steatosis and atherosclerosis in diet-induced insulin-resistant mice. *Cell Metabolism*, *13*(4), 376–88. doi:10.1016/j.cmet.2011.03.009

32. Yin, D., Huang, P., Wu, J., & Song, H. (2014). Drosophila protein phosphatase V regulates lipid homeostasis via the AMPK pathway. *Journal of Molecular Cell Biology*, *6*(1), 100–2. doi:10.1093/jmcb/mjt050

33. Scarpulla, R. C. (2011). Metabolic control of mitochondrial biogenesis through the PGC-1 family regulatory network. *Biochimica et Biophysica Acta*, *1813*(7), 1269–78. doi:10.1016/j.bbamcr.2010.09.019

34. Scarpulla, R. C., Vega, R. B., & Kelly, D. P. (2012). Transcriptional integration of mitochondrial biogenesis. *Trends in Endocrinology and Metabolism: TEM*, *23*(9), 459–66. doi:10.1016/j.tem.2012.06.006

35. Handschin, C., Kobayashi, Y. M., Chin, S., Seale, P., Campbell, K. P., & Spiegelman, B. M. (2007). PGC-1alpha regulates the neuromuscular junction program and ameliorates Duchenne muscular dystrophy. *Genes & Development*, *21*(7), 770–83. doi:10.1101/gad.1525107

36. Wenz, T., Diaz, F., Spiegelman, B. M., & Moraes, C. T. (2008). Activation of the PPAR/PGC-1alpha pathway prevents a bioenergetic deficit and effectively improves a mitochondrial myopathy phenotype. *Cell Metabolism*, *8*(3), 249–56. doi:10.1016/j.cmet.2008.07.006

37. Rera, M., Bahadorani, S., Cho, J., Koehler, C. L., Ulgherait, M., Hur, J. H., … Walker, D. W. (2011). Modulation of longevity and tissue homeostasis by the drosophila PGC-1 homolog. *Cell Metabolism*, *14*(5), 623–634.

38. Jäger, S., Handschin, C., St-Pierre, J., & Spiegelman, B. M. (2007). AMP-activated protein kinase (AMPK) action in skeletal muscle via direct phosphorylation of PGC-1alpha. *Proceedings of the National Academy of Sciences of the United States of America*, *104*(29), 12017–22. doi:10.1073/pnas.0705070104

39. Johnson, S. C., Rabinovitch, P. S., & Kaeberlein, M. (2013). mTOR is a key modulator of ageing and age-related disease. *Nature*, *493*(7432), 338–45. doi:10.1038/nature11861

40. Laplante, M., & Sabatini, D. M. (2012). mTOR signaling in growth control and disease. *Cell*, *149*(2), 274–93. doi:10.1016/j.cell.2012.03.017

41. Magnuson, B., Ekim, B., & Fingar, D. C. (2012). Regulation and function of ribosomal protein S6 kinase (S6K) within mTOR signalling networks. *The Biochemical Journal*, *441*(1), 1–21. doi:10.1042/BJ20110892

42. Rubinsztein, D. C., Mariño, G., & Kroemer, G. (2011). Autophagy and aging. *Cell*, *146*(5), 682–95. doi:10.1016/j.cell.2011.07.030

43. Gwinn, D. M., Shackelford, D. B., Egan, D. F., Mihaylova, M. M., Mery, A., Vasquez, D. S., … Shaw, R. J. (2008). AMPK phosphorylation of raptor mediates a metabolic checkpoint. *Molecular Cell*, *30*(2), 214–26. doi:10.1016/j.molcel.2008.03.003

44. Inoki, K., Zhu, T., & Guan, K.-L. (2003). TSC2 Mediates Cellular Energy Response to Control Cell Growth and Survival. *Cell*, *115*(5), 577–590. doi:10.1016/S0092-8674(03)00929-2

45. Kim, J., Kundu, M., Viollet, B., & Guan, K.-L. (2011). AMPK and mTOR regulate autophagy through direct phosphorylation of Ulk1. *Nature Cell Biology*, *13*(2), 132–41. doi:10.1038/ncb2152

46. Egan, D. F., Shackelford, D. B., Mihaylova, M. M., Gelino, S., Kohnz, R. A., Mair, W., … Shaw, R. J. (2011). Phosphorylation of ULK1 (hATG1) by AMP-activated protein kinase connects energy sensing to mitophagy. *Science (New York, N.Y.)*, *331*(6016), 456–61. doi:10.1126/science.1196371

47. Ravikumar, B., Sarkar, S., Davies, J. E., Futter, M., Garcia-Arencibia, M., Green-Thompson, Z. W., … Rubinsztein, D. C. (2010). Regulation of mammalian autophagy in physiology and pathophysiology. *Physiological Reviews*, *90*(4), 1383–435. doi:10.1152/physrev.00030.2009

48. Scott, R. C., Juhász, G., & Neufeld, T. P. (2007). Direct induction of autophagy by Atg1 inhibits cell growth and induces apoptotic cell death. *Current Biology : CB*, *17*(1), 1–11. doi:10.1016/j.cub.2006.10.053

49. Kim, J., Kim, Y. C., Fang, C., Russell, R. C., Kim, J. H., Fan, W., … Guan, K.-L. (2013). Differential regulation of distinct Vps34 complexes by AMPK in nutrient stress and autophagy. *Cell*, *152*(1-2), 290–303. doi:10.1016/j.cell.2012.12.016

50. Cuervo, A. M. (2008). Autophagy and aging: keeping that old broom working. *Trends in Genetics : TIG*, *24*(12), 604–12. doi:10.1016/j.tig.2008.10.002

51. Meléndez, A., Tallóczy, Z., Seaman, M., Eskelinen, E.-L., Hall, D. H., & Levine, B. (2003). Autophagy genes are essential for dauer development and life-span extension in C. elegans. *Science (New York, N.Y.)*, *301*(5638), 1387–91. doi:10.1126/science.1087782

52. Bjedov, I., Toivonen, J. M., Kerr, F., Slack, C., Jacobson, J., Foley, A., & Partridge, L. (2010). Mechanisms of life span extension by rapamycin in the fruit fly Drosophila melanogaster. *Cell Metabolism*, *11*(1), 35–46. doi:10.1016/j.cmet.2009.11.010

53. Demontis, F., & Perrimon, N. (2010). FOXO/4E-BP signaling in Drosophila muscles regulates organism-wide proteostasis during aging. *Cell*, *143*(5), 813–25. doi:10.1016/j.cell.2010.10.007

54. Pyo, J.-O., Yoo, S.-M., Ahn, H.-H., Nah, J., Hong, S.-H., Kam, T.-I., … Jung, Y.-K. (2013). Overexpression of Atg5 in mice activates autophagy and extends lifespan. *Nature Communications*, *4*, 2300. doi:10.1038/ncomms3300

55. Simonsen, A., Cumming, R. C., Brech, A., Isakson, P., Schubert, D. R., & Finley, K. D. (2008). Promoting basal levels of autophagy in the nervous system enhances longevity and oxidant resistance in adult Drosophila. *Autophagy*, *4*(2), 176–184.

56. Burkewitz, K., Zhang, Y., & Mair, W. (2014). AMPK at the Nexus of Energetics and Aging. *Cell Metabolism*, 1–16. doi:10.1016/j.cmet.2014.03.002

57. Curtis, R., O'Connor, G., & DiStefano, P. S. (2006). Aging networks in Caenorhabditis elegans: AMP-activated protein kinase (aak-2) links multiple aging and metabolism pathways. *Aging Cell*, *5*(2), 119–26. doi:10.1111/j.1474-9726.2006.00205.x

58. Apfeld, J., O'Connor, G., McDonagh, T., DiStefano, P. S., & Curtis, R. (2004). The AMP-activated protein kinase AAK-2 links energy levels and insulin-like signals to lifespan in C. elegans. *Genes & Development*, *18*(24), 3004–9. doi:10.1101/gad.1255404

59. Mair, W., Morantte, I., Rodrigues, A. P. C., Manning, G., Montminy, M., Shaw, R. J., & Dillin, A. (2011). Lifespan extension induced by AMPK and calcineurin is mediated by CRTC-1 and CREB. *Nature*, *470*(7334), 404–8. doi:10.1038/nature09706

60. Greer, E. L., Dowlatshahi, D., Banko, M. R., Villen, J., Hoang, K., Blanchard, D., … Brunet, A. (2007). An AMPK-FOXO pathway mediates longevity induced by a novel method of dietary restriction in C. elegans. *Current Biology : CB*, *17*(19), 1646–56. doi:10.1016/j.cub.2007.08.047

61. Cantó, C., & Auwerx, J. (2011). Calorie restriction: is AMPK a key sensor and effector? *Physiology (Bethesda, Md.)*, *26*(4), 214–24. doi:10.1152/physiol.00010.2011

62. Mair, W., Panowski, S. H., Shaw, R. J., & Dillin, A. (2009). Optimizing dietary restriction for genetic epistasis analysis and gene discovery in C. elegans. *PloS One*, *4*(2), e4535. doi:10.1371/journal.pone.0004535

63. Spasić, M. R., Callaerts, P., & Norga, K. K. (2008). Drosophila alicorn is a neuronal maintenance factor protecting against activity-induced retinal degeneration. *The Journal of Neuroscience : The Official Journal of the Society for Neuroscience*, *28*(25), 6419–29. doi:10.1523/JNEUROSCI.1646-08.2008

64. Poels, J., Spasić, M. R., Gistelinck, M., Mutert, J., Schellens, A., Callaerts, P., & Norga, K. K. (2012). Autophagy and phagocytosis-like cell cannibalism exert opposing effects on cellular survival during metabolic stress. *Cell Death and Differentiation*, *19*(10), 1590–601. doi:10.1038/cdd.2012.37

65. Stenesen, D., Suh, J. M., Seo, J., Yu, K., Lee, K.-S., Kim, J.-S., … Graff, J. M. (2013). Adenosine nucleotide biosynthesis and AMPK regulate adult life span and mediate the longevity benefit of caloric restriction in flies. *Cell Metabolism*, *17*(1), 101–12. doi:10.1016/j.cmet.2012.12.006

66. Poirier, L., Shane, A., Zheng, J., & Seroude, L. (2008). Characterization of the Drosophila gene-switch system in aging studies: a cautionary tale. *Aging Cell*, *7*(5), 758–70. doi:10.1111/j.1474-9726.2008.00421.x

67. Nikoletopoulou, V., Kyriakakis, E., & Tavernarakis, N. (2014). Cellular and molecular longevity pathways: the old and the new. *Trends in Endocrinology and Metabolism: TEM*, *25*(4), 212–23. doi:10.1016/j.tem.2013.12.003

68. Rera, M., Clark, R. I., & Walker, D. W. (2012). Intestinal barrier dysfunction links metabolic and inflammatory markers of aging to death in Drosophila. *Proceedings of the National Academy of Sciences of the United States of America*, *109*(52), 21528–33. doi:10.1073/pnas.1215849110

69. Kirkwood, T. B. L. (2004). Intrinsic ageing of gut epithelial stem cells. *Mechanisms of Ageing and Development*, *125*(12), 911–5. doi:10.1016/j.mad.2004.09.004

70. Katz, D., Hollander, D., Said, H. M., & Dadufalza, V. (1987). Aging-associated increase in intestinal permeability to polyethylene glycol 900. *Digestive Diseases and Sciences*, *32*(3), 285–288.

71. Stechmiller, J. K., Treloar, D., & Allen, N. (1997). Gut dysfunction in critically ill patients: A review of the literature. *American Journal of Critical Care*, *6*(3), 204–209.

72. Nair, K. S. (2005). Aging muscle. In *American Journal of Clinical Nutrition* (Vol. 81, pp. 953–963).

73. Augustin, H., & Partridge, L. (2009). Invertebrate models of age-related muscle degeneration. *Biochimica et Biophysica Acta*, *1790*(10), 1084–94. doi:10.1016/j.bbagen.2009.06.011

74. Rana, A., Rera, M., & Walker, D. W. (2013). Parkin overexpression during aging reduces proteotoxicity, alters mitochondrial dynamics, and extends lifespan. *Proceedings of the National Academy of Sciences of the United States of America*, *110*(21), 8638–43. doi:10.1073/pnas.1216197110

75. Rhodenizer, D., Martin, I., Bhandari, P., Pletcher, S. D., & Grotewiel, M. (2008). Genetic and environmental factors impact age-related impairment of negative geotaxis in Drosophila by altering age-dependent climbing speed. *Experimental Gerontology*, *43*(8), 739–48. doi:10.1016/j.exger.2008.04.011

76. Copeland, J. M., Cho, J., Lo, T., Hur, J. H., Bahadorani, S., Arabyan, T., … Walker, D. W. (2009). Extension of Drosophila life span by RNAi of the mitochondrial respiratory chain. *Current Biology : CB*, *19*(19), 1591–8. doi:10.1016/j.cub.2009.08.016

77. Kenyon, C. (2005). The plasticity of aging: insights from long-lived mutants. *Cell*, *120*(4), 449–60. doi:10.1016/j.cell.2005.02.002

78. Duffy, J. B. (2002). GAL4 system in Drosophila: A fly geneticist's Swiss army knife. *Genesis*.

79. Brand, A. H., & Perrimon, N. (1993). Targeted gene expression as a means of altering cell fates and generating dominant phenotypes. *Development*, *118*(2), 401–415.

80. Burgess, D. J. (2011). Model organisms: the dangers lurking in the genetic background. *Nature Reviews. Genetics*, *12*(11), 742. doi:10.1038/nrg3089

81. Roman, G., Endo, K., Zong, L., & Davis, R. L. (2001). P[Switch], a system for spatial and temporal control of gene expression in Drosophila melanogaster. *Proceedings of the National Academy of Sciences of the United States of America*, *98*(22), 12602–7. doi:10.1073/pnas.221303998

CHAPTER II:

NEURONAL OVEREXPRESSION OF AMPK EXTENDS ORGANISMAL LIFESPAN AND INDUCES SYSTEMIC AUTOPHAGY

Neuronal overexpression of AMPK is sufficient to stimulate kinase function and suppress TOR signaling

To better understand the relationship between neuronal energy homeostasis and organismal aging, we sought to examine the impact of neuron-specific upregulation of the catalytic (α) AMPK subunit (hereafter referred to as AMPK) on *Drosophila* lifespan. To do so, we used the pan-neuronal *Elav-Gene-Switch* (GS) driver line [1] to activate two different AMPK transgenes: an untagged "*UAS-AMPK*" insertion and an mCherry-tagged "*UAS-mCh-AMPK*" insertion specifically in adult neurons. Firstly, we confirmed that induction of the *ELAV-GS>UAS-mch-AMPK* flies upregulated total levels of AMPK RNA in head tissue of RU486-fed female flies **(Fig. 2-1A)**. As AMPK functions as an obligate heterotrimeric complex, we sought to determine if endogenous transcripts of AMPK and partner subunits were increased upon transgenic AMPK overexpression in brain tissue. Using primer sets that specifically amplify only endogenous transcripts of AMPK and partner subunits, we saw increased levels of endogenous AMPK (α), Alicorn (β), and Snf4a (γ) message. These data provide evidence for a conserved transcriptional linkage. When levels of the AMPKα are increased, compensatory gene expression for all subunits is increased accordingly **(Fig. 2-1A)**.

As *Drosophila* AMPK is only active when phosphorylated on Thr184, we sought to confirm that transgenic expression of AMPK can increase AMPK-phosphorylation/activity in nervous system tissue. Western blot analysis using a phospho-specific antibody revealed a significant increase in total phospho-Thr184-AMPK levels in head tissue lysates from *ElavGS>UAS-mCh-AMPK* flies upon RU486 treatment compared to uninduced controls **(Fig. 2-1B quantification right)**. Using this construct, it is easy to differentiate between the higher molecular weight exogenous-tagged forms of AMPK from the endogenous protein due to lower mobility by SDS-PAGE/western blot. We found that most of the increase in total

phosphorylation of AMPK is due to overexpression of the tagged transgene. Endogenous AMPK is phosphorylated to a similar degree in both RU486-treated and untreated flies. As confirmation of this phenomenon, we tested the additional untagged *UAS-AMPK* insert via western blot **(Fig. 2-1C quantification right)**. Similarly, we observed a significant increase in the total amount of active phosphorylated AMPK in this line.

Exploring the effects of increased AMPK activity in the adult nervous system on downstream pathways, we first measured phosphorylation of the S6 ribosomal subunit kinase (S6K), a well-characterized downstream target of TOR kinase, by western blotting using a phospho-Thr398-dependent S6K antibody. We observed reduced levels of phospho-T398-S6K in head lysates of *ElavGS>UAS-mCh-AMPK* flies upon RU486 treatment compared to uninduced controls **(Fig. 2-1D and quantification right),** suggesting that TOR signaling is downregulated in adult neurons upon AMPK activation. To ensure this downstream suppression in TOR signaling is not specific exclusively to the *UAS-mCH-AMPK* line, we tested the additional untagged line *UAS-AMPK*, and saw similarly decreased S6k phosphorylation **(Fig. 2-1E)**. Additionally, to rule out the possibility that the drug RU486 accounted for these biochemical changes, we tested the *ElavGS* line crossed to W^{1118} flies as a control. *ElavGS>*W^{1118} flies exposed to RU486 showed no difference in AMPK transcripts, AMPK phosphorylation, or S6K phosphorylation **(Fig. 2-2)**.

Activation of AMPK in neurons extends organismal lifespan and upregulates markers of autophagy cell-autonomously

Next, we examined whether neuronal AMPK activation is sufficient to extend lifespan. The gene-switch system eliminates the potential confounding effect of genetic background differences between test and controls strains, as the only difference between conditions is the presence of the inducing agent (RU486) or diluent (ethanol) in the food [1, 2]. Adult-onset,

neuronal upregulation of AMPK resulted in increases in median lifespan in female flies, and had variable effects on male lifespan **(Figure 2-3A, Table A1).** As the AMPK-mediated longevity effects were stronger in females, we used female flies throughout the rest of this study.

TOR and AMPK act in concert to control autophagy induction [3]. As the induction of autophagy can be accompanied by an increase in mRNA levels of certain autophagy-related genes (ATGs) [4, 5], we examined the transcript levels of ATGs in response to AMPK activation. Indeed, Atg1, Atg8a, and Atg8b levels were significantly increased in head tissue of *ElavGS>UAS-mCh-AMPK* flies upon RU486 treatment **(Fig. 2-3B).** To further investigate the impact of neuronal AMPK activation on autophagy, we utilized a transgenic autophagosome marker, GFP-tagged Atg8a under the control of its endogenous promoter (*pGFP-Atg8a*), generated by [6]. We observed a significant increase in GFP puncta in brain tissue of *ElavGS>UAS-mCh-AMPK* flies upon RU486 treatment **(Fig. 2-3C, quantification Fig. 2-3D).** As a reduction in food intake can extend organismal lifespan, we sought to determine whether neuronal AMPK activation affects feeding behavior. Using two independent methods, a capillary feeding (CAFE) assay [7] and a dye-tracking assay [8], we failed to observe alterations in feeding behavior in *ElavGS>UAS-mCh-AMPK* flies upon RU486 treatment **(Fig. 2-3E, F)**. Control flies exposed to RU486 showed no difference in lifespan, feeding or autophagy markers in head tissue **(Fig. 2-4).** Together, these data indicate that activation of AMPK in the adult nervous system can induce autophagy in this target tissue and prolong lifespan.

Overexpression of AMPK in neurons causes moderate heat and oxidative stress resistance, but sensitizes flies to starvation

To better understand neuronal AMPK-mediated lifespan extension, we examined a number of behavioral and physiological parameters in long-lived flies. As there are often observed decreases in reproductive success in life-extending genetic manipulation, we first

assessed fecundity of the flies. Long-lived flies with increased neuronal AMPK activity showed normal fecundity throughout their lifespan **(Fig. 2-5A).** Frequently, *Drosophila* with extended longevity exhibit markedly increased resistance to external stressors, such as increased temperature, and hyperoxia. Neuronal AMPK activation confers a moderate increase in resistance to both hyperoxia **(Fig. 2-5B)** and heat stress **(Fig. 2-5C).**

As AMPK is activated by energy deprivation [9], we hypothesized that increased levels of AMPK activity in the nervous system could affect organismal survival under starvation conditions. Indeed, neuronal activation of AMPK conferred a decrease in survival when flies were maintained on an agar-only diet to induce starvation **(Fig. 2-5D).** To better understand this observation, we examined mass and triacylglyceride (TAG) levels in neuronal AMPK flies and controls in response to starvation. Interestingly, we observed rapid weight loss **(Fig. 2-5E)** and depletion of TAG stores **(Fig. 2-5F)** in response to starvation in *ElavGS>UAS-mCh-AMPK* flies upon RU486 treatment. Feeding RU486 to control flies did not influence stress resistance, mass, or TAG levels in response to starvation, and produced a moderate decrease in fecundity **(Fig. 2-6)**. Taken together, these data show that neuronal AMPK-mediated lifespan extension is not linked to reduced food consumption, physical activity, or reproductive output. However, increased AMPK activity in the adult nervous system, which extends lifespan when food is present, leads to rapid loss of TAG stores and early-onset mortality in the absence of food.

AMPK activation in neuronal tissue slows intestinal aging and induces autophagy in a cell non-autonomous manner

Neuron-specific activation of AMPK could promote organismal survival by slowing aging exclusively within the nervous system. Alternatively, neuronal AMPK activation could impact systemic aging via cell non-autonomous effects in distal, non-neuronal cells. In recent years, maintenance of intestinal homeostasis has been shown to play a key role in lifespan

determination in *Drosophila* [10, 11]. Indeed, loss of intestinal integrity in aged flies is linked to multiple markers of organismal aging and, critically, is a harbinger of death [12]. To determine whether neuronal AMPK-mediated lifespan extension acts via a cell autonomous or non-autonomous mechanism, we examined intestinal integrity via our smurf assay during aging in response to upregulation of AMPK in adult neurons. Using the constitutive *ELAV-GAL4* driver, we sought to both knockdown and upregulate AMPK in the nervous system and assess the impact on intestinal aging. Using this approach, we observed that neuron-specific RNAi of AMPK accelerated intestinal aging, while neuron-specific upregulation of AMPK delayed the onset of intestinal aging **(Fig. 2-7A)**. Similarly, we observed a delay in the onset of intestinal barrier dysfunction in *ElavGS>UAS-mCh-AMPK* flies upon RU486 treatment **(Fig. 2-7B)**, indicating a delay in intestinal aging at the tissue level.

Intrigued by the manner in which neuronal AMPK can modulate intestinal aging, we hypothesized that AMPK may be acting in a cell non-autonomous fashion. To better understand how neuron-specific expression of an AMPK transgene could impact intestinal tissues of the fly, we assayed markers of autophagy in the intestine upon neuronal activation of AMPK. Interestingly, we observed increased mRNA levels of *Atg1*, *Atg8a*, and *Atg8b* in intestinal tissue from *ElavGS>UAS-mCh-AMPK* flies upon RU486 treatment **(Fig. 2-7C).** These findings led us to question whether AMPK activation in neurons could stimulate autophagy in the intestinal epithelium. Following that line of questioning, we examined the transgenic autophagosome marker *pGFP-Atg8a* in the intestinal epithelium of flies with and without neuronal AMPK activation. We observed a significant increase in GFP puncta in posterior mid-gut enterocytes in *ElavGS>UAS-mCh-AMPK* flies upon RU486 treatment **(Fig. 2-7D, quantification Fig. 2-7E).** Upregulation of AMPK in neurons also significantly increased the amount of lysosomal foci

found in the mid-gut enterocytes as marked by the acidophilic dye lysotracker **(Fig. 2-7F, quantification Fig. 2-7G).** To further validate this observed upregulation in autophagy markers, live imaging of Lysotracker, and GFP-atg8a was performed simultaneously on dissected intestines of *ElavGS>UAS-mCh-AMPK* with or without RU486 feeding **(Fig. 2-8A).** The density of GFP-Atg8a, Lysotracker, and colocalized "autolysosomal" vesicles were all increased upon AMPK activation **(Fig. 5-7B).** Feeding RU486 to control flies did not affect intestinal aging, Atg transcript levels, autophagosome formation or lysosomal foci in intestinal tissue **(Fig. 2-9).**

Previous studies have reported that *ElavGS* displays RU486-dependent gene expression exclusively in the nervous system [1,13]. To rule out the possibility that transgenic AMPK is being misexpressed in other tissues of the fly, we examined expression of the exogenous AMPK transgene in various tissues of the fly— heads, thoraces, and intestines, in *ElavGS>UAS-mCh-AMPK* flies with and without RU486 induction. Only RNA isolated from head tissue showed a significant RU486-dependant increase in exogenous AMPK **(Fig. 2-10A).** Furthermore, western blot analysis of lysates from different tissues of *ElavGS>UAS-eGFP* flies also showed a visible RU486-dependent increase in GFP levels in only head tissue **(Fig. 2-10B).** In total, our findings support a model whereby neuronal activation of AMPK modulates intestinal aging via a cell non-autonomous mechanism.

Neuronal AMPK delays age-related decline in proteostasis and slows muscle aging

To better understand the cell non-autonomous nature of AMPK-mediated lifespan extension, we set out to determine whether neuronal AMPK activation can influence protein homeostasis in aging muscle tissue. First, we characterized the age-related deposition of protein aggregates in thoracic muscles by immunofluorescence. Importantly, neuronal AMPK activation led to reduced levels of protein aggregates during muscle aging **(Fig. 2-11A and quantification**

Fig. 2-11B). In a complementary approach, we examined the levels of insoluble ubiquitinated proteins, by western blotting, in thoraces of neuronal AMPK flies and controls during aging. Consistent with the immunofluorescence data, we observed that neuronal upregulation of AMPK reduced levels of insoluble ubiquitinated proteins during muscle aging **(Fig. 2-11C and quantification Fig. 2-11D).** Moreover, neuronal upregulation of AMPK improved climbing ability during aging **(Fig. 2-11E).** Concordantly, the levels of *Atg1*, *Atg8a*, and *Atg8b*, were significantly increased in thoracic tissue from *ElavGS>UAS-mCh-AMPK* flies upon RU486 treatment **(Fig. 2-11F).** Control flies fed RU486 showed no changes in markers of muscle aging or ATG transcript levels of thoracic tissue **(Fig. 2-12).** In total, these findings indicate that neuron-specific AMPK activation can maintain protein homeostasis during muscle aging, which is associated with improved muscle function in aged flies.

Summary of findings and discussion

In this chapter, I have shown that neuron-specific overexpression of *Drosophila* AMPKα is sufficient to increase the abundance of endogenous AMPK subunits and increase overall kinase activity as marked by activating phosphorylation. I have also described that *Drosophila* AMPK overexpression is able to suppress TOR signaling and induce autophagy in neurons, while extending organismal lifespan. Furthermore, neuronal AMPK activation is sufficient to induce autophagy in distal tissues of the organism in a cell non-autonomous manner while slowing systemic tissue aging **(Graphical Summary Fig. 2-13)**. This work, coupled with others', strengthens the concept that stress responses and anti-aging interventions can be coordinated across multiple tissues [14].

While we observe transcriptionally increased Atg expression, exactly how AMPK is capable of upregulating transcription of autophagy genes is not known. Furthermore, it is yet

undetermined if neuronal AMPK-mediated life extension is dependent upon autophagy-gene expression. Likewise, are the cell non-autonomous delayed tissue aging effects of neuronal AMPK activation reliant upon increased autophagy induction? While neuronal AMPK is able to extend lifespan in the constant presence of food, the same intervention sensitizes flies to starvation. It may be possible that the autophagy pathways play a role in this starvation sensitivity. In the next chapter, I will test and discuss the requirement of autophagy induction in the context of AMPK-mediated cell non-autonomous signaling and lifespan extension.

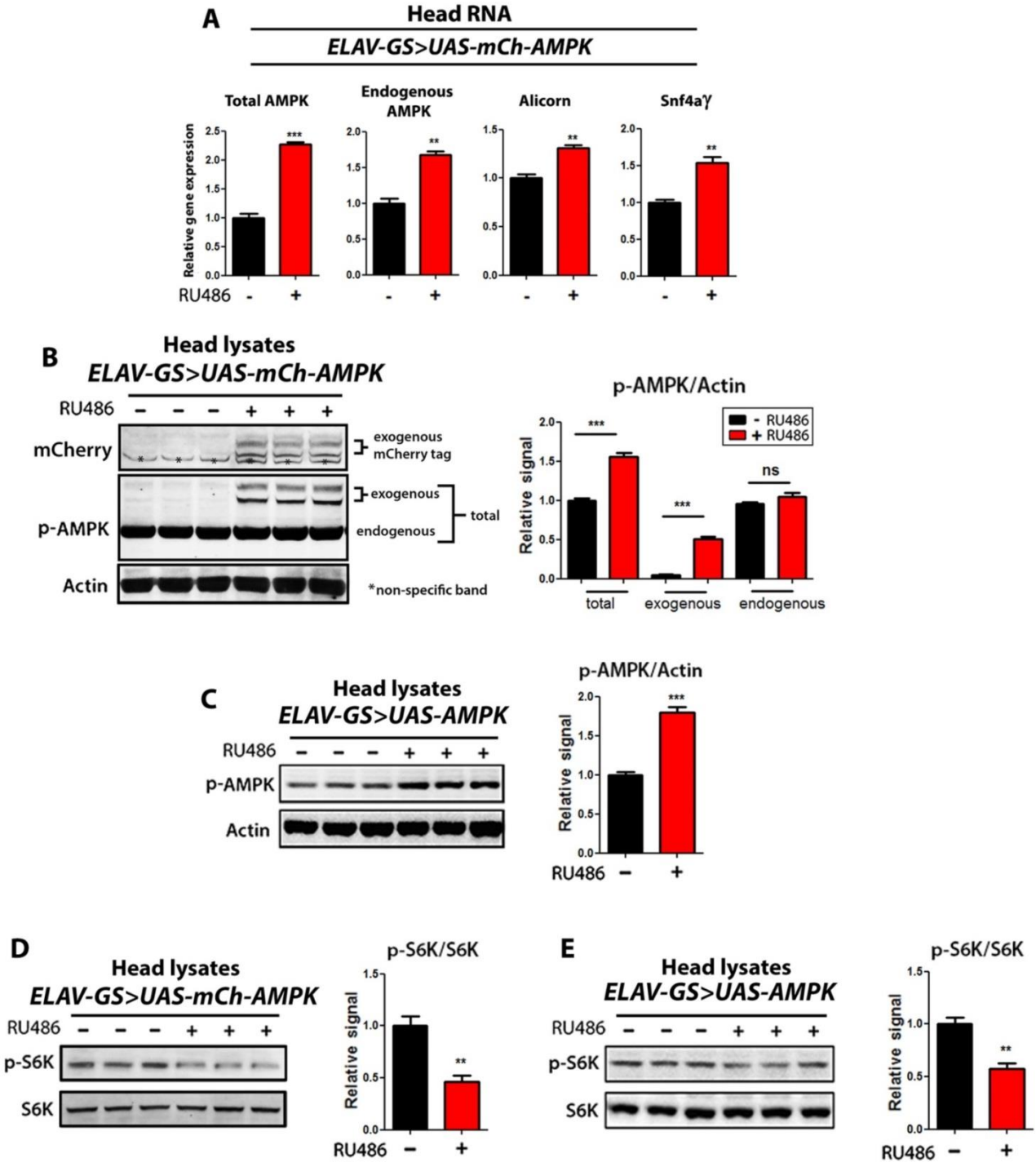

Figure2-1. Overexpression of AMPK in neuronal tissue, increased transcript levels of endoegenous AMPK subunits, increased the amount of active phosphorylated AMPK, and decreased S6K phosphorylation.

(A) Transcript levels of total AMPK and endogenous subunits, upon neuron-specific overexpression of AMPK. RNA was extracted from female flies at 10 days of age. Total levels of AMPK, endogenous AMPK, Alicorn, and Snf4aγ are significantly increased upon RU486 transgene induction (*$p<0.01$; t-test; n=3, of RNA extracted from 10 heads/replicate*).

(B) Western blot analysis of exogenous AMPK (mCherry tag), AMPK phosphorylated on T184 (p-AMPK), and loading control (actin) from head lysates of 10 day old female *ELAV-GS>UAS-mCH-AMPK* with or without RU486-mediated transgene induction. Densitometry quantification (right) shows that overexpression of exogenous mCherry-tagged AMPK is sufficiently phosphorylated to increase the total amount of phospho-AMPK present in head protein extracts (*p<0.001; t-test; n=3 replicates; 10 heads/replicate*).

(C) Western blot analysis of AMPK phosphorylated on T184 (p-AMPK) and loading control (actin) from head lysates of 10 day old female *ELAV-GS>UAS-AMPK* with or without RU486-mediated transgene induction. Validation that overexpression of AMPK increases the amount of active phosphorylated AMPK, using an additional UAS insertion line. Densitometry quantification (right) (*p<0.0001; t-test; n=3 replicates; 10 heads/replicate*).

(D) Western blot analysis of S6K phosphorylated at T398 and total S6K from head lysates of 10 day old *ELAV-GS>UAS*-mCh-*AMPK* females with or without RU486-mediated transgene induction. Overexpression of AMPK significantly reduced the amount of active, phosphorylated S6Kinase. Densitometry quantification (right) (*p<0.0098; t-test; n=3 replicates; 10 heads/replicate*).

(E) Western blot analysis of S6K phosphorylated at T398 and total S6K from head lysates of 10 day old *ELAV-GS>UAS -AMPK* females with or without RU486-mediated transgene induction. Validation that overexpression of AMPK decreased the amount of active S6Kinase, using an additional UAS insertion line. Densitometry quantification (right) (*p<0.0098; t-test; n=3 replicates; 10 heads/replicate*).

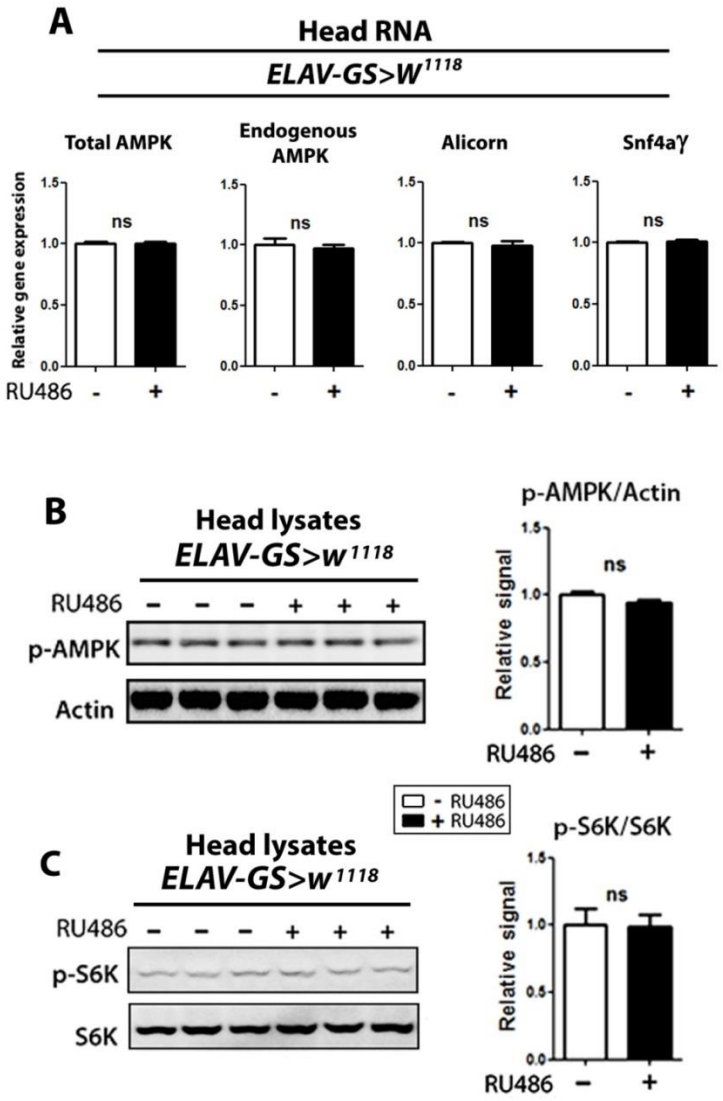

Figure 2-2. Feeding RU486 to control flies has no influence on AMPK transcript levels, AMPK phosphorylation, or S6K phosphorylation.

(A) Transcript levels of total AMPK and endogenous subunits upon RU486 feeding to control flies. RNA was extracted from female flies at 10 days of age. Total levels of AMPK, endogenous AMPK, Alicorn, and Snf4aγ are not effected by RU486 treatment of control strains (*p<0.01; t-test; n=3, of RNA extracted from 10 heads/replicate*).

(B) Western blot analysis of AMPK phosphorylated on T184 (p-AMPK) and loading control (actin) from head lysates of 10 day old *ELAV-GS>W^{1118}* female flies. Densitometry quantification (right) showed no significant increase in phosphorylation of AMPK upon RU486 feeding (*p>0.05*; *t-test; n=3 replicates; 10 heads/replicate*).

(C) Western blot analysis of S6K phosphorylated at T398 and total S6K from head lysates from *ELAV-GS>W^{1118}* female flies at 10 days of adulthood. Densitometry (right) showed no significant change in S6K phosphorylation upon RU486 feeding (*p>0.05*; *t-test; n=3 replicates; 10 heads/replicate*).

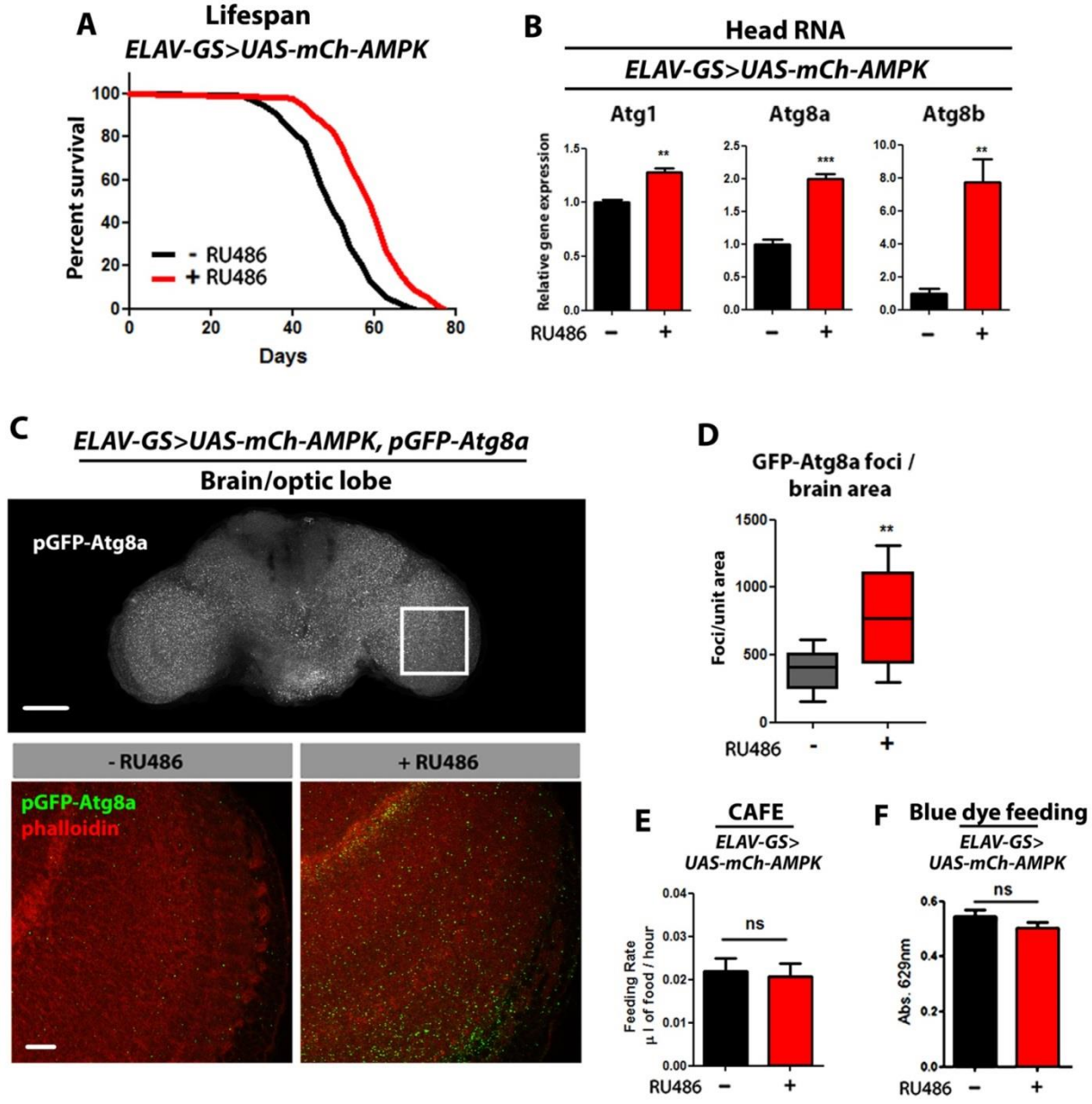

Figure 2-3. Neuronal overexpression of AMPK extends organismal lifespan and induces autophagy in brain tissue.

(A) Survival curves of *ELAV-GS>UAS*-mCh-*AMPK* females with or without RU486-mediated transgene induction. Neuron-specific overexpression of AMPK increased median lifespan by 18% (*p<0.0001; log-rank test; n>247 flies*).

(B) Expression of autophagy genes in head tissue of *ELAV-GS>UAS-mCH-AMPK* female flies at 10 days of adulthood. Upon AMPK induction, significantly increased Atg1, Atg8a, and Atg8b RNA levels are observed (*t-test; n=3 of RNA extracted from 10 heads/replicate*).

(C) GFP-Atg8a localization in adult brain with 10X objective (above) and representative images (below) from optic lobes of 10 day old female *ELAV-GS>UAS-mCh-AMPK, pGFP-Atg8a* flies with or without RU486-mediated transgene induction (*red channel-phalloidin, green channel-GFP-Atg8a, upper scale bar represents 50μm, lower scale bar represents 10μm*).

(D) Quantification of optic lobe pAtg8a foci reveals that overexpression of AMPK in neuronal tissue significantly increases GFP-Atg8a puncta at 10 days of adulthood (*p<0.004; t-test; n>10 confocal stacks from optic lobes/condition; one brain/replicate stack*).

(E) Capillary feeding assay (CAFE) of 10 day old *ELAV-GS>UAS-mCh-AMPK*, flies with or without RU486 induction. Neuronal AMPK overexpression had no effect on the feeding rate of female flies *(p>0.05*; *t-test, n>7 vials of 10 flies/condition*).

(F) Blue dye feeding assay of 10 day old *ELAV-GS>UAS-mCH-AMPK* with or without RU486 induction. Neuronal AMPK overexpression had no effect on the amount of blue food consumed by 10 day old female flies (*p>0.05*; *t-test; n>37 flies/condition*).

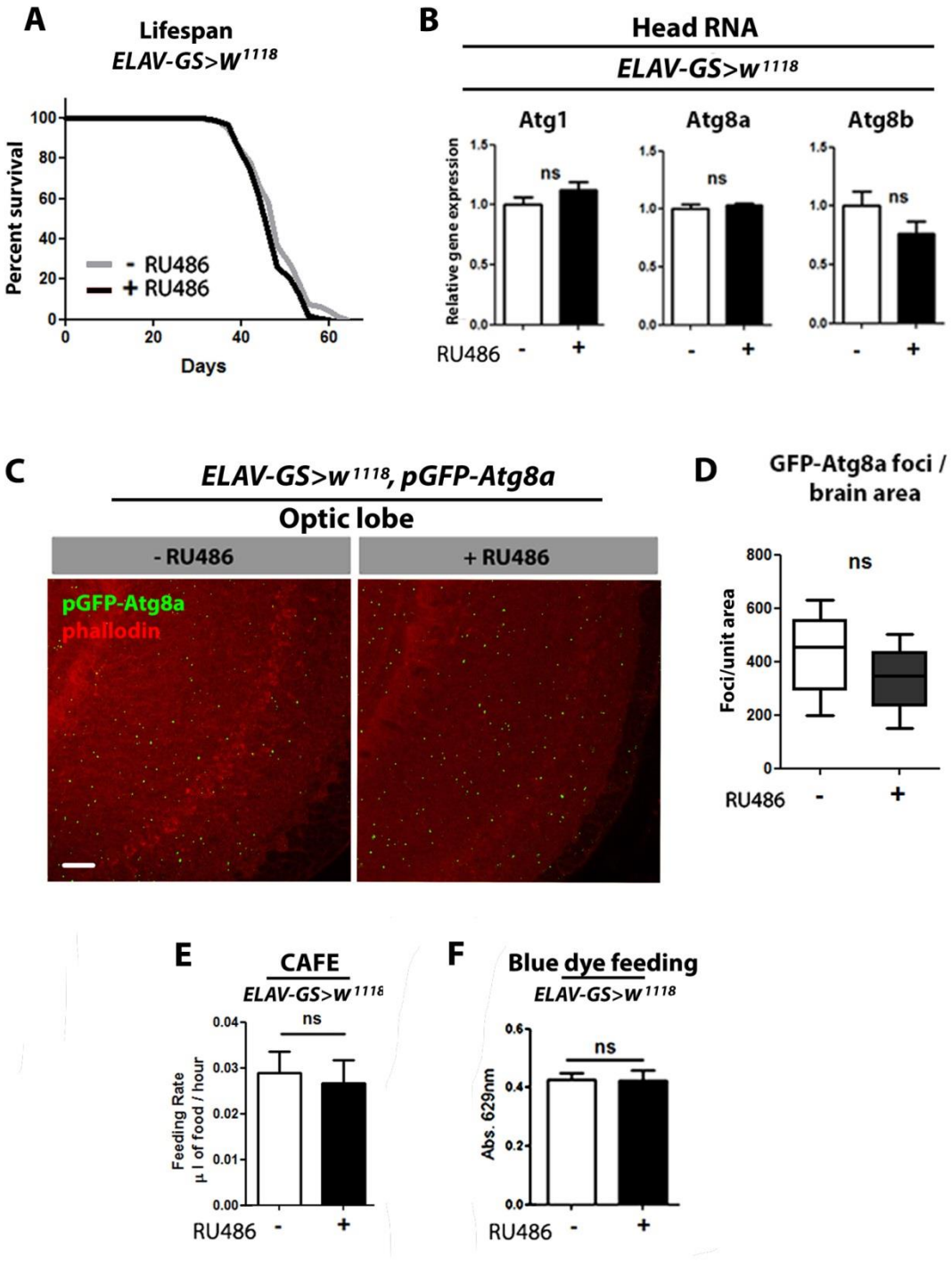

Figure 2-4. Feeding RU486 to control flies has no influence on lifespan, autophagy markers, and feeding behavior.

(A) Survival curves of *ELAV-GS>W^{1118}* females with or without RU486 treatment. No significant effect on lifespan was observed (*p>0.05; log-rank test; n>100 flies/condition*).

(B) Expression of autophagy genes in head tissue of *ELAV-GS>W^{1118}* female control flies at 10 days of adulthood. RU486 feeding had no significant effect on Atg1, Atg8a, and Atg8b RNA levels (*p>0.05*; *t-test; n=3 of RNA extracted from 10 heads/replicate*).

(C) Brain GFP-atg8a staining. Representative images from optic lobes of 10 day old female *ELAV-GS>W^{1118}*, *pGFP-Atg8a* flies (*red channel-phalloidin, green channel-GFP-Atg8a, scale bar represents 10μm*).

(F) Quantification of brain Atg8a foci in *ELAV-GS>W^{1118}*, *pGFP-Atg8a* control flies. RU486 feeding had no influence on the number of GFP-Atg8a foci (*p>0.05*; *t-test; n>10 confocal stacks from brains/condition, one brain per replicate stack*).

(G) Capillary feeding assay (CAFE) of 10 day old *ELAV-GS>W^{1118}* flies. RU486 treatment had no effect on feeding rate of control flies *(p>0.05*; *t-test, n>7 vials of 10 flies/condition*).

(H) Blue dye feeding assay of 10 day old *ELAV-GS>W^{1118}* control flies. RU486 treatment had no effect on the amount of blue dye consumed by control flies (*p>0.05*; *t-test; n>37 flies/condition*).

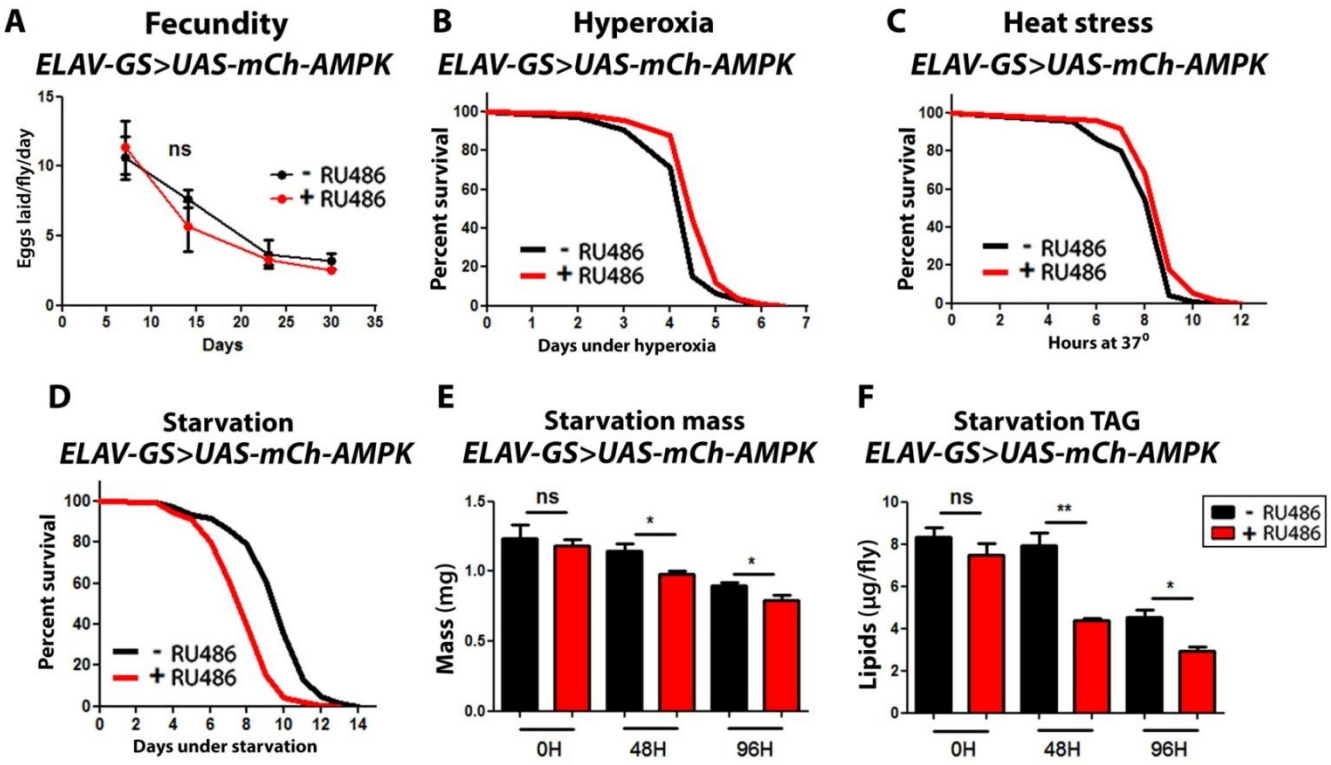

Figure 2-5. Upregulation of AMPK in the nervous systems renders flies more resistant to oxidative stress, heat stress, and sensitizes flies to starvation by rapid depletion of mass and energy stores.

(A) Fecundity timecourse of *ELAV-GS>UAS-mCH-AMPK* flies. Induction of AMPK in the nervous system had no effect on the number of eggs laid over the lifespan of the organisms (*p>0.05*; *t-test; n>7 vials of 10 flies/condition*).

(B) Hyperoxia survival curves of 10 day old female *ELAV-GS>UAS-mCh-AMPK* flies. Neuronal upregulation of AMPK moderately increased survival under 80% atmospheric oxygen (*p<0.0001; log-rank; n>173 flies/condition*).

(C) Heat stress survival curves of 10 day old female *ELAV-GS>UAS-mCh-AMPK* flies. Neuronal upregulation of AMPK moderately increased survival at 37° C. (*p<0.0001; log-rank; n>136 flies/condition*).

(D) Wet starvation survival curves of female *ELAV-GS>UAS-mCh-AMPK* flies with or without RU486-mediated transgene induction. AMPK overexpression in neurons caused early mortality when deprived of nutrition (*p<0.0001; log-rank; n>122 flies/condition*).

(E) Body mass during starvation of *ELAV-GS>UAS-mCh-AMPK* females with or without RU486-mediated transgene induction. AMPK overexpression in neurons caused rapid mass depletion upon starvation, compared to uninduced flies (*p<0.05, at 48hours and 96 hours of starvation; t-test; n>6 samples/condition; 10 flies weighed/sample).*

(F) Whole body lipid stores during starvation of *ELAV-GS>UAS-mCh-AMPK* females with or without RU486-mediated transgene induction. Neuronal AMPK induction caused rapid lipid depletion upon

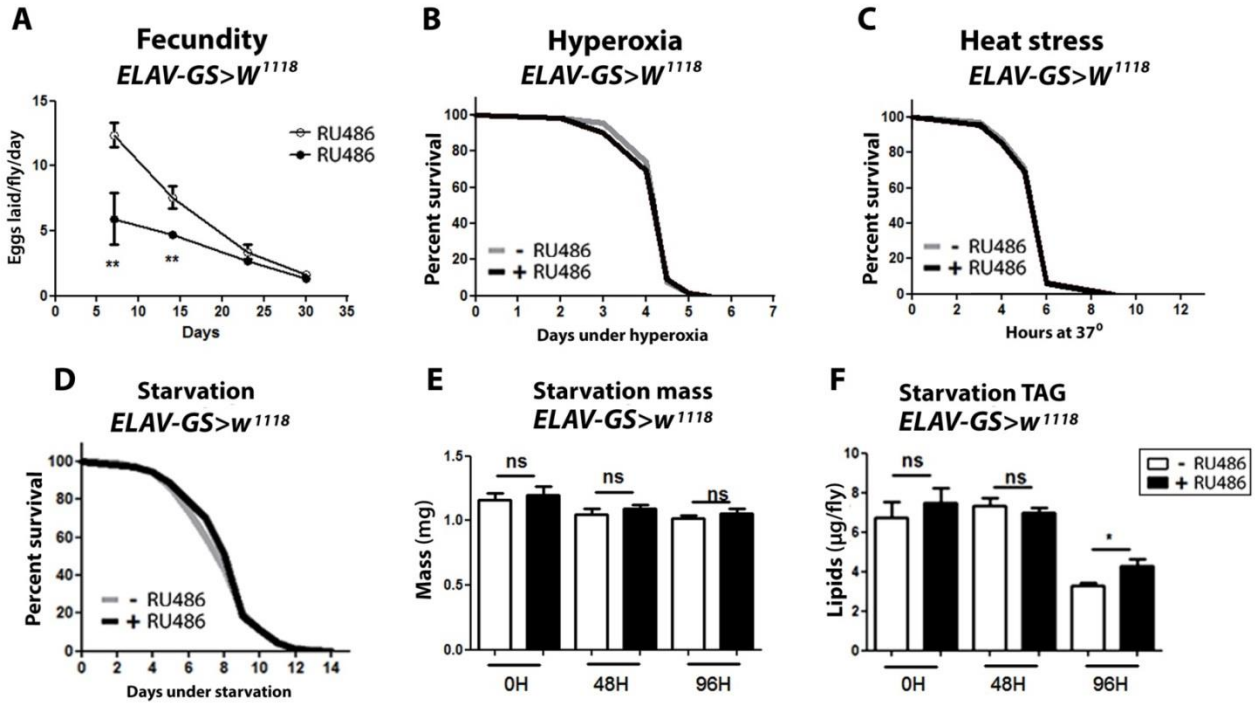

starvation (*p<0.01 at 48 hours, and p<0.05 at 96 hours of starvation; t-test; n>3 samples/condition/timepoint; lipids extracted from 5 flies per sample).*

Figure 2-6. Feeding RU486 to control flies has minimal impact on fecundity, starvation, and no impact on hyperoxia and heat-stress resistance.

(A) Fecundity timecourse of control *ELAV-GS>W^{1118}* flies. RU486 feeding significantly reduced the number of eggs laid at early timepoints (*p<0.01*; *t-test; n>7 vials of 10 flies/condition*).

(B) Starvation survival curves of *ELAV-GS>W^{1118}* controls. Female control flies fed RU486 for 10 days had no significant effect on starvation lifespan (*p>0.05*; *log-rank; n>203 flies*).

(C) Body mass during starvation of *ELAV-GS>W^{1118}* controls. RU486 feeding had no significant influence over mass of control flies (*p>0.05*; *t-test; n>6 samples/condition from 10 flies weighed/sample*)

(D) Whole body lipid stores during starvation of *ELAV-GS>W^{1118}* controls. RU486 feeding of control flies moderately increased the amount of lipids at 96 hours of starvation compared to ethanol-fed flies (*p<0.05; t-test; n>3 samples /condition; lipids extracted from 5 flies/sample*).

(E) Hyperoxia survival curves of 10-day-old female *ELAV-GS>W^{1118}* controls. RU486 feeding had no effect on survival under 80% atmospheric oxygen (*p>0.05; log-rank; n>130 flies/condition*).

(F) Heat stress survival curves of 10-day-old female *ELAV-GS>W^{1118}* controls. RU486 feeding had no effect on survival at 37° C. (*p>0.05; log-rank; n>133 flies/condition*).

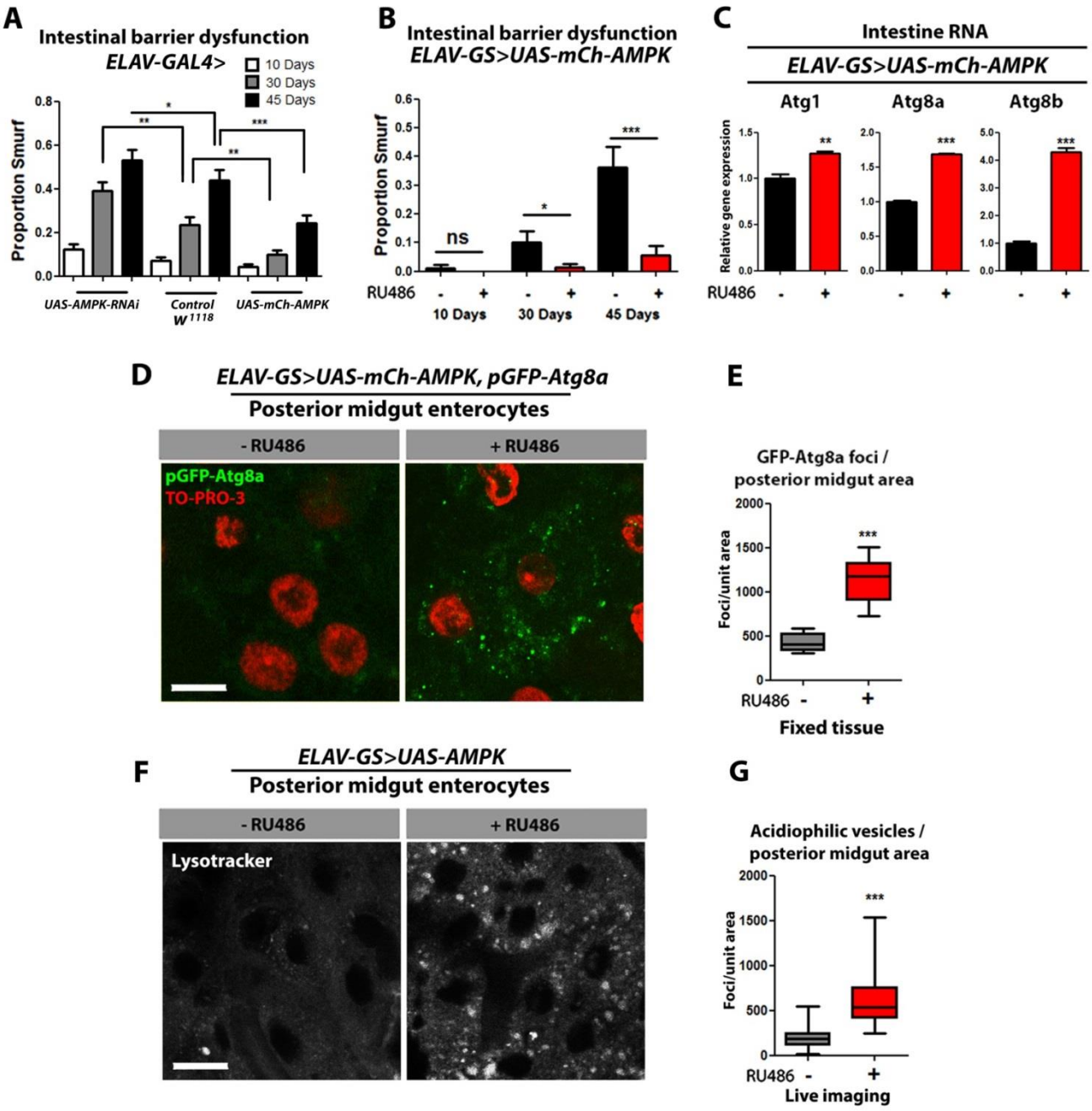

Figure 2-7. Neuronal AMPK activation maintains intestinal integrity during aging, and causes a cell non-autonomous induction of autophagy.

(A) Intestinal integrity during aging with constitutive neuronal expression of *AMPK-RNAi, mCH-AMPK,* and W^{1118} controls. *ELAV-GAL4>AMPK-RNAi* had significantly increased numbers of smurf flies at 30 and 45 days adulthood compared to *ELAV-GAL4>* W^{1118} controls. Flies constitutively overexpressing mCh-AMPK showed reduced numbers of smurfs compared to *ELAV-GAL4>* W^{1118} controls (*binomial test; n>96 flies/condition*).

(B) Intestinal integrity during aging in *ELAV-GS>UAS-mCH-AMPK* females with or without RU486-mediated transgene induction. Inducible upregulation of AMPK in neurons significantly decreases the proportion of flies exhibiting intestinal barrier dysfunction at old age timepoints (*$p<0.05$; binomial test, at 30 days of age, and $p<0.01$ at 45 days; n>60 flies/condition*).

(C) Intestinal expression of autophagy genes in *ELAV-GS>UAS-mCH-AMPK* females at 10 days of adulthood. Neuronal upregulation of AMPK increases autophagy gene expression in the intestine (*$p<0.01$ for Atg1, $p<0.001$ for Atg8a and Atg8b; t-test; n=3 of RNA extracted from 15 intestines/replicate*).

(D) GFP-Atg8a staining. Representative images of enterocytes from the posterior midgut of 10- day old *ELAV-GS>UAS-mCh-AMPK, pGFP-Atg8a* females with or without RU486-mediated transgene induction in neurons (*red channel-TO-PRO-3 DNA stain, green channel-GFP-Atg8a, scale bar represents 10μm*).

(E) Quantification of posterior midgut pGFP-Atg8a foci. Neuronal upregulation of AMPK increased the number of GFP-Atg8a puncta compared to uninduced controls (*$p<0.0001$; t-test; n>10 confocal stacks from posterior midgut/condition; one fly per replicate stack*).

(E) Lysotracker Red staining. Representative images of posterior midgut enterocytes from 10 day old *ELAV-GS>UAS-AMPK* females with or without RU486-mediated transgene induction (*scale bars represent 10μm*).

(F) Quantification of acidophilic vesicles. Neuronal upregulation of AMPK increased the number of acidophilic vesicles in the intestine compared to uninduced controls (*$p<0.0001$; t-test; n>19 confocal stacks from posterior midgut/condition; one fly per replicate stack*).

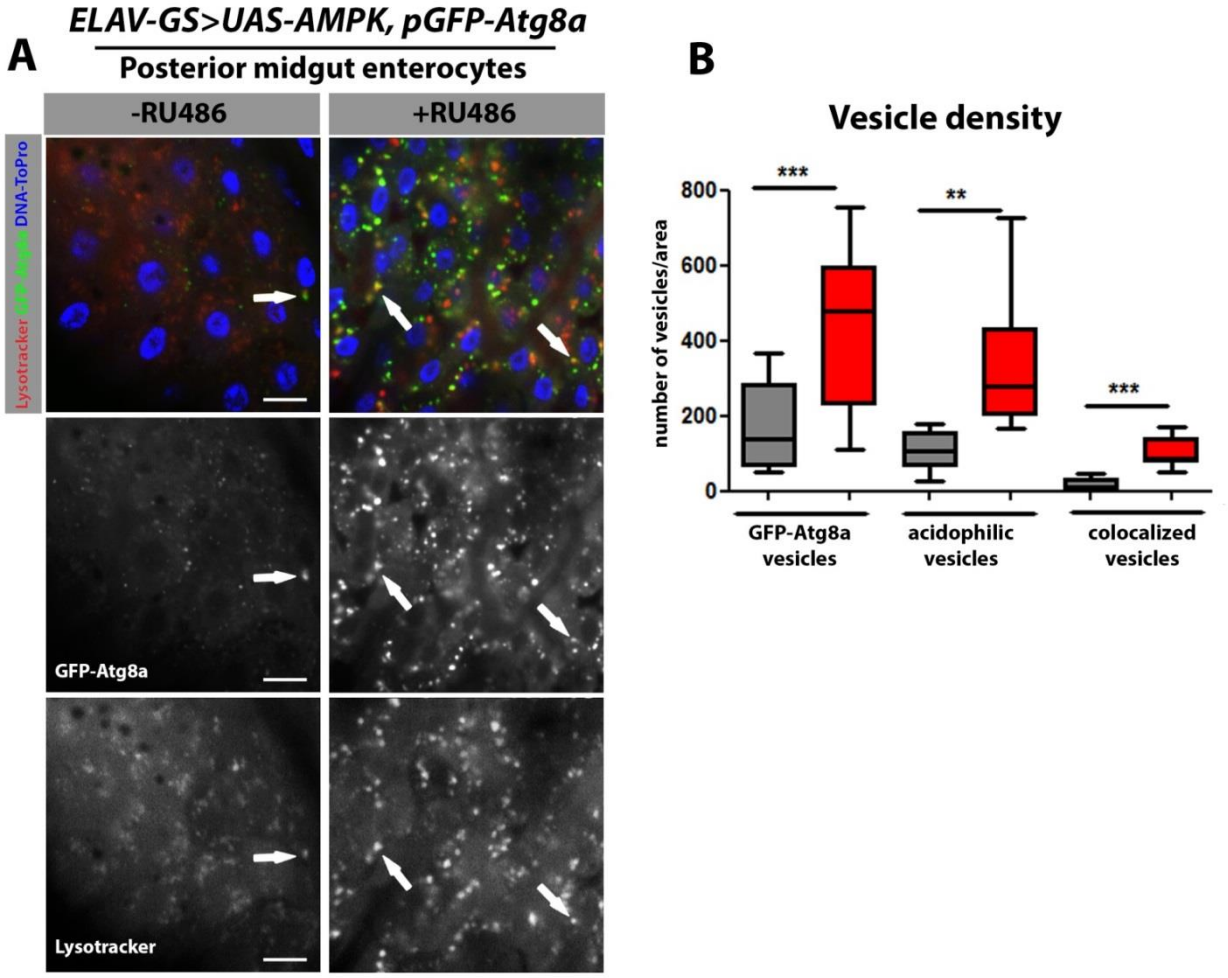

Figure 2-8. Neuronal AMPK activation causes a cell-non autonomous induction of autophagy when monitored via live imaging of dissected intestinal enterocytes.

(A) Representative images of enterocytes from the posterior midgut of 10 day old *ELAV-GS>UAS-mCh-AMPK, pGFP-Atg8a* females with or without RU486-mediated transgene induction in neurons (*red channel-Lysotracker Red, blue channel-ToPro-3 DNA stain, green channel-GFP-Atg8a, scale bar represents 10μm, arrows indicate colocalized autolysosomes*).

(B) Quantification of acidophilic vesicles, GFP-atg8a vesicles, and colocalized "autolysosomal" vesicles/midgut area. Induction of AMPK in neuronal tissue increased density of GFP-atg8a vesicles, acidophilic vesicles, and colocalized vesicles compared to uninduced controls (*$p<0.01$; t-test; $n>10$ guts/condition*).

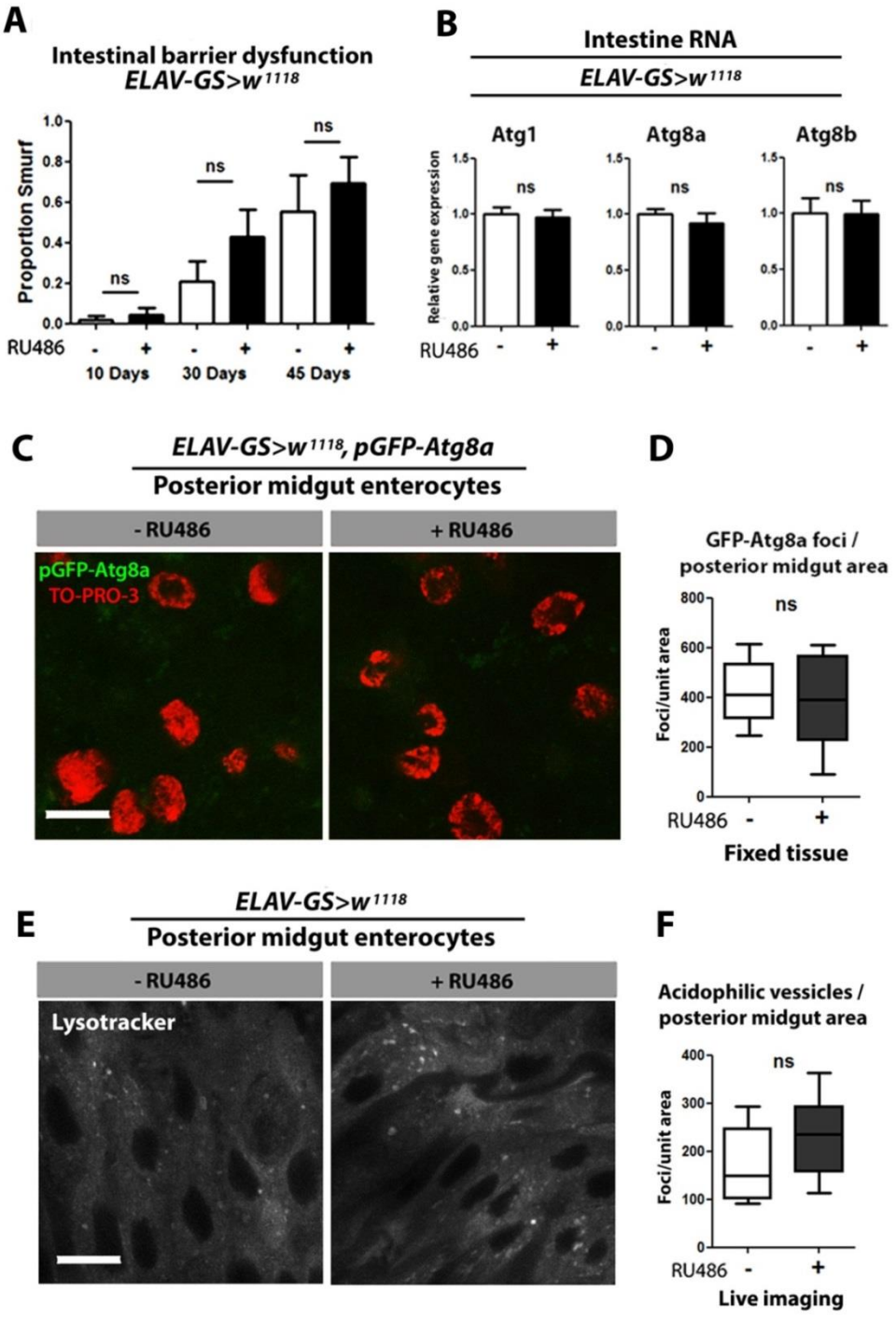

Figure 2-9. Feeding RU486 to control flies does not influence intestinal barrier dysfunction, or markers of autophagy.

(A) Intestinal integrity during aging in *ELAV-GS>W*^{1118} controls. RU486 has no effect on the proportion of flies exhibiting intestinal barrier dysfunction. (*p>0.05*; *binomial test; n>40 flies/condition*)

(B) Expression of autophagy genes in the intestines of female *ELAV-GS>W^{1118}* control flies at 10 days of adulthood. RU486 feeding had no significant effect on Atg1, Atg8a, and Atg8b RNA levels (*p>0.05*; *t-test; n=3 of RNA extracted from 15 intestines/replicate*).

(C) GFP-Atg8a staining. Representative images of enterocytes from the posterior midgut of 10 day old female *ELAV-GS>W^{1118}, pGFP-Atg8a* flies fed RU486 and vehicle (*red channel-TO-PRO-3 DNA stain, green channel-GFP-Atg8a, scale bar represents 10μm*).

(D) Quantification of posterior midgut Atg8a foci. Control flies fed RU486 showed no difference in foci number (*p>0.05*; *t-test; n>10 confocal stacks from posterior midgut/condition, one fly per replicate stack*).

(E) Lysotracker Red staining. Representative images of posterior midgut enterocytes from 10 day old female *ELAV-GS>W^{1118}* flies stained with the acidophilic dye.

(F) Quantification of acidophilic vesicles. Feeding control flies RU486 had no effect on the number of acidophilic vesicles (*t-test*; *n>9 confocal stacks from posterior midgut/condition, one fly per replicate stack*).

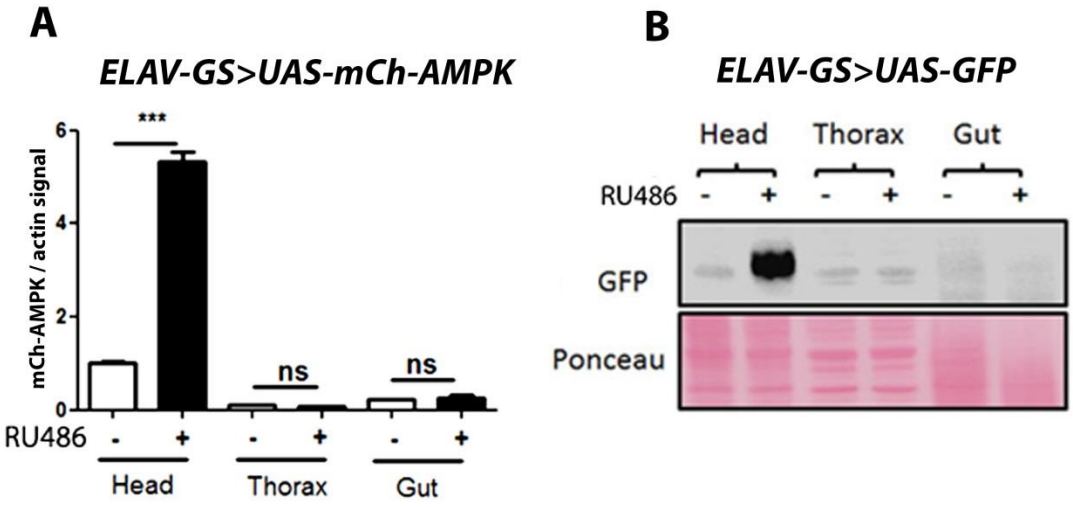

Figure 2-10. Expression specificity for ELAV-GS driver.

(A) Exogenous mCherry-tagged AMPK expression levels of RNA extracted from body parts of *ELAV-GS>UAS-mCH-AMPK* female flies at 10 days of age. Statistically significant increase in exogenous mCherry-AMPK is only detectable in the head tissue of RU486-fed flies compared to uninduced controls. (*p<0.001; t-test; n=3 of RNA extracted from 10 body parts/replicate*)

(B) Western blot analysis for GFP and membrane stain for loading control (Poncea S.) of protein extracted from body parts of *ELAV-GS>UAS-eGFP* flies at 10 days of age. An RU486-dependent increase of GFP-signal was only observed in the head tissue flies.

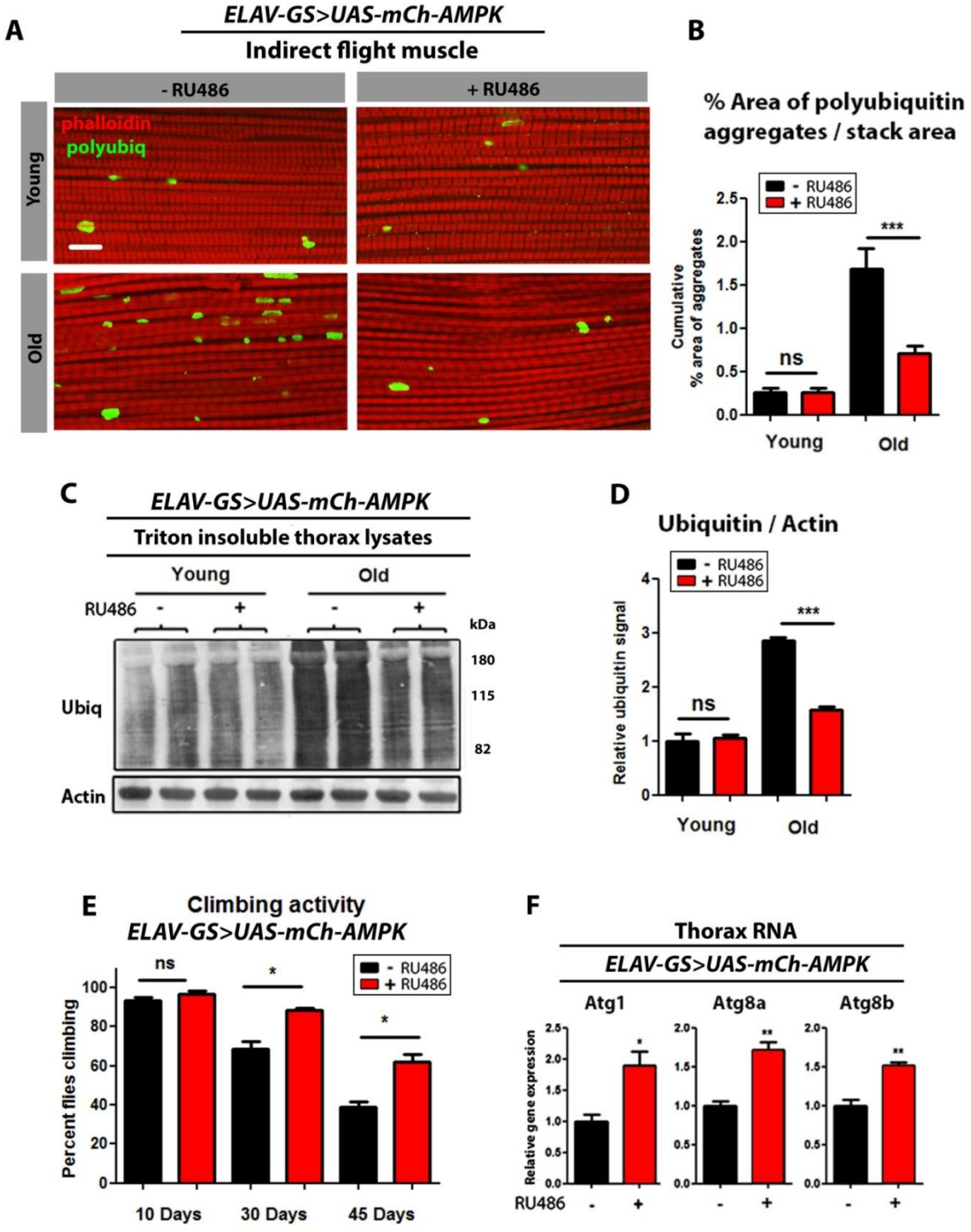

Figure 2-11. Neuronal AMPK activation maintains muscle proteostasis during aging.

(A) Confocal images of indirect flight muscle in *ELAV-GS>UAS-mCH-AMPK* females with or without RU486-mediated transgene induction, showing protein polyubiquitinated aggregates at young (10 days),

and old (30 days) timepoints (*red channel-phalloidin/F-actin, green channel- anti-polyubiquitin, scale bar represents 10μm*).

(B) Quantification of polyubiquitin aggregates in muscle. Neuronal AMPK activation decreased the accumulation of polyubiquitinated proteins during aging compared to uninduced controls (*p<0.001; t-test; n>10; one fly/replicate stack*).

(C) Western blot detection of total ubiquitin-conjugated proteins from thorax detergent-insoluble extracts of young (10 days) and aged (30 days) *ELAV-GS>UAS-mCH-AMPK* females with or without RU486-mediated transgene induction.

(D) Densitometry of ubiquitin blots from thoraces of *ELAV-GS>UAS-mCH-AMPK* flies. AMPK activation in neurons decreased the amount of insoluble ubiquitinated proteins at 30 days of age compared to uninduced controls (*p<0.001; t-test; n=4 samples/condition; 10 thoraces/sample).*

(E) Climbing activity of *ELAV-GS>UAS-mCH-AMPK* females with or without RU486-mediated transgene induction. Upregulation of AMPK in neurons allows flies to maintain active climbing ability with age compared to uninduced controls (*p<0.05*; *t-test; n>6 vials/condition; 30 flies/vial).*

(F) Expression of autophagy genes in dissected thoraces of female *ELAV-GS>UAS-mCH-AMPK* flies at 10 days of adulthood. AMPK induction in the nervous system significantly increased Atg1, Atg8a, and Atg8b gene expression levels(*t-test; n>3 of RNA extracted from 10 thoraces/replicate*).

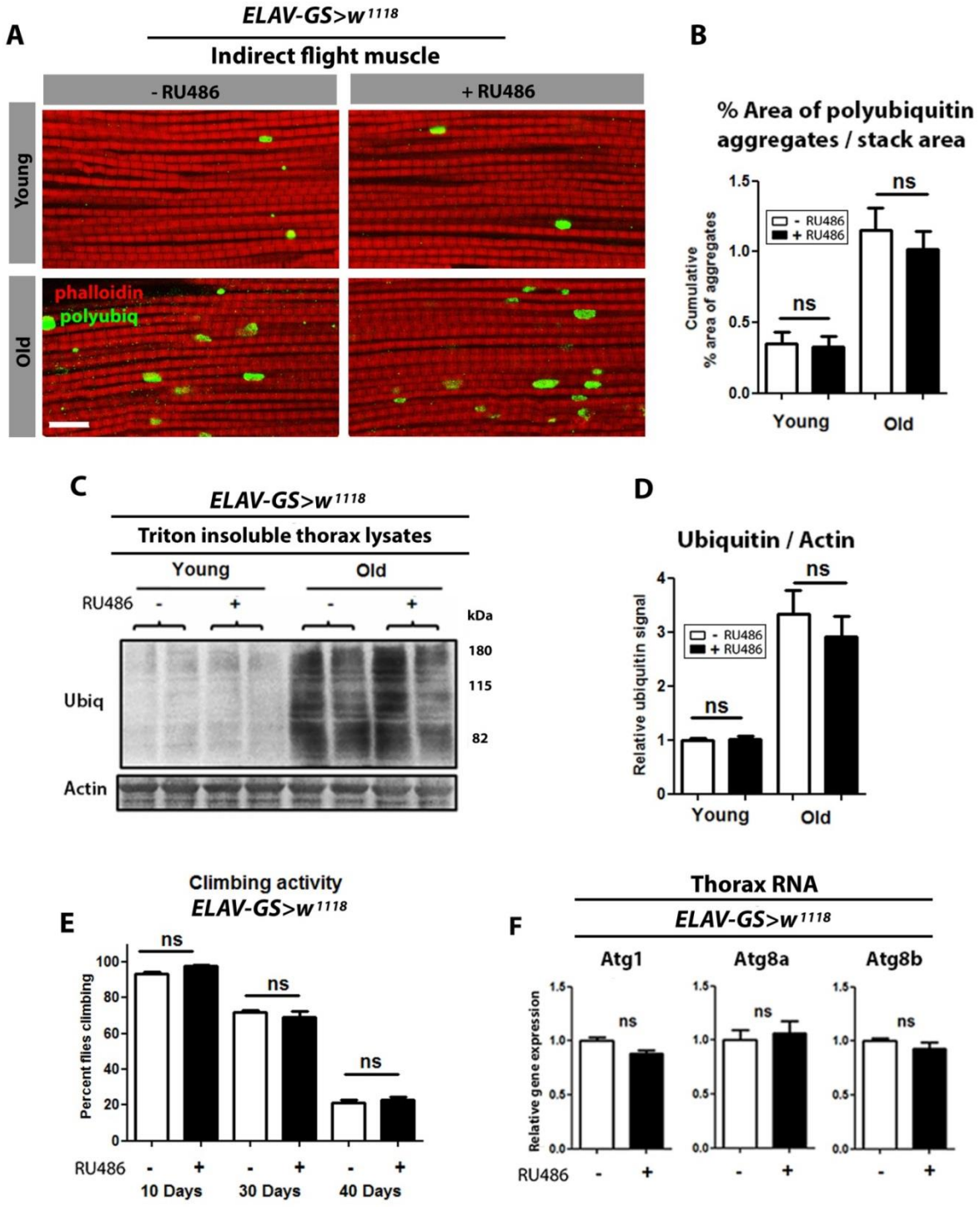

Figure 2-12 . RU486 feeding has no effect on muscle proteostasis in control flies.

(A) Confocal imaging of adult female *ELAV-GS>W*^{1118} flight muscle showing protein polyubiquitinated aggregates at young (10 days), and old (30 days) timepoints (*red channel-phalloidin/F-actin, green channel- anti-polyubiquitin, scale bar represents 10μm*).

(B) Quantification of polyubiquitin aggregates in the muscle of *ELAV-GS>W^{1118}* flies. Feeding control flies RU486 had no effect on protein aggregate accumulation with age (*p>0.05*; *t-test, n>10, one fly / replicate stack*).

(C) Western blot detection of total ubiquitin-conjugated proteins from thorax detergent-insoluble extracts of young (10 days) and aged (30 days) *ELAV-GS>W^{1118}* female flies.

(D) Densitometry of ubiquitin blots from thoraces of flies. RU486 feeding had no effect on amount of thoracic detergent-insoluble ubiquitin-conjugated proteins, normalized to actin, in aged flies (*p>0.05*; *t-test; n=4 samples/condition; 10 thoraces/sample).*

(E) Climbing activity of *ELAV-GS>W^{1118}* controls. Female control flies fed RU486 for 10 days had no significant effect on climbing activity with age (*p>0.05*; *t-test; n=6 vials/condition; 30 flies/vial).*

(F) Expression of autophagy genes in dissected thoraces of female *ELAV-GS>W^{1118}* control flies at 10 days of adulthood. RU486 feeding showed no significant changes in Atg1, Atg8a, and Atg8b gene expression levels (*p>0.05*; *t-test; n=3 of RNA extracted from 10 thoraces /replicate*)

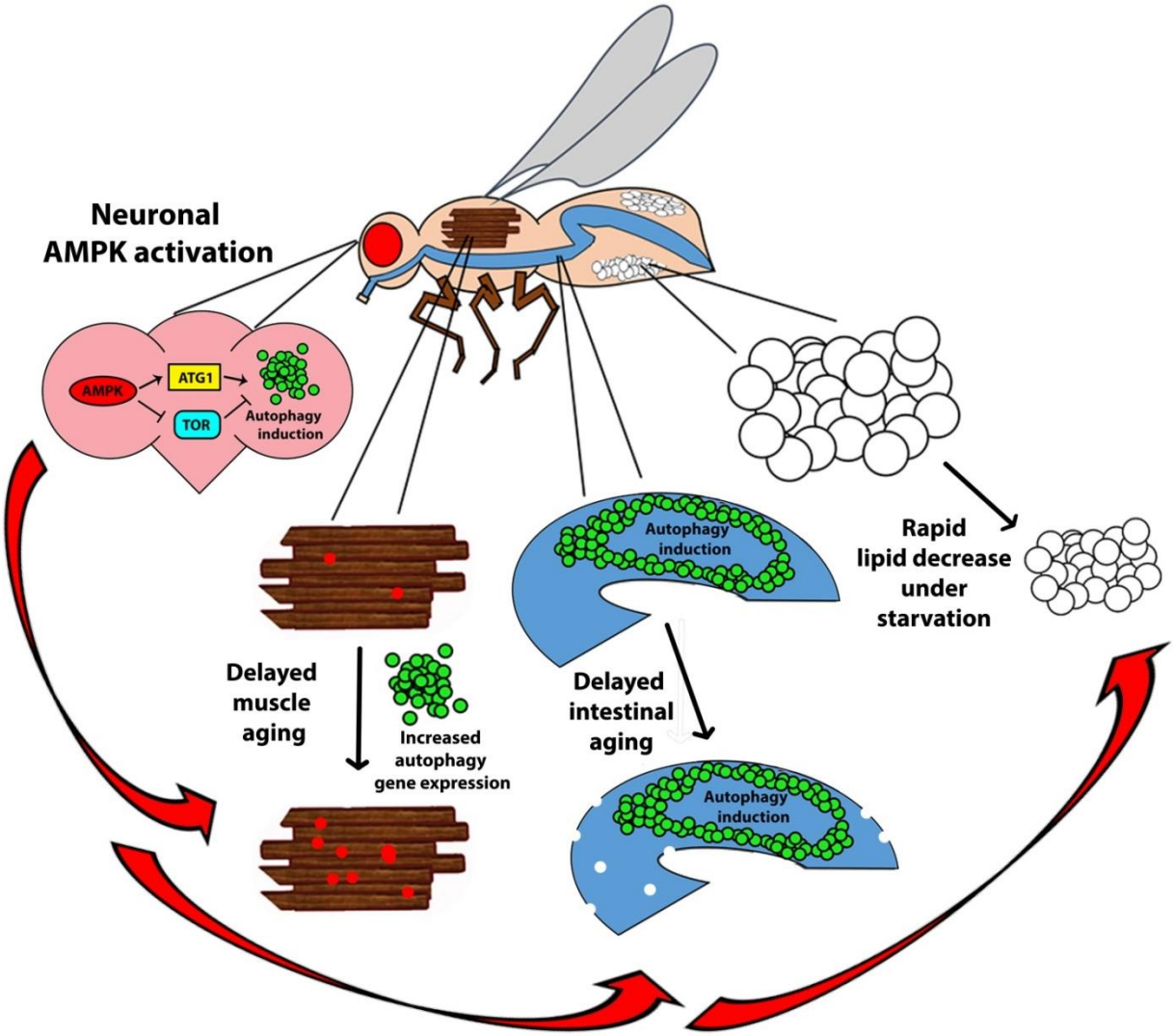

Figure 2-13 . Summary of neuronal AMPK upregulation in aging and physiology.

AMPK overexpression in the brain/nervous system causes a cell non-autonomous upregulation in markers of autophagy in the thorax and intestine, with a concordant delay in muscle aging and intestinal barrier dysfunction. Upregulation of AMPK in the nervous system also causes a striking increase in starvation sensitivity, with rapid decrease in body mass and lipid stores compared to uninduced controls.

REFERENCES:

1. Poirier, L., Shane, A., Zheng, J., & Seroude, L. (2008). Characterization of the Drosophila gene-switch system in aging studies: a cautionary tale. *Aging Cell*, *7*(5), 758–70. doi:10.1111/j.1474-9726.2008.00421.x

2. Roman, G., Endo, K., Zong, L., & Davis, R. L. (2001). P[Switch], a system for spatial and temporal control of gene expression in Drosophila melanogaster. *Proceedings of the National Academy of Sciences of the United States of America*, *98*(22), 12602–7. doi:10.1073/pnas.221303998

3. Rubinsztein, D. C., Mariño, G., & Kroemer, G. (2011). Autophagy and aging. *Cell*, *146*(5), 682–95. doi:10.1016/j.cell.2011.07.030

4. Klionsky, D.J., Abdalla, F.C., Abeliovich, H., Abraham, R.T., Acevedo-Arozena, A., Adeli, K., Agholme, L., Agnello, M., Agostinis, P., Aguirre-Ghiso, J.A., et al. (2012). Guidelines for the use and interpretation of assays for monitoring autophagy. *Autophagy* 8, 445-544.

5. Lapierre, L.R., De Magalhaes Filho, C.D., McQuary, P.R., Chu, C.C., Visvikis, O., Chang, J.T., Gelino, S., Ong, B., Davis, A.E., Irazoqui, J.E., et al. (2013). The TFEB orthologue HLH-30 regulates autophagy and modulates longevity in Caenorhabditis elegans. *Nature communications* 4, 2267.

6. Denton, D., Shravage, B., Simin, R., Mills, K., Berry, D. L., Baehrecke, E. H., & Kumar, S. (2009). Autophagy, not apoptosis, is essential for midgut cell death in Drosophila. *Current Biology : CB*, *19*(20), 1741–6. doi:10.1016/j.cub.2009.08.042

7. Ja, W.W., Carvalho, G.B., Mak, E.M., de la Rosa, N.N., Fang, A.Y., Liong, J.C., Brummel, T., and Benzer, S. (2007). Prandiology of Drosophila and the CAFE assay. *Proceedings of the National Academy of Sciences of the United States of America* 104, 8253-8256.

8. Wong, R., Piper, M.D., Wertheim, B., and Partridge, L. (2009). Quantification of food intake in Drosophila. *PloS one* 4, e6063.

9. Hardie, D. G., Ross, F. a, & Hawley, S. a. (2012). AMPK: a nutrient and energy sensor that maintains energy homeostasis. *Nature Reviews. Molecular Cell Biology*, *13*(4), 251–62. doi:10.1038/nrm3311

10. Rera, M., Bahadorani, S., Cho, J., Koehler, C. L., Ulgherait, M., Hur, J. H., … Walker, D. W. (2011). Modulation of longevity and tissue homeostasis by the drosophila PGC-1 homolog. *Cell Metabolism*, *14*(5), 623–634.

11. Hur, J. H., Bahadorani, S., Graniel, J., Koehler, C. L., Ulgherait, M., Rera, M., … Walker, D. W. (2013). Increased longevity mediated by yeast NDI1 expression in Drosophila intestinal stem and progenitor cells. *Aging*, *5*(9), 662–81.

12. Rera, M., Clark, R. I., & Walker, D. W. (2012). Intestinal barrier dysfunction links metabolic and inflammatory markers of aging to death in Drosophila. *Proceedings of the National Academy of Sciences of the United States of America*, *109*(52), 21528–33. doi:10.1073/pnas.1215849110

13. Shen, J., Curtis, C., Tavare, S., and Tower, J. (2009). A screen of apoptosis and senescence regulatory genes for life span effects when over-expressed in Drosophila. *Aging* 1, 191-211.

14. Taylor, R.C., Berendzen, K.M., and Dillin, A. (2014). Systemic stress signalling: understanding the cell non-autonomous control of proteostasis. *Nature reviews. Molecular cell biology* 15, 211-217.

CHAPTER III:

AMPK-MEDIATED LIFESPAN EXTENSION IS DEPENDENT UPON ATG1 EXPRESSION

On determining the requirement and sufficiency of Atg1 in AMPK-mediated longevity

In the previous chapter we showed AMPK-mediated induction of autophagy in the adult nervous system is associated with increased lifespan, delayed muscle aging, improved intestinal homeostasis during aging, and increased sensitivity to starvation. To seek evidence for a causal role of autophagy in mediating these effects, we set out to directly manipulate Atg1, a Ser/Thr protein kinase involved in the initiation of autophagosome formation [1, 2]. To test for Atg1 requirement in AMPK-mediated longevity, we can simultaneously overexpress AMPK, and knockdown Atg1, to determine subsequent effects on lifespan, markers of aging, and stress resistance. As a control, we will knockdown Atg1 alone, and determine the influence of reduced Atg1 expression on lifespan and markers of aging. Lastly, we can assess if Atg1 is mediating these lifespan effects by overexpressing Atg1 in neurons alone. All lines will be backcrossed into the W^{1118}/cyo genetic background to ensure baseline homogeneity of effect on lifespan. Summary of epistasis paradigm can be found in **(Fig. 3-1).**

Atg1 is required for neuronal AMPK-mediated lifespan extension/delayed markers of aging, and Atg1 overexpression alone is sufficient to extend longevity

First, we set out to confirm that simultaneous transgenic AMPK overexpression and Atg1 knockdown was sufficient to alter both AMPK and Atg1 transcript levels. As we have seen previously, induced *ElavGS>UAS-mCh-AMPK* flies increased Atg1 transcript levels a moderate 23% in head tissue compared to uninduced controls **(Fig. 3-2 A-left)**. Next, we confirmed that simultaneous induction of AMPK overexpression and Atg1 knockdown *(ElavGS>UAS-mCh-AMPK, UAS-Atg1-RNAi)* was sufficient to reduce Atg1 transcript levels compared to uninduced controls **(Fig. 3-2 A- middle)**. As an added control, Atg1-RNAi alone was adequate to reduce Atg1 levels **(Fig 3-2A-right)**. Moreover, we wanted to rule out that manipulation of Atg1 did

not alter AMPK levels in our transgenic *mCh-AMPK* line. As seen before, *ElavGS >UAS-mCh-AMPK* flies were able to increase total AMPK levels by about 2 fold on RU486 induction **(Fig. 3-2 B – left)**. Simultaneous AMPK overexpression and Atg1 knockdown flies still had sufficiently increased levels of AMPK **(Fig. 3-2 B – middle)**. Atg1 knockdown in neurons alone did not alter AMPK levels **(Fig. 3-2B – right).**

After establishing that simultaneous overexpression of AMPK and knockdown of Atg1 is possible, we then set out to determine if AMPK-mediated lifespan extension was dependent upon Atg1 expression levels. We found that induced RNAi of Atg1 in adult neurons suppressed the lifespan extension associated with neuronal upregulation of AMPK **(Fig. 3-3 A-F).** RNAi knockdown of Atg1 alone did not shorten lifespan in control flies **(Fig. 3-3 H-I).** This result indicates that neuronal AMPK-mediated longevity is dependent on Atg1 gene activity. In previous work, Atg1 overexpression has been shown to directly induce autophagy in *Drosophila* [1, 2]. However, the question of whether Atg1 can slow aging or extend animal lifespan has not been addressed. Given our findings with neuronal AMPK activation, we sought to examine the impact of neuron-specific upregulation of Atg1 on *Drosophila* aging. To do so, we used the *Elav-GS* driver to activate a *UAS-Atg1* transgene [1]. Adult-onset, neuronal upregulation of Atg1 resulted in increased median and maximum lifespan in female flies **(Fig. 3-3 J-L and Table 3-1).** These data indicate that Atg1 expression is required for neuronal AMPK life extension, and Atg1 overexpression is sufficient to phenocopy AMPK-mediated longevity.

Having shown that Atg1 is required and sufficient to mediate the lifespan extension phenotype of AMPK overexpression in neurons, we sought to analyze markers of distal tissue aging in these flies. As before, flies overexpressing AMPK alone showed decreased polyubiquitinated protein aggregates in the muscle of 30-day-old flies, and greater maintained

climbing ability with age **(Fig. 3-4 A, B, C)**. Additionally, we saw decreased incidence of intestinal barrier dysfunction at aged timepoints **(Fig. 3-4 D).** Flies with induced simultaneous overexpression of AMPK and knockdown of Atg1 showed no difference in muscle aging or intestinal aging markers. This indicates that neuronal Atg1 expression is required for the anti-aging effects of AMPK **(Fig. 3-4 E-H)**. Neuronal Atg1 knockdown alone did not influence muscle or intestinal aging over the lifespan of the organism **(Fig. 3-4 I-L).** Also, Atg1 overexpression in neurons was sufficient to delay muscle and intestinal aging **(Fig. 3-4 M-P).** Taken together, this evidence indicates that Atg1 is both required and sufficient to mediate the distal tissue anti-aging effects of AMPK overexpression in neurons.

While neuronal AMPK overexpression extends longevity in *Drosophila*, it has the biological trade-off of increased mortality under starvation, including rapid depletion of body mass and lipid stores **(Fig. 3-5 A-C).** To determine if Atg1 plays a contributory role in this starvation sensitivity, we then assayed starvation survival, mass, and lipid content of flies that both overexpress AMPK and knockdown Atg1 in neurons. Knockdown of Atg1 protected AMPK overexpression flies from starvation sensitivity **(Fig. 3-5 D-F).** Atg1 knockdown in neurons alone had no effect on survival under starvation **(Fig. 3-5 G-I)**, and overexpression of Atg1 in neurons produced starvation sensitivity similar to that of AMPK overexpression **(Fig. 3-5 J-L).** In a cumulative manner, this data highlights the importance of Atg1 regulating starvation stress and lipid metabolism downstream of Atg1.

Atg1 activation in neuronal tissue causes a systemic induction of autophagy

The autophagy induction kinase Atg1 clearly plays an important role in lifespan extension and reduction of distal tissue aging markers downstream of AMPK. To assess whether Atg1 is mediating the autonomous and cell non-autonomous induction of autophagy observed in

AMPK flies, we sought to monitor if Atg1 expression alone was sufficient to mediate these effects. Initially we looked at markers of autophagy in the brain. Levels of *Atg1*, *Atg8a*, and *Atg8b* were significantly increased in head tissue **(Fig. 3-6A)**. Moreover, using the transgenic autophagosome marker *pGFP-Atg8a,* we observed a significant increase in GFP puncta in the brain tissue of *ElavGS>UAS*-Atg1 flies upon RU486 treatment **(Fig. 3-6 B, quantification Fig. C).** Together, these data indicate that upregulation of *Atg1* in the adult nervous system can induce autophagy in the target tissue.

As with AMPK, neuronal Atg1 overexpression was associated with improved intestinal homeostasis during aging **(Fig. 3-7A).** Next, we set out to determine whether Atg1 can induce autophagy in a cell non-autonomous manner similar to that of AMPK. Remarkably, upregulation of Atg1 in adult neurons significantly increased mRNA levels of *Atg1*, *Atg8a*, and *Atg8b* in intestinal tissue **(Fig. 3-7 B)**. Additionally, using the transgenic autophagosome marker *pGFP-Atg8a,* we observed a significant increase in GFP puncta in posterior midgut enterocytes in *ElavGS>UAS-Atg1* flies upon RU486 treatment **(Fig. 3-6 C, quantification 3-6 D).** Upregulation of Atg1 in neurons also significantly increased the amount of lysosomal foci found in the midgut enterocytes as marked by the acidophilic dye Lysotracker **(Fig 3-6 E, quantification 3-6 F).** In a complimentary live staining approach, the amount of GFP-Atg8a puncta, Lysotracker puncta, and colocalized vesicles was increased in the posterior-midgut upon Atg1 activation in neurons **(Fig. 3-7 A and quantification 3-7 B)**. These data indicate that direct upregulation of the autophagy pathway in adult neurons can produce intertissue effects during aging in a similar fashion to neuronal AMPK activation.

Overexpression of Atg1 in neurons does not alter feeding behavior and causes moderate heat and oxidative stress resistance

To determine whether altered feeding behavior may play a role in mediating these effects, we assayed food intake in response to neuron-specific Atg1 upregulation. As was the case with neuronal AMPK-mediated longevity, long-lived flies overexpressing Atg1 in the adult nervous system did not show altered feeding behavior **(Fig. 3-8 A).** Similar to AMPK as well, overexpression of Atg1 in neurons conferred moderately increased survival under oxidative and heat stress **(Fig. 3-8 B, C).** Given these discoveries, Atg1 overexpression in neuronal tissue is at least partially sufficient to phenocopy stress resistance seen in neuronal AMPK activation.

Summary and discussion

In this chapter we have shown that neuronal AMPK-mediated life extension is dependent upon Atg1 expression levels in the brain. Furthermore, the intertissue influence of delayed intestinal and thoracic muscle aging is also reliant on the autophagy pathway in AMPK activated flies. Along these lines, Atg1 overexpression in neurons is sufficient to phenocopy all of the observed AMPK-mediated effects on lifespan, stress resistance, delayed distal tissue aging, and both autonomous and non-autonomous autophagy induction. These genetic interactions are summarized in **(Fig. 3-9).**

While we have shown both the requirement and sufficiency of Atg1 in transducing AMPK-mediated signals for distal tissue communication, we have not described the mechanism by which this intertissue communication is transduced. As the *ElavGS* driver is expressed in nearly all neuronal populations [3, 4], it is possible that this cell non-autonomous signal is being mediated by a specific subset of neurons that innervate distal tissues of the fly. Alternatively,

this cell non-autonomous action could be mediated by a secretory/endocrine system in *Drosophila* [5]. Chapter IV describes the subpopulation of neurons, and the endocrine regulatory systems involved in this cell non-autonomous response to neuron-specific AMPK activation.

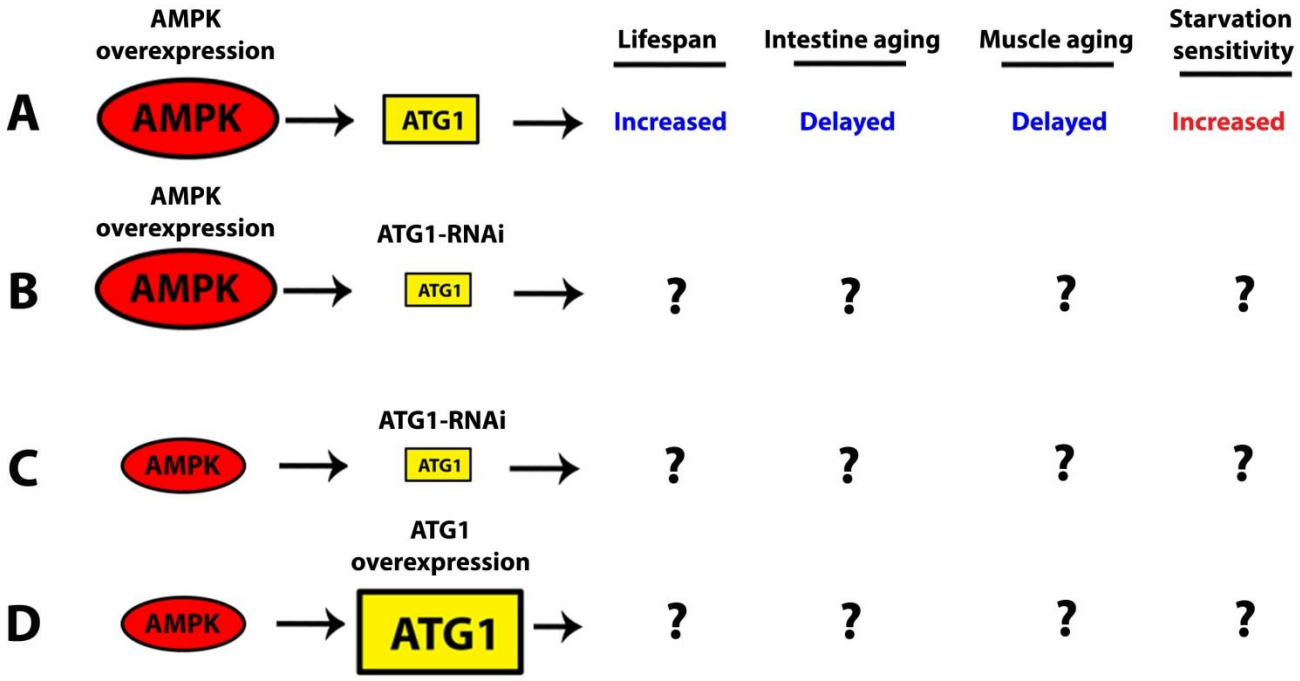

Figure 3-1. Schematic for the determination of necessity, and sufficiency of Atg1 on AMPK mediated life-extension and physiology.

(A) AMPK overexpression in neuronal tissue alone is sufficient to extend lifespan, cause a cell-non-autonomous delay in muscle aging/intestinal aging, and an increase in starvation sensitivity.

(B) To determine if AMPK overexpression lifespan extension and physiology is dependent on Atg1 gene expression levels, simultaneous overexpression of AMPK and knockdown of Atg1 will be performed in neuronal tissue. If AMPK-mediated lifespan effects are masked by Atg1 RNAi, Atg1 is epistatic to AMPK.

(C) As a control to show Atg1 is epistatic to AMPK, Atg1 will be knocked down in neuronal tissue alone.

(D) To determine Atg1 upregulation is sufficient to increase lifespan, Atg1 will be overexpressed in neuronal tissue alone.

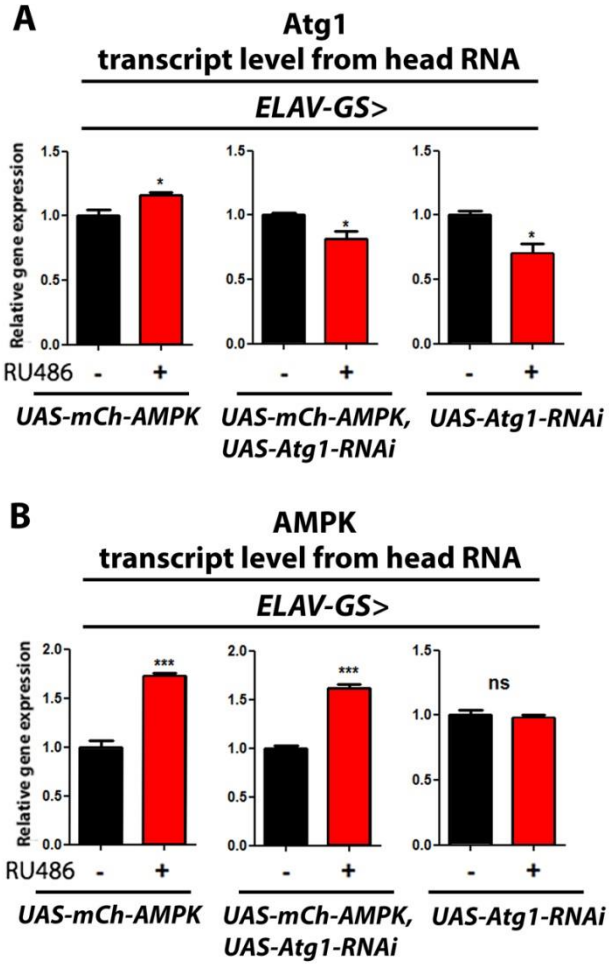

Figure 3-2. Confirmation of AMPK overexpression and Atg1 knockdown for epistasis analysis.

(A) Expression level of Atg1 in dissected heads of indicated genotypes of female flies at 10 days of adulthood. AMPK induction in the nervous system significantly increased Atg1 transcript levels. Simultaneous overexpression of AMPK, and knockdown of Atg1significantly reduced Atg1 transcript levels upon RU486 induction. Atg1 knockdown alone significantly decreased Atg1 transcript in heads of female flies. (*t-test; n>3 of RNA extracted from 10 heads /replicate*).

(B) Expression level of AMPK in dissected heads of indicated genotypes of female flies at 10 days of adulthood. AMPK induction in the nervous system significantly increased AMPK transcript levels. Flies with simultaneous overexpression of AMPK, and knockdown of Atg1significantly maintain increased AMPK transcript levels upon RU 486 induction. Atg1 knockdown alone does not influence AMPK transcript levels in heads of female flies (*t-test; n>3 of RNA extracted from 10 heads /replicate*).

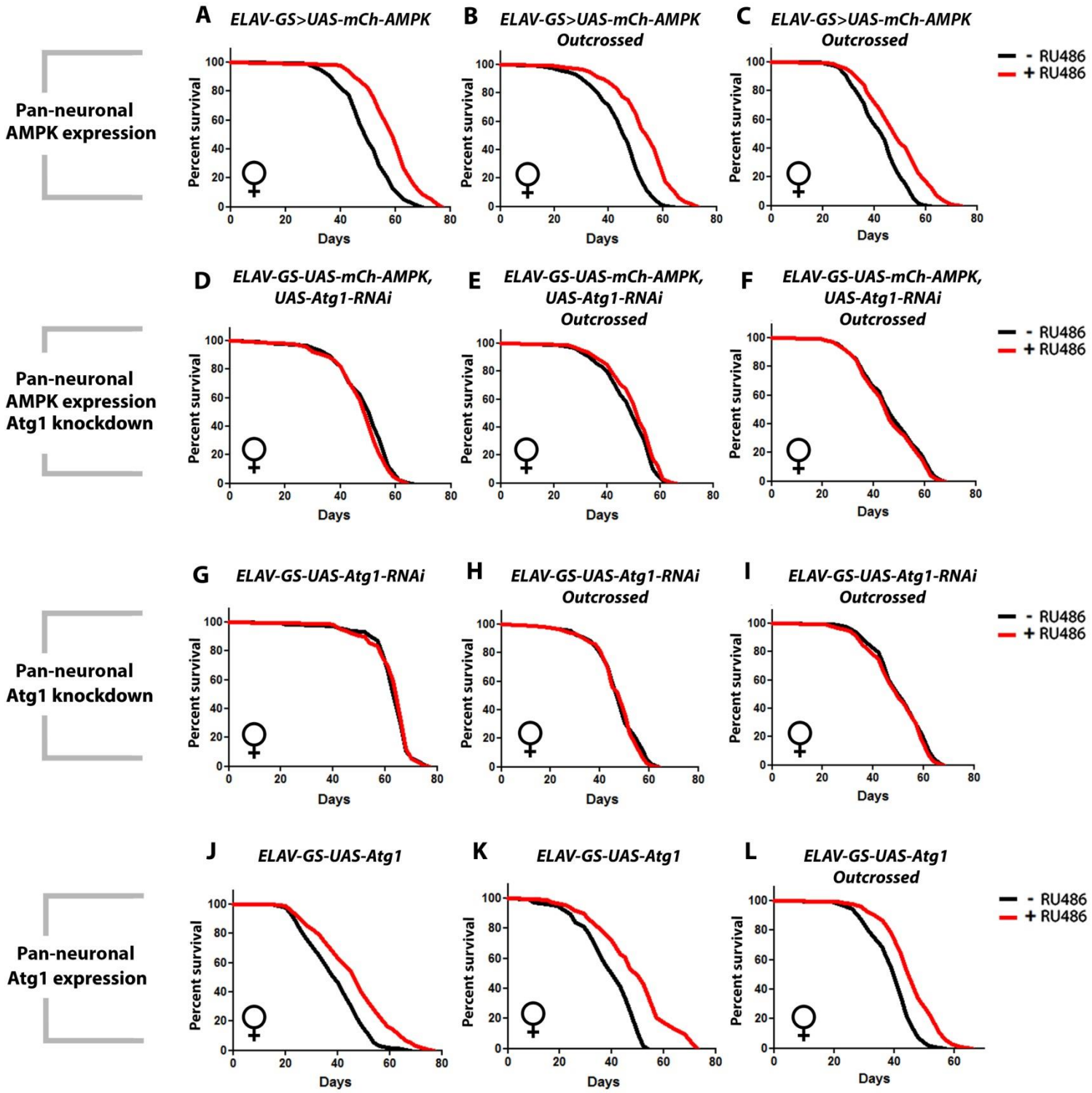

Figure 3-3. Atg1expression in neuronal tissue is both necessary and sufficient to increase lifespan.

(A-C) Repeat survival curves of AMPK overexpression in neurons alone, *ELAV-GS>UAS-mCh-AMPK* females with or without RU486-mediated transgene induction.

(A) Neuronal AMPK overexpression increased median lifespan by 18% (repeat from figure???) (*p<0.0001; log-rank test; n>247 flies/condition*).

(B) Survival curve of *ELAV-GS>UAS-mCh-AMPK* outcrossed to W^{1118}/cyo. AMPK overexpression in neurons increased median lifespan by 18.1% (*p<0.0001; log-rank test; n>138 flies/condition*).

(C) Repeat survival curve of *ELAV-GS>UAS-mCh-AMPK* outcrossed to W^{1118}/cyo. AMPK overexpression in neurons increased median lifespan by 9.1% (*p<0.0001; log-rank test; n>396 flies/condition*).

(D-F) Repeat survival curves of AMPK overexpression with simultaneous knockdown of Atg1, *ELAV-GS>UAS-mCh-AMPK, UAS-Atg1-RNAi* females with or without RU486-mediated transgene induction.

(D) Survival curves of *ELAV-GS> UAS-mCH-AMPK, UAS-Atg1-RNAi* females with or without RU486-mediated transgene induction. Simultaneous overexpression of AMPK and knockdown of Atg1 resulted in no lifespan extension (*p=0.136; log-rank test; n>196 flies/condition*).

(E) Survival curves of *ELAV-GS> UAS-mCH-AMPK, UAS-Atg1-RNAi* outcrossed to W^{1118}/cyo. Simultaneous overexpression of AMPK and knockdown of Atg1 resulted in a very small 4% lifespan extension (*p<0.0284; log-rank test; n>210 flies/condition*).

(F) Repeat survival curve of *ELAV-GS>UAS-mCh-AMPK, UAS-Atg1-RNAi* outcrossed to W^{1118}/cyo. Simultaneous overexpression of AMPK and knockdown of Atg1 resulted in no lifespan extension (*p>0.21; log-rank test; n>306 flies/condition*).

(G-I) Repeat survival curves of Atg1 knockdown alone, *ELAV-GS>UAS-Atg1-RNAi* females with or without RU486-mediated transgene induction.

(G) Survival curves of *ELAV-GS>UAS-Atg1-RNAi* with or without RU486-mediated transgene induction. Knockdown of Atg1alone resulted in no lifespan alteration compared to uninduced controls (*p=0.51; log-rank test; n>205 flies/condition*).

(H) Survival curves of *ELAV-GS>UAS-Atg1-RNAi* outcrossed to W^{1118}/cyo. Knockdown of Atg1 resulted in no lifespan alteration compared to uninduced controls (*p=0.98; log-rank test; n>111 flies/condition*).

(I) Repeat survival curves of *ELAV-GS>UAS-Atg1-RNAi* outcrossed to W^{1118}/cyo. Knockdown of Atg1 resulted in no lifespan alteration compared to uninduced controls (*p=0.258; log-rank test; n>238 flies/condition*).

(J-L) Repeat survival curves of Atg1 overexpression in neuronal tissue, *ELAV-GS>UAS-Atg1* females with or without RU486-mediated transgene induction.

(J) Survival curves of *ELAV-GS>UAS-Atg1* females with or without RU486-mediated transgene induction. Overexpression of Atg1 alone increased lifespan by 15% (*p<0.0001; log-rank test; n>386 flies/condition*).

(K) Repeat survival curves of *ELAV-GS>UAS-Atg1* females with or without RU486-mediated transgene induction. Overexpression of Atg1 alone increased lifespan by 25% (*p<0.0001; log-rank test; n>151 flies/condition*).

(L) Survival curves of *ELAV-GS>UAS-Atg1* outcrossed to W^{1118}/cyo. Overexpression of Atg1 is sufficient to increase lifespan by 11% (*p<0.0001; log-rank test; n>328 flies/condition*).

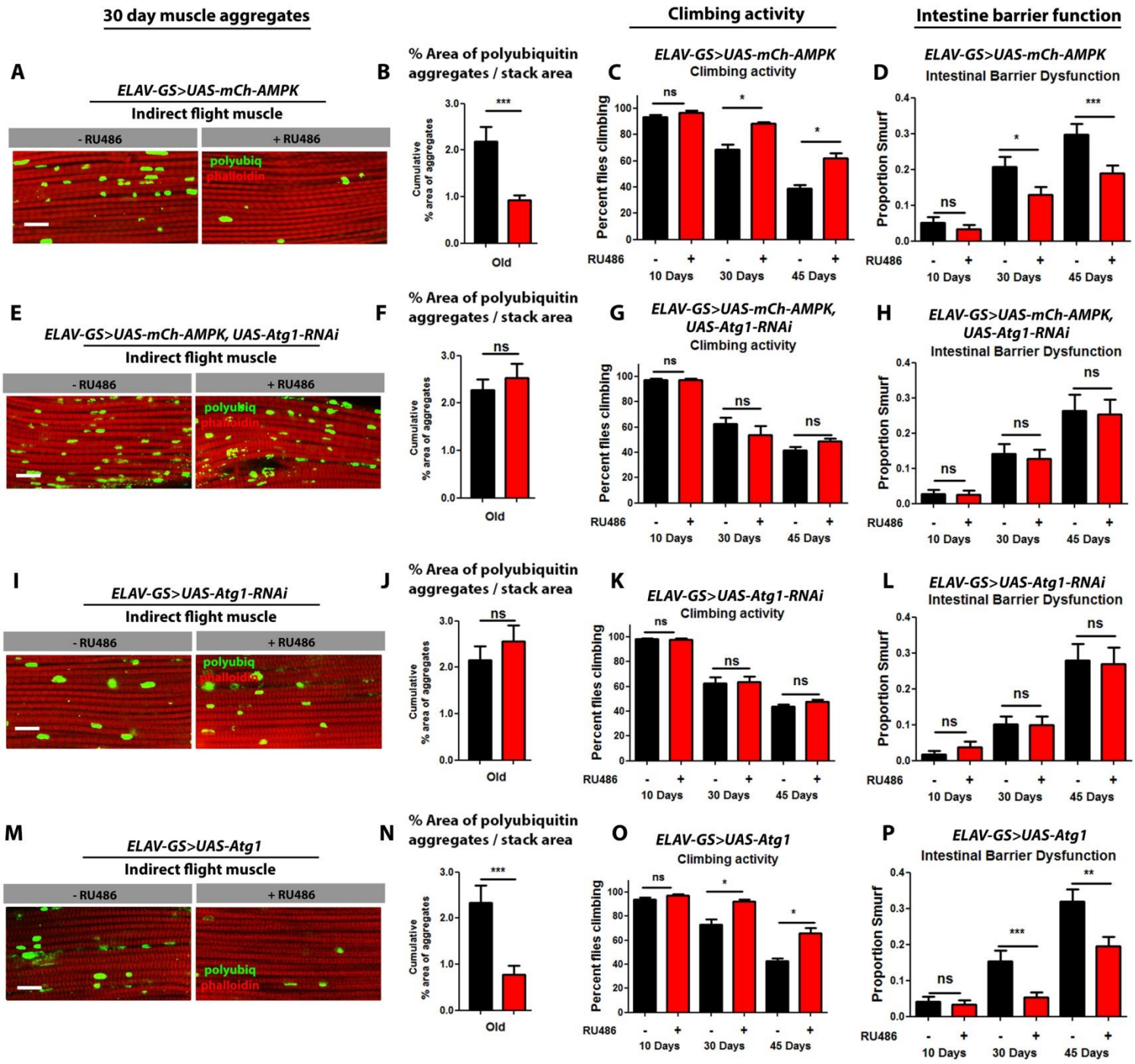

Figure 3-4. Atg1 expression level in neurons is necessary for AMPK-mediated delay in muscle aging, intestinal aging, and Atg1 overexpression is sufficient to delay these phenotypes.

(A) Confocal images of indirect flight muscle, in *ELAV-GS>UAS-mCH-AMPK* females with or without RU486-mediated transgene induction, showing protein polyubiquitinated aggregates at old (30 days) timepoints.

(B) Repeat quantification of polyubiquitin aggregates in muscle. Neuronal AMPK activation decreased the accumulation of polyubiquitinated proteins during aging compared to uninduced controls (*p<0.001; t-test; n>10; one fly/replicate stack*).

(C) Repeat climbing activity of *ELAV-GS>UAS-mCH-AMPK* females with or without RU486-mediated transgene induction. Upregulation of AMPK in neurons allows flies to maintain active climbing ability with age compared to uninduced controls (*p<0.05*; *t-test; n>6 vials/condition; 30 flies/vial).*

(D) Repeat intestinal integrity assay during aging in *ELAV-GS>UAS-mCH-AMPK* females. Inducible upregulation of AMPK in neurons significantly decreases the proportion of flies exhibiting intestinal barrier dysfunction at old age time points (*p<0.05; binomial test, at 30 days of age, and p<0.01 at 45 days; n>90 flies/condition*).

(E) Representative confocal images of indirect flight muscle, in *ELAV-GS>UAS-mCH-AMPK, UAS-Atg1-RNAi* females with or without RU486-mediated transgene induction.

(F) Quantification of polyubiquitin aggregates in muscle at 30 days. Simultaneous neuronal AMPK activation and Atg1 knockdown had no influence on polyubiquitinated protein accumulation with age compared to uninduced controls (*p>0.05; t-test; n>10; one fly/replicate stack*).

(G) Climbing activity of *ELAV-GS>UAS-mCH-AMPK, UAS-Atg1-RNAi* females with or without RU486-mediated transgene induction. Simultaneous neuronal AMPK activation and Atg1 knockdown had no influence on climbing activity compared to uninduced controls (*p>0.05*; *t-test; n>6 vials/condition; 30 flies/vial).*

(H) Intestinal integrity assay during aging in *ELAV-GS>UAS-mCH-AMPK, UAS-Atg1-RNAi* females with or without RU486-mediated transgene induction. Simultaneous neuronal AMPK activation and Atg1 knockdown had no influence on intestinal barrier function compared to uninduced controls (*p>0.05; binomial test, at 30 days of age, n>100 flies/condition*).

(I) Representative confocal images of indirect flight muscle, in *ELAV-GS> UAS-Atg1-RNAi* females with or without RU486-mediated transgene induction.

(J) Quantification of polyubiquitin aggregates in muscle. Neuronal Atg1 knockdown had no effect on the accumulation of polyubiquitinated proteins during aging compared to uninduced controls (*p>0.05; t-test; n>10; one fly/replicate stack*).

(K) Repeat climbing activity of *ELAV-GS>UAS-Atg1-RNAi* females with or without RU486-mediated transgene induction. Neuronal Atg1 knockdown had no effect on climbing activity during aging compared to uninduced controls (*p>0.05*; *t-test; n>6 vials/condition; 30 flies/vial).*

(L) Intestinal integrity assay during aging in *ELAV-GS> UAS-Atg1-RNAi* females with or without RU486-mediated transgene induction. Atg1 knockdown in neurons had no influence on intestinal barrier function compared to uninduced controls (*p>0.05; binomial test, at 30 days of age, n>100 flies/condition*).

(M) Confocal images of indirect flight muscle, in *ELAV-GS>UAS-Atg1* females with or without RU486-mediated transgene induction.

(N) Quantification of polyubiquitin aggregates in muscle. Neuronal Atg1upregulation decreased the accumulation of polyubiquitinated proteins during aging compared to uninduced controls (*p<0.001; t-test; n>10; one fly/replicate stack*).

(O) Climbing activity of *ELAV-GS>UAS-Atg1* females with or without RU486-mediated transgene induction. Upregulation of Atg1 in neurons allows flies to maintain active climbing ability with age compared to uninduced controls (*p<0.05*; *t-test; n>6 vials/condition; 30 flies/vial).*

(P) Intestinal integrity assay during aging in *ELAV-GS>UAS-Atg1* females with or without RU486-mediated transgene induction. Inducible upregulation of Atg1 in neurons significantly decreases the proportion of flies exhibiting intestinal barrier dysfunction at old age time points (*p<0.001; binomial test, at 30 days of age, and p<0.01 at 45 days; n>120 flies/condition*).

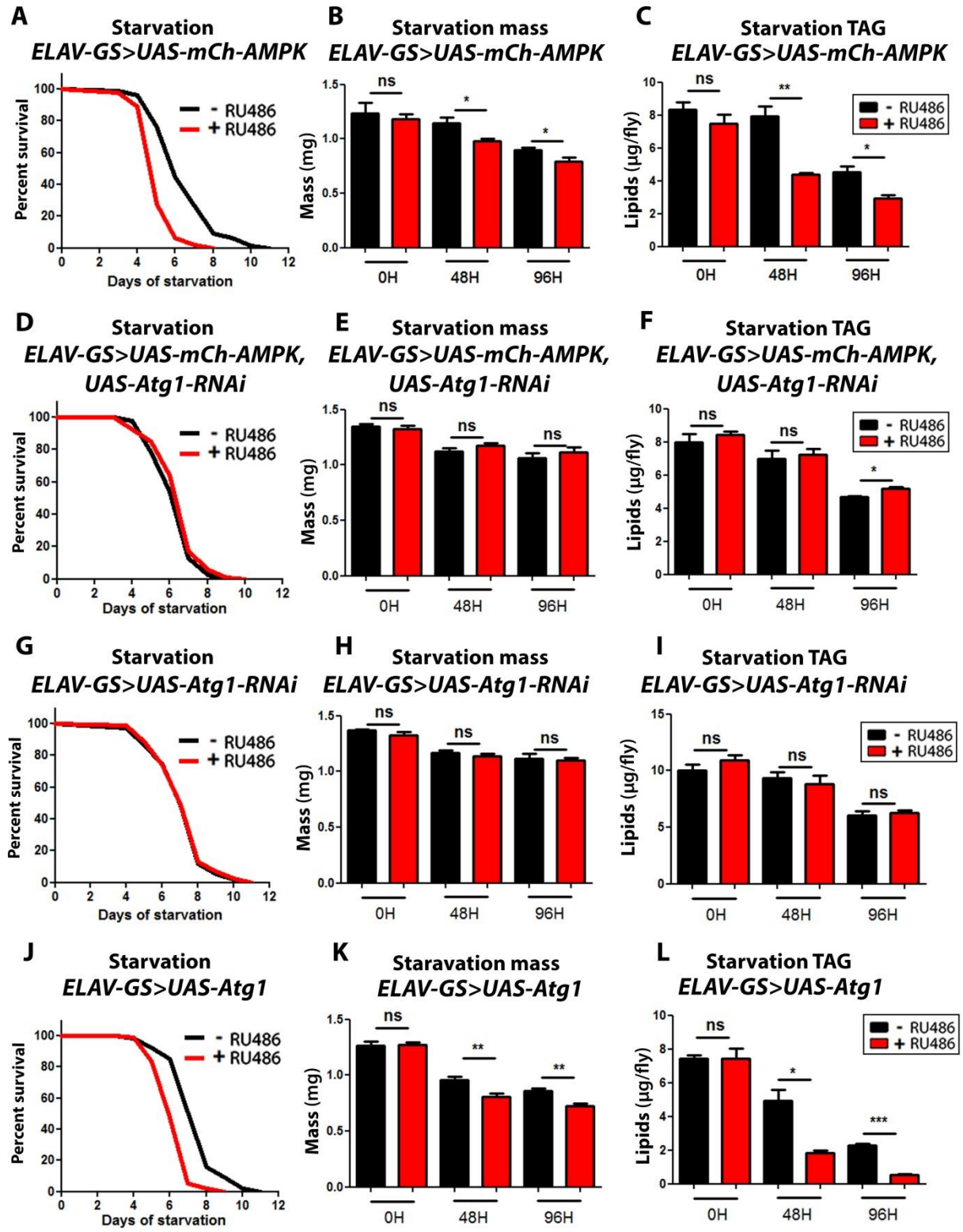

Figure 3-5. Neuronal AMPK-mediated starvation sensitivity is dependent upon Atg1 expression levels, and Atg1 overexpression in neurons phenocopies starvation sensitivity.

(A) Repeat wet starvation survival curves of female *ELAV-GS>UAS-mCh-AMPK* flies (originally depicted in figure 2). AMPK overexpression in neurons caused early mortality when deprived of nutrition (*p<0.0001; log-rank; n>122 flies/condition*).

(B) Repeat body mass during starvation of *ELAV-GS>UAS-mCh-AMPK* females. AMPK overexpression in neurons caused rapid mass depletion upon starvation, compared to uninduced flies (*p<0.05, at 48hours and 96 hours of starvation; t-test; n>6 samples/condition; 10 flies weighed/sample).*

(C) Repeat whole body lipid stores during starvation of *ELAV-GS>UAS-mCh-AMPK* females with or without RU486-mediated transgene induction. Neuronal AMPK induction caused rapid lipid depletion upon starvation (*p<0.01 at 48 hours, and p<0.05 at 96 hours of starvation; t-test; n>3 samples/condition/timepoint; lipids extracted from 5 flies per sample).*

(D) Wet starvation survival curves of *ELAV-GS>UAS-mCH-AMPK, UAS-Atg1-RNAi* females with or without RU486-mediated transgene induction. Simultaneous neuronal AMPK activation and Atg1 knockdown had no influence on starvation survival compared to uninduced controls (*p=0.54*; *log-rank; n>206 flies/condition).*

(E) Body mass during starvation of *ELAV-GS>UAS-mCH-AMPK, UAS-Atg1-RNAi* females Simultaneous neuronal AMPK activation and Atg1 knockdown had no influence on starvation body mass compared to uninduced controls (*p>0.05,; t-test; n>6 samples/condition; 10 flies weighed/sample).*

(F) Whole body lipid stores during starvation of *ELAV-GS>UAS-mCH-AMPK, UAS-Atg1-RNAi* females. Simultaneous neuronal AMPK activation and Atg1 knockdown had minimal influence on lipid quantity compared to uninduced controls (*p<0.05 at 96 hours hours of starvation; t-test; n>3 samples/condition/timepoint; lipids extracted from 5 flies per sample).*

(G) Wet starvation survival curves of female *ELAV-GS>UAS-Atg1-RNAi* flies with or without RU486-mediated transgene induction. Neuronal Atg1 knockdown had no effect on the starvation survival compared to uninduced controls (*p=0.7091; log-rank; n>202 flies/condition*).

(H) Body mass during starvation of *ELAV-GS>UAS-Atg1-RNAi* females. Neuronal Atg1 knockdown had no effect on starvation body massl compared to uninduced controls (*p>0.05, n>6 samples/condition; 10 flies weighed/sample).*

(I) Whole body lipid stores during starvation of *ELAV-GS>UAS-Atg1-RNAi* females. Neuronal Atg1 knockdown had no effect on whole body lipid content during starvation compared to uninduced controls(*p>0.05; t-test; n>3 samples/condition/timepoint; lipids extracted from 5 flies per sample).*

(J) Wet starvation survival curves of female *ELAV-GS>UAS-Atg1* flies with or without RU486-mediated transgene induction. Atg1overexpression in neurons caused early mortality when deprived of nutrition (*p<0.0001; log-rank; n>107 flies/condition*).

(K) Body mass during starvation of *ELAV-GS>UAS-Atg1* females. Atg1 overexpression in neurons caused rapid mass depletion upon starvation, compared to uninduced flies (*p<0.01, at 48hours and 96 hours of starvation; t-test; n>6 samples/condition; 10 flies weighed/sample).*

(L) Whole body lipid stores during starvation of *ELAV-GS>UAS-Atg1* females. Neuronal AMPK induction caused rapid lipid depletion upon starvation (*p<0.05 at 48 hours, and p<0.001 at 96 hours of starvation; t-test; n>3 samples/condition/timepoint; lipids extracted from 5 flies per sample).*

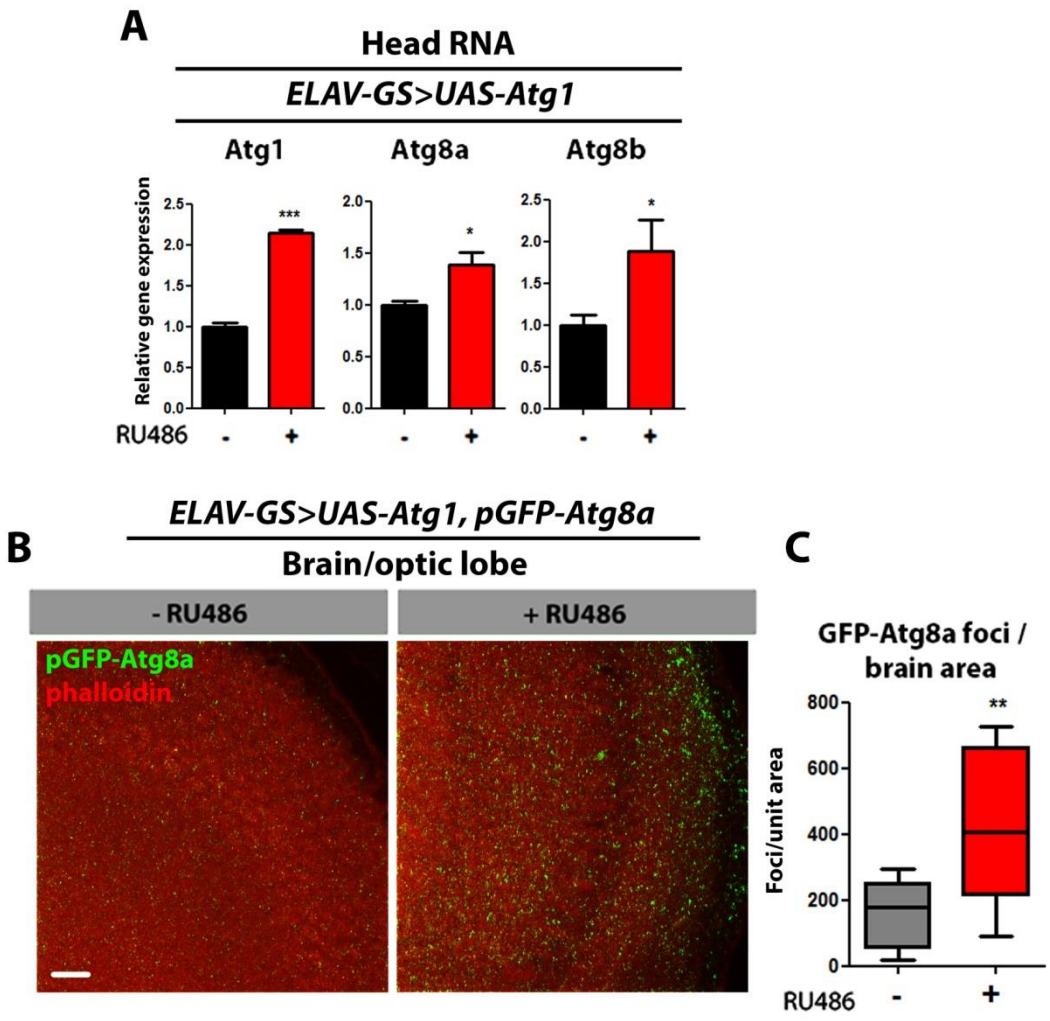

Figure 3-6. Neuronal Atg1 overexpression induces autophagy in the brain.

(A) Expression levels of autophagy genes in heads of *ELAV-GS>UAS-Atg1* flies at 10 days of adulthood. Atg1 induction in neurons significantly increased Atg1, Atg8a, and Atg8b RNA levels in the heads of female flies (*t-test; n>3 of RNA extracted from 10 heads/replicate*).

(B) Brain GFP-Atg8a Staining. Representative images from optic lobes of 10- day old *ELAV-GS>UAS-Atg1, pGFP-Atg8a* females with or without RU486-mediated transgene expression (*red channel-phalloidin, green channel-GFP-Atg8a, scale bar represents 10μm*).

(C) Quantification of brain pGFP-Atg8a foci. Neuronal upregulation of Atg1 increased the amount of GFP-Atg8a puncta compared to uninduced controls (*p<0.0082; t-test; n>10 confocal stacks from optic lobes/condition; one brain/replicate stack*).

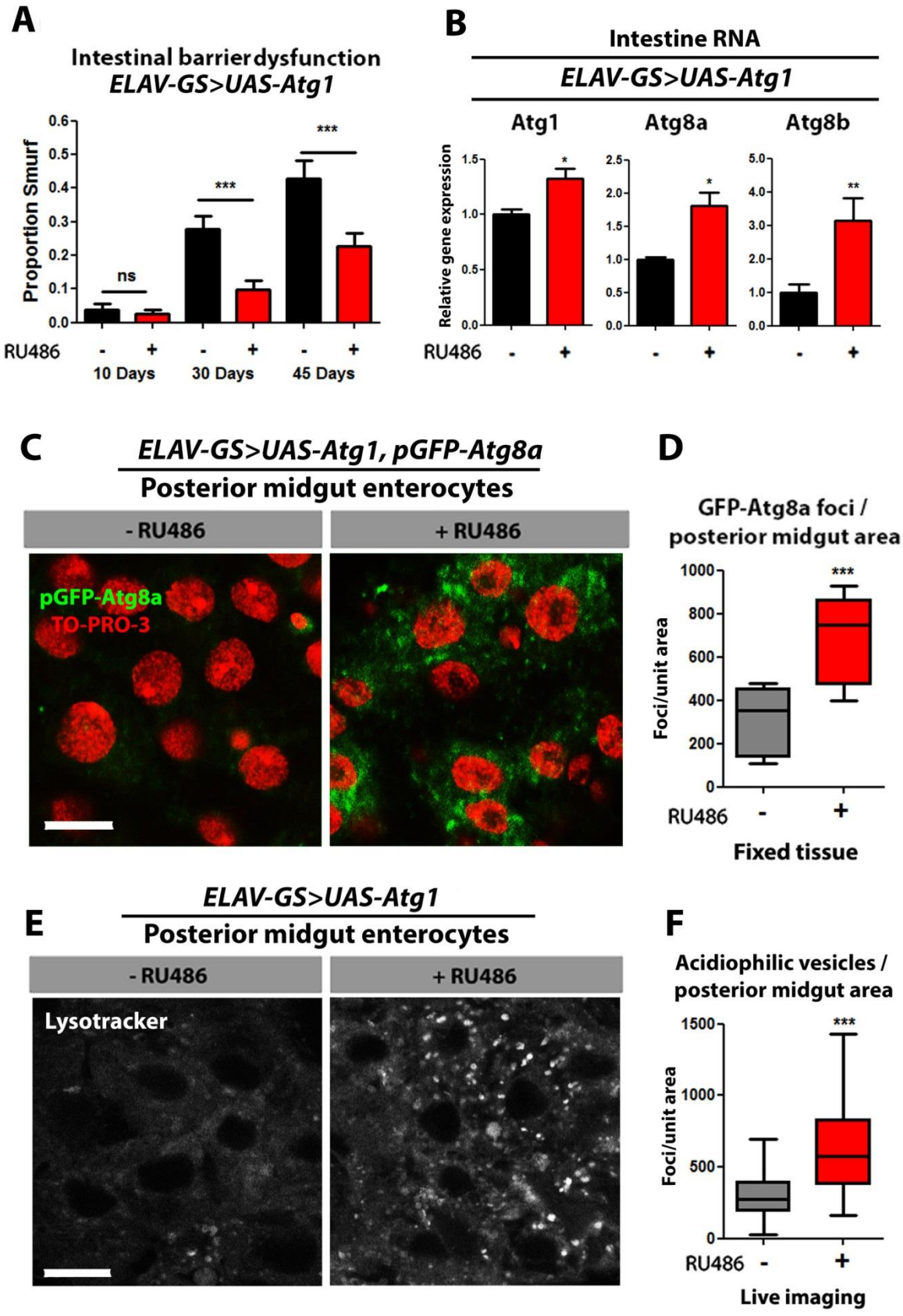

Figure 3-7. Atg1 overexpression in neurons induces autophagy in the intestine, and delays intestinal aging.

(A) Repeat intestinal integrity assay during aging in *ELAV-GS>UAS-Atg1* females. Inducible upregulation of Atg1 in neurons significantly decreases the proportion of flies exhibiting intestinal barrier dysfunction at old age time points (*p<0.001; binomial test, at 30, and 45 days of age; n>91 flies/condition*).

(B) Expression levels of autophagy genes in the intestines of *ELAV-GS>UAS-Atg1* female flies at 10 days of adulthood. Upon Atg1 induction in neurons significantly increased Atg1, Atg8a, and Atg8b RNA levels are observed in the gut (*t-test; n>3 of RNA extracted from 15 intestines/replicate*).

(C) GFP-Atg8a staining. Representative images of enterocytes from the posterior midgut of 10 day old *ELAV-GS, pGFP-Atg8a>UAS-Atg1* females with or without RU486-mediated transgene induction in neurons (*red channel-TO-PRO-3 DNA stain, green channel-GFP-Atg8a, scale bar represents 10μm*).

(D) Quantification of posterior midgut pGFP-Atg8a foci. Atg1 overexpression in neurons increased the number of GFP-Atga puncta in the intestine compared to uninduced controls (*p<0.0001; t-test; n>10 confocal stacks from posterior midgut/condition; one fly per replicate stack*).

(E) Lysotracker Red staining. Representative images of posterior midgut enterocytes from 10 day old *ELAV-GS-GAL4>UAS-Atg1* females with or without RU486-mediated transgene induction stained with the acidophilic dye (*scale bar represents 10μm*).

(F) Quantification of acidophilic vesicles. Atg1 overexpression in neurons increased the number of acidophilic vesicles in the intestine compared to uninduced controls (*p<0.0001; t-test; n>25 confocal stacks from posterior midgut/condition; one fly per replicate stack*).

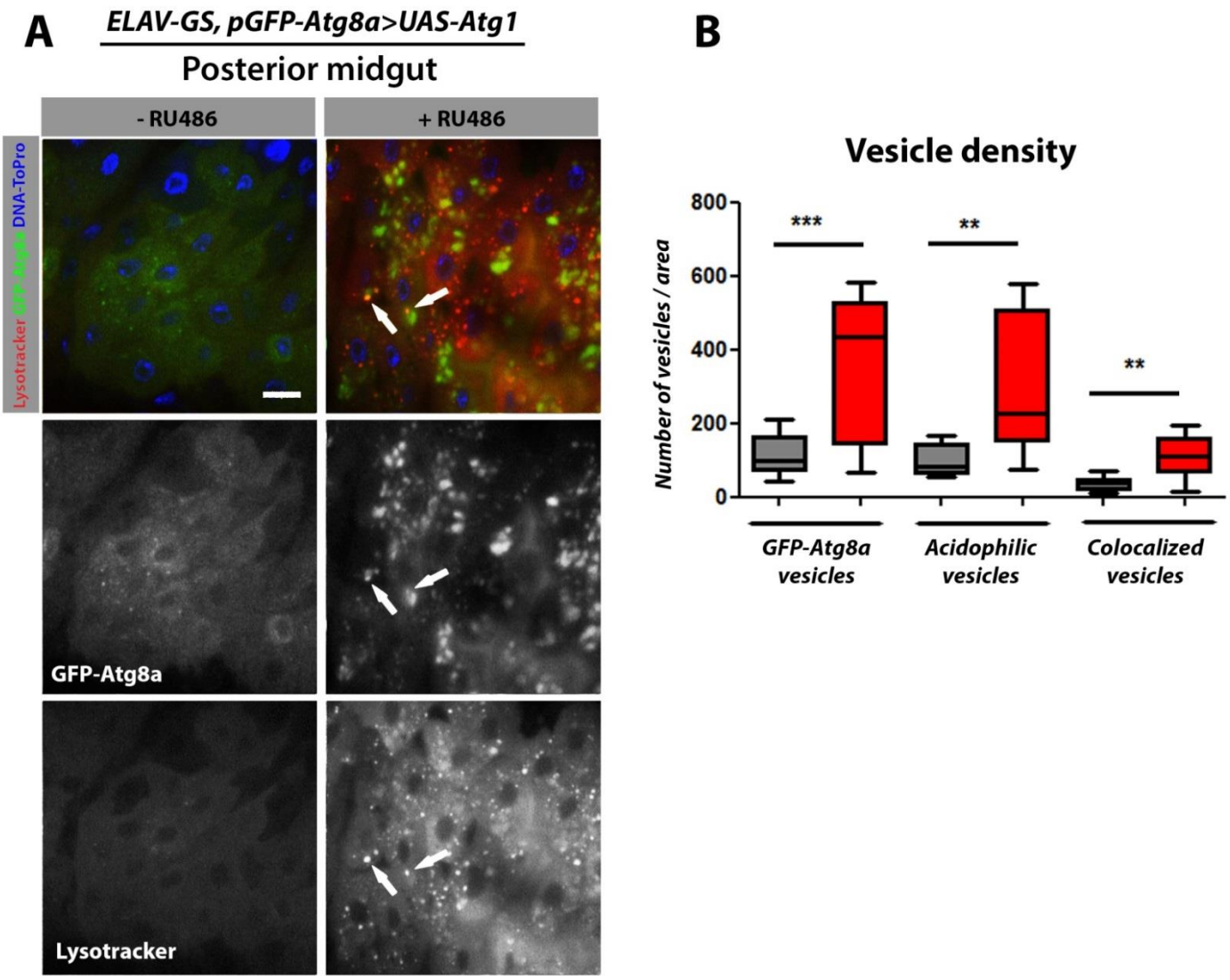

Figure 3-8. Neuronal Atg1 upregulation causes a cell-non autonomous induction of autophagy when monitored via live imaging of dissected intestinal enterocytes.

(A) Representative images of enterocytes from the posterior midgut of 10 day old *ELAV-GS, pGFP-Atg8a>UAS-atg1,* females with or without RU486-mediated transgene induction in neurons (*red channel-Lysotracker Red, blue channel-ToPro-3 DNA stain, green channel-GFP-Atg8a, scale bar represents 10μm, arrows indicate colocalized autolysosomes*).

(B) Quantification of acidophilic vesicles, GFP-atg8a vesicles, and colocalized "autolysosomal" vesicles/midgut area. Induction of AMPK in neuronal tissue increased density of GFP-atg8a vesicles, acidophilic vesicles, and colocalized vesicles compared to uninduced controls (*$p<0.01$; t-test; $n>10$ guts/condition*).

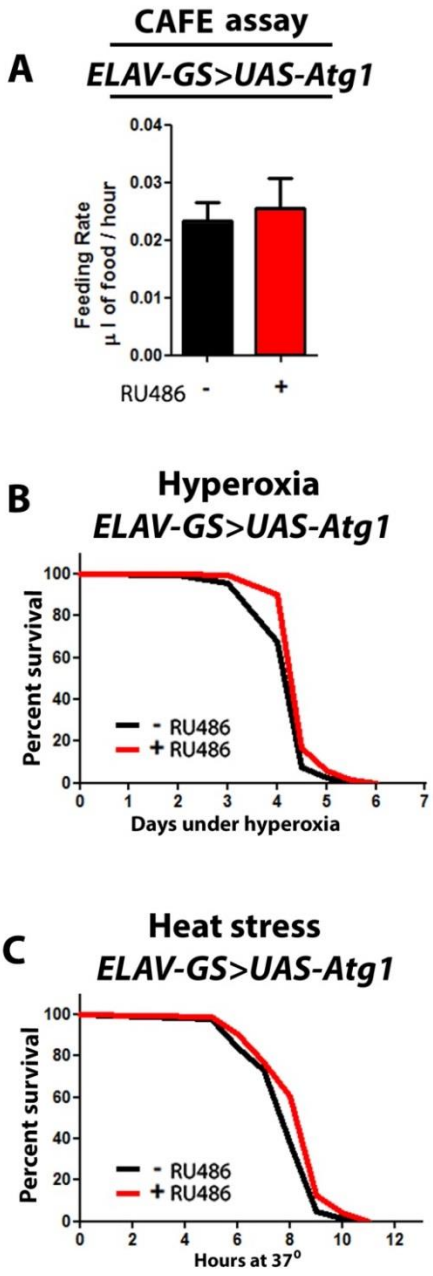

Figure 3-9. Atg1 overexpression in neurons causes moderate stress resistance and does not influence feeding behavior.

(A) Capillary feeding assay (CAFE) of 10 day old *ELAV-GS>UAS-Atg1* flies. RU486 transgene induction had no effect on feeding rate of female flies *($p>0.05$; t-test, n>7 vials of 10 flies/condition*).

(B) Hyperoxia survival curves of 10 day old female *ELAV-GS>UAS-Atg1* flies. Neuronal upregulation of Atg1 moderately increased survival under 80% atmospheric oxygen (*$p<0.0001$; log-rank; n>172 flies/condition*).

(C) Heat stress survival curves of 10 day old female *ELAV-GS>UAS-Atg1* flies. Neuronal upregulation of Atg1moderately increased survival at 37° C. (*$p<0.0097$; log-rank; n>73 flies/condition*).

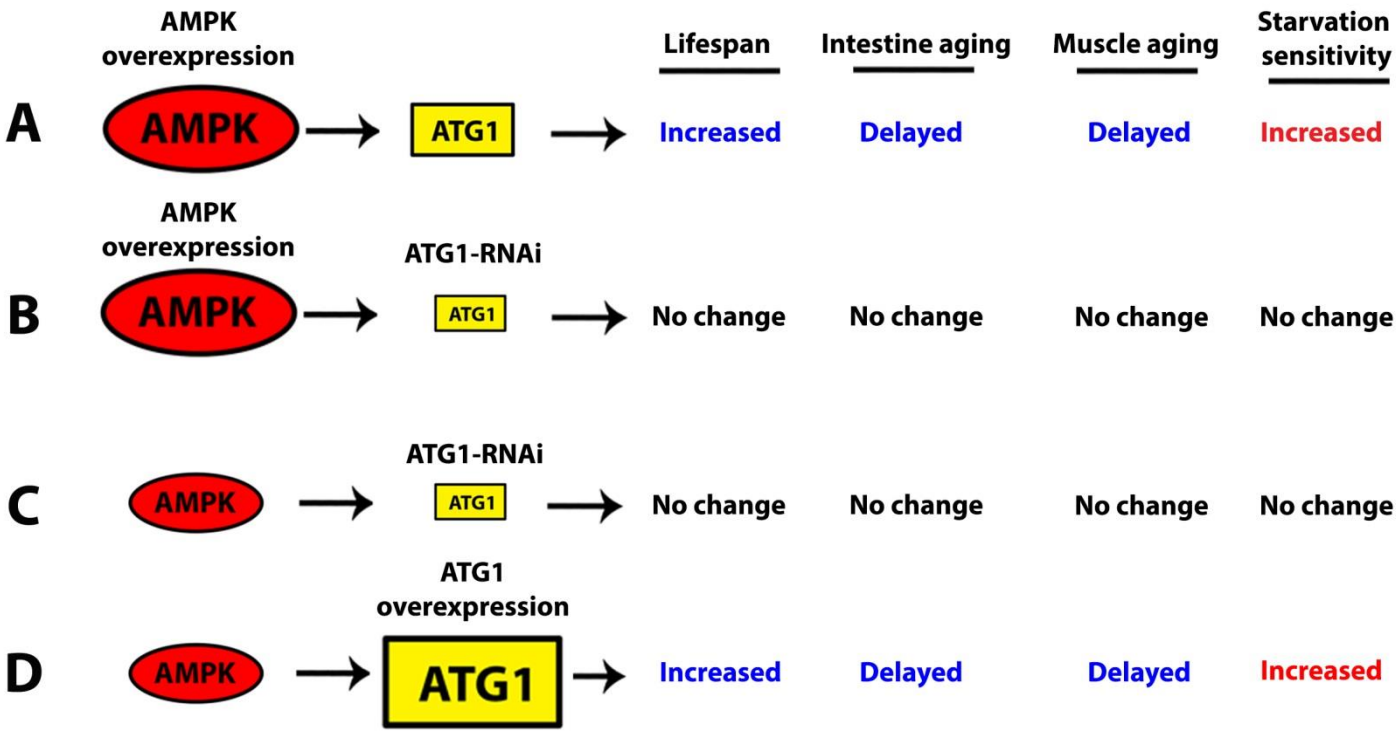

Figure 3-10. Experimental summary indicating neuronal Atg1 expression is required for AMPK-mediated lifespan extension, and Atg1 overexpression alone phenocopies the aging and physiology effects of AMPK overexpression in neurons.

(A) AMPK overexpression in neuronal tissue alone is sufficient to extend lifespan, cause a cell-non-autonomous delay in muscle aging/intestinal aging, and an increase in starvation sensitivity.

(B) Knockdown of Atg1 in AMPK overexpression background reverts flies to normal lifespan, with no reduction in markers of aging, and no starvation sensitivity.

(C) Atg1 knockdown in neurons alone results in no lifespan extension, no reduction in markers of aging, and no starvation sensitivity.

(D) Atg1 overexpression in neuronal tissue alone is sufficient to extend lifespan, cause a cell-non-autonomous delay in muscle aging/intestinal aging, and an increase in starvation sensitivity.

TABLE 3-1. Lifespan data associated to figure 3-3

Repeat	Genotype	RU-486 dose µG / ml of food	Sex	Median lifespan days	Percent change median lifespan to "0 RU"	Sample size	Log Rank p-value
1	ELAV-GS>UAS-mCh-AMPK	0	F	50		266	
	ELAV-GS>UAS-mCh-AMPK	25	F	59	+18.0	263	< 0.0001
	ELAV-GS>UAS-mCh-AMPK	50	F	57	+14.0	247	< 0.0001
1	ELAV-GS>UAS-mCh-AMPK, OC	0	F	47		197	
	ELAV-GS>UAS-mCh-AMPK, OC	25	F	50	+6.38	272	< 0.0001
	ELAV-GS>UAS-mCh-AMPK, OC	50	F	55.5	+18.0	138	< 0.0001
2	ELAV-GS>UAS-mCh-AMPK, OC	0	F	44		397	
	ELAV-GS>UAS-mCh-AMPK, OC	50	F	48	+9.09	396	< 0.0001
1	ELAV-GS>UAS-Atg1-RNAi	0	F	64.5		228	
	ELAV-GS>UAS-Atg1-RNAi	25	F	66	NS	205	NS
	ELAV-GS>UAS-Atg1-RNAi	50	F	63	-2.32	272	0.0002
1	ELAV-GS>UAS-Atg1-RNAi, OC	0	F	50		238	
	ELAV-GS>UAS-Atg1-RNAi, OC	50	F	50	NS	248	NS
2	ELAV-GS>UAS-Atg1-RNAi, OC	0	F	47		111	
	ELAV-GS>UAS-Atg1-RNAi, OC	50	F	50	NS	116	NS
1	ELAV-GS>UAS-mCh-AMPK, Atg1-RNAi	0	F	52		196	
	ELAV-GS>UAS-mCh-AMPK, Atg1-RNAi	25	F	50	NS	200	NS
	ELAV-GS>UAS-mCh-AMPK, Atg1-RNAi	50	F	50	-3.84	216	0.0003
1	ELAV-GS>UAS-mCh-AMPK, Atg1-RNAi, OC	0	F	50		210	
	ELAV-GS>UAS-mCh-AMPK, Atg1-RNAi, OC	25	F	54	+8.00	210	0.0112
	ELAV-GS>UAS-mCh-AMPK, Atg1-RNAi, OC	50	F	52	+4.00	217	0.0284
1	ELAV-GS>UAS-mCh-AMPK, Atg1-RNAi, OC	0	F	46		306	
	ELAV-GS>UAS-mCh-AMPK, Atg1-RNAi, OC	50	F	46	NS	324	NS
controls	ELAV-GS>W^{1118},Sco,Cyo	0	F	44		184	
	ELAV-GS>W^{1118},Sco,Cyo	25	F	45	NS	198	NS
	ELAV-GS>W^{1118},Sco,Cyo	50	F	43	NS	338	NS
1	ELAV-GS>UAS-Atg1	0	F	40		716	
	ELAV-GS>UAS-Atg1	25	F	47	+17.50	386	< 0.0001
	ELAV-GS>UAS-Atg1	50	F	46	+15.00	494	< 0.0001
controls	ELAV-GS>W^{1118}	0	F	38		200	
	ELAV-GS>W^{1118}	25	F	38	NS	196	NS
	ELAV-GS>W^{1118}	50	F	36	NS	126	NS
2	ELAV-GS>UAS-Atg1	0	F	39		274	
	ELAV-GS>UAS-Atg1	25	F	42	+7.69	137	< 0.0001
	ELAV-GS>UAS-Atg1	50	F	49	+25.64	209	< 0.0001
1	ELAV-GS>UAS-Atg1, OC	0	F	42		328	
	ELAV-GS>UAS-Atg1, OC	50	F	46	+9.52	340	< 0.0001
3	ELAV-GS>UAS-Atg1	0	F	40		151	
	ELAV-GS>UAS-Atg1	25	F	47	+17.50	179	< 0.0001
	ELAV-GS>UAS-Atg1	50	F	50	+25.00	186	< 0.0001

REFERENCES:

1. Scott, R. C., Juhász, G., & Neufeld, T. P. (2007). Direct induction of autophagy by Atg1 inhibits cell growth and induces apoptotic cell death. *Current Biology : CB*, *17*(1), 1–11. doi:10.1016/j.cub.2006.10.053

2. Chang, Y.-Y., & Neufeld, T. P. (2009). An Atg1/Atg13 complex with multiple roles in TOR-mediated autophagy regulation. *Molecular Biology of the Cell*, *20*(7), 2004–14. doi:10.1091/mbc.E08-12-1250

3. Poirier, L., Shane, A., Zheng, J., & Seroude, L. (2008). Characterization of the Drosophila gene-switch system in aging studies: a cautionary tale. *Aging Cell*, *7*(5), 758–70. doi:10.1111/j.1474-9726.2008.00421.x

4. Shen, J., Curtis, C., Tavare, S., and Tower, J. (2009). A screen of apoptosis and senescence regulatory genes for life span effects when over-expressed in Drosophila. *Aging* 1, 191-211.

5. Taylor, R.C., Berendzen, K.M., and Dillin, A. (2014). Systemic stress signalling: understanding the cell non-autonomous control of proteostasis. *Nature reviews. Molecular cell biology* 15, 211-217.

CHAPTER IV:

AMPK/ATG1-MEDIATED LIFESPAN EXTENSION IS LINKED TO SUPPRESSED INSULIN-LIKE SIGNALING

Introduction to Insulin-like signaling control of growth, metabolism, and organismal lifespan.

The expression and secretion of *Drosophila*-insulin-like peptides (DILPs) have been shown to cell-non-autonomously regulate key metabolic functions involving metabolism and cellular growth [1]. Consistent with a role in systemic metabolism, DILPs can control fertility, stress response, aging, and lifespan in the fly [2, 3]. In *Drosophila* there are 8 known DILP proteins, and only one well characterized receptor, the Insulin/Inuslin-like-growth factor receptor (InR/IGFR). In the adult fly, DILP 2, 3, 5, 6, and 7 are known to be expressed and influence nutrition/metabolic signaling [4]. The most widely studied of these being DILP2, and DILP5. During the adult phase DILP 2, and 5 are produced and secreted from the median-neurosecretory-cells (mNSCs, also known as Insulin-producing cells or IPCs) of the brain. When the fly is actively feeding on media containing a high density of nutrients, DILPs are secreted from the IPCs, signaling to InRs located in local and distal tissues for increased growth and anabolic processes. If the fly is placed on media that is poor in nutrition and starved of nutrients, DILPs are retained in the IPCs, and InR remains inactive suppressing growth and starting catabolic processes to maintain active energy status of the organism [4].

At the molecular level, activation of InR upon DILP binding allows for phosphorylation of InR substrates leading to activation of AKT kinase [5]. Phosphorylated AKT activates the TOR pathway. Upregulation of TOR results in S6K stimulation and phosphorylation of the S6 protein of the ribosome allowing for increased protein synthesis and cell growth. Simultaneously, TOR inactivates the translational repressor 4E-BP, aiding in the increased protein synthesis signal. AKT is also able to inhibit the *Drosophila* FOXO (dFOXO)

transcription factor. When FOXO is phosphorylated by AKT, translocation into the nucleus is inhibited, preventing transcription of target genes including 4E-BP [5].

In the absence of DILP binding to InR, AKT is less active and TOR signaling is suppressed. This decrease in TOR activity leads to decreased repression of 4E-BP, inhibiting translation and suppressing cell growth. Moreover, decreased AKT activity leads to increased FOXO transcription factor activity. FOXO can then translocate to the nucleus and increase levels of 4E-BP, further inhibiting translation. FOXO activity is required for many enhanced longevity paradigms in a number model systems including *Drosophila* [5] **(Schematic Summary Fig 4-1).**

The insulin/IGF pathway can modulate lifespan through autonomous and non-autonomous actions [1, 4, 5]. Overexpression of dFOXO in the fat body or muscle has been shown to extend lifespan in *Drosophila* [6,7]. In particular, dFOXO upregulation in muscle has been shown to autonomously decrease the accumulation of insoluble ubiquitinated proteins in the muscle, while also upregulating markers of autophagy [7]. These muscle-specific effects of dFOXO upregulation also function cell-non-autonomously to reduce the accumulation of aggregated proteins in the distal tissues of the fly. This cell-non-autonomous decrease in aggregated polyubiquitinated proteins is accompanied by decreased DILP secretion in the IPCs of these long-lived flies [7].

Ablation of IPCs and inhibition of DILP secretion has been shown to extend lifespan in *Drosophila* [2,8]. Using the *Drosophila* pro-apoptotic gene Reaper, expressed solely in IPCs using the *Dilp2>GAL4* driver results in flies of decreased body mass and organ size, with enhanced longevity and stress resistance [2]. Furthermore, certain neurons present in the mNSCs have been shown to directly innervate the intestine, controlling water balance gut transit [9] **(Fig. 4-2).** Given the physical connection of IPCs/mNSCs to the intestine, and the ability for DILP

expression in these cells to mediate systemic organismal responses that influence aging processes, the insulin-like signaling system appears a likely candidate in neuronal AMPK/Atg1 control of systemic aging.

Overexpression of AMPK and Atg1 in the brain suppresses insulin-like signaling.

To explore a potential role for insulin signaling in mediating the systemic effects associated with tissue-specific AMPK/Atg1 activation, we first examined whether pan-neuronal AMPK activation affects DILP levels in the brain. Indeed, we observed a significant decrease in DILP2 in the insulin producing cells (IPCs) of *ElavGS>UAS-mCh-AMPK* flies upon RU486 treatment **(Fig. 4-3A, quantification Fig. 4-3B)** and a decrease in both *dilp2* and *dilp5* mRNAs in head tissue **(Fig. 4-3C)**. As, the translational regulator *4E-BP* is a direct transcriptional target of *Drosophila* FOXO (dFOXO) that is induced when insulin signaling is repressed, we used transcript levels of 4E-BP as a readout of insulin signaling (Puig et al., 2003). Importantly, *4E-BP* transcript levels were increased in the head and non-autonomously in both the thorax and intestine upon neuronal AMPK activation, consistent with a systemic reduction in insulin signaling. In a similar fashion, neuronal up-regulation of Atg1 reduced DILP levels in the brain **(Fig. 4-3E-G)** and was associated with a systemic increase in *4E-BP* expression **(Fig. 4-3H).** RU486 feeding to ELAV-GS control flies did not alter markers of insulin signaling **(Fig 4-4).**

Summary of findings / Discussion.

In this chapter we have shown that overexpression of AMPK or Atg1 specifically in in nuerons is sufficient to inhibit DILP expression. These findings are the first instance of AMPK and Atg1 being able to suppress DILP expression, influencing systemic response to aging**.** Uninduced flies quickly accumulate age-related pathologies of the muscle and intestine, showing

lower levels of autophagy than transgenic AMPK and Atg1 flies. While we have shown that expression of AMPK/Atg1 in the brain is able to reduce DILP expression and increase systemic 4E-BP transcript levels, we have not determined the downstream mechanism by which autophagy is upregulated in these distal tissues. As insulin-like signaling suppression-mediated lifespan extension is often associated with elevated levels of the transcription factor DAF-16/FOXO, which has been known to transcriptionally regulate autophagy gene expression in *Drosophila*, it may be possible that FOXO is mediating this systemic induction of autophagy [7,13]. Furthermore, AMPK has been shown to activate FOXO activity post-translationally in worms and mammals [14, 15].

While it is a possibility that FOXO is partially facilitating these effects, there is some confounding evidence suggesting that FOXO is not a completely critical component in regulating the cell-non-autonomous mechanism of insulin signaling control of longevity. Surprisingly, dFOXO knockout flies exhibit high levels of 4E-BP gene expression, even though 4E-BP transcription is known to be enhanced by elevated FOXO levels [16]. 4E-BP is often used as the sole readout of FOXO activity in *Drosophila* aging, while this data suggests a redundancy or alternative mechanism of 4E-BP transcriptional regulation. Furthermore, long-lived flies that overexpress transgenic FOXO in the fat body exhibit cell-non-autonomous reduction in markers of muscle aging [6]. Contrary to this, genetic manipulations that have removed the endogenous FOXO from the genome, but overexpress transgenic FOXO exclusively in fat cells, still show increased lifespan and delayed muscle aging [17]. This indicating that FOXO activity in distal tissues of the fly is not required for beneficial cell-non-autonomous signaling [17]. In the following chapter, I offer an alternative hypothesis for AMPK-mediated cell-non-autonomous

signaling, whereby transgenic-AMPK activation in one tissue is able to increase endogenous AMPK activity in distal tissues, leading to autophagy induction and delayed aging.

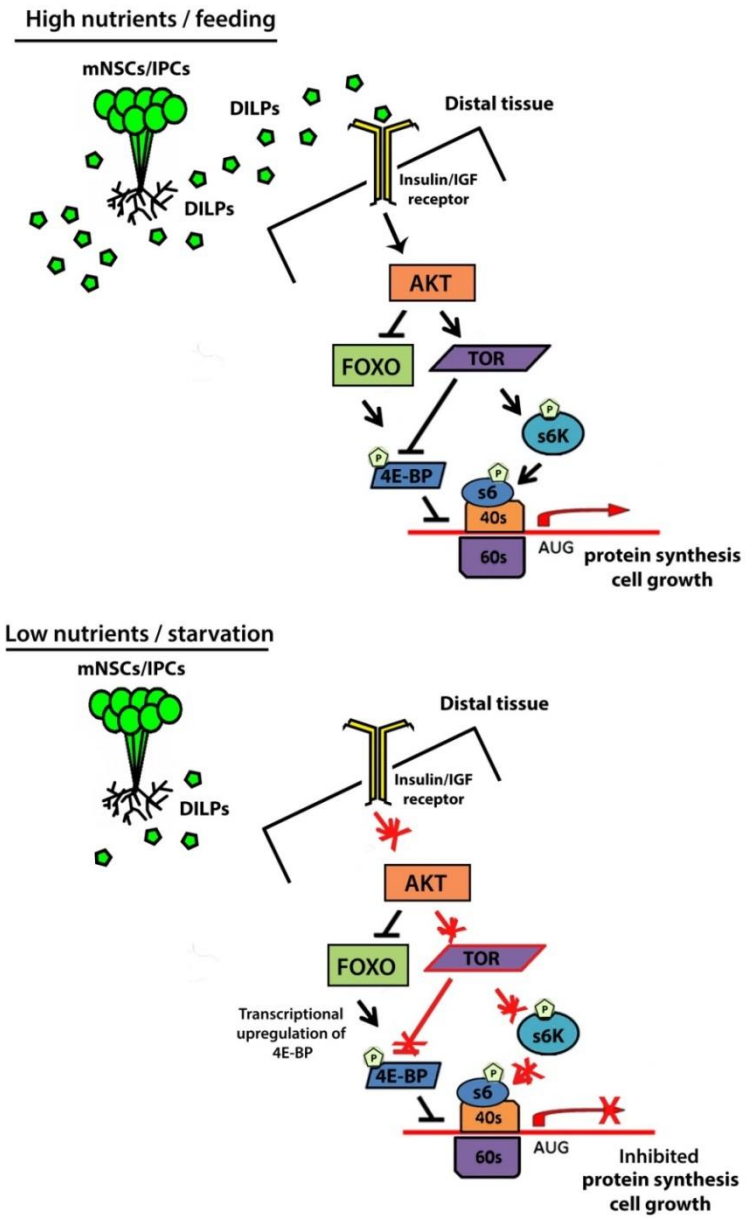

Figure 4-1. Schematic of insulin-like signaling in response to nutrition in the fly.

Under normal feeding conditions, DILPs are released from the IPCs of the *Drosophila* brain into the hemolymph of the fly. DILPs can then bind Insulin-like/IGF receptor (InR) in distal tissues, signaling for increased downstream AKT kinase activity and repression of FOXO transcription factor activity and increased TOR kinase activity resulting in increased protein synthesis and systemic growth. Under poor nutritional conditions, lack of Insulin-like signaling allows for increased FOXO transcriptional activity and upregulation of the translational repressor 4E-BP, resulting in decreased protein synthesis and systemic growth.

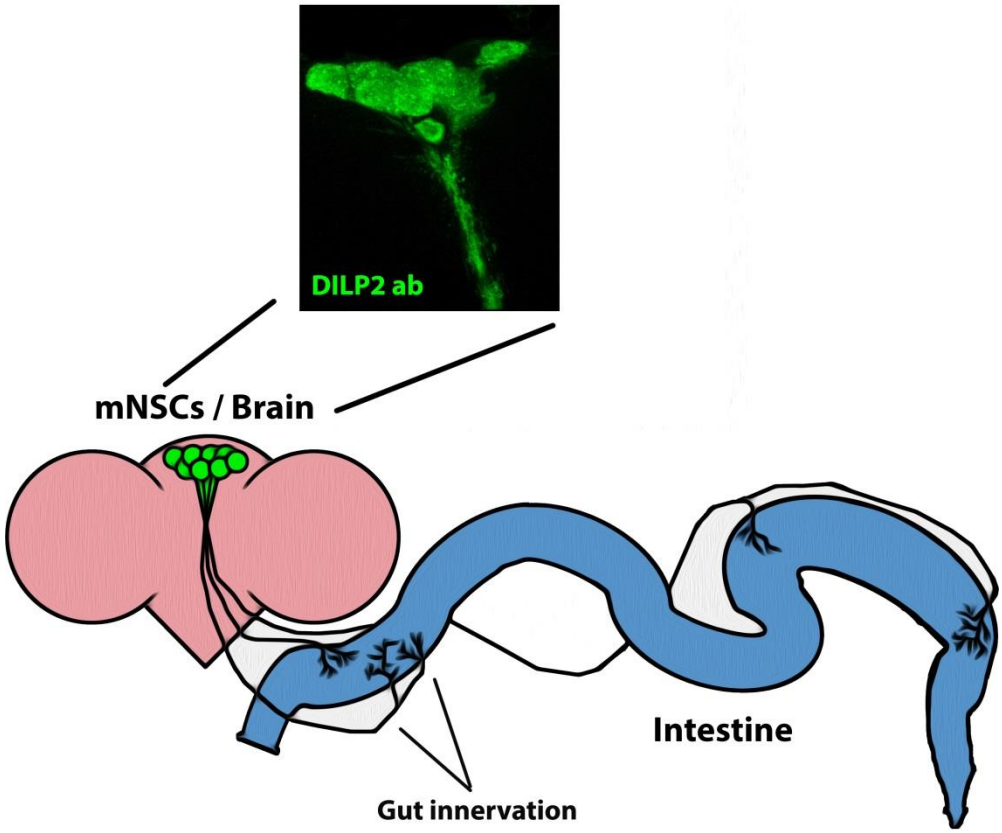

Figure 4-2. Diagram of median neurosecretory cells (mNSCs) of the *Drosophila* brain, and representative image of insulin-like peptide staining specific to insulin producing cells (IPCs) of the (mNSCs).

Neurons that specifically express and secrete *Drosophila* insulin-like peptides (DILPs) specifically innervate the gut and may play a role in the cell-non-autonomous physiological changes found in pan-neuronal AMPK and Atg1 expressing flies. Antibody staining of Dilp2 reveals staining specifically in the mNSCs, secreted DILP peptides may also play a role in AMPK/Atg1 mediated organ to organ communication.

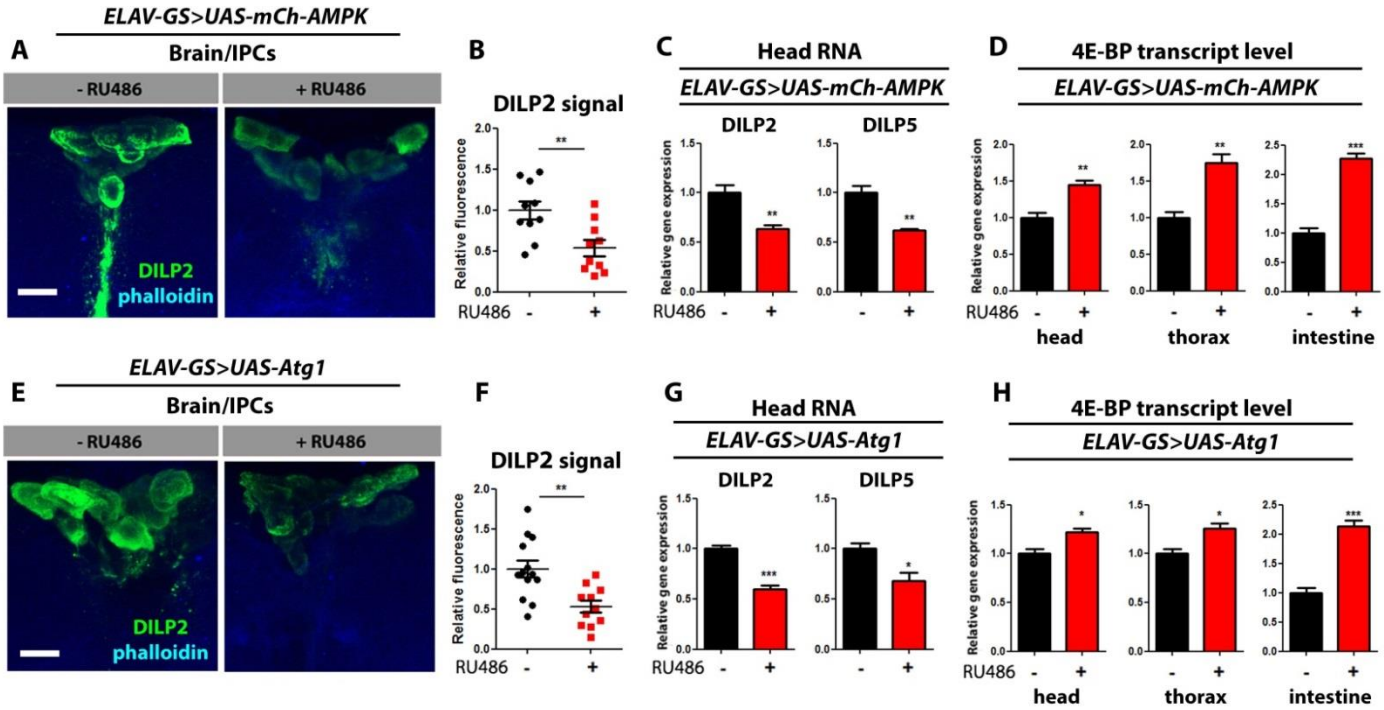

Figure 4-3. Neuronal AMPK and Atg1 expression represses systemic insulin signaling.

(A) Representative images of DILP2 antibody stained insulin producing cells (IPCs) from 10 day old female *ELAV-GS>UAS-mCh-AMPK* flies *(green channel – Dilp2 antibody, blue channel – phalloidin, scale bars represent 10μm).*

(B) Quantification of DILP2 fluorescence from IPCs of 10 day old female *ELAV-GS>UAS-mCh-AMPK* flies. Neuronal AMPK expression significantly reduced DILP2 signal in IPCs *(p<0.01; t-test; n>10 brains/condition).*

(C) Expression level of Dilp genes from dissected heads of *ELAV-GS>UAS-mCh-AMPK* female flies at 10 days of adulthood. Upregulation of AMPK in neurons significantly decreased Dilp2 and Dilp5 transcript levels in head tissue (*p<0.01; t-test; n>3 of RNA extracted from 10 heads /replicate*).

(D) Expression level of 4E-BP from dissected body parts of *ELAV-GS>UAS-mCh-AMPK* female flies at 10 days of adulthood. Neuronal induction of AMPK significantly increased 4E-BP transcript in the indicated tissues (*p<0.01; t-test; n=3 of RNA extracted from 10 body parts/replicate*).

(E) Representative images of DILP2 antibody stained IPCs from 10 day old female *ELAV-GS>UAS-Atg1* flies *(green channel – Dilp2 antibody, blue channel – phalloidin, scale bars represent 10μm).*

(F) Quantification of DILP2 fluorescence from IPCs of 10 day old female *ELAV-GS>UAS-Atg1* flies. Neuronal Atg1 expression significantly reduced DILP2 signal in IPCs *(p<0.01; t-test; n>10 brains/condition).*

(G) Expression level of Dilp genes from dissected heads of *ELAV-GS>UAS-Atg1* female flies at 10 days of adulthood. Upregulation of Atg1 in neurons significantly decreased Dilp2 and Dilp5 transcript levels in head tissue (*p<0.05; t-test; n>3 of RNA extracted from 10 heads /replicate*).

(H) Expression level of 4E-BP from dissected body parts of *ELAV-GS> UAS-Atg1* female flies at 10 days of adulthood. Neuronal induction of Atg1 significantly increased 4E-BP transcript in the indicated tissues (*p<0.05; t-test; n=3 of RNA extracted from 10 body parts/replicate*).

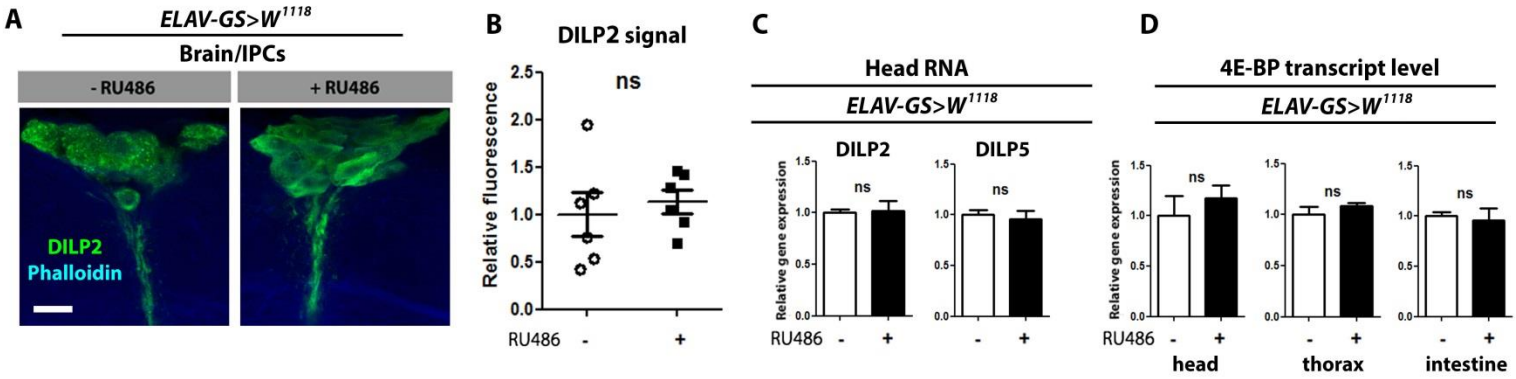

Figure 4-4. RU486 feeding has no effect on insulin-like signaling in control flies.

(A) Representative images of DILP2 antibody stained insulin producing cells (IPCs) from 10 day old female *ELAV-GS>W^{1118}* flies *(green channel – Dilp2 antibody, blue channel – phalloidin, scale bars represent 10 μm).*

(B) Quantification of DILP2 fluorescence from insulin producing cells of 10 day old female *ELAV-GS>W^{1118}* flies. RU486 feeding had no effect on the relative fluorescence of Dilp2 in IPCs *(p>0.05; t-test; n>6 brains/condition).*

(C) Expression level of Dilp genes from dissected heads of *ELAV-GS>W^{1118}* female control flies at 10 days of adulthood. RU486 feeding showed no difference in the levels of Dilp2, or Dilp5 RNA (*p>0.05; t-test; n=3 of RNA extracted from 10 heads /replicate*).

(D) Expression level of 4E-BP from dissected body parts of *ELAV-GS>W^{1118}* female control flies at 10 days of adulthood. RU486 feeding showed no difference in the levels 4E-BP RNA in the indicated tissues (*p>0.05; t-test; n=3 of RNA extracted from 10 body parts/replicate*).

REFERENCES:

1. Rajan, A., & Perrimon, N. (2011). Drosophila as a model for interorgan communication: lessons from studies on energy homeostasis. *Developmental Cell*, *21*(1), 29–31. doi:10.1016/j.devcel.2011.06.034

2. Broughton, S. J., Piper, M. D. W., Ikeya, T., Bass, T. M., Jacobson, J., Driege, Y., … Partridge, L. (2005). Longer lifespan, altered metabolism, and stress resistance in Drosophila from ablation of cells making insulin-like ligands. *Proceedings of the National Academy of Sciences of the United States of America*, *102*(8), 3105–10. doi:10.1073/pnas.0405775102

3. Broughton, S. J., Slack, C., Alic, N., Metaxakis, A., Bass, T. M., Driege, Y., & Partridge, L. (2010). DILP-producing median neurosecretory cells in the Drosophila brain mediate the response of lifespan to nutrition. *Aging Cell*, *9*(3), 336–46. doi:10.1111/j.1474-9726.2010.00558.x

4. Nässel, D. R., Kubrak, O. I., Liu, Y., Luo, J., & Lushchak, O. V. (2013). Factors that regulate insulin producing cells and their output in Drosophila. *Frontiers in Physiology*, *4*, 252. doi:10.3389/fphys.2013.00252

5. Partridge, L., Alic, N., Bjedov, I., & Piper, M. D. W. (2011). Ageing in Drosophila: the role of the insulin/Igf and TOR signalling network. *Experimental Gerontology*, *46*(5), 376–81. doi:10.1016/j.exger.2010.09.003

6. Hwangbo, D. S., Gershman, B., Gersham, B., Tu, M.-P., Palmer, M., & Tatar, M. (2004). Drosophila dFOXO controls lifespan and regulates insulin signalling in brain and fat body. *Nature*, *429*(6991), 562–6. doi:10.1038/nature02549

7. Demontis, F., & Perrimon, N. (2010). FOXO/4E-BP signaling in Drosophila muscles regulates organism-wide proteostasis during aging. *Cell*, *143*(5), 813–25. doi:10.1016/j.cell.2010.10.007

8. Broughton, S., Alic, N., Slack, C., Bass, T., Ikeya, T., Vinti, G., … Partridge, L. (2008). Reduction of DILP2 in Drosophila triages a metabolic phenotype from lifespan revealing redundancy and compensation among DILPs. *PloS One*, *3*(11), e3721. doi:10.1371/journal.pone.0003721

9. Cognigni, P., Bailey, A. P., & Miguel-Aliaga, I. (2011). Enteric neurons and systemic signals couple nutritional and reproductive status with intestinal homeostasis. *Cell Metabolism*, *13*(1), 92–104. doi:10.1016/j.cmet.2010.12.010

10. Zhang, H., Liu, J., Li, C. R., Momen, B., Kohanski, R. A., & Pick, L. (2009). Deletion of Drosophila insulin-like peptides causes growth defects and metabolic abnormalities. *Proceedings of the National Academy of Sciences of the United States of America*, *106*(46), 19617–22. doi:10.1073/pnas.0905083106

11. Tatar, M., Kopelman, A., Epstein, D., Tu, M. P., Yin, C. M., & Garofalo, R. S. (2001). A mutant Drosophila insulin receptor homolog that extends life-span and impairs neuroendocrine function. *Science (New York, N.Y.)*, *292*(5514), 107–10. doi:10.1126/science.1057987

12. Clancy, D. J., Gems, D., Harshman, L. G., Oldham, S., Stocker, H., Hafen, E., … Partridge, L. (2001). Extension of life-span by loss of CHICO, a Drosophila insulin receptor substrate protein. *Science (New York, N.Y.)*, *292*(5514), 104–6. doi:10.1126/science.1057991

13. Bai, H., Kang, P., Hernandez, A. M., & Tatar, M. (2013). Activin signaling targeted by insulin/dFOXO regulates aging and muscle proteostasis in Drosophila. *PLoS Genetics*, *9*(11), e1003941. doi:10.1371/journal.pgen.1003941

14. Greer, E. L., Oskoui, P. R., Banko, M. R., Maniar, J. M., Gygi, M. P., Gygi, S. P., & Brunet, A. (2007). The energy sensor AMP-activated protein kinase directly regulates the mammalian FOXO3 transcription factor. *The Journal of Biological Chemistry*, *282*(41), 30107–19. doi:10.1074/jbc.M705325200

15. Greer, E. L., Dowlatshahi, D., Banko, M. R., Villen, J., Hoang, K., Blanchard, D., … Brunet, A. (2007). An AMPK-FOXO pathway mediates longevity induced by a novel method of dietary restriction in C. elegans. *Current Biology : CB*, *17*(19), 1646–56. doi:10.1016/j.cub.2007.08.047

16. Slack, C., Giannakou, M. E., Foley, A., Goss, M., & Partridge, L. (2011). dFOXO-independent effects of reduced insulin-like signaling in Drosophila. *Aging Cell*, *10*(5), 735–48. doi:10.1111/j.1474-9726.2011.00707.x

17. Alic, N., Tullet, J. M., Niccoli, T., Broughton, S., Hoddinott, M. P., Slack, C., … Partridge, L. (2014). Cell-nonautonomous effects of dFOXO/DAF-16 in aging. *Cell Reports*, *6*(4), 608–16. doi:10.1016/j.celrep.2014.01.015

CHAPTER V:

INTESTINE-SPECIFIC AMPK ACTIVATION EXTENDS LIFESPAN AND INDUCES SYSTEMIC AUTOPHAGY

Neuronal exogenous AMPK overexpression causes a systemic increase in endogenous AMPK phosphorylation and subunit expression

In the previous chapters we have shown that neuronal AMPK activation is sufficient to suppress insulin signaling which may lead to a cell non-autonomous regulation of tissue aging. To better understand if endogenous AMPK is involved in mediating this upregulation in autophagy downstream of its function in insulin suppression, we performed QPCR for endogenous transcripts of AMPK subunits in RNA extracted from the intestine and thorax of flies with neuronal AMPK overexpression **(Fig. 5-1 A, C)**. Surprisingly, endogenous transcripts for AMPK subunits are significantly upregulated in the distal tissues of the fly. Furthermore, endogenous AMPK is phosphorylated to a greater degree, than the uninduced controls**(Fig. 5-1 B, D)**. This indicates that endogenous AMPK activity is increased in these distal tissues, in flies overexpressing transgenic AMPK in neurons**.** Feeding RU486 to *ElavGS* control flies did not alter the expression of endogenous AMPK subunits in distal tissues **(Fig. 5-2A,B)**. It could then be hypothesized that this cell-non-autonomous upregulation of endogenous AMPK, upon exogenous AMPK expression in neurons, is partly responsible for AMPK-mediated lifespan extension.

Intestine-specific AMPK activation extends lifespan and induces autophagy cell-autonomously

To better understand the relationships between exogenous AMPK upregulation in neurons creating a systemic increase in active endogenous AMPK, we set out to determine whether AMPK up-regulation in the intestine alone was sufficient to activate autophagy in the target tissue and/or prolong lifespan. To do so, we utilized the intestine-specific Gene-Switch (GS) driver line *TIGS-2* [1] to activate *UAS-mCh-AMPK*. To validate the tissue-specificity of *TIGS-2*, we examined the expression of the exogenous AMPK transgene in heads, thoraces, and

intestines, in *TIGS-2>UAS*-mCh-AMPK flies with and without RU486 induction **(Fig. 5-3A)**. Only RNA isolated from intestinal tissue showed a significant RU486-dependant increase in exogenous AMPK transcript**.** Furthermore, Western blot analysis of lysates from different tissues of *TIGS-2>UAS-eGFP* flies also showed a visible RU486-dependent increase in GFP levels in intestinal tissue **(Fig 5-3B).**

To determine if transgenic AMPK overexpression in the intestine is able to increase the expression and activation of endogenous AMPK subunits in the intestine, we overexpressed AMPK via the *TIGS-2* driver and monitored the expression of endogenous AMPK subunits via QPCR **(Fig. 5-4A).** Similar to neuronal AMPK expression, exogenous upregulation of AMPK in the intestine increased the abundance of endogenous AMPK transcripts. Additionally, exogenous AMPK overexpression in the intestine also increased the total amount of active phosphorylated AMPK as viewed by western blot **(Fig. 5-4b and quantification, right).** Unexpectedly, the amount of endogenous AMPK that is phosphorylated increased as well. RU486 treatment of control *TIGS-2* flies did not influence endogenous AMPK expression levels **(Fig. 5-5A).**

After confirming the tissue specificity and phosphorylation state of AMPK overexpressed in the intestine via the *TIGS-2* driver, several rounds of lifespan analysis were conducted. Adult-onset, intestine-specific up-regulation of AMPK resulted in increased median and maximum lifespan in female flies by approximately 30% **(Fig. 5-6A)** with a smaller lifespan increase in male flies **(Table A1)**. To determine whether exogenous overexpression of AMPK was sufficient to improve tissue homeostasis in the aging intestine, we examined intestinal integrity as a function of age. Importantly, we observed a delay in the onset of intestinal barrier dysfunction in *TIGS-2>UAS-mCh-AMPK* flies upon RU486 treatment compared to uninduced controls **(Fig. 5-6B).** Next, we examined markers of autophagy in response to up-regulation of

AMPK in the intestine. The levels of autophagy-related genes, *Atg1*, *Atg8a*, and *Atg8b*, were significantly increased in intestinal tissue from *TIGS-2>UAS-mCh-AMPK* flies upon RU486 treatment **(Fig. 5-6C).** Moreover, using *pGFP-Atg8a*, we observed a significant increase in GFP puncta in the posterior mid-gut enterocytes of *TIGS-2>UAS-mCh-AMPK* flies upon RU486 treatment compared to uninduced controls **(Fig. 5-6D, quantification 5-6E).** Upregulation of AMPK in the intestine also significantly increased the amount of lysosomal foci found in the mid-gut enterocytes as marked by the acidophilic dye lysotracker **(Fig. 5-4F, quantification 5-6G).** To further validate this upregulation in autophagy, live imaging of lysotracker, and pGFP-atg8a was performed simultaneously on dissected intestines of *TIGS-2>UAS-mCh-AMPK* with or without RU486 feeding **(Fig. 5-7).** The density of GFP-Atg8a, Lysotracker, and colocalized vesicles, were all increased upon AMPK activation **(Fig. 5-7B).** Feeding RU486 to control flies did not affect lifespan, intestinal barrier dysfunction, Atg transcript levels in intestinal tissue, autophagosome formation or lysosomal foci **(Fig. 5-8).** Taken together, these findings indicate that intestine-specific up-regulation of AMPK induces autophagy and maintains intestinal homeostasis during aging, which is associated with increased lifespan at the organismal level.

Overexpression of AMPK in the intestine causes increased heat and oxidative stress tolerance, but sensitizes flies to starvation

As was the case with neuronal AMPK-mediated longevity, long-lived flies overexpressing AMPK in the intestine did not show reduced feeding behavior or fecundity **(Fig. 5-9A, B, C).** However, intestine-specific AMPK overexpression did confer sensitivity to starvation conditions, including early-onset mortality **(Fig. 5-9F)**, rapid loss of body weight **(Fig. 5-9G)** and TAG stores **(Fig. 5-9H)** . Additionally, AMPK activation in gut tissue increased tolerance to both hyperoxia **(Fig. 5-9D)** and heat stress **(Fig. 5-9E).** Feeding RU486 to control flies did not affect feeding, fecundity or sensitivity to stress conditions **(Fig. 5-10).**

Intestine-specific AMPK upregulation increases endogenous AMPK expression in the thorax and slows muscle aging.

As neuronal expression of exogenous AMPK can cause a systemic increase in endogenous AMPK expression and activation, we sought to confirm if this phenomenon can travel from the gut to the thoracic muscle of the fly. Monitoring the expression of endogenous AMPK subunits via QPCR, we found that intestinal overexpression of exogenous AMPK is sufficient to increase endogenous AMPK transcript abundance in the thorax **(Fig. 5-11A).** Likewise, the quantity of phosphorylated active AMPK is also increased in the thoracic muscle **(Fig. 5-11B).** RU486 treatment of control flies did not alter endogenous AMPK gene expression in the thorax **(Fig. 5-12).**

To further explore the cell-non-autonomous consequences of up-regulating AMPK in the intestine, we set out to examine markers of muscle aging. Upregulation of AMPK in the intestine significantly reduces levels of protein aggregates during muscle aging **(Fig. 5-13A, quantification Fig. 5-13B).** Consistent with the immunofluorescence data, we observed reduced levels of insoluble ubiquitinated proteins by Western blot in the aged muscle of flies with intestinal AMPK activation **(Fig.5-13C, and quantification Fig. 5-13D)** with improved climbing ability during aging **(Fig. 5-13E)**. Additionally, these reduced markers of muscle aging are associated with an increase in Autophagy-related gene expression in the thorax muscle **(Fig. 5-13F).** Feeding RU486 to control flies did not affect protein homeostasis during muscle aging, or ATG transcript levels in thoracic tissue (**Fig. 5-14).** Taken together, these findings indicate that intestine-specific AMPK activation can maintain protein homeostasis during muscle aging, which is associated with reduced levels of proteotoxicity in aged muscles.

Activation of AMPK in the intestine causes a cell-non-autonomous upregulation of autophagy in the brain.

As transgenic up-regulation of AMPK in the adult nervous system can increase markers of endogenous AMPK activation and autophagy in the intestine, we wanted to assess the converse by up-regulating AMPK in the intestine followed by monitoring AMPK activation and autophagy markers in the brain. Firstly, we determined the levels of endogenous AMPK subunits in the brain by QPCR **(Fig. 5-15A).** As with other tissues of the fly, upregulation of AMPK in the intestine increased endogenous AMPK transcripts and phosphorylation in brain tissues **(Fig. 5-15B)**. Feeding RU486 to control flies did not influence endogenous AMPK levels **(Fig.5-16).**

To evaluate the effects of intestine-specific exogenous AMPK expression on brain autophagy markers, we monitored ATG gene expression in RNA extracted from heads of 10 day old female flies. Interestingly, *Atg1*, *Atg8a*, and *Atg8B* were moderately increased in head tissue upon intestine-specific up-regulation of AMPK **(Fig. 5-17A).** To extend these findings, we examined the transgenic autophagosome marker, *pGFP-Atg8a,* in the brain of flies with and without intestine-specific AMPK induction. In doing so, we observed a significant increase in GFP puncta in brain tissue of *TIGS-2>UAS-mCh-AMPK* flies upon RU486 treatment compared to uninduced controls **(Fig. 5-17A, quantification Fig. 5-17B).** Feeding RU486 to control flies did not affect ATG transcript levels, and GFP-Atg8a foci formation in head tissue **(Fig 5-18).** These findings indicate that targeted up-regulation of AMPK in adult intestinal cells can induce autophagy in brain tissue.

Intestine-specific upregulation of AMPK is sufficient to suppress insulin-like signaling contributing to cell-non-autonomous changes in physiology

As neuronal AMPK overexpression can directly suppress DILP gene expression resulting in cell-non-autonomous increases in autophagy and slowed aging, we wanted to address whether intestinal AMPK activation could also impact DILP levels in the brain and/or systemic 4E-BP expression. We observed a significant decrease in DILP2 in the IPCs of *TIGS-2>UAS-mCh-AMPK* flies upon RU486 treatment **(Fig. 5-19A, quantification Fig. 5-19B)** and a decrease in both *dilp2* and *dilp5* mRNAs in head tissue **(Fig. 5-19C).** Furthermore, *4E-BP* transcript levels were increased in the head, thorax and intestine upon intestinal AMPK activation **(5-19D).** Feeding RU486 to control flies did not affect DILP levels or 4E-BP expression **(Fig 5-20).**

Intestine-specific AMPK-mediated lifespan extension is dependent upon Atg1.

To determine if the lifespan extension of AMPK overexpression in the gut is dependent upon Atg1 gene expression levels, epistasis analysis was conducted by simultaneously overexpressing AMPK and knockdown of Atg1. All lines were back-crossed into W^{1118}/ cyo. To confirm, AMPK overexpression in the intestine is sufficient to increase organismal lifespan in this genetic background *TIGS-2>UAS-AMPK* flies were monitored for survival with or without RU486-mediated transgene induction **(Fig. 5-21 A).** Consistent with previous data, AMPK activation in the intestine resulted in an over 25% increase in median lifespan. Simultaneously overexpressing AMPK, while reducing Atg1 levels via RNAi resulted in no lifespan extension **(Fig. 5-21 B).** This result indicates that gut AMPK-mediated lifespan extension is dependent upon sufficient levels of Atg1. As a control, Atg1 was knocked down in the intestine alone, with no significant reduction in lifespan **(Fig. 5-21 C).** To determine if Atg1 overexpression in the intestine is sufficient to increase organismal lifespan, survival analysis was conducted on *TIGS-2>UAS-Atg1* female flies with or without RU486-mediated transgene induction **(Fig. 5-21 D).**

Contrary to when Atg1 is overexpressed in neurons, intestine-specific upregulation of Atg1 resulted in toxicity and decreased lifespan.

Summary.

In this chapter we have shown, that specific overexpression of transgenic AMPK in neuronal tissue is sufficient to increase endogenous AMPK levels and activation throughout the fly. Intestine-specific activation of AMPK is sufficient to delay tissue aging in the muscle, and intestine. This delayed tissue aging is accompanied by a systemic induction of autophagy, and extended longevity **(Schematic Summary in Fig. 5-22).**. These alterations are also linked to a decrease in markers of insulin signaling, resulting in 4E-BP transcript increase in the distal tissues of the fly. Simply expressing AMPK in one organ system of the fly is able to transduce an increase in autophagy and anti-aging effects to distal tissues. This delay in mortality is dependent upon sufficient levels of Atg1, but Atg1 overexpression in the intestine alone is inadequate to increase lifespan of *Drosophila*.

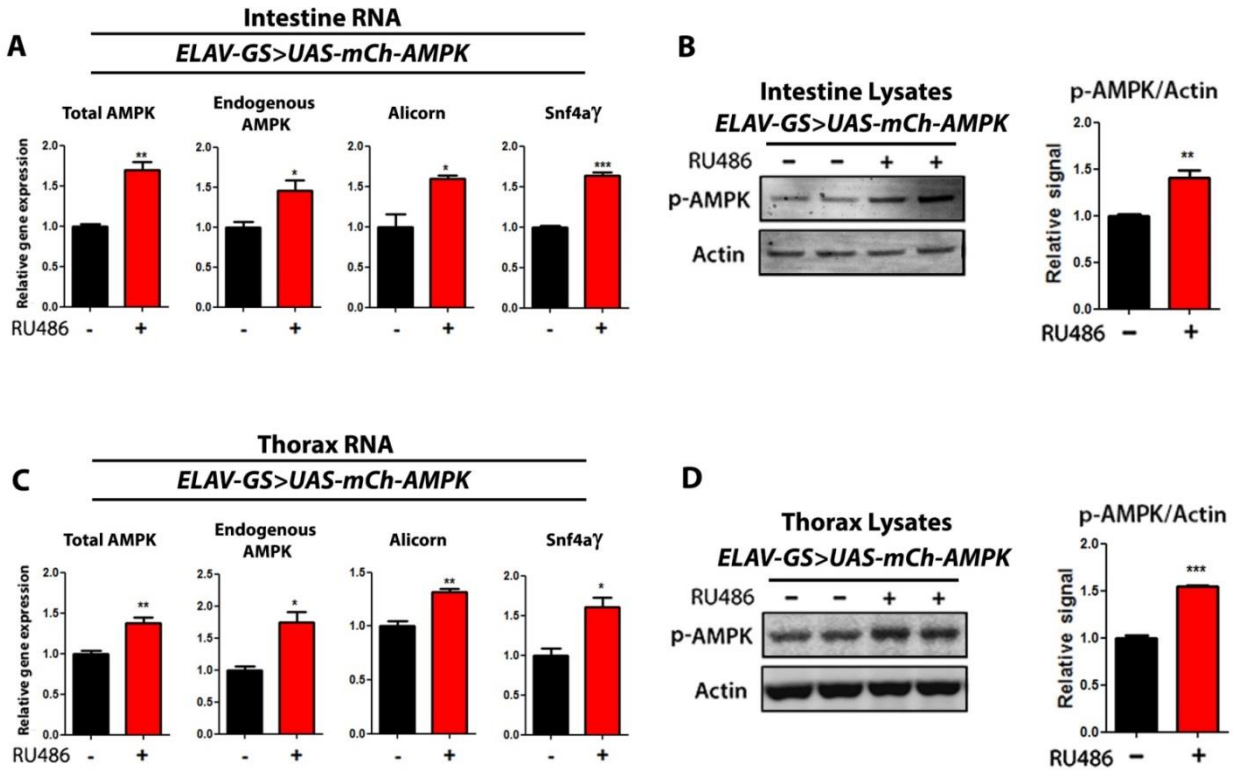

Figure 5-1. Overexpression of AMPK in neuronal tissue, increased transcript levels of endoegenous AMPK subunits, and endogenous AMPK phosphorylation in distal tissues.

(A) Transcript levels of total AMPK and endogenous subunits in the intestine, upon neuron-specific overexpression of AMPK. RNA was extracted from female flies at 10 days of age. Total levels of AMPK, endogenous AMPK, Alicorn, and Snf4aγ are significantly increased upon RU486 transgene induction (*p<0.05; t-test; n=3, of RNA extracted from 10 intestines/replicate*).

(B) Western blot analysis of AMPK phosphorylated on T184 (p-AMPK) and loading control (actin) from intestine lysates of 10 day old female *ELAV-GS>UAS-mCh-AMPK* with or without RU486-mediated transgene induction. Upregulation of AMPK in neurons significantly increased phosphorylated AMPK in gut tissue. Densitometry quantification (right) (*p<0.01; t-test; n=4 replicates; 10 intestines/replicate*).

(C) Transcript levels of total AMPK and endogenous subunits in thorax tissue, upon neuron-specific overexpression of AMPK. RNA was extracted from female flies at 10 days of age. Total levels of AMPK, endogenous AMPK, Alicorn, and Snf4aγ are significantly increased upon RU486 transgene induction (*p<0.05; t-test; n=3, of RNA extracted from 10 intestines/replicate*).

(D) Western blot analysis of AMPK phosphorylated on T184 (p-AMPK) and loading control (actin) from thorax lysates of 10 day old female *ELAV-GS>UAS-mCh-AMPK* with or without RU486-mediated transgene induction. Upregulation of AMPK in neurons significantly increased phosphorylated AMPK in thorax tissue. Densitometry quantification (right) (*p<0.001; t-test; n=4 replicates; 10 intestines/replicate*).

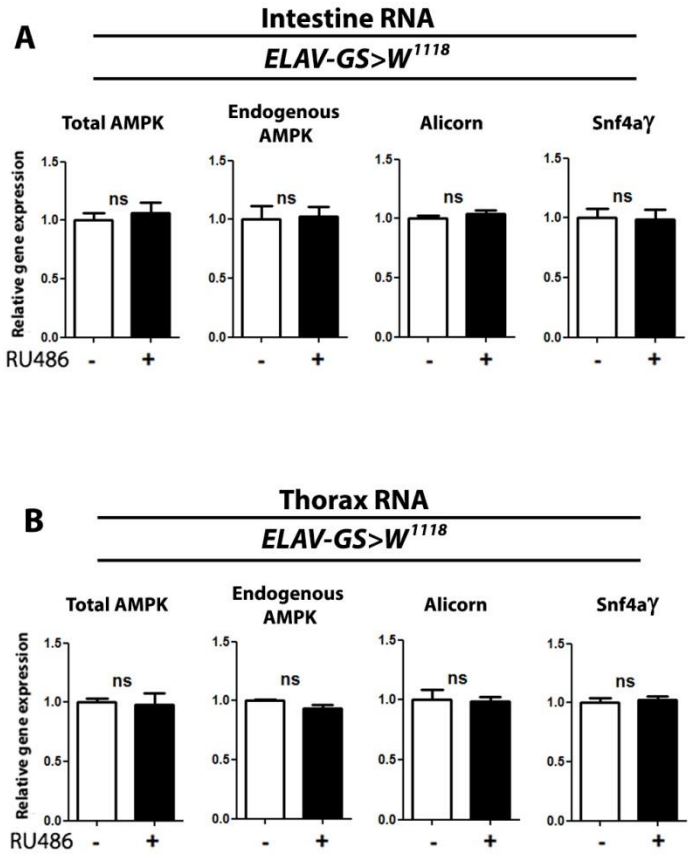

Figure 5-2. RU486 feeding does not influence expression of AMPK subunits.

(A) Transcript levels of total AMPK and endogenous subunits upon RU486 feeding to control flies. RNA was extracted from intestines of female flies at 10 days of age. Total levels of AMPK, endogenous AMPK, Alicorn, and Snf4aγ are not effected by RU486 treatment of control strains (*p<0.01; t-test; n=3, of RNA extracted from 10 heads/replicate*).

(B) Transcript levels of total AMPK and endogenous subunits upon RU486 feeding to control flies. RNA was extracted from thoraces of female flies at 10 days of age. Total levels of AMPK, endogenous AMPK, Alicorn, and Snf4aγ are not effected by RU486 treatment of control strains (*p<0.01; t-test; n=3, of RNA extracted from 10 heads/replicate*).

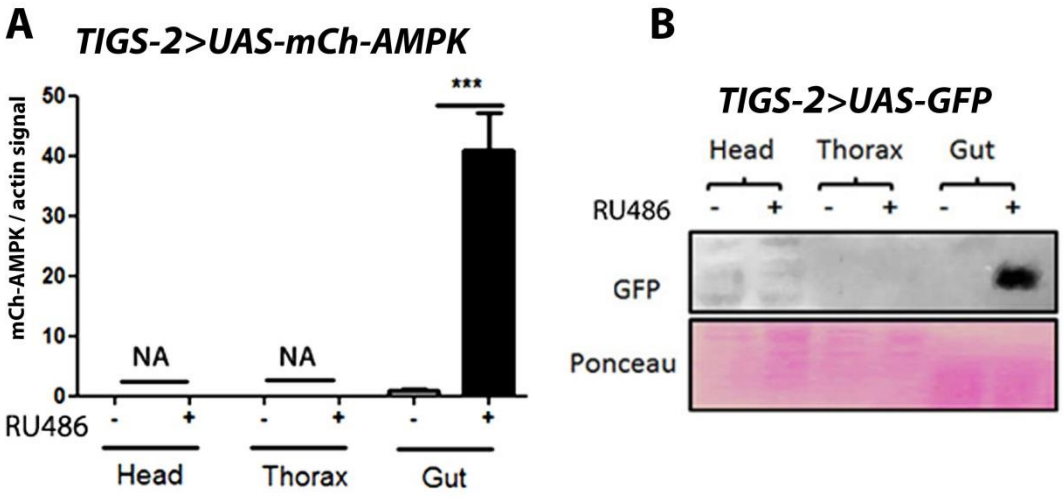

Figure 5-3. Expression specificity for *TIGS-2* driver.

(A) Exogenous mCherry-tagged AMPK expression levels of RNA extracted from body parts of *TIGS-2>UAS-mCH-AMPK* female flies at 10 days of age. Statistically significant increase in exogenous mCherry-AMPK is only detectable in the intestines of RU486 fed flies compared to uninduced controls. (*$p<0.001$; t-test; NA indicates "no amplification detectable after 45 cycles;" n=3 of RNA extracted from 10 body parts/replicate*)

(B) Western blot analysis for GFP and membrane stain for loading (Poncea S.) of protein extracted from body parts of *TIGS-2>UAS-eGFP* flies at 10 days of age. An RU486-dependent increase of GFP-signal was only observed in the intestines flies.

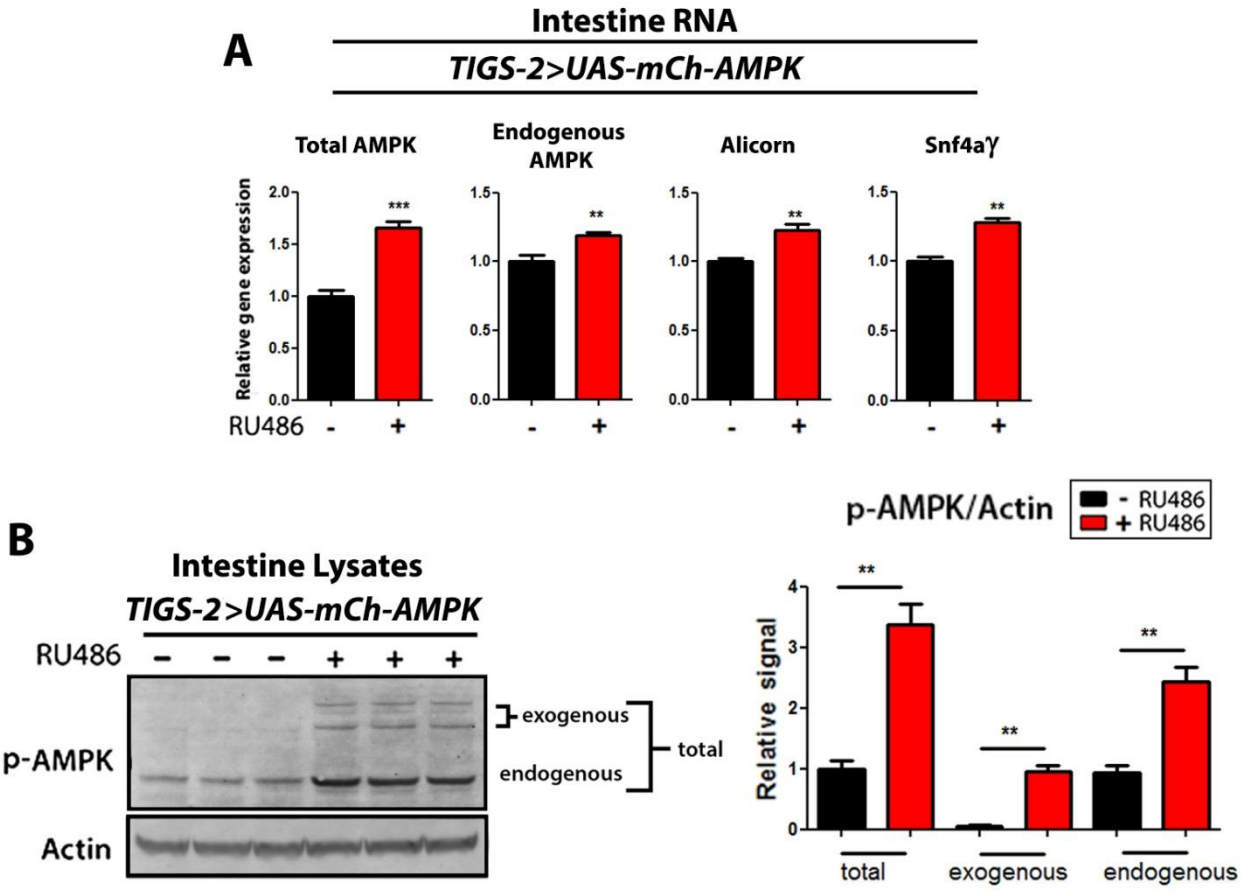

Figure 5-4. Overexpression of AMPK in the intestine, increased transcript levels of endoegenous AMPK subunits, and increased the amount of active phosphorylated AMPK.

(A) Transcript levels of total AMPK and endogenous subunits, upon intestine-specific overexpression of AMPK. RNA was extracted from female flies at 10 days of age. Total levels of AMPK, endogenous AMPK, Alicorn, and Snf4aγ are moderately increased upon RU486 transgene induction (*p<0.01; t-test; n=3, of RNA extracted from 10 heads/replicate*).

(B) Western blot analysis of AMPK phosphorylated on T184 (p-AMPK), and loading control (actin) from head lysates of 10 day old female *TIGS-2>UAS-mCH-AMPK* with or without RU486-mediated transgene induction. Densitometry quantification (right) shows that overexpression of exogenous mCherry-tagged AMPK is sufficiently phosphorylated to increase the total amount of phospho-AMPK present in head protein extracts. Additionally, the amount of endogenous AMPK is phosphorylated to higher degree (*p<0.01; t-test; n=3 replicates; 10 intestines/replicate*).

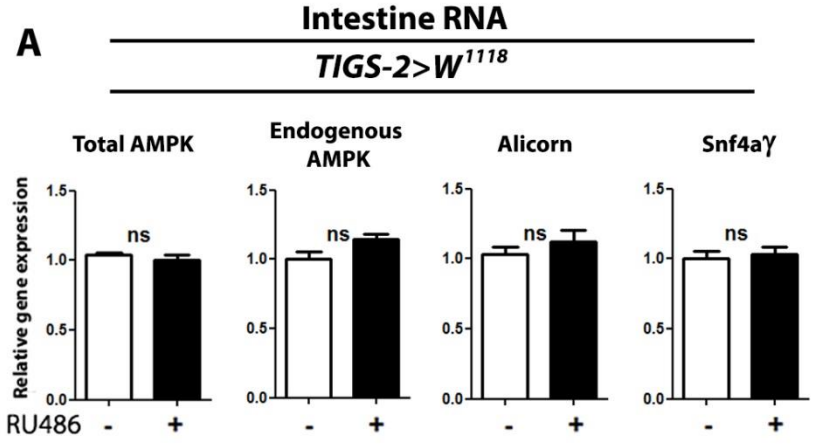

Figure 5-5. RU486 feeding does not influence expression of AMPK subunits in the *TIGS-2* genetic background.

(A) Transcript levels of total AMPK and endogenous subunits upon RU486 feeding to control flies. RNA was extracted from intestines of female flies at 10 days of age. Total levels of AMPK, endogenous AMPK, Alicorn, and Snf4aγ are not effected by RU486 treatment of control strains (*p<0.01; t-test; n=3, of RNA extracted from 10 intestines/replicate*).

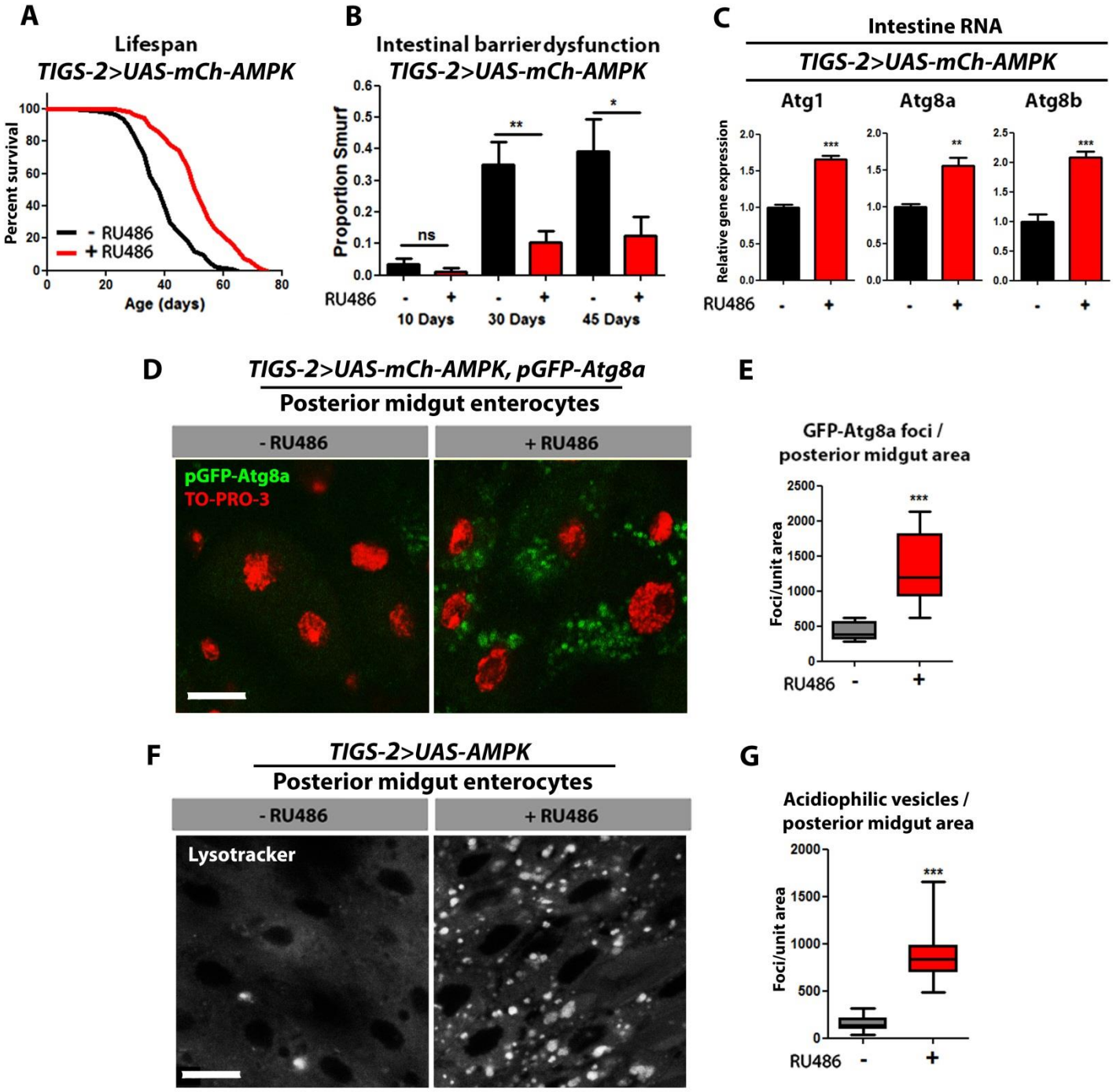

Figure 5-6. Intestinal AMPK activation extends lifespan and upregulates markers of autophagy.

(A) Survival curves of *TIGS-2>UAS-mCh-AMPK* females with or without RU486-mediated transgene induction. Intestine activation of AMPK significantly increased fly longevity (*p<0.0001; log-rank test; n>116 flies*).

(B) Intestinal integrity during aging in *TIGS-2>UAS-mCh-AMPK* females with or without RU486-mediated transgene induction. Overexpression of AMPK in the gut significantly reduced the proportion

of flies exhibiting intestinal barrier dysfunction with age (*p<0.01, at 30 days, p<0.05 at 45 days; binomial test; n>127 flies/condition*).

(C) Expression levels of autophagy genes in from intestines of *TIGS-2>UAS-mCH-AMPK* female flies at 10 days of adulthood. Upon gut-specific AMPK induction significantly increased Atg1, Atg8a, and Atg8b RNA levels are observed in the intestine (*t-test; n>3 of RNA extracted from 15 intestines/replicate*).

(D) GFP-Atg8a staining. Representative images of enterocytes from the posterior midgut of 10 day old *TIGS-2>UAS-mCh-AMPK, pGFP-Atg8a* females with or without RU486-mediated transgene expression (*red channel-TO-PRO-3 DNA stain, green channel-GFP-Atg8a, scale bar represents 10μm*).

(E) Quantification of posterior midgut pGFP-Atg8a foci. Gut-specific AMPK upregulation increased the amount of GFP-Atg8a puncta in gut enterocytes (*p<0.0001; t-test; n>10 confocal stacks from posterior midgut/condition; one fly per replicate stack*).

(F) Lysotracker Red staining. Representative images of posterior midgut enterocytes from 10 day old *TIGS-2>UAS-AMPK* females with or without RU486-mediated transgene induction (*scale bar represents 10μm*).

(G) Quantification of acidophilic vesicles. Gut-specific AMPK upregulation increased the amount of acidophilic foci in gut enterocytes (*p<0.0001; t-test; n>10 confocal stacks from posterior midgut/condition; one fly per replicate stack*).

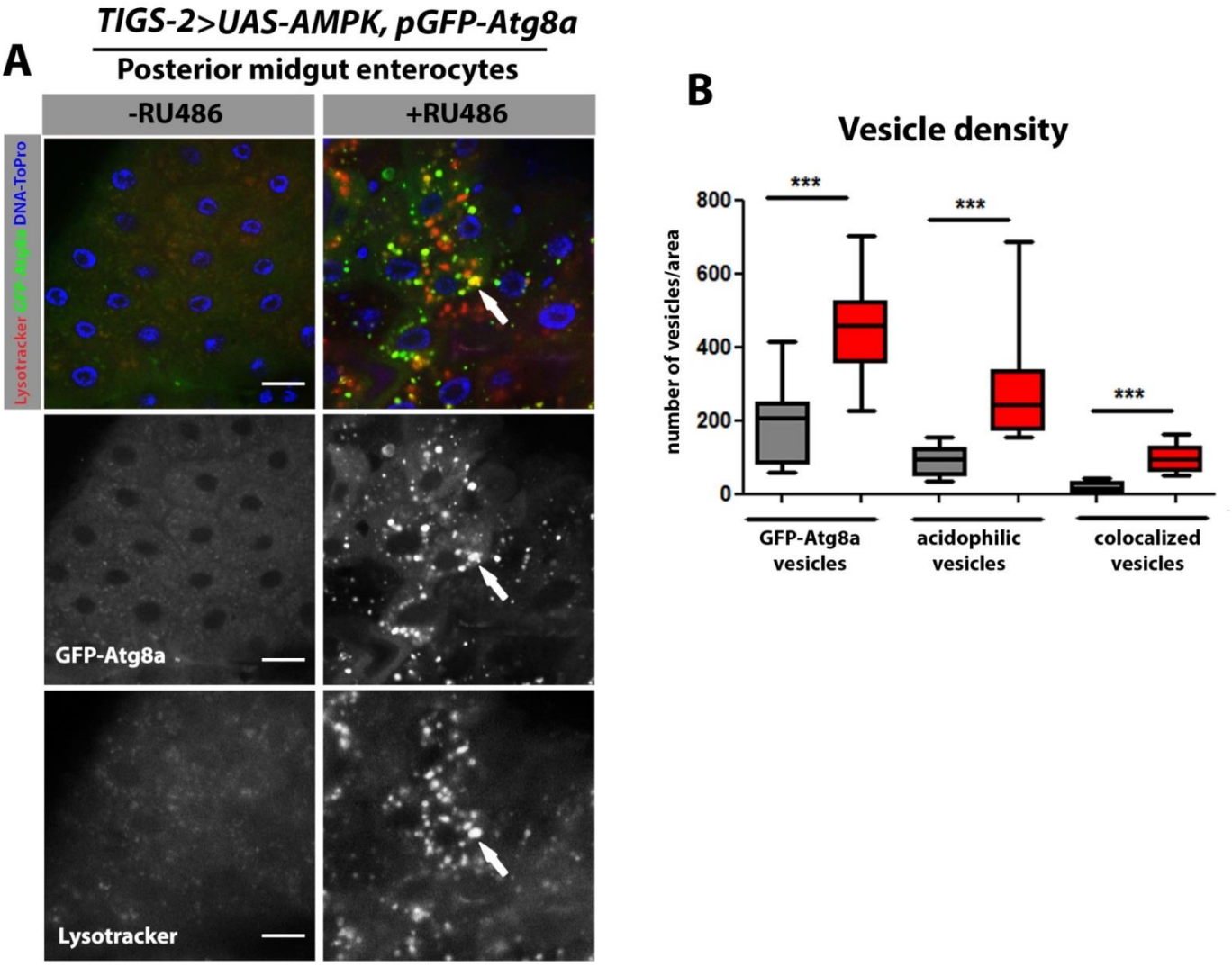

Figure 5-7. Intestine-specific AMPK activation causes an induction of autophagy when monitored via live imaging of dissected intestinal enterocytes.

(A) Representative images of enterocytes from the posterior midgut of 10 day old *TIGS-2>UAS-mCh-AMPK, pGFP-Atg8a* females with or without RU486-mediated transgene induction in neurons (*red channel-Lysotracker Red, blue channel-ToPro-3 DNA stain, green channel-GFP-Atg8a, scale bar represents 10μm, arrows indicate colocalized autolysosomes*).

(B) Quantification of acidophilic vesicles, GFP-atg8a vesicles, and colocalized "autolysosomal" vesicles/midgut area. Induction of AMPK in gut tissue increased density of GFP-atg8a vesicles, acidophilic vesicles, and colocalized vesicles compared to uninduced controls (*$p<0.001$; t-test; $n>10$ guts/condition*).

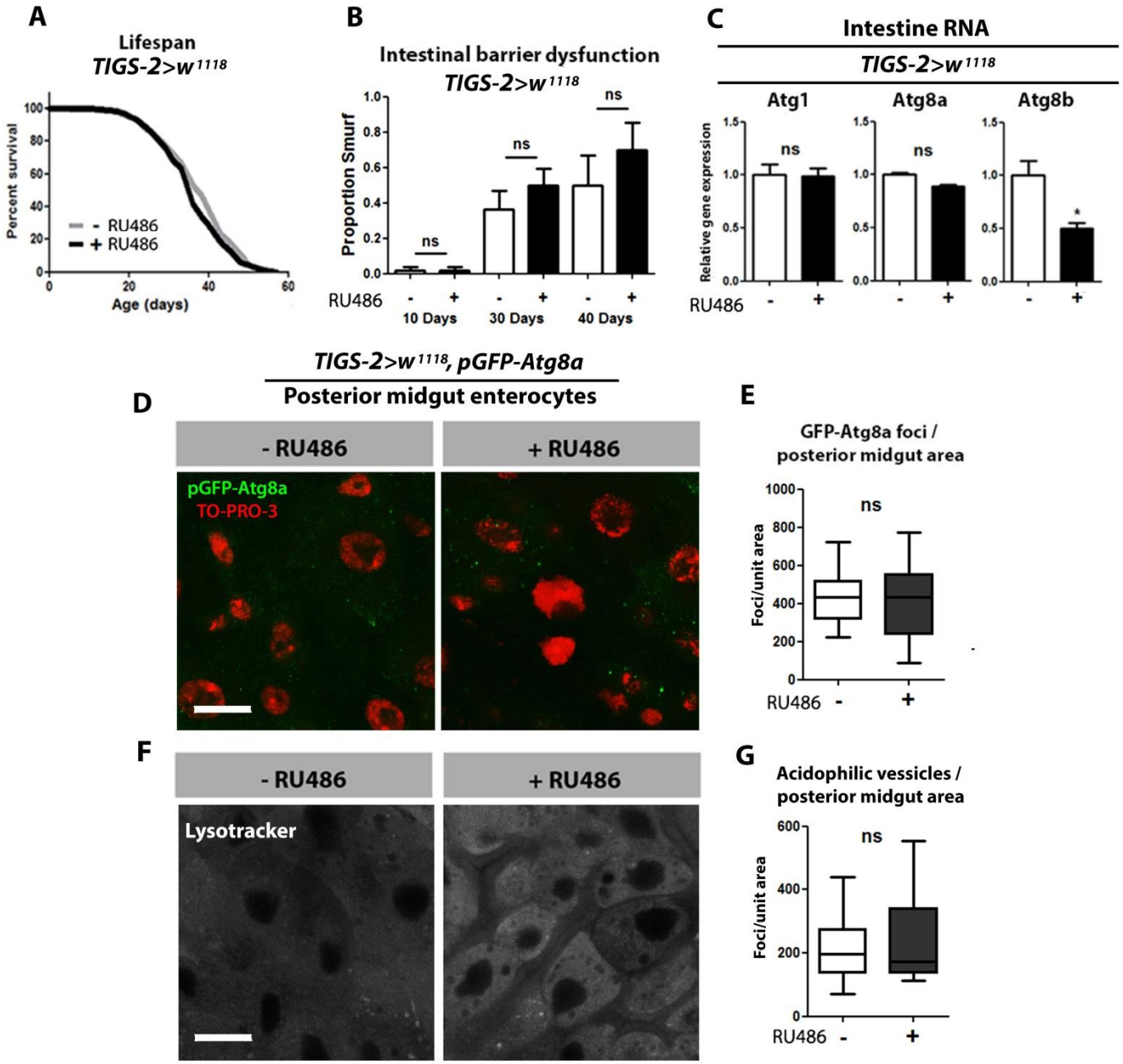

Figure 5-8. RU486 feeding does not influence aging and autophagy in the *TIGS-2* genetic background.

(A) Survival curves of *TIGS-2>W^{1118}* flies with or without RU486 feeding. There was no significant effect on the lifespan of control flies fed RU486 (*p>0.05*; *log-rank test; n>171 flies*).

(B) Intestinal integrity during aging in *TIGS-2>W^{1118}* controls. RU486 has no effect on the proportion of flies exhibiting intestinal barrier dysfunction (*p>0.05*; *binomial test; n>30 flies/condition*)

(C) Expression levels of autophagy genes from intestines of *TIGS-2>W^{1118}* control flies at 10 days of adulthood. RU486 feeding showed no significant increase Atg1, Atg8a, and Atg8b gene expression levels (*t-test; n=3 of RNA extracted from 15 intestines/replicate*)

(D) GFP atg8a foci staining. Representative images of enterocytes from the posterior midgut of 10 day old female *TIGS-2>W^{1118}, pGFP-Atg8a* flies fed RU486 and vehicle (*red channel-TO-PRO-3 DNA stain, green channel-GFP-Atg8a, scale bar represents 10μm*).

(E) Quantification of posterior midgut Atg8a foci. Control flies fed RU486 showed no difference in foci number (*p>0.05*; *t-test; n>10 confocal stacks from posterior midgut/condition, one fly per replicate stack*).

(F) Lysotracker Red staining. Representative images of posterior midgut enterocytes from 10 day old female *TIGS-2>W^{1118}* flies stained with the acidophilic dye.

(G) Quantification of acidophilic vesicles. Feeding control flies RU486 had no effect on the number of acidophilic vesicles (*p>0.05*; *t-test*; *n>10 confocal stacks from posterior midgut/condition, one fly per replicate stack*).

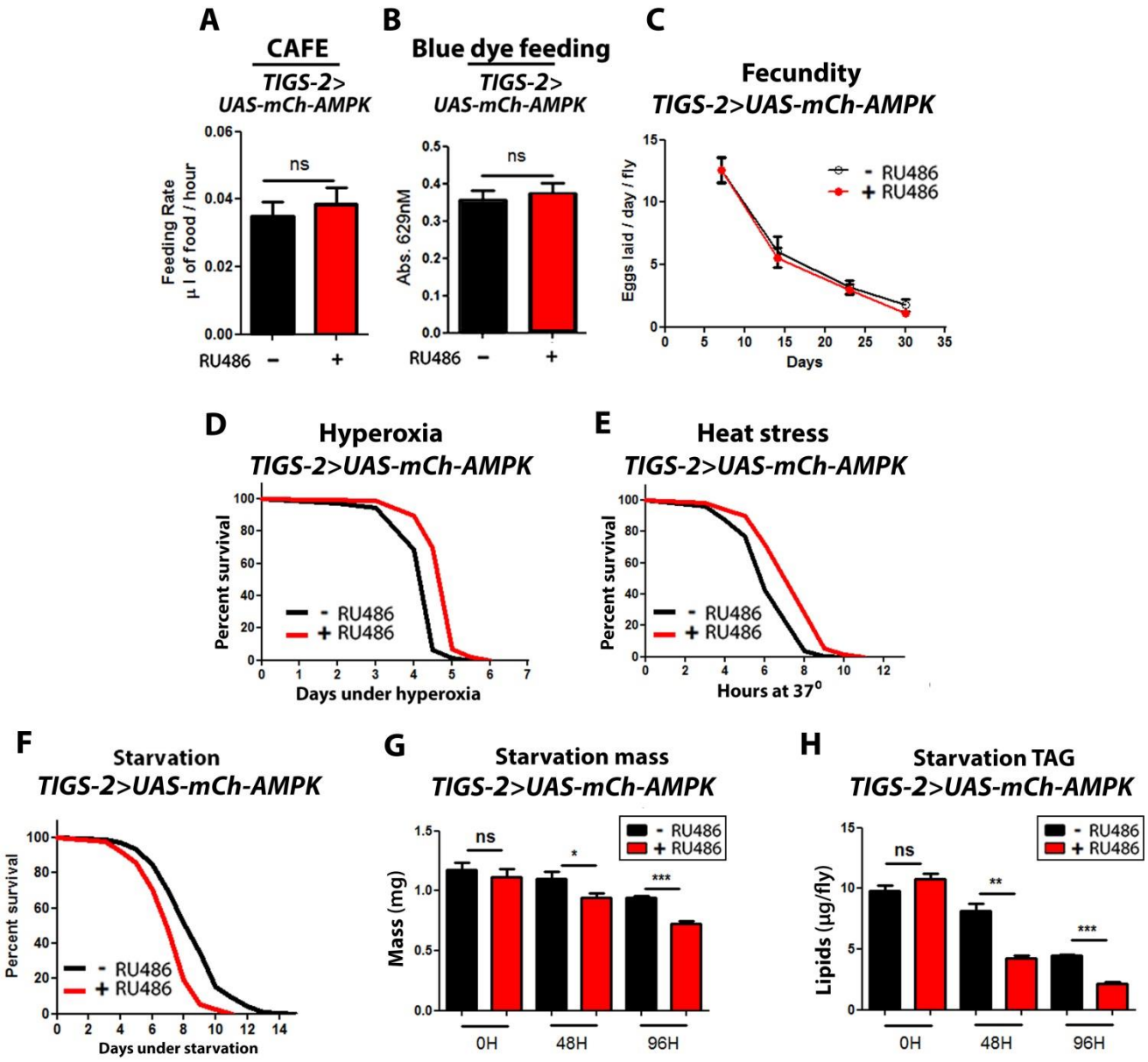

Figure 5-9. Intestine-specific AMPK upregulation mediates enhanced oxidative and heat stress resistance, with sensitivity to starvation.

(A) Capillary feeding assay (CAFE) of 10 day old *TIGS-2>UAS-mCh-AMPK* flies. RU486 treatment had no effect on feeding rate of flies overexpressing AMPK in the intestine (*p>0.05*; *t-test, n>7 vials of 10 flies/condition*).

(B) Blue dye feeding assay of 10 day old *TIGS-2>UAS-mCH-AMPK* flies. Induction of AMPK in the gut had no effect on the amount of blue food consumed (*p>0.05*; *t-test; n>37 flies/condition*).

(C) Fecundity timecourse of *TIGS-2>UAS-mCH-AMPK* flies. Induction of AMPK in the intestine had no effect on the number of eggs laid over lifespan of the organisms (*p>0.05*; *t-test; n>7 vials of 10 flies/condition*).

(D) Hyperoxia survival curves of 10 day old female *TIGS-2>UAS-mCH-AMPK* flies. Gut upregulation of AMPK significantly increased survival under 80% atmospheric oxygen (*p<0.0001; log-rank; n>154 flies/condition*).

(E) Heat stress survival curves of 10 day old female *TIGS-2>UAS-mCH-AMPK* flies. Gut-specific upregulation of AMPK significantly increased survival at 37° C. (*p<0.0001; log-rank; n>118 flies/condition*).

(F) Wet starvation survival curves of female *ELAV-GS>UAS-mCh-AMPK* flies with or without RU486-mediated transgene induction. AMPK overexpression in neurons caused early mortality when deprived of nutrition. (*p<0.001; log-rank; n>257 flies*).

(G) Body mass during starvation of *ELAV-GS>UAS-mCh-AMPK* females with or without RU486-mediated transgene induction. AMPK overexpression in neurons caused rapid mass depletion upon starvation, compared to uninduced flies (*p<0.05, at 48hours and p<0.01 at 96 hours of starvation; t-test; n>6 samples/condition; 10 flies weighed/sample).*

(H) Whole body lipid stores during starvation of *ELAV-GS>UAS-mCh-AMPK* females with or without RU486-mediated transgene induction. Neuronal AMPK induction caused rapid lipid depletion upon starvation (*p<0.01 at 48 hours, and p<0.001 at 96 hours of starvation; t-test; n>3 samples/condition/timepoint; lipids extracted from 5 flies/sample).*

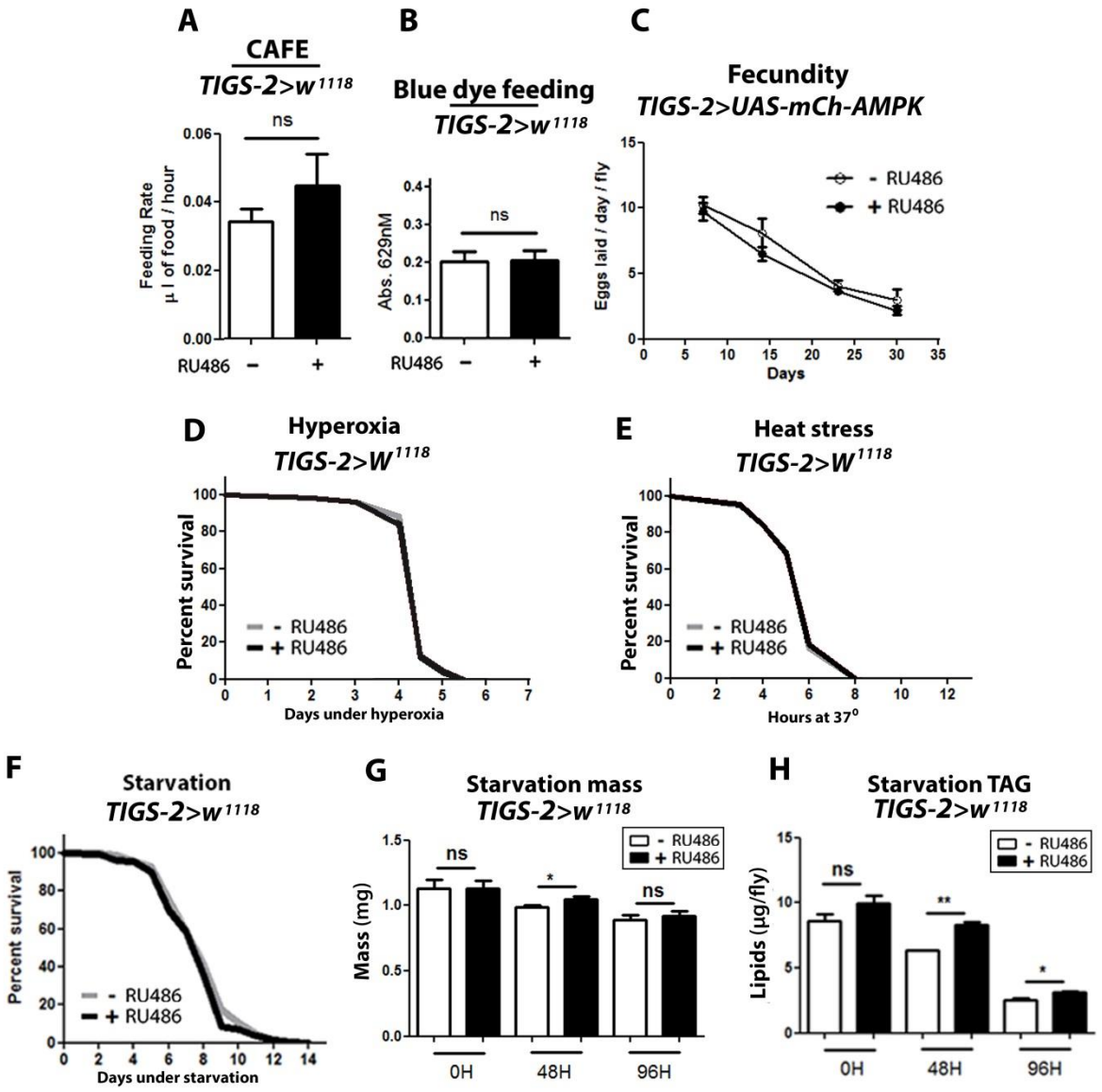

Figure 5-10. RU486 treatment does not influence feeding and stress resistance in the *TIGS-2* genetic background.

(A) Capillary feeding assay (CAFE) of 10 day old *TIGS-2>W^{1118}* control flies. RU486 feeding had no effect on the amount of food consumed by control flies (*p>0.05*; *t-test; n>70 flies/condition*).

(B) Blue dye feeding assay of 10 day old *TIGS-2>W^{1118}* control flies. RU486 feeding had no effect on the amount of blue food consumed by control flies (*p>0.05*; *t-test; n>40 flies/condition*).

(C) Fecundity timecourse of control *TIGS-2>W^{1118}* flies. RU486 feeding had no effect on the number of eggs laid over lifespan of the organisms (*p>0.05*; *t-test; n>7 vials of 10 flies/condition*).

(D) Hyperoxia survival curves of 10 day old female *TIGS-2>W^{1118}* controls. RU486 feeding had no effect on survival under 80% atmospheric oxygen (*p>0.05; log-rank; n>125 flies/condition*).

(E) Heat stress survival curves of 10 day old female *TIGS-2>W^{1118}* controls. RU486 feeding had no effect on survival at 37° C. (*p>0.05; log-rank; n>139 flies/condition*).

(F) Starvation survival curves of *TIGS-2>W^{1118}* controls. Female control flies fed RU486 for 10 days had no significant effect on starvation lifespan (*p>0.05*; *log-rank; n>203 flies*).

(G) Body mass during starvation of *TIGS-2>W^{1118}* controls. RU486 fed flies showed a minimal increase in body mass at 48 hours compared to control flies (*p<0.05*; *t-test; n>6 samples/condition from 10 flies weighed/sample*)

(H) Whole body lipid stores during starvation of *TIGS-2>W^{1118}* controls. RU486 feeding of control flies moderately increased the amount of lipids at 48 and 96 hours of starvation compared to ethanol fed flies (*p<0.01 at 48 hours; p<0.05 at 96 hours; t-test; n>3 samples /condition; lipids extracted from 5 flies/sample*).

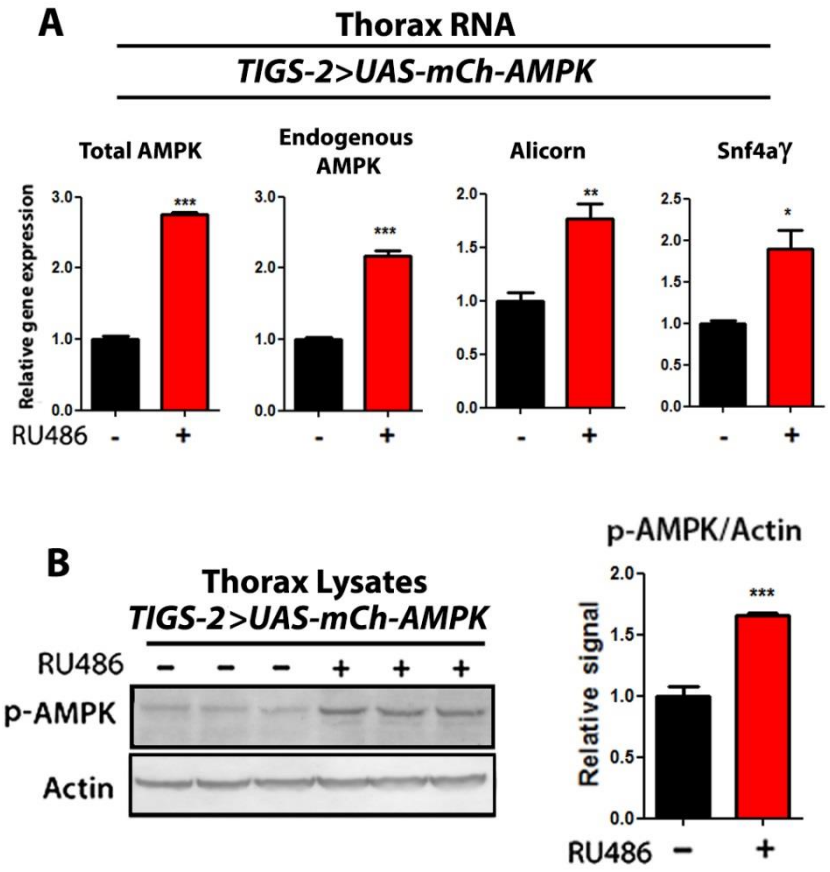

Figure 5-11. Intestine-specific upregulation of AMPK causes a cell-non-autonomous increase in AMPK transcripts and phosphorylation in thorax tissue.

(A) Transcript levels of total AMPK and endogenous subunits in the thorax, upon intestine-specific overexpression of AMPK. RNA was extracted from female flies at 10 days of age. Total levels of AMPK, endogenous AMPK, Alicorn, and Snf4aγ are significantly increased in the head RNA upon RU486 transgene induction (*p<0.05; t-test; n=3, of RNA extracted from 10 thoraces/replicate*).

(B) Western blot analysis of AMPK phosphorylated on T184 (p-AMPK) and loading control (actin) from thorax of 10 day old female *ELAV-GS>UAS-mCh-AMPK* with or without RU486-mediated transgene induction. Upregulation of AMPK in the intestine significantly increased phosphorylated AMPK in gut tissue. Densitometry quantification (right) (*p<0.001; t-test; n=4 replicates; thoraces/replicate*).

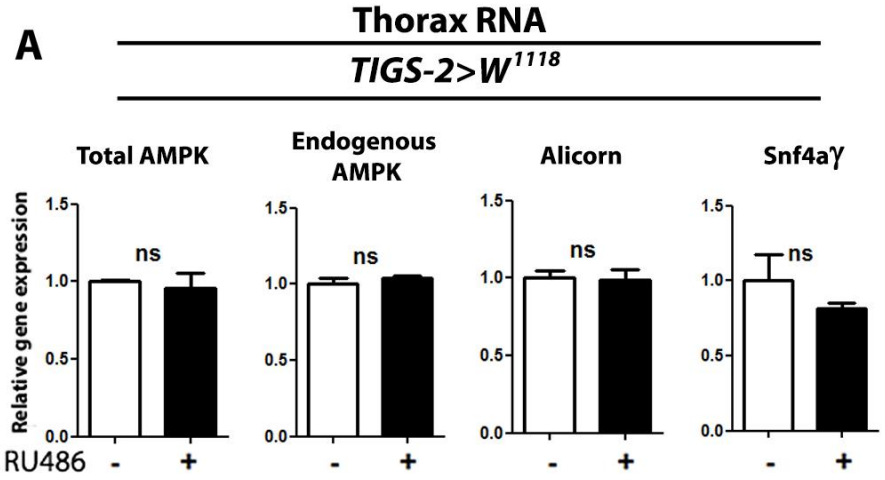

Figure 5-12. RU486 feeding does not influence thorax expression of AMPK subunits in the *TIGS-2* genetic background.

(A) Transcript levels of total AMPK and endogenous subunits upon RU486 feeding to control flies. RNA was extracted from intestines of female flies at 10 days of age. Total levels of AMPK, endogenous AMPK, Alicorn, and Snf4aγ are not effected by RU486 treatment of control strains (*$p<0.01$; t-test; n=3, of RNA extracted from 10 intestines/replicate*).

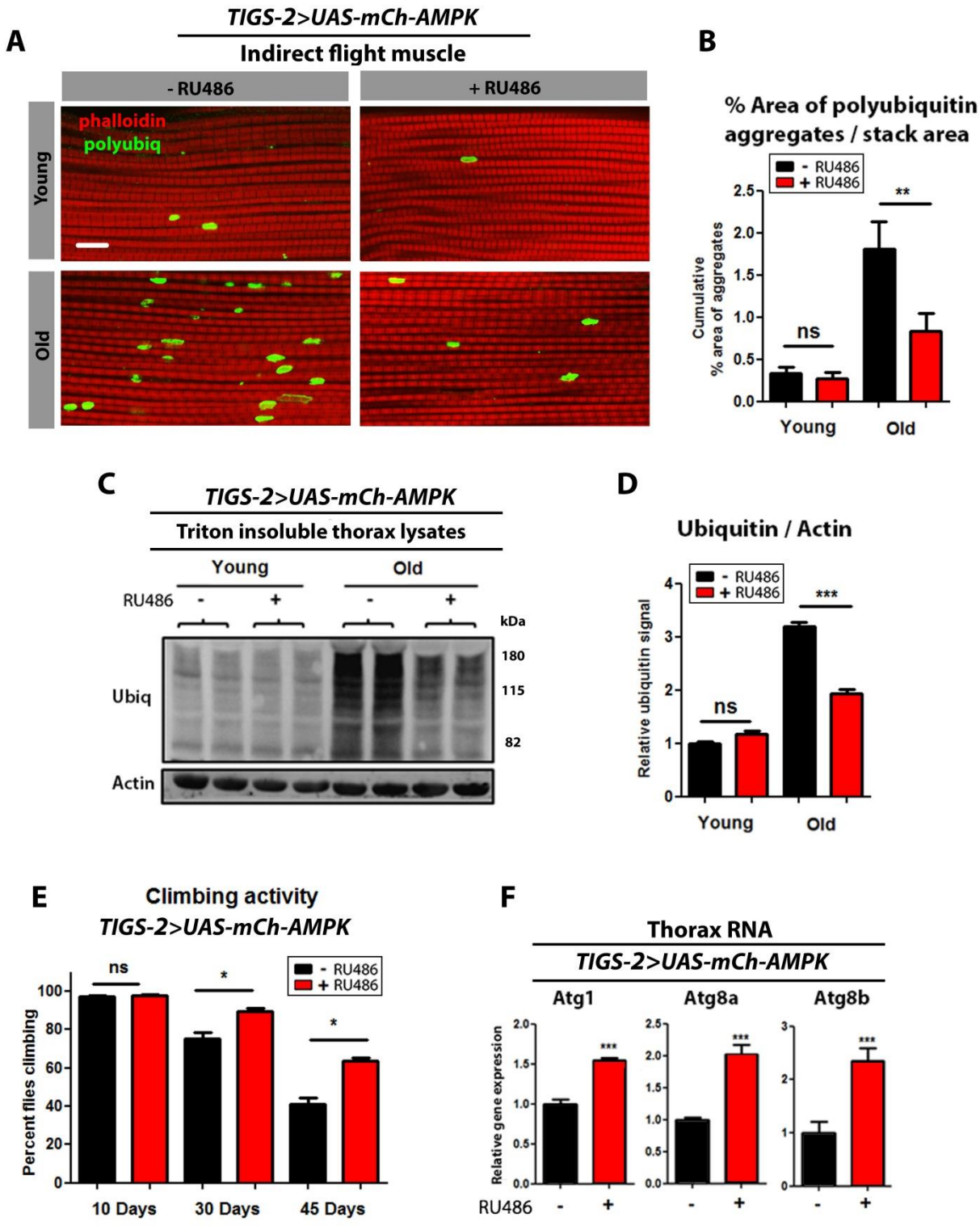

Figure 5-13. AMPK upregulation in the intestine maintains muscle proteostasis with aging.

(A) Confocal imaging of flight muscle of *TIGS-2>UAS-mCh-AMPK* females with or without RU486-mediated transgene induction showing protein polyubiquitinated aggregates at young (10 days), and old

(30 days) timepoints (*red channel-phalloidin/F-actin, green channel- anti-polyubiquitin, scale bar represents 10μm*).

(B) Quantification of polyubiquitin aggregates in muscle. Intestine-specific overexpression of AMPK reduced the accumulation of protein aggregates in the muscle at 30 days of age (*p<0.01; t-test; n>10; one fly/replicate stack*).

(C) Western blot detection of total ubiquitin-conjugated proteins from thorax detergent-insoluble extracts of young (10 days) and aged (30 days) *TIGS-2>UAS-mCH-AMPK* females with or without RU486-mediated transgene induction.

(D) Densitometry of ubiquitin blots. Intestine-specific overexpression of AMPK reduced the accumulation of insoluble protein aggregates in the thoracic muscle at 30 days of age (*p<0.001; t-test; n=4 samples/condition; 10 thoraces/sample).*

(E) Climbing activity of *TIGS-2>UAS-mCh-AMPK* females with or without RU486-mediated transgene induction. Upregulation of AMPK in the intestine maintains active climbing ability with age compared to uninduced controls *(p<0.05; t-test; n=6 vials/condition; 30 flies/vial).*

(F) Expression levels of autophagy genes from dissected thoraces of *TIGS-2>UAS-mCH-AMPK* female flies at 10 days of adulthood. Upon AMPK induction in the intestine we see significantly increased Atg1, Atg8a, and Atg8b gene expression levels in the thorax (*p<0.001*; *t-test; n>3 of RNA extracted from 10 thoraces/replicate*).

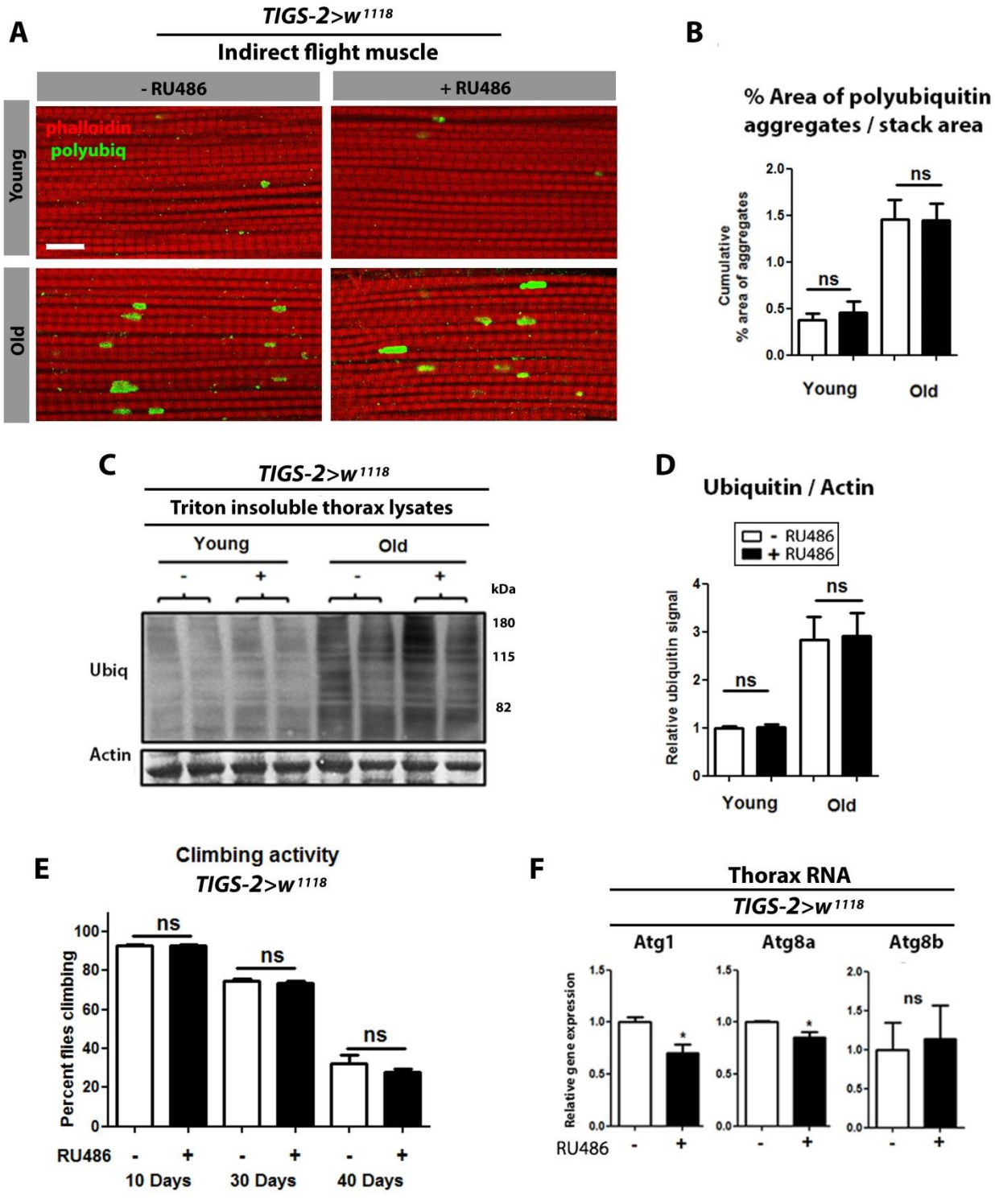

Figure 5-14. RU486 does not influence muscle proteostasis with aging in the TIGS-2 genetic background.

(A) Confocal imaging of adult female *TIGS-2>W^{1118}* flight muscle showing protein polyubiquitinated aggregates at young (10 days), and old (30 days) timepoints (*red channel-phalloidin/F-actin, green channel- anti-polyubiquitin, scale bar represents 10μm*).

(B) Quantification of polyubiquitin aggregates in the muscle of *TIGS-2>W^{1118}* flies. RU486 feeding had no effect on protein aggregate accumulation with age. *(p>0.05*; *t-test, n>10, one fly / replicate stack*).

(C) Western blot detection of total ubiquitin-conjugated proteins from thorax detergent-insoluble extracts of young (10 days) and aged (30 days) *TIGS-2>W^{1118}* female flies.

(D) Densitometry of ubiquitin blots from thoraces of flies. RU486 feeding had no effect on amount of thoracic detergent-insoluble ubiquitin-conjugated proteins, normalized to actin, in aged flies *(p>0.05*; *t-test; n=4 samples/condition; 10 thoraces/sample*).

(E) Climbing activity of *TIGS-2>W^{1118}* female flies with age. RU486 feeding had no effect on climbing activity of control flies *(p>0.05; t-test; n=6 vials; 30 flies/vial)*.

(F) Expression level of autophagy genes from dissected thoraces of *TIGS-2>W^{1118}* female control flies at 10 days of adulthood. RU486 feeding showed a moderate reduction in the levels of Atg1 and Atg8a gene expression levels (*t-test; n=3 of RNA extracted from 10 thoraces /replicate*).

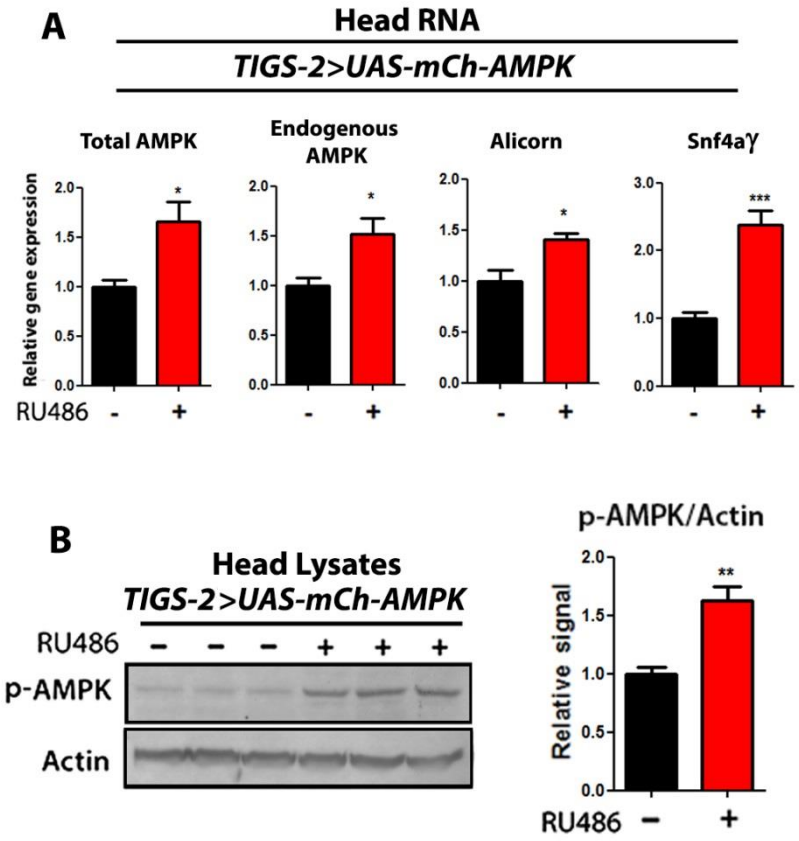

Figure 5-15. Intestine-specific upregulation of AMPK causes a cell-non-autonomous increase in AMPK transcripts and phosphorylation in head tissue.

(A) Transcript levels of total AMPK and endogenous subunits in head RNA upon intestine-specific overexpression of AMPK. RNA was extracted from female flies at 10 days of age. Total levels of AMPK, endogenous AMPK, Alicorn, and Snf4aγ are significantly increased in the head RNA upon RU486 transgene induction (*p<0.05; t-test; n=3, of RNA extracted from 10 intestines/replicate*).

(B) Western blot analysis of AMPK phosphorylated on T184 (p-AMPK) and loading control (actin) from intestine lysates of 10 day old female *ELAV-GS>UAS-mCh-AMPK* with or without RU486-mediated transgene induction. Upregulation of AMPK in the intestine significantly increased phosphorylated AMPK in gut tissue. Densitometry quantification (right) (*p<0.01; t-test; n=4 replicates; 10 intestines/replicate*).

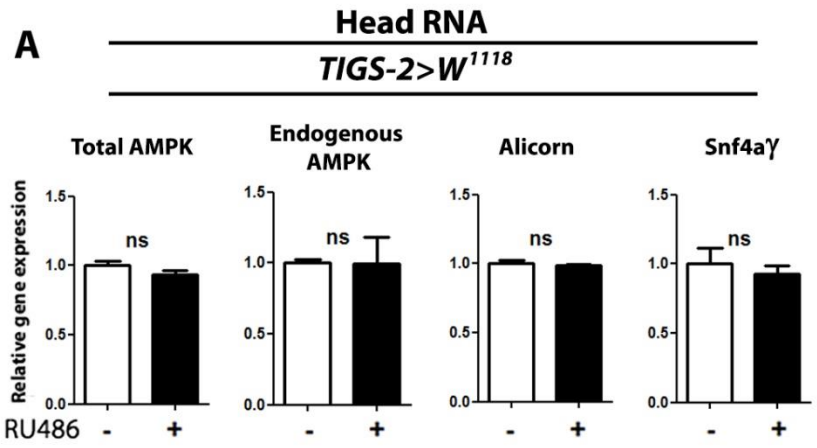

Figure 5-16. RU486 feeding does not influence expression of AMPK subunits in the *TIGS-2* genetic background.

(A) Transcript levels of total AMPK and endogenous subunits upon RU486 feeding to control flies. RNA was extracted from heads of female flies at 10 days of age. Total levels of AMPK, endogenous AMPK, Alicorn, and Snf4aγ are not effected by RU486 treatment of control strains (*$p<0.01$; t-test; n=3, of RNA extracted from 10 heads/replicate*).

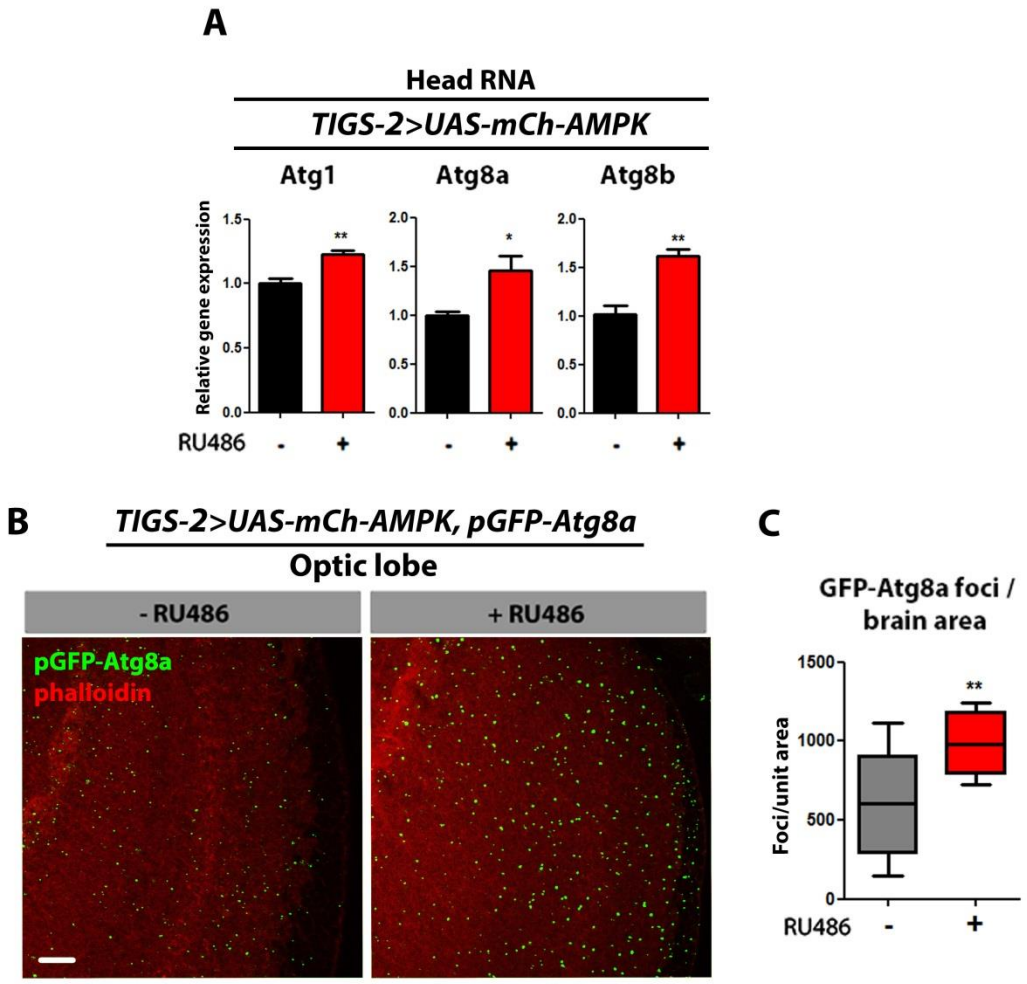

Figure 5-17. Intestinal AMPK activation induces autophagy in the brain.

(A) Expression levels of autophagy genes in heads of *TIGS-2>UAS-mCH-AMPK* flies at 10 days of adulthood. Upon AMPK induction in the intestine significantly increased Atg1, Atg8a, and Atg8b RNA levels are observed in the heads of female flies (*p<0.05*; *t-test; n>3 of RNA extracted from 10 heads/replicate*).

(B) Brain GFP-Atg8a Staining. Representative images from optic lobes of 10 day old *TIGS-2>UAS-mCH-AMPK, pGFP-Atg8a* females with or without RU486-mediated transgene expression (*red channel-phalloidin, green channel-GFP-Atg8a, scale bar represents 10μm*).

(C) Quantification of brain pAtg8a foci. Overexpression of AMPK in the intestine increased the amount of GFP-Atg8a foci in the brain (*p<0.007; t-test; n>10 confocal stacks from optic lobes/condition; one brain/replicate stack*).

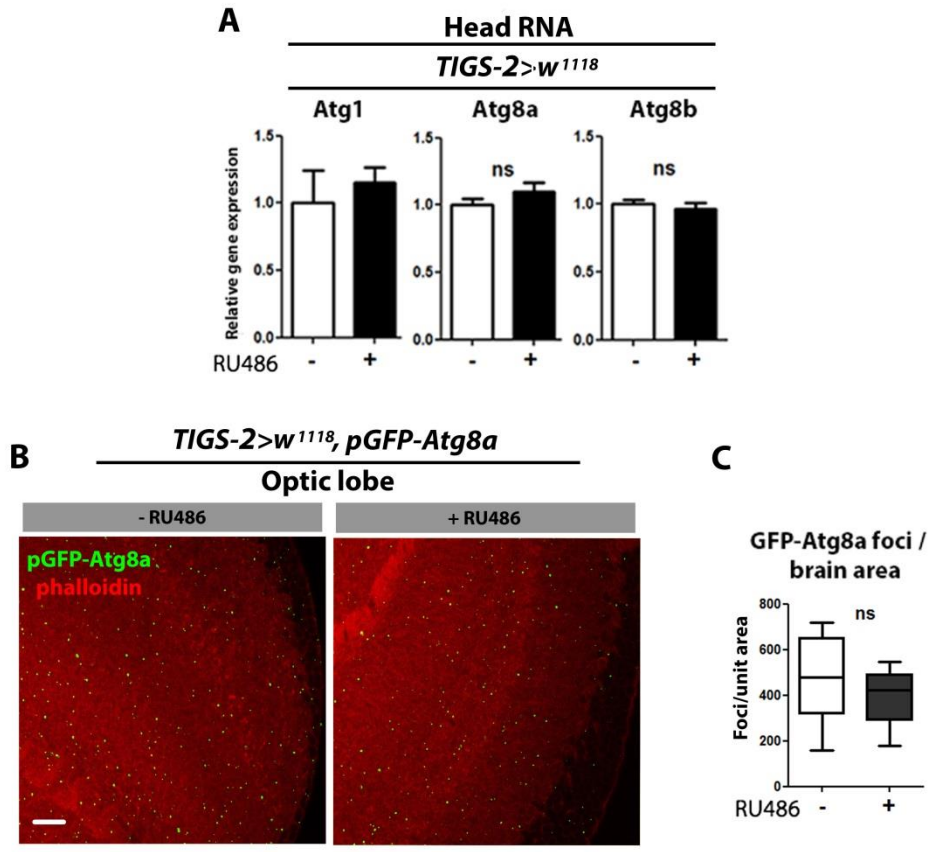

Figure 5-18. RU486 feeding does not influence brain autophagy in the *TIGS-2* background.

(A) Expression level of autophagy genes from dissected heads of *TIGS-2>W^{1118}* female control flies at 10 days of adulthood. RU486 feeding showed no effects on autophagy gene transcription in heads (*t-test; n=3 of RNA extracted from 10 heads /replicate*).

(B) GFP atg8a foci staining. Representative images from optic lobes of 10 day old female *TIGS-2>W^{1118}, pGFP-Atg8a* flies fed RU486 and vehicle (*red channel-TO-PRO-3 DNA stain, green channel-GFP-Atg8a, scale bar represents 10μm*).

(C) Quantification of brain Atg8a foci. Control flies fed RU486 showed no difference in foci number (*p>0.05*; *t-test; n>10 confocal stacks from optic lobes/condition, one fly per replicate stack*).

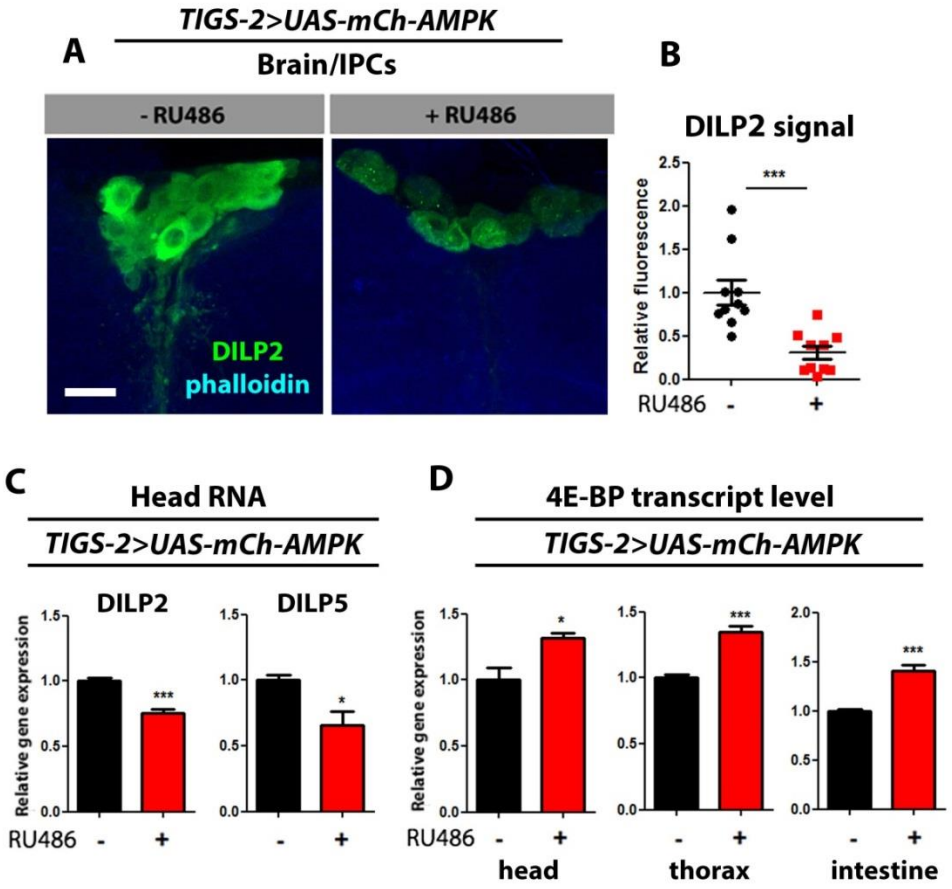

Figure 5-19. Expression of AMPK in the intestine suppresses insulin-like signaling.

(A) Representative images of DILP2 antibody stained insulin producing cells from 10 day old female *TIGS-2>UAS-mCh-AMPK* flies *(green channel – Dilp2 antibody, blue channel – phalloidin, scale bars represent 10μm).*

(B) Quantification of DILP2 fluorescence from insulin producing cells of 10 day old female *TIGS-2>UAS-mCh-AMPK* flies. Induction of AMPK in the intestines of flies significantly reduced DILP2 fluorescence in IPCs compared to uninduced controls *($p<0.001$; t-test; $n>10$ brains/condition).*

(C) Expression level of Dilp genes from dissected heads of *TIGS-2>UAS-mCh-AMPK* female flies at 10 days of adulthood. Intestine-specific upregulation of AMPK decreased Dilp2 and Dilp5 transcript levels in head tissue (*$p<0.05$; t-test; $n=3$ of RNA extracted from 10 heads /replicate*).

(D) Expression level of 4E-BP from dissected body parts of *TIGS-2>UAS-mCh-AMPK* female flies at 10 days of adulthood. Intestine-specific upregulation of AMPK significantly increased 4E-BP transcript levels in the indicated tissues (*$p<0.05$; t-test; $n=3$ of RNA extracted from 10 body parts/replicate*).

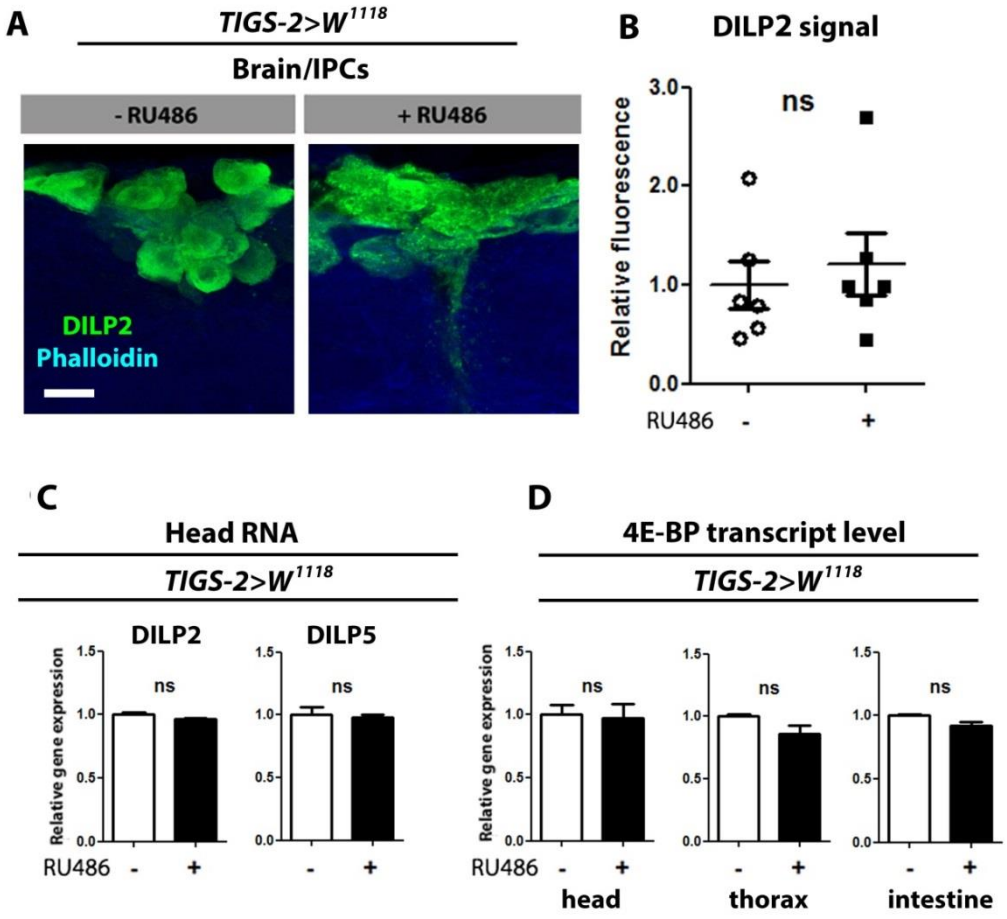

Figure 5-20. RU486 treatment has no influence on DILP expression in TIGS-2 control lines.

(A) Representative images of DILP2 antibody stained insulin producing cells from 10 day old female *TIGS-2>W^{1118}* flies *(green channel – Dilp2 antibody, blue channel – phalloidin, scale bars represent 10μm).*

(B) Quantification of DILP2 fluorescence from insulin producing cells of 10 day old female *TIGS-2>W^{1118}* flies. RU486 feeding had no effect on the relative fluorescence of Dilp2 in IPCs *(p>0.05; t-test; n>6 brains/condition).*

(C) Expression level of Dilp genes from dissected heads of *TIGS-2>W^{1118}* female control flies at 10 days of adulthood. RU486 feeding showed no difference in the levels of Dilp2, or Dilp5 RNA (*p>0.05; t-test; n=3 of RNA extracted from 10 heads /replicate*).

(D) Expression level of 4E-BP from dissected body parts of *TIGS-2>W^{1118}* female control flies at 10 days of adulthood. RU486 feeding showed no difference in the levels 4E-BP RNA in the indicated tissues (*p>0.05; t-test; n=3 of RNA extracted from 10 body parts/replicate*).

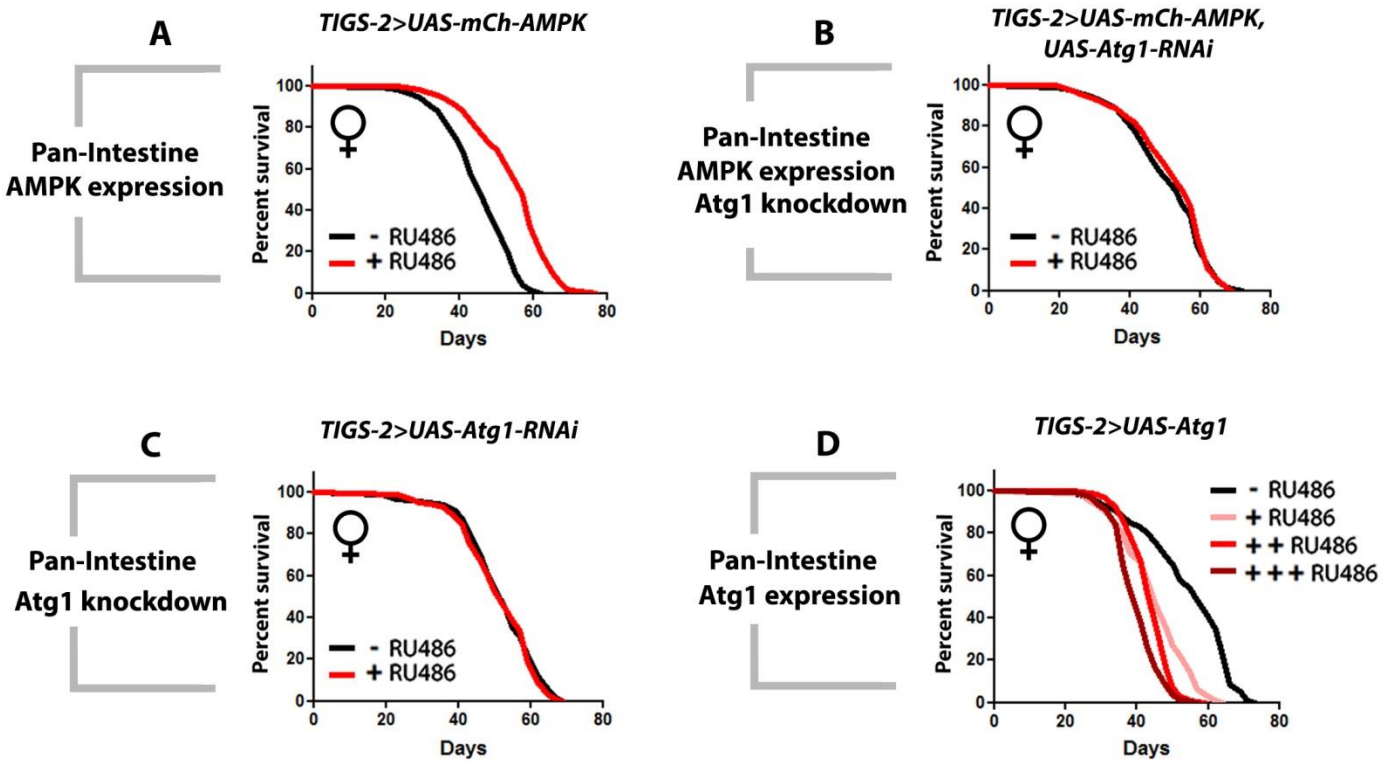

Figure 5-21. Atg1 is required for intestine-specific AMPK-mediated lifespan extension, but intestine-Atg1 overexpression is not sufficient to mediate extended longevity extension.

(A) Survival curves of AMPK overexpression in the intestine alone, *TIGS-2>UAS-mCh-AMPK* females with or without RU486-mediated transgene induction. Intestine-specific overexpression of AMPK extends median lifespan by over 25% (*p<0.0001; log-rank; n>326/ condition*).

(B) Survival curves simultaneous AMPK overexpression, and Atg1 knockdown in the intestine *TIGS-2>UAS-mCh-AMPK, UAS-Atg1-RNAi* females with or without RU486-mediated transgene induction. Simultaneous overexpression of AMPK, and knockdown of Atg1 did not alter lifespan *(p>0.05; log-rank; n>302 /condition).*

(C) Survival curves of Atg1 knockdown in the intestine alone, *TIGS-2>UAS-Atg1-RNAi* females with or without RU486-mediated transgene induction. Intestine-specific knockdown of Atg1 did not alter lifespan *(p>0.05; log-rank; n>141/condition).*

(D) Survival curves of Atg1 overexpression in the intestine alone, *TIGS-2>UAS-Atg1* females with or without RU486-mediated transgene induction. Intestine-specific overexpression of Atg1significantly reduced lifespan in all RU486 induced conditions *(p<0.0001; log-rank; n>293 / condition).*

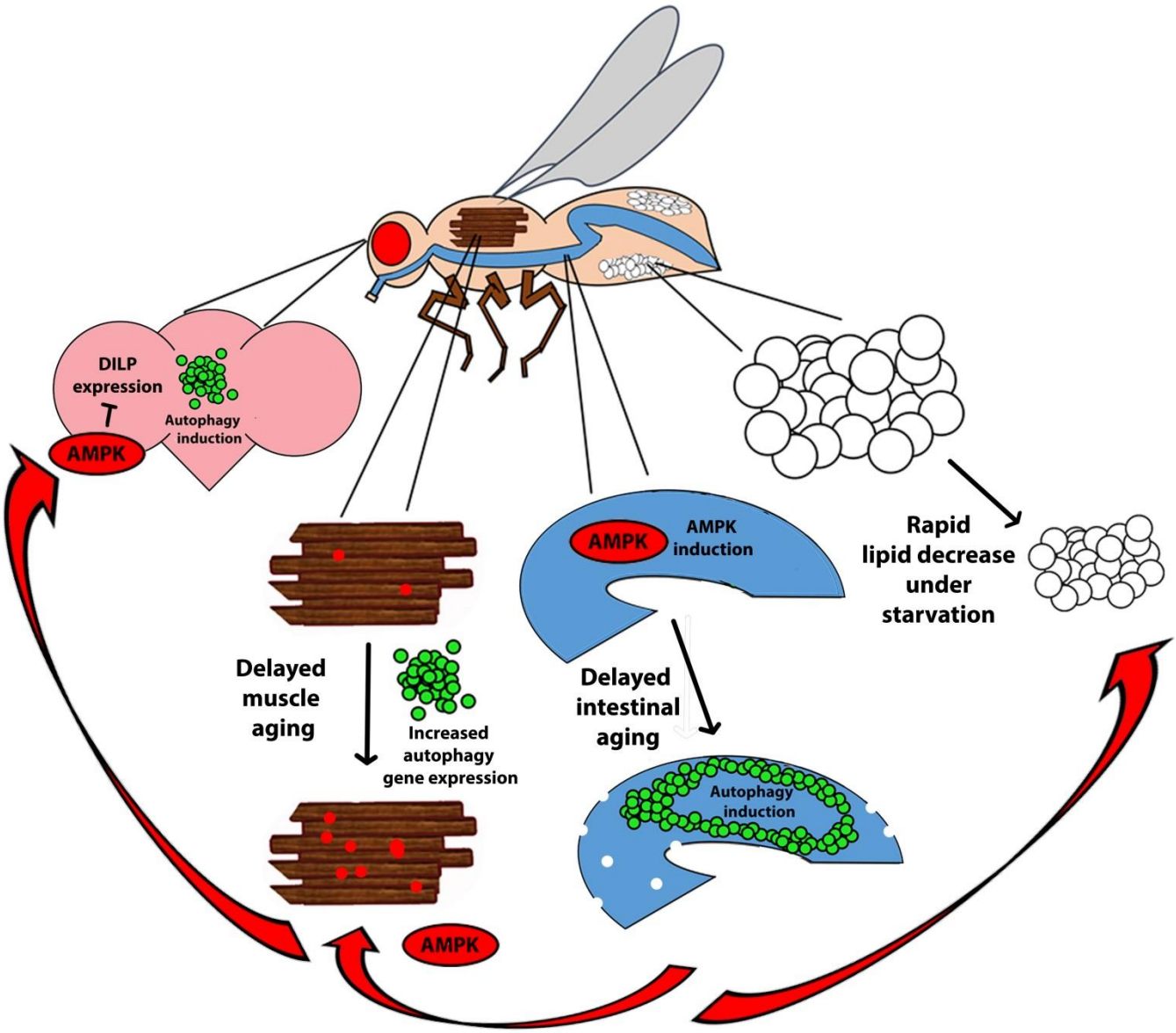

Figure 5-22. Schematic summary of physiological effects due to intestine-specific AMPK overexpression.

Overexpression of transgenic AMPK in the intestine is able to induce autophagy in the gut and delay intestinal aging. Exogenous gut-specific AMPK is able to induce expression and activation of endogenous AMPK in distal tissues, resulting in delayed muscle aging, repressed insulin signaling, and increased systemic autophagy. Gut-specific AMPK overexpression is comes with a biological trade-off: inducing rapid weight loss, lipid decrease, and early mortality when deprived of food.

REFERENCE:

1. Poirier, L., Shane, A., Zheng, J., & Seroude, L. (2008). Characterization of the Drosophila gene-switch system in aging studies: a cautionary tale. *Aging Cell*, *7*(5), 758–70. doi:10.1111/j.1474-9726.2008.00421.x

CHAPTER VI:

CONCLUDING REMARKS:

AMPK AS A RELAY FOR SYSTEMIC CONTROL OF NUTRITIONAL SIGNALING AND AGING

In the previous chapters we have shown that neuronal overexpression of AMPK is sufficient to extend lifespan and delay tissue-aging in a cell-non-autonomous manner (Chapter II). The increased longevity and delayed markers of tissue aging mediated by neuron-specific AMPK activation are dependent upon the downstream autophagy induction kinase Atg1 (Chapter III). This intertissue signal may be transduced by the insulin-like-signaling system (Chapter IV). Additionally, transgenic AMPK overexpression in neurons is sufficient to upregulate endogenous AMPK expression in distal tissues including the intestine. Transgenic AMPK activation in the intestine alone is sufficient to extend lifespan, delay systemic aging, induce autophagy cell autonomously. Surprisingly, intestine-specific AMPK expression is capable of cell-non-autonomously signaling to the brain, inducing autophagy and suppressing DILP signaling (Chapter V).

From this work it can be established that AMPK is able to function as a relay for systemic nutritional signaling from neurons-to-gut, or gut-to-neurons **(Fig. 6-1).** This AMPK activity represents a novel brain-to-gut and gut-to-brain signaling axis in *Drosophila*. Contrary to this, another aging-related cell-non-autonomous mechanism described by Andrew Dillin's Lab shows only singular directionality in systemic signaling [1,2]. Dillin's work was able to display that life extending inhibition of the electron transport chain (ETC) in neurons is sufficient to induce cell-non-autonomous changes in the mito-UPR stress response of the intestine of *C. elegans*. However, they were unable to show that the signal can travel from gut-to-neurons in the worm. Our work represents the first instance of an intestine-specific, or neuron-specific genetic signal that is capable of mediating cell-non-autonomous autophagy induction.

As stated previously, the cellular recycling process of autophagy can exert anti-aging effects in diverse species [3,4] Although AMPK, a key regulator of autophagy [5], has also been

linked to aging and lifespan determination [6] little was known about the relationships between AMPK and autophagy in the coordination of tissue and organismal aging. Our work, along with others, strengthens the emerging concept that stress responses can be transduced among various different tissues [1,2,7]. Of note, muscle-specific dFOXO/4E-BP/activin signaling can induce autophagy autonomously and, thereby, retard muscle aging. These effects in muscle are linked to altered DILP levels in the brain, dampened systemic insulin-like signaling and extended organismal lifespan [8,9]. Our findings are consistent with a model where tissue-specific AMPK/Atg1 up-regulation antagonizes DILP signaling leading to slowed organismal aging. Although, the exact mechanism by which AMPK/Atg1 activity antagonizes DILP signaling both from brain-to-gut and gut-to-brain, is undetermined.

As AMPK has been shown to directly activate FOXO activity in *C. elegans* and mammalian cells [10, 11], it could be speculated that an AMPK-dFOXO-autophagy circuit may play a role in our findings. As stated previously in Chapter IV, it has recently been reported that up-regulation of dFOXO in the fat body of flies can cell-non-autonomously slow markers of aging in the absence of endogenous dFOXO in the responding tissue [12]. In a similar fashion, it will be interesting to determine whether distal-tissue endogenous AMPK, or FOXO expression is required for the changes in autophagy gene expression, physiology and lifespan observed upon targeted transgenic AMPK/Atg1 induction.

Indeed, our work raises several questions concerning the regulation of autophagy by AMPK both autonomously and non-autonomously. As we observe increased mRNA levels of several autophagy genes upon AMPK activation, an interesting area of future investigation will be to explore the transcriptional control of autophagy in AMPK overexpressing flies. Recently, William Mair and Andrew Dillin have shown that cAMP-responsive element-binding protein (CREB)-regulated transcriptional coactivators (CRTCs) link AMPK activity to

the transcriptional regulation of lifespan [13]. The CRTC family of genes function as transcriptional cofactors involved in nutritional signaling, energy homeostasis, mitochondrial biogenesis, and stress response [14]. AMPK can directly target CRTCs for regulation [14]. In *C. elegans*, transgenic activation of AMPK and inhibition of calcineurin both extend longevity in *C. elegans* by regulating the activity of CRTC-1 [13]. Additionally, calcineurin-mediated longevity requires a functioning autophagic pathway to exert beneficial lifespan effect [15]. Quite possibly, CRTC orthologs may play a role in AMPK-mediated transcriptional regulation of autophagy genes in *Drosophila*.

In any case, a plausible interpretation of our findings is that the AMPK/Atg1-mediated induction of autophagy slows aging (both autonomously and nonautonomously) by increasing the turnover of damaged macromolecules and/or organelles. While we have shown that neuronal AMPK and Atg1 overexpression is able to reduce the accumulation of polyubiquitin rich aggregated proteins in thoracic muscle, a pressing challenge will be to identify other relevant autophagic cargo in the context of aging. During the aging process, it may be that the autophagy machinery is overloaded with specific aggregation-prone proteins [16]. Identifying this cargo may aid in possible therapeutic intervention.

While up-regulation of either AMPK or Atg1 can slow *Drosophila* aging in the constant presence of food, these same interventions have the biological trade-off in that they sensitize flies to starvation conditions. This information could prove useful when designing therapeutic interventions based around AMPK and/or autophagy induction. Particularly, the ability of AMPK and Atg1 to mediate rapid weight loss and triglyceride reduction may be of interest to those who study weight loss and weight gain prevention in mammals. Additionally, AMPK and the macro-autophagy pathway have been proposed to mediate the beneficial effects of Resveratrol, Metformin, Rapamycin and AICAR respectively [4,6]. In the future, it will be

interesting to determine whether AMPK is required for the benefits of these pharmacological treatments. More promising is the possibility that AMPK activation in a single tissue (e.g.the nervous system/intestine) may induce an organism-wide response to delay systemic aging in mammals.

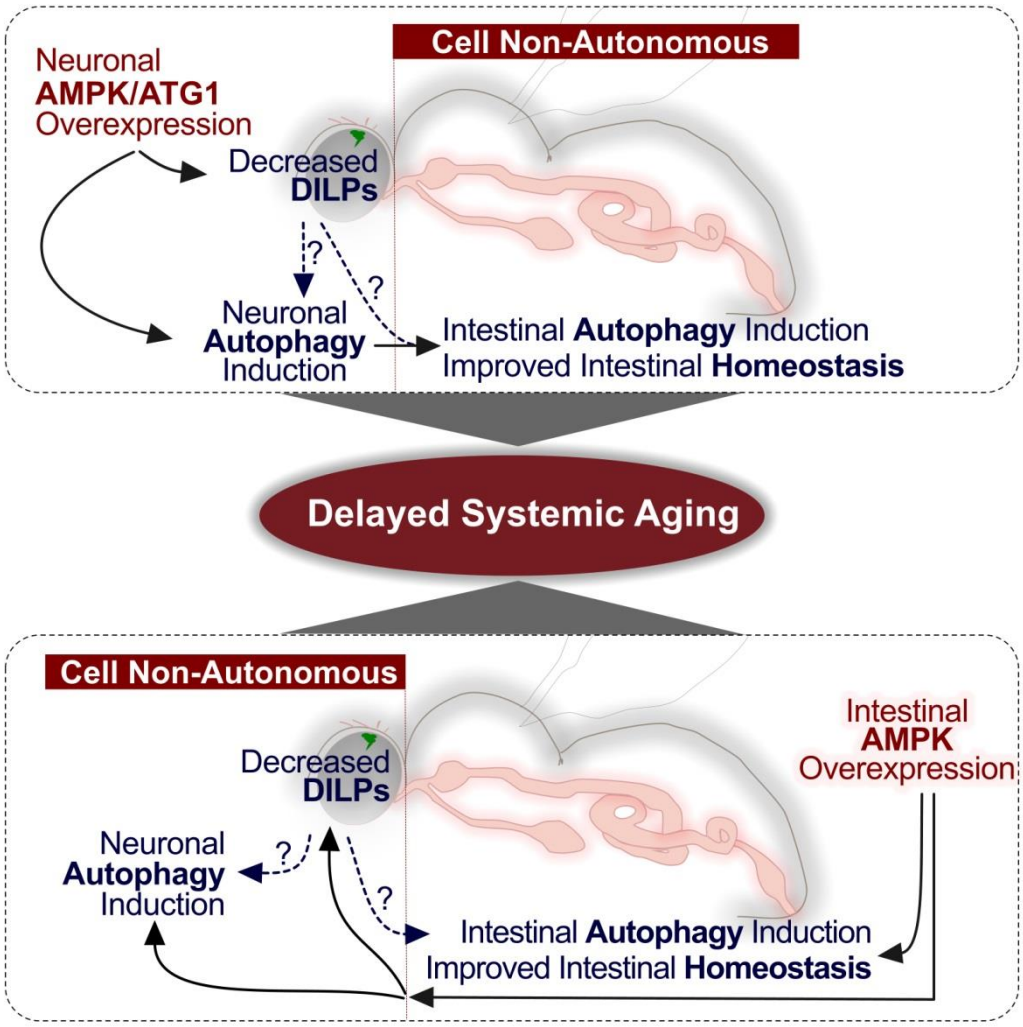

Figure 6-1. AMPK as a novel relay for brain-to-gut and gut-to-brain signaling.

Neuronal AMPK activation results in autonomous autophagy induction and DILP suppression in the brain, with a concordant upregulation of autophagy in the intestine resulting in slowed systemic aging.

Intestine-specific AMPK activation causes an autonomous induction of autophagy in the intestine, and a simultaneous upregulation of autophagy in the brain along with suppressed DILP signaling in IPCs.

REFERENCES:

1. Durieux, J., Wolff, S., & Dillin, A. (2011). The cell-non-autonomous nature of electron transport chain-mediated longevity. *Cell*, *144*(1), 79–91. doi:10.1016/j.cell.2010.12.016

2. Taylor, R. C., & Dillin, A. (2013). XBP-1 is a cell-nonautonomous regulator of stress resistance and longevity. *Cell*, *153*(7), 1435–47. doi:10.1016/j.cell.2013.05.042

3. Gelino, S., and Hansen, M. (2012). Autophagy - An Emerging Anti-Aging Mechanism. *Journal of clinical & experimental pathology* Suppl 4.

4. Rubinsztein, D. C., Mariño, G., & Kroemer, G. (2011). Autophagy and aging. *Cell*, *146*(5), 682–95. doi:10.1016/j.cell.2011.07.030

5. Alers, S., Löffler, A. S., Wesselborg, S., & Stork, B. (2012). Role of AMPK-mTOR-Ulk1/2 in the regulation of autophagy: cross talk, shortcuts, and feedbacks. *Molecular and Cellular Biology*, *32*(1), 2–11. doi:10.1128/MCB.06159-11

6. Burkewitz, K., Zhang, Y., & Mair, W. (2014). AMPK at the Nexus of Energetics and Aging. *Cell Metabolism*, 1–16. doi:10.1016/j.cmet.2014.03.002

7. Rajan, A., & Perrimon, N. (2011). Drosophila as a model for inter organ communication: lessons from studies on energy homeostasis. *Developmental Cell*, *21*(1), 29–31. doi:10.1016/j.devcel.2011.06.034

8. Demontis, F., & Perrimon, N. (2010). FOXO/4E-BP signaling in Drosophila muscles regulates organism-wide proteostasis during aging. *Cell*, *143*(5), 813–25. doi:10.1016/j.cell.2010.10.007

9. Bai, H., Kang, P., Hernandez, A. M., & Tatar, M. (2013). Activin signaling targeted by insulin/dFOXO regulates aging and muscle proteostasis in Drosophila. *PLoS Genetics*, *9*(11), e1003941. doi:10.1371/journal.pgen.1003941

10. Greer, E. L., Dowlatshahi, D., Banko, M. R., Villen, J., Hoang, K., Blanchard, D., … Brunet, A. (2007). An AMPK-FOXO pathway mediates longevity induced by a novel method of dietary restriction in C. elegans. *Current Biology : CB*, *17*(19), 1646–56. doi:10.1016/j.cub.2007.08.047

11. Greer, E. L., Oskoui, P. R., Banko, M. R., Maniar, J. M., Gygi, M. P., Gygi, S. P., & Brunet, A. (2007). The energy sensor AMP-activated protein kinase directly regulates the mammalian FOXO3 transcription factor. *The Journal of Biological Chemistry*, *282*(41), 30107–19. doi:10.1074/jbc.M705325200

12. Alic, N., Tullet, J. M., Niccoli, T., Broughton, S., Hoddinott, M. P., Slack, C., … Partridge, L. (2014). Cell-nonautonomous effects of dFOXO/DAF-16 in aging. *Cell Reports*, *6*(4), 608–16. doi:10.1016/j.celrep.2014.01.015

13. Mair, W., Morantte, I., Rodrigues, A. P. C., Manning, G., Montminy, M., Shaw, R. J., & Dillin, A. (2011). Lifespan extension induced by AMPK and calcineurin is mediated by CRTC-1 and CREB. *Nature*, *470*(7334), 404–8. doi:10.1038/nature09706

14. Altarejos, J. Y., & Montminy, M. (2011). CREB and the CRTC co-activators: sensors for hormonal and metabolic signals. *Nature Reviews. Molecular Cell Biology*, *12*(3), 141–51. doi:10.1038/nrm3072

15. Dwivedi, M., Song, H.-O., & Ahnn, J. (2009). Autophagy genes mediate the effect of calcineurin on life span in C. elegans. *Autophagy*, *5*(5), 604–607. doi:10.4161/auto.5.5.8157

16. Cuervo, A. M. (2008). Autophagy and aging: keeping that old broom working. *Trends in Genetics : TIG*, *24*(12), 604–12. doi:10.1016/j.tig.2008.10.002

CHAPTER VII:

MATERIALS AND PROCEDURES

Fly Strains and media

UAS-AMPK flies were obtained from Jongkyeong Chung. pGFP-Atg8a flies were provided by Eric Baehrecke. The following lines were obtained from the Bloomington Stock Center: UAS-mCH-AMPK (32109), AMPK-RNAi (35137), UAS-Atg1-6B (51655), and Dilp2-GAL4. UAS-Atg1-RNAi line was received from the Vienna Drosophila RNAi (VDRC) Center (stock no. 16133). ELAV-GAL4, Da-GAL4 constitutive (Bloomington) expression experiments were performed on flies that have undergone 12 rounds of backcrossing into a W^{1118} background. All epistasis experiments were performed on flies that have undergone 12 rounds of backcrossing into a W^{1118} background. *Drosophila* were reared in vials containing cornmeal medium (1% agar, 3% yeast,1.9% sucrose, 3.8% dextrose, 9.1% cornmeal, 1% acid mix, and 1.5% methylparaben, all concentrations given in wt/vol) throughout all experiments.

Lifespan analysis and starvation.

Flies that eclosed over a 36 hour period were collected and allowed to mate for approximately 60 hours. Female or male flies were collected under light nitrogen-induced anesthesia and maintained at a density of 30-35 flies per vial in a humidified, temperature-controlled (25° C.) incubator with a 12 hour light-dark cycle. Flies were transferred to new vials every 2-3 days and scored for death. For starvation analysis female flies were aged for 10 days in vials containing cornmeal medium and then transferred to 1% agar solution in a humidified, temperature-controlled incubator with 12 h on/off light cycle at 25° C. Percentage of survival was measured every day, with survivors transferred to fresh vials every 2 days.

Immunostaining procedure for DILP2 or GFP-Atg8a in brain/intestinal tissues.

Female flies were anesthetized on ice and intestines/brains were dissected in cold PBS. Samples were then fixed in 4% formaldehyde in PBS at room temp for 30 minutes, rinsed three times in PBS + 0.2% Triton X-100 for 10 minutes at room temperature. Blocking was performed in 5% BSA in PBS + 0.2% triton X-100 for one hour at room temperature. Primary antibody mouse anti-DILP2 (a generous gift from Dr. Seung Kim), or rabbit anti-GFP (Cell Signaling, D5.1, XP), was added 1:250 in 5% BSA in PBS + 0.2% triton X-100 and incubated overnight at 4 degrees Celsius. Samples were then rinsed three times in PBS + 0.2% Triton X-100 for 10 minutes at room temperature, and secondary antibody incubation, anti-rabbit AlexaFluor-488, or anti-mouse AlexaFluor-488 (Invitrogen) was added 1:200, and To-Pro-3 DNA stain (Invitrogen) 1:200, or phalloidin AlexaFlour-633 (Invitrogen) 1:200, in 5% BSA in PBS + 0.2% triton X-100 for 4 hours at room temperature. Samples were rinsed three times in PBS + 0.2% triton X-100 for 10 minutes at room temperature. Intestines/brains were then mounted in Vectashield mounting medium (Vector Labs) and Imaged using Zeiss single point LSM 5 exciter confocal microscope.

Quantification of DILP2 signal was performed similarly to (Broughton et al., 2010). Briefly, confocal Z stacks were taken to capture all IPCs of the brain, with identical excitation parameters for all conditions. Stacks were merged as projections using Axiovision v. 4.8 and average fluorescent intensity was measured using Image J. Average fluorescent intensity of IPCs of a given area per brain was analyzed via student's t-test. A minimum of 6 brains were used for all conditions. For number and size of IPCs, cells were outlined via automated procedures using the count particle function in Image J. Information about the size of the cells was also obtained using the particle counter plugin.

For brain GFP-Atg8a foci quantifications, Z stacks of the optic lobe were taken using identical settings with the 63X objective. For Intestinal quantification of GFP-atg8a foci, Z stacks of enterocytes in regions 200–500 μm anterior to the pylorus were imaged. The average number of foci in either the gut or brain was counted using the local maxima tool in Image J. Statistical analysis was conducted on mean autophagosome counts averaged from a set area of 120 μm^2 for each midgut or brain using a two-tailed, unpaired Student's t test (n>9 brains or guts were used per condition).

Lysotracker Red.

Female flies were anesthetized on ice and intestines were dissected in cold PBS**.** Intestines were washed once in PBS, followed by three 30s rinses in freshly prepared 1 μM Lysotracker Red (Invitrogen) in PBS at room temperature. Intestines were washed five times for 30s in PBS at room temperature, then mounted in Vectashield, and imaged immediately. Imaging should not proceed for very long as apoptosis can be observed after approximately 60 min. Quantification of acidophilic vesicles was performed similarly to above GFP-atg8a quantification.

Immunostaining procedure for dissected indirect flight muscle.

Staining was performed similarly to (Rana et al., 2013). Hemithoraces were dissected and fixed for 20 minutes in PBS with 4% paraformaldehyde and 0.2% Triton X-100. After washing, samples were incubated overnight at 4 °C with an antibody detecting polyubiquitinated proteins at 1:250 mouse mAb FK2 (Enzo). Washed thoroughly and incubated with secondary anti-mouse AlexaFlour-568 (1:250), with phalloidin AlexaFlour-633. Samples were rinsed three times in PBS + 0.2% triton X-100 for 10 minutes at room temperature, then mounted in

Vectashield mounting medium (Vector Labs) and Imaged. For quantification of protein aggregates in hemithoraces, single-channel images were converted into grayscale and the area and total number of protein aggregates was measured using ImageJ. Statistical analysis was conducted the area of protein aggregates/indirect flight muscle region averaged using a two-tailed, unpaired Student's t test (n>10 thoraces were used per condition).

Western blot.

Heads of 10 day old female flies were dissected and lysates were separated by SDS page using standard procedures. Membranes were probed with antibodies against AMPK phospho-T184 at 1:1000 (Cell Signaling, 40H9), anti-phospho-S6K T398 (Cell Signaling, 9209), anti-total S6K 1:300 (Santa Cruz, C-18, SC-230), anti-Ubiquitin added at 1:1000 (Cell Signaling, P4D1), and with horseradish peroxidase-conjugated monoclonal mouse antibody against Actin diluted 1:5000 (Sigma). The rabbit antibodies were detected using horseradish peroxidase-conjugated anti-rabbit IgG antibodies at 1:2000 (Sigma). The mouse antibodies were detected using horseradish peroxidase-conjugated anti-mouse IgG antibodies 1:2000 dilution (Sigma). ECL 2 chemiluminescent/chemifluorescent reagent (Pierce) was used to visualize horse radish peroxidase activity, and the chemifluorescence was detected using a Typhoon scanner (GE Healthcare).

Triton-Insoluble protein extracts.

Dissected thoraces were homogenized in ice-cold PBS with 1% Triton X-100 and protease inhibitors. The mixture was spun for 10 min at 4 °C, and the pellet and supernatant were collected. The Triton X-100–insoluble pellet was washed and resuspended in lysis solution with

5% lithium dodecyl sulfate (LDS) (NuPAGE LDS Sample Buffer; Invitrogen). N>4 independent samples of 5 thoraces were used for densitometry post-blotting.

Quantitative real-time PCR.

Head, thorax, or intestines were dissected on ice, and then total RNA was extracted using TRIzol reagent (Invitrogen) following manufacturer protocols. Samples were treated with DNase, and then cDNA was synthesized using the standard kit (Fermentas). Equalized amplicons of Actin5C were used as a reference to normalize exogenous AMPK—mCherry RFP fwd-CCACAACGAGGACTACACCA and AMPK rev-GGTAGTGCCCAATCTTGACC, total AMPK— fwd-CAAGATCCGGCGTGAGAT and rev-GCTTGCCGTGCTTCACAATA, Atg1— fwd- GCTTCTTTGTTCACCGCTTC and rev- GCTTGACCAGCTTCAGTTCC, Atg8a— fwd-AGTCCCAAAAGCAAACGAAG and rev-TTGTCCAAATCACCGATGC, Atg8b— fwd-AATGTGATCCCACCGACATC and rev-TTGAGCGAGTAGTGCCAATG, Actin5C—fwd-TTGTCTGGGCAAGAGGATCAG and rev-ACCACTCGCACTTGCACTTTC. Dilp2—fwd-GCTTTAATACGCTGCCAAGG and rev-CGGATCCGTACAGATTGGTT. Dilp5—fwd-AGAGAACTTTGGACCCCGTGA and rev-TGAACCGAACTATCACTCAAC. 4E-BP—fwd-TACACGTCCAGCGGAAAGTT and rev- CCTCCAGGAGTGGTGGAGTA.

Mass/weight.

Flies were weighed in groups of 10 in preweighed microcentrifuge tubes, using an analytical scale (Torbal, Clifton, NJ, USA).

Quantification of Triglycerides.

Lipids were extracted from five whole female flies in a chloroform:ethanol solution (2:1 vol/vol), and nonpolar lipids (fatty acid, triacylglycerol) were separated by thin-layer chromatography with a n-hexane/diethylether/glacial acetic acid solution (70:30:1, vol/vol/vol). Plates were air-dried and stained (with 0.2% Amido Black 10B in 1 M NaCl), and lipid bands were quantified by photo densitometry using ImageJ.

Intestinal barrier dysfunction assay.

The 'Smurf fly'/intestinal barrier dysfunction assay was performed similarly to (Rera et al., 2012). Flies were aged on standard medium until the day of the Smurf assay. Dyed medium was prepared using standard medium with blue dye no. 1 added at a concentration of (2.5% wt/vol). The blue no. 1 was purchased from SPS Alfachem. A fly was counted as a Smurf when dye coloration was observed outside the digestive tract. Comparisons of Smurf proportion per time point were carried out using binomial tests to calculate the probability of having as many Smurfs in population A as in population B. The binomial tests were performed using R version 2.14.2.

Feeding assays.

Quantification of food intake was assayed at 10 d of age using two different approaches. Firstly, food intake was assayed based upon the uptake of a blue food dye (FD&C Blue Dye No. 1; SPS Alfachem) as described in (Hur et al., 2013; Rana et al., 2013; Wong et al., 2009). Three vials of female flies of each genotype were transferred onto fresh medium containing blue dye 2.5% wt/vol at 9:00 AM hours for 2 hours. Flies were frozen, decapitated, and homogenized separately in 250µl H2O. Cell debris was pelleted via centrifugation, and absorbance (629nm) of a 1:2.5 dilution of the supernatant was used to determine whether the fly ate (flies were categorized as

having eaten if they had A629nm greater than 110% of the absorbance outside of the dye absorption range, at 800nm), and if so, the relative meal size (A629-A800) and absorbance was measured at 630 nm using an Epoch spectrophotometer (BioTek).

Analysis of capillary feeding ("the CAFE assay") was performed similarly to (Hur et al., 2013; Ja et al., 2007) with minor modifications. Briefly, 10 flies were placed in vials with wet tissue paper as a water source and a capillary food source (5% sucrose, 5% yeast extract, 2.5% FD&C Blue No. 1) Feeding was monitored from 1 h after lights on until lights off, with capillaries being replaced and feeding amounts recorded every hour, for 11-12 hours.

Fecundity.

Eight vials of mated female flies (10 flies per vial) were collected and kept in a humidified, temperature-controlled incubator with 12 h on/off light cycle at 25 °C. Eggs laid per fly in 24 h were counted on days 7, 14, 23, and 30 post-eclosion.

Spontaneous Activity Assay.

Spontaneous activity was measured via the Drosophila Activity Monitor (DAM) system as in (Rana et al., 2013). Each experiment was performed on 3 vials of 10 flies each, with average number of beam breaks condensed into 10 minute intervals over 24 hours of a 12 hour light/dark cycle.

Climbing Assay.

Assessment of climbing ability was performed similarly to (Copeland et al., 2009) with minor modifications. Briefly, 30 flies were placed in a standard 23mmX95mm plastic vial and gently

tapped to the bottom. The number of flies that reached the top 1/4 of the vial within 20 seconds were then scored as climbing. Each experiment was performed on a minimum of 6 vials of 30 flies.

Hyperoxia lifespan.

Vials of 10 day old flies were maintained on food with or without RU486, kept in a humidified Plexiglas chamber where oxygen was constantly passed through at a rate sufficient to maintain an atmospheric concentration of 80%. Flies were scored for death 1-2 times daily, and media was changed every 2 days.

Heat stress.

Vials of 10 day old flies were maintained on food with or without RU486, kept in a humidified incubator at 37°C. Flies were scored for death every hour to ½ hour.

REFERENCES:

Broughton, S.J., Slack, C., Alic, N., Metaxakis, A., Bass, T.M., Driege, Y., and Partridge, L. (2010). DILP-producing median neurosecretory cells in the Drosophila brain mediate the response of lifespan to nutrition. Aging cell *9*, 336-346.

Copeland, J.M., Cho, J., Lo, T., Jr., Hur, J.H., Bahadorani, S., Arabyan, T., Rabie, J., Soh, J., and Walker, D.W. (2009). Extension of Drosophila life span by RNAi of the mitochondrial respiratory chain. Current biology : CB *19*, 1591-1598.

Hur, J.H., Bahadorani, S., Graniel, J., Koehler, C.L., Ulgherait, M., Rera, M., Jones, D.L., and Walker, D.W. (2013). Increased longevity mediated by yeast NDI1 expression in Drosophila intestinal stem and progenitor cells. Aging *5*, 662-681.

Ja, W.W., Carvalho, G.B., Mak, E.M., de la Rosa, N.N., Fang, A.Y., Liong, J.C., Brummel, T., and Benzer, S. (2007). Prandiology of Drosophila and the CAFE assay. Proceedings of the National Academy of Sciences of the United States of America *104*, 8253-8256.

Rana, A., Rera, M., and Walker, D.W. (2013). Parkin overexpression during aging reduces proteotoxicity, alters mitochondrial dynamics, and extends lifespan. Proceedings of the National Academy of Sciences of the United States of America *110*, 8638-8643.

Rera, M., Clark, R.I., and Walker, D.W. (2012). Intestinal barrier dysfunction links metabolic and inflammatory markers of aging to death in Drosophila. Proceedings of the National Academy of Sciences of the United States of America *109*, 21528-21533.

Wong, R., Piper, M.D., Wertheim, B., and Partridge, L. (2009). Quantification of food intake in Drosophila. PloS one *4*, e6063.

APPENDIX I:

DATA IN SUPPORT OF AMPK REGULATION OF AGING AND AUTOPHAGY

Lifespan screens for tissue-specific AMPK interventions.

When I initially began the AMPK project we set out to determine in which tissues AMPK overexpression could extend lifespan. To accomplish this, I set out to manipulate AMPK via inducible, and constitutive activation in various tissue-subtypes in *Drosophila.* **Figures A1-A4 and Tables A1-A4** represent the sum total of these lifespan screens. This includes manipulating constitutively active (CA) T184D-AMPK, "kinase dead" (DN) K56R- AMPK, RNAi knockdown of AMPK, as well as the normal *wild-type* AMPK gene.

Interesting highlights from these data conclude the following:

1. Inducible AMPK overexpression in neurons /intestine increased lifespan **(Fig/Table. A1).**

2. Inducible ubiquitous, fat-body, and intestinal stem cell (ISC) overexpression of AMPK fail to extend lifespan **(Fig/Table. A1).**

3. Inducible ubiquitous overexpression of AMPK-CA extends lifespan **(Fig. A3).**

4. Inducible ubiquitous overexpression of AMPK-DN severely shortens lifespan **(Fig. A3).**

5. Constitutive overexpression of AMPK, and AMPK-CA extend lifespan in muscle, neurons, pan-intestinal tissue, and intestinal stem cells/enteroblasts, while RNAi of AMPK shortens lifespan in these tissues **(Fig/Table. A4).**

6. Control flies fed RU486 show no positive effects on lifespan **(Fig/Table. A2)**

Ubiquitous overexpression of AMPK can induce markers of autophagy.

While inducible Ubiquitous AMPK overexpression fails to extend lifespan of flies, it is still capable of inducing autophagy markers in the fly **(Fig. A5).** RU486 feeding to control flies showed no change in autophagy genes **(Fig. A6)**.

AMPK controls autophagy and colocalizes to autophagosomes.

Ubiquitously overexpressing an mCherry-tagged form of AMPK (mCh-AMPK), along with the pGFP-Atg8a reporter, I noticed that AMPK (Red) colocalized to autophagosomes (Green) in the *Drosophila* intestine upon acute starvation **(Fig. A7-A)**. Additionally, overexpression of AMPK increases the number of Atg8a foci in the starved intestine compared to control flies **(Fig. A7-B)**, along with increased Atg8 reporter expression at the RNA level **(Fig. A7-C)**,. Additionally, ubiquitous AMPK overexpression sensitizes flies to starvation **(Fig. A7-D).**

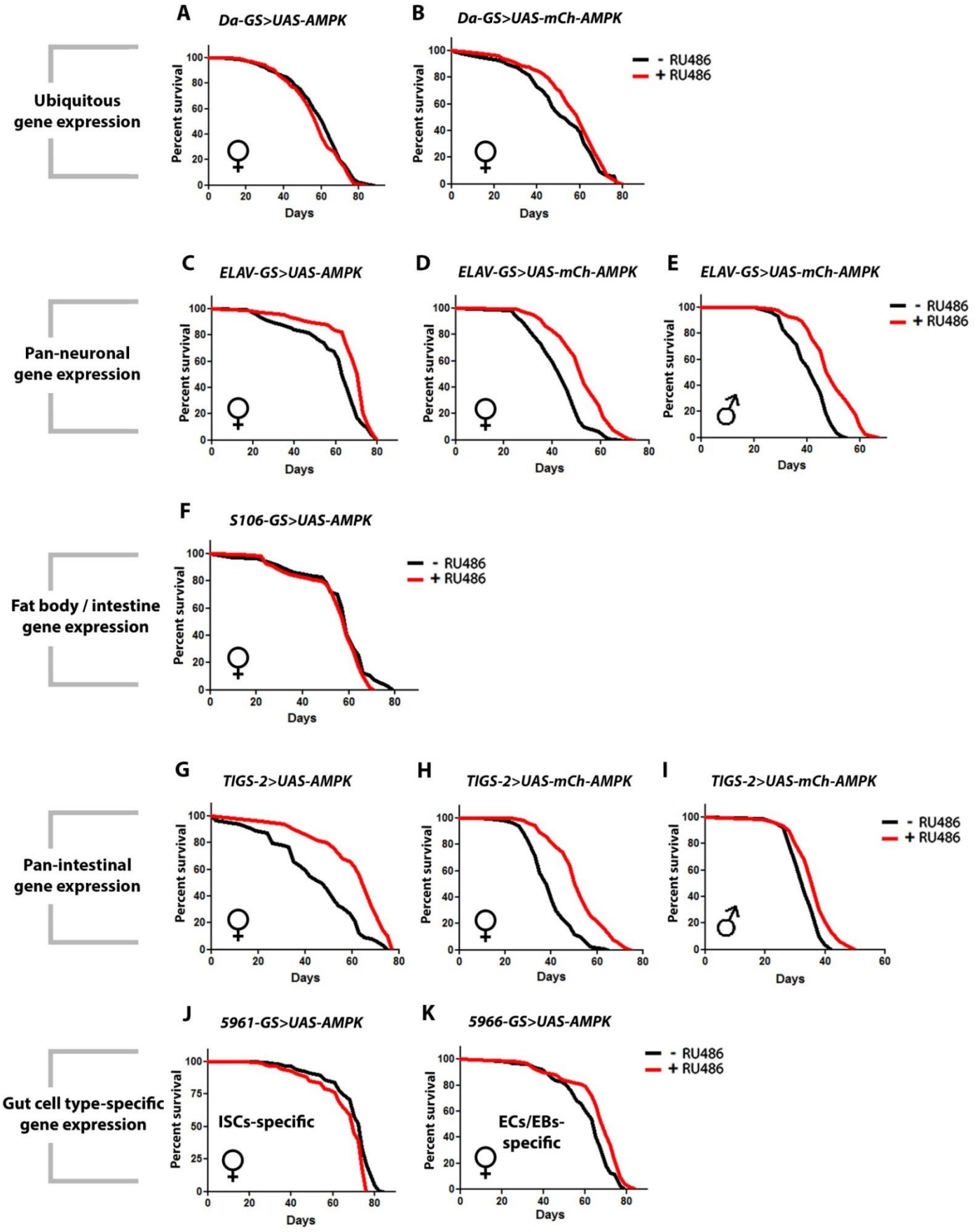

Figure A1. Representative lifespan curves from tissue-specific AMPK expression screen via inducible gene-switch system.

(A) Survival curves of female *Daughterless-GS>UAS- AMPK* flies with or without RU486 induction. Ubiquitous Daughterless gene-switch expression of untagged AMPK does not extend lifespan *(p>0.05; log-rank; n>238 flies/condition).*

(B) Survival curves of female *Daughterless-GS>UAS- AMPK* flies with or without RU486 induction. Ubiquitous expression of mCherry-tagged AMPK does not extend lifespan *(p>0.05; log-rank; n>132 flies/condition).*

(C) Survival curves of female *ELAV-GS>UAS- AMPK* flies with or without RU486 induction. Neuronal gene-switch expression of untagged AMPK extends lifespan by 13% *(p<0.0001; log-rank; n>106 flies/condition).*

(D) Survival curves of female *ELAV-GS>UAS-mCh-AMPK* flies with or without RU486 induction. Neuronal gene-switch expression of mCherry-tagged AMPK extends lifespan by over 20% *(p<0.0001; log-rank; n>159 flies/condition).*

(E) Survival curves of male *ELAV-GS>UAS-mCh-AMPK* flies with or without RU486 induction. Neuronal gene-switch expression of mCherry-tagged AMPK extends male lifespan by over 16% *(p<0.0001; log-rank; n>94 flies/condition).*

(F) Survival curves of female *S106-GS>UAS- AMPK* flies with or without RU486 induction. Fat body gene-switch expression of untagged AMPK does not extend lifespan *(p>0.05; log-rank; n>110 flies/condition).*

(G) Survival curves of female *TIGS-2>UAS- AMPK* flies with or without RU486 induction. Intesine-specific gene-switch expression of untagged AMPK extends lifespan by 31% *(p<0.0001; log-rank; n>65 flies/condition).*

(H) Survival curves of female *TIGS-2>UAS-mCh-AMPK* flies with or without RU486 induction. Intesine-specific gene-switch expression of mCherry-tagged AMPK extends lifespan by over 39% *(p<0.0001; log-rank; n>104 flies/condition).*

(I) Survival curves of male *TIGS-2>UAS-mCh-AMPK* flies with or without RU486 induction. Intestinal gene-switch expression of mCherry-tagged AMPK extends male lifespan by over 9% *(p<0.0001; log-rank; n>95 flies/condition).*

(J) Survival curves of female *5961-GS>UAS- AMPK* flies with or without RU486 induction. Intesinal stem cell-specific (ISCs) gene-switch expression of untagged AMPK does not extend lifespan *(p>0.05; log-rank; n>335 flies/condition).*

(K) Survival curves of female 5966-GS>*UAS- AMPK* flies with or without RU486 induction. Enterocyte/enteroblast-specific gene-switch expression of untagged AMPK extends lifespan by 9% *(p<0.0001; log-rank; n>104 flies/condition).*

TABLE A1. Lifespan data associated to figure A1

Repeat	Genotype	RU-486 dose µG / ml of food	Sex	Median lifespan days	Percent change median lifespan to "0 RU"	Sample size	Log Rank p-value
1	Daughterless-GS>UAS-AMPK	0	F	63		308	
	Daughterless-GS>UAS-AMPK	25	F	58	-8.62	292	0.0299
	Daughterless-GS>UAS-AMPK	50	F	56	-12.5	273	< 0.0001
2	Daughterless-GS>UAS-AMPK	0	F	59		247	
	Daughterless-GS>UAS-AMPK	25	F	54	-9.25	238	0.0394
	Daughterless-GS>UAS-AMPK	50	F	53	-11.32	104	0.0116
1	Daughterless-GS>UAS-AMPK	0	M	44		300	
	Daughterless-GS>UAS-AMPK	25	M	44	NS	289	NS
	Daughterless-GS>UAS-AMPK	50	M	44	NS	287	NS
1	Daughterless-GS>UAS-mCh-AMPK	0	F	53		175	
	Daughterless-GS>UAS-mCh-AMPK	25	F	53	NS	142	NS
	Daughterless-GS>UAS-mCh-AMPK	50	F	56	NS	132	0.0746
1	ELAV-GS>UAS-AMPK	0	F	63		119	
	ELAV-GS>UAS-AMPK	25	F	65	**+3.17**	188	0.0112
	ELAV-GS>UAS-AMPK	50	F	71.5	**+13.49**	106	< 0.0001
2	ELAV-GS>UAS-AMPK	0	F	51		239	
	ELAV-GS>UAS-AMPK	50	F	56	**+9.8**	226	< 0.0001
3	ELAV-GS>UAS-AMPK	0	F	43		281	
	ELAV-GS>UAS-AMPK	50	F	48	**+11.6**	284	< 0.0001
1	ELAV-GS>UAS-AMPK	0	M	43		162	
	ELAV-GS>UAS-AMPK	50	M	48	NS	120	NS
1	ELAV-GS>UAS-mCh-AMPK	0	F	46		120	
	ELAV-GS>UAS-mCh-AMPK	25	F	64	**+39.1**	105	< 0.0001
2	ELAV-GS>UAS-mCh-AMPK	0	F	49		180	
	ELAV-GS>UAS-mCh-AMPK	25	F	55	**+12.2**	165	0.0034
3	ELAV-GS>UAS-mCh-AMPK	0	F	49		205	
	ELAV-GS>UAS-mCh-AMPK	25	F	59	**+20.4**	159	< 0.0001
1	ELAV-GS>UAS-mCh-AMPK	0	M	42		87	
	ELAV-GS>UAS-mCh-AMPK	25	M	40	NS	85	NS
	ELAV-GS>UAS-mCh-AMPK	100	M	49	**+16.6**	94	< 0.0001
1	S106-GS>UAS-AMPK	0	F	59		110	
	S106-GS>UAS-AMPK	25	F	59	NS	185	NS
1	TIGS-2>UAS-AMPK	0	F	48		64	
	TIGS-2>UAS-AMPK	25	F	65	**+35.4**	50	0.001
	TIGS-2>UAS-AMPK	50	F	63	**+31.2**	67	<0.0001
2	TIGS-2>UAS-AMPK	0	F	36		266	
	TIGS-2>UAS-AMPK	25	F	43	**+19.4**	244	<0.0001
3	TIGS-2>UAS-AMPK	0	F	40		258	
	TIGS-2>UAS-AMPK	25	F	43	**+7.5**	284	0.0135

TABLE A1 continued . Lifespan data associated to figure A1

Repeat	Genotype	RU-486 dose µG / ml of food	Sex	Median lifespan days	Percent change median lifespan to "0 RU"	Sample size	Log Rank p-value
1	TIGS-2>UAS-AMPK	0	M	49		295	
	TIGS-2>UAS-AMPK	25	M	46	NS	292	NS
	TIGS-2>UAS-AMPK	50	M	49	NS	228	NS
1	TIGS-2>UAS-mCh-AMPK	0	F	25		117	
	TIGS-2>UAS-mCh-AMPK	100	F	50	**+100**	81	< 0.0001
2	TIGS-2>UAS-mCh-AMPK	0	F	38		116	
	TIGS-2>UAS-mCh-AMPK	100	F	53	**+39.47**	104	< 0.0001
3	TIGS-2>UAS-mCh-AMPK	0	F	45		106	
	TIGS-2>UAS-mCh-AMPK	100	F	51	**+13.3**	120	< 0.0001
1	TIGS-2>UAS-mCh-AMPK	0	M	41		95	
	TIGS-2>UAS-mCh-AMPK	100	M	45	**+9.75**	110	0.002
1	5961-GS>UAS-AMPK	0	F	74		416	
	5961-GS>UAS-AMPK	25	F	70	-5.4	376	< 0.0001
	5961-GS>UAS-AMPK	50	F	72	-2.7	335	< 0.0001
1	5966-GS>UAS-AMPK	0	F	65		144	
	5966-GS>UAS-AMPK	25	F	70	**+9.75**	104	< 0.0001

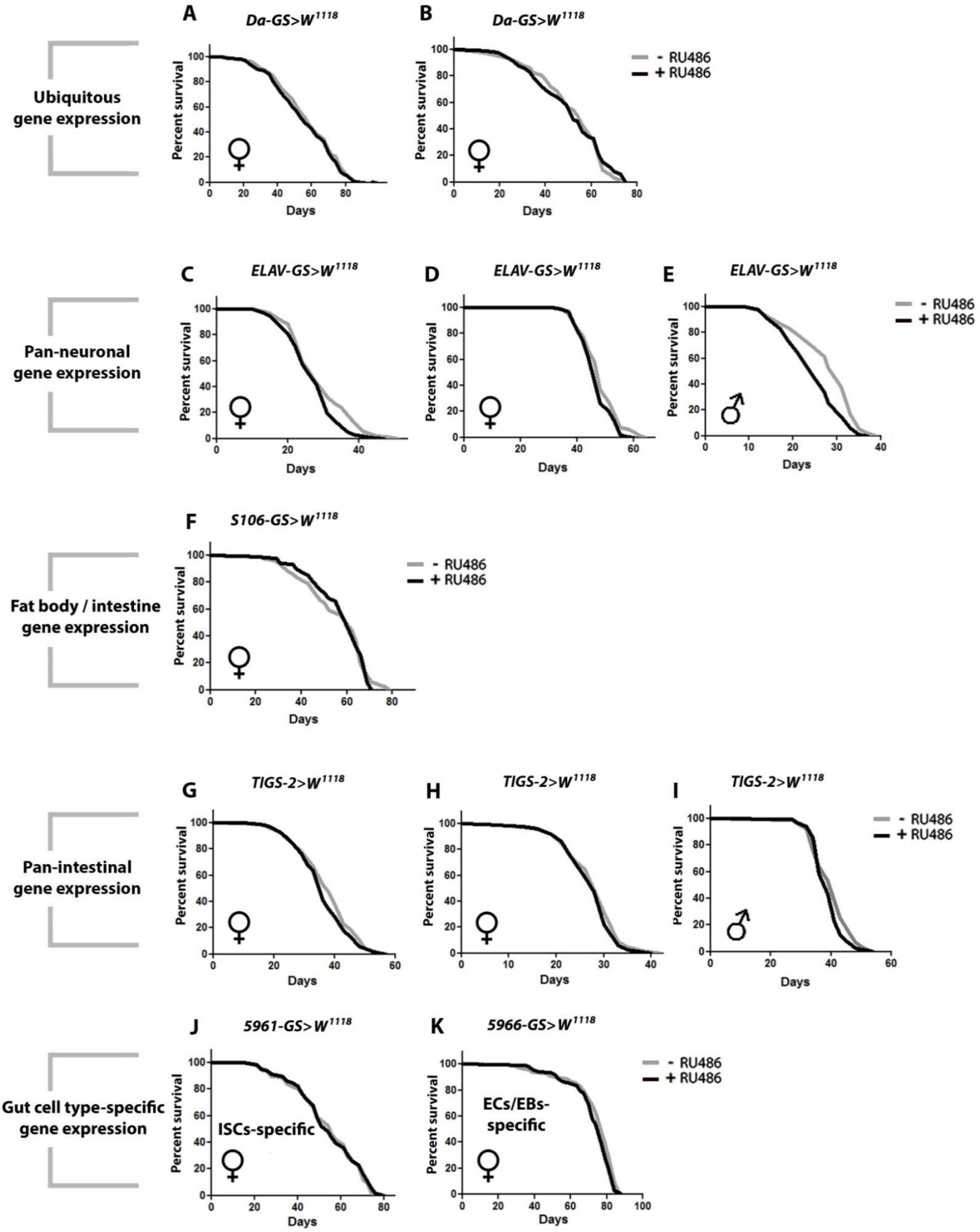

Figure A2. Control W^{1118} lifespan curves from tissue-specific expression screen via inducible gene-switch system.

(A) Survival curves of female *Daughterless-GS>W^{1118}* flies with or without RU486 induction. Feeding RU486 to control flies does not influence lifespan *(p>0.05; log-rank; n>131 flies/condition).*

(B) Repeat survival curves of female *Daughterless-GS>W^{1118}* flies with or without RU486 induction. Feeding RU486 to control flies does not influence lifespan *(p>0.05; log-rank; n>300 flies/condition).*

(C) Survival curves of female *ELAV-GS>W^{1118}* flies with or without RU486 induction. Feeding RU486 to control flies does not influence lifespan *(p>0.05; log-rank; n>121 flies/condition).*

(D) Repeat survival curves of female *ELAV-GS>W^{1118}* flies with or without RU486 induction. Feeding RU486 to control flies does not influence lifespan *(p>0.05; log-rank; n>168 flies/condition).*

(E) Survival curves of male *ELAV-GS>W^{1118}* flies with or without RU486 induction. Feeding RU486 to male control reduces lifespan *(p<0.0001; log-rank; n>140 flies/condition).*

(F) Survival curves of female *S106-GS>W^{1118}*flies with or without RU486 induction Feeding RU486 to female controls did not influence lifespan *(p>0.05; log-rank; n>138 flies/condition).*

(G) Survival curves of female *TIGS-2>W^{1118}* flies with or without RU486 induction Feeding RU486 to female controls did not influence lifespan *(p>0.05; log-rank; n>98 flies/condition).*

(H) Repeat survival curves of female *TIGS-2>W^{1118}* flies with or without RU486 induction. Feeding RU486 to female controls did not influence lifespan *(p>0.05; log-rank; n>252 flies/condition).*

(I) Survival curves of male *TIGS-2>W^{1118}* flies with or without RU486 induction Feeding RU486 to male controls moderately reduced lifespan *(p<0.01; log-rank; n>291 flies/condition).*

(J) Survival curves of female *5961-GS>W^{1118}* flies with or without RU486 induction. Feeding RU486 to female controls did not influence lifespan *(p>0.05; log-rank; n>290 flies/condition).*

(K) Survival curves of female 5966-GS>*W^{1118}* flies with or without RU486 induction. Feeding RU486 to female controls did not influence lifespan *(p>0.05; log-rank; n>135 flies/condition).*

TABLE A2. Lifespan data associated to control figure A2

Repeat	Genotype	RU-486 dose µG / ml of food	Sex	Median lifespan days	Percent change median lifespan to "0 RU"	Sample size	Log Rank p-value
1	Daughterless-GS>W^{1118}	0	F	58		300	
	Daughterless-GS>W^{1118}	25	F	56	NS	287	NS
	Daughterless-GS>W^{1118}	50	F	56	NS	283	NS
2	Daughterless-GS>W^{1118}	0	F	56		131	
	Daughterless-GS>W^{1118}	25	F	52	NS	133	NS
	Daughterless-GS>W^{1118}	50	F	54	NS	132	NS
3	Daughterless-GS>W^{1118}	0	M	44		301	
	Daughterless-GS>W^{1118}	25	M	51	NS	305	NS
	Daughterless-GS>W^{1118}	50	M	51	NS	283	NS
1	ELAV-GS>W^{1118}	0	F	47		121	
	ELAV-GS>W^{1118}	25	F	42	-11.9	122	< 0.0001
	ELAV-GS>W^{1118}	50	F	45	-4.4	118	0.037
2	ELAV-GS>W^{1118}	0	F	48		202	
	ELAV-GS>W^{1118}	50	F	46	-4.3	168	0.033
3	ELAV-GS>W^{1118}	0	F	35		218	
	ELAV-GS>W^{1118}	50	F	35	NS	171	NS
1	ELAV-GS>W^{1118}	0	M	30		140	
	ELAV-GS>W^{1118}	50	M	28	NS	172	NS
1	ELAV-GS>W^{1118}	0	F	28		153	
	ELAV-GS>W^{1118}	25	F	26	-7.6	108	0.0146
2	ELAV-GS>W^{1118}	0	F	37		116	
	ELAV-GS>W^{1118}	25	F	29	-27.5	92	< 0.0001
3	ELAV-GS>W^{1118}	0	F	40		187	
	ELAV-GS>W^{1118}	25	F	35	-14.2	176	0.0003
2	ELAV-GS>W^{1118}	0	M	31		98	
	ELAV-GS>W^{1118}	25	M	24	-22.5	93	0.01564
	ELAV-GS>W^{1118}	100	M	24	-22.5	88	< 0.0001
1	S106-GS> W^{1118}	0	F	62		138	
	S106-GS> W^{1118}	25	F	62	NS	170	NS
1	TIGS-2>W^{1118}	0	F	40		126	
	TIGS-2>W^{1118}	25	F	43	+6.9	106	0.0121
	TIGS-2>W^{1118}	50	F	39		98	NS
2	TIGS-2>W^{1118}	0	F	38		291	
	TIGS-2>W^{1118}	25	F	36	-5.5	292	0.0143
3	TIGS-2>W^{1118}	0	F	41		252	
	TIGS-2>W^{1118}	25	F	43	NS	325	NS

TABLE A2 continued . Lifespan data associated to control figure A2

Repeat	Genotype	RU-486 dose µG / ml of food	Sex	Median lifespan days	Percent change median lifespan to "0 RU"	Sample size	Log Rank p-value
1	TIGS-2>W^{1118}	0	M	46		287	
	TIGS-2>W^{1118}	25	M	42	-9.5	288	< 0.0001
	TIGS-2>W^{1118}	50	M	42	-9.5	276	< 0.0001
1	TIGS-2>W^{1118}	0	F	32		145	
	TIGS-2>W^{1118}	100	F	29	-10.3	159	0.0048
2	TIGS-2>W^{1118}	0	F	28		131	
	TIGS-2>W^{1118}	100	F	28	NS	123	NS
3	TIGS-2>W^{1118}	0	F	41		146	
	TIGS-2>W^{1118}	100	F	39	NS	152	NS
1	TIGS-2>W^{1118}	0	M	41		104	
1	TIGS-2>W^{1118}	100	M	39	-5.1	107	0.0006
1	5961-GS> W^{1118}	0	F	56		413	
	5961-GS> W^{1118}	25	F	54	NS	709	NS
	5961-GS> W^{1118}	50	F	49	-12.5	290	0.001
1	5966-GS> W^{1118}	0	F	79		172	
	5966-GS> W^{1118}	25	F	77	NS	135	NS

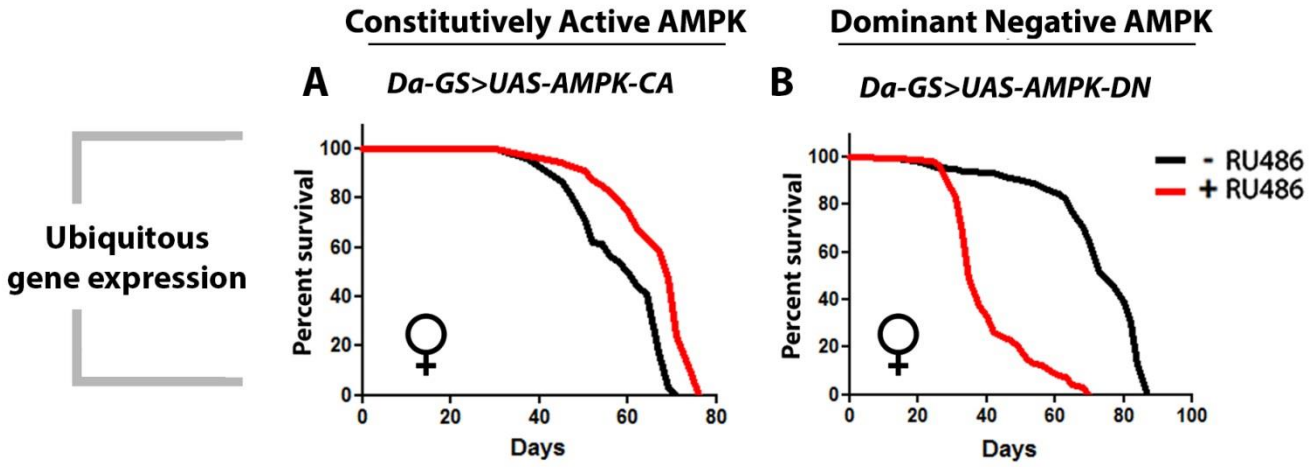

Figure A3. Ubiquitous overexpression of constitutively active (CA) phosphomimetic (Thr184D) AMPK extends lifespan, and upregulation of dominant negative (DN) kinase dead (K56R) AMPK shortens lifespan.

(A) Representative survival curves of female *Daughterless-GS>UAS-AMPK-CA* flies with or without RU486 induction. Ubiquitous overexpression of constitutively active AMPK extends lifespan by over 15% *(p<0.0001; log-rank; n>147 flies/condition).*

(B) Representative survival curves of female *Daughterless-GS>UAS-AMPK-DN* flies with or without RU486 induction. Ubiquitous overexpression of dominant negative AMPK strongly shortens lifespan by over 50% *(p<0001; log-rank; n>131 flies/condition).*

TABLE A3. Lifespan data associated to control figure A3

Repeat	Genotype	RU-486 dose µG / ml of food	Sex	Mean lifespan days	Percent change mean lifespan to "0 RU"	Sample size	Log Rank p-value
1	Daughterless-GS>UAS-AMPK-CA	0	F	70		147	
	Daughterless-GS>UAS-AMPK-CA	50	F	84	**+20**	151	< 0.0001
2	Daughterless-GS>UAS-AMPK-CA	0	F	60		163	
	Daughterless-GS>UAS-AMPK-CA	50	F	69	**+15**	168	< 0.0001
1	Daughterless-GS>UAS-AMPK-DN	0	F	67		220	
	Daughterless-GS>UAS-AMPK-DN	50	F	33	-50.7	121	< 0.0001

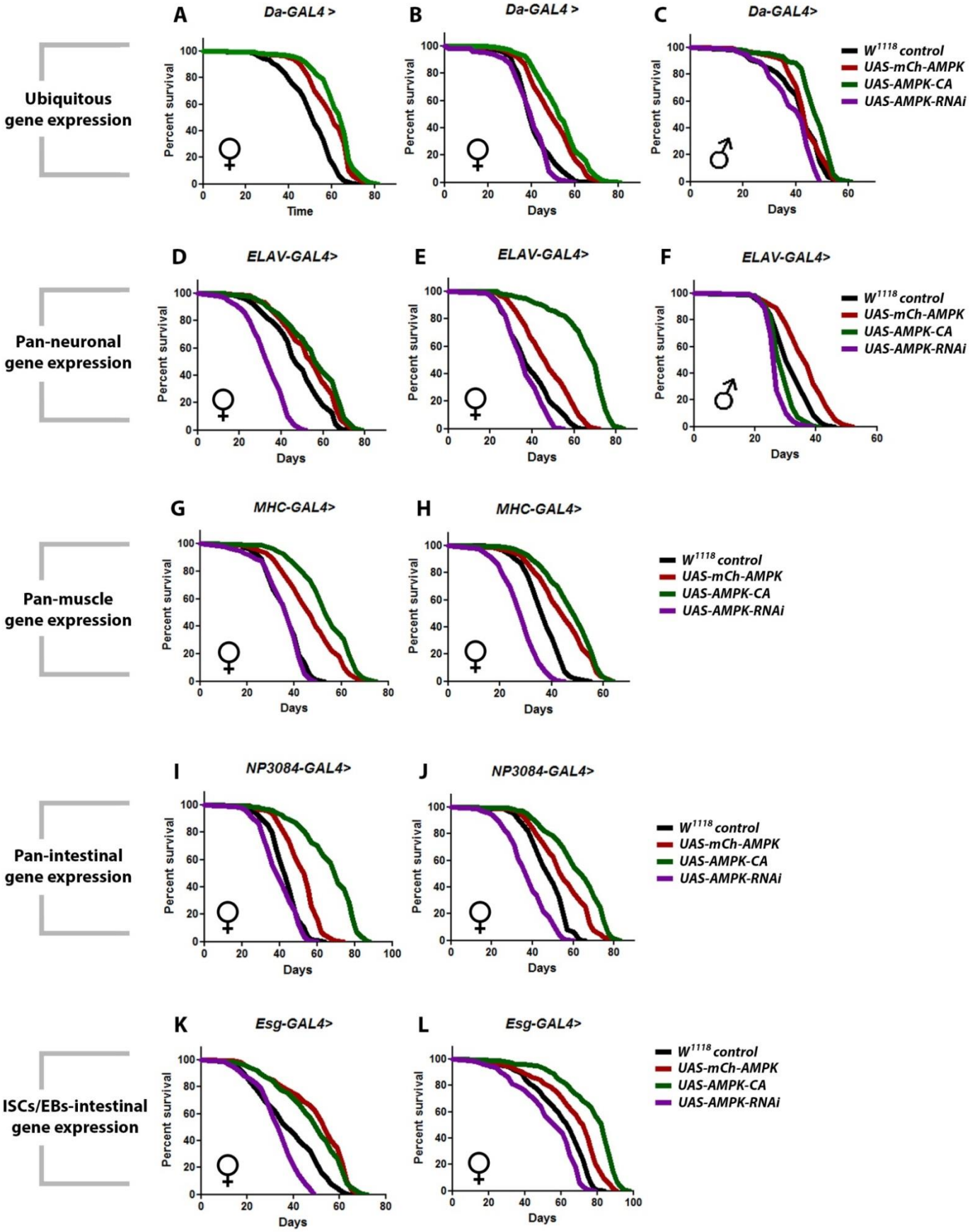

Figure A4. Representative lifespan curves from tissue-specific AMPK expression screen via constitutive UAS-GAL4 system.

(A) Survival curves of outcrossed female *Daughterless-GAL4>* flies crossed to outcrossed *UAS-mCh-AMPK, UAS-AMPK-CA,* and W^{1118} controls. Ubiquitous expression of AMPK, and constitutively active AMPK both significantly extend lifespan compared to W1118 control strain *(p<0.0001; log-rank; n>184 flies/condition).*

(B) Survival curves of outcrossed female *Daughterless-GAL4>* flies crossed to *UAS-mCh-AMPK, UAS-AMPK-CA,UAS-AMPK-RNAi* and W^{1118} controls. Ubiquitous expression of AMPK, and constitutively active AMPK both significantly extend lifespan compared to W^{1118} control strain, AMPK-RNAi moderately shortens lifespan *(p<0.0001; log-rank; n>161 flies/condition).*

(C) Survival curves of male *Daughterless-GAL4>* flies crossed to *UAS-mCh-AMPK, UAS-AMPK-CA,UAS-AMPK-RNAi* and W^{1118} controls. Ubiquitous expression of AMPK-CA significantly extends lifespan compared to W^{1118} control strain. mCH-AMPK and AMPK-RNAi do not affect lifespan compared to controls *(mCh-AMPK, p<0.0001; log-rank; n>148 flies/condition).*

(D) Survival curves of outcrossed female *ELAV-GAL4>* flies crossed to *UAS-mCh-AMPK, UAS-AMPK-CA,UAS-AMPK-RNAi* and W^{1118} controls. Neuronal expression of AMPK, and constitutively active AMPK both significantly extend lifespan compared to W^{1118} control strain, AMPK-RNAi shortens lifespan *(p<0.0001; log-rank; n>198 flies/condition).*

(E) Survival curves of outcrossed female *ELAV-GAL4>* flies crossed to *UAS-mCh-AMPK, UAS-AMPK-CA,UAS-AMPK-RNAi* and W^{1118} controls. Neuronal expression of AMPK, and constitutively active AMPK both significantly extend lifespan compared to W^{1118} control strain. AMPK-RNAi shortens lifespan *(p<0.0001; log-rank; n>331 flies/condition).*

(F) Survival curves of male *ELAV-GAL4>* flies crossed to *UAS-mCh-AMPK, UAS-AMPK-CA,UAS-AMPK-RNAi* and W^{1118} controls. Neuronal expression of AMPK significantly extends lifespan compared to W^{1118} control strain. AMPK-CA, and AMPK-RNAi moderately reduce lifespan compared to controls *(mCh-AMPK, p<0.0001; log-rank; n>148 flies/condition).*

(G) Survival curves of outcrossed female *MHC-GAL4>* flies crossed to *UAS-mCh-AMPK, UAS-AMPK-CA,UAS-AMPK-RNAi* and W^{1118} controls. Muscle-specific expression of AMPK, and constitutively active AMPK both significantly extend lifespan compared to W^{1118} control strain, AMPK-RNAi shows no lifespan effects *(p<0.0001; log-rank; n>247 flies/condition).*

(H) Survival curves of outcrossed female *MHC-GAL4>* flies crossed to *UAS-mCh-AMPK, UAS-AMPK-CA,UAS-AMPK-RNAi* and W^{1118} controls. Muscle-specific expression of AMPK, and constitutively active AMPK both significantly extend lifespan compared to W^{1118} control strain, AMPK-RNAi shortens lifespan *(p<0.0001; log-rank; n>174 flies/condition).*

(I) Survival curves of outcrossed female *NP3084-GAL4>* flies crossed to *UAS-mCh-AMPK, UAS-AMPK-CA,UAS-AMPK-RNAi* and W^{1118} controls. Intestine-specific expression of AMPK, and constitutively active AMPK both significantly extend lifespan compared to W^{1118} control strain, AMPK-RNAi shortens lifespan *(p<0.0001; log-rank; n>319 flies/condition).*

(J) Survival curves of outcrossed female *NP3084-GAL4>* flies crossed to *UAS-mCh-AMPK, UAS-AMPK-CA,UAS-AMPK-RNAi* and W^{1118} controls. Intestine-specific expression of AMPK, and

constitutively active AMPK both significantly extend lifespan compared to W^{1118} control strain, AMPK-RNAi shortens lifespan *(p<0.0001; log-rank; n>220 flies/condition).*

(K) Survival curves of outcrossed female *Esg-GAL4>* flies crossed to *UAS-mCh-AMPK, UAS-AMPK-CA,UAS-AMPK-RNAi* and W^{1118} controls. ISC/EB-specific expression of AMPK, and constitutively active AMPK both significantly extend lifespan compared to W^{1118} control strain, AMPK-RNAi shortens lifespan *(p<0.0001; log-rank; n>185 flies/condition).*

(L) Survival curves of outcrossed female *Esg-GAL4>* flies crossed to *UAS-mCh-AMPK, UAS-AMPK-CA,UAS-AMPK-RNAi* and W^{1118} controls. ISC/EB-specific expression of AMPK, and constitutively active AMPK both significantly extend lifespan compared to W^{1118} control strain, AMPK-RNAi shortens lifespan *(p<0.0001; log-rank; n>158 flies/condition).*

TABLE A4. Lifespan data associated to control figure A4

Repeat	Genotype	Sex	Median lifespan days	median lifespan % change	Sample size	Log Rank
1	DA-GAL4>W^{1118}	F	39		350	
	DA-GAL4>UAS-mCh-AMPK	F	51	**+30.7**	296	<0.00001
	DA-GAL4>UAS-AMPK-CA	F	53	**+35.89**	361	<0.00001
	DA-GAL4>UAS-AMPK-RNAi	F	41	NS	161	NS
2	DA-GAL4>W^{1118}	F	52		208	
	DA-GAL4>UAS-mCh-AMPK	F	61	**+17.3**	184	<0.00001
	DA-GAL4>UAS-AMPK-CA	F	66	**+26.9**	193	<0.00001
3	DA-GAL4>W^{1118}	F	49		171	
	DA-GAL4>UAS-mCh-AMPK	F	49	NS	215	NS
	DA-GAL4>UAS-AMPK-CA	F	52	**+6.12**	243	<0.00001
	DA-GAL4>UAS-AMPK-RNAi	F	46	-3.11	135	0.015
1	DA-GAL4>W^{1118}	M	44		109	
	DA-GAL4>UAS-mCh-AMPK	M	44	NS	119	NS
	DA-GAL4>UAS-AMPK-CA	M	49	**+11.3**	135	<0.00001
	DA-GAL4>UAS-AMPK-RNAi	M	42	NS	154	NS

TABLE A4 continued. Lifespan data associated to control figure A4

Repeat	Genotype	Sex	Median lifespan days	median lifespan % change	Sample size	Log Rank
1	ELAV-GAL4>W^{1118}	F	37		358	
	ELAV-GAL4> mCh-AMPK	F	46	**+24.3**	363	<0.00001
	ELAV-GAL4> AMPK-CA	F	70	**+89.1**	331	<0.00001
	ELAV-GAL4> AMPK-RNAi	F	35	-5.4	387	<0.00001
2	ELAV-GAL4>W^{1118}	F	47		270	
	ELAV-GAL4> mCh-AMPK	F	56	**+19.1**	212	<0.00001
	ELAV-GAL4> AMPK-CA	F	59	**+25.5**	289	<0.00001
	ELAV-GAL4> AMPK-RNAi	F	34	-27.6	198	<0.00001
1	ELAV-GAL4>W^{1118}	M	30		168	
	ELAV-GAL4> mCh-AMPK	M	37	**+30.3**	148	<0.00001
	ELAV-GAL4> AMPK-CA	M	28	-6.67	209	<0.00001
	ELAV-GAL4> AMPK-RNAi	M	27	-10.0	164	<0.00001
1	MHC-GAL4>W^{1118}	F	38		384	
	MHC-GAL4> mCh-AMPK	F	47	**+23.6**	414	<0.00001
	MHC-GAL4> AMPK-CA	F	56	**+47.3**	414	<0.00001
	MHC-GAL4> AMPK-RNAi	F	38	NS	247	NS
2	MHC-GAL4>W^{1118}	F	38		360	
	MHC-GAL4> mCh-AMPK	F	45	**+18.4**	232	<0.00001
	MHC-GAL4> AMPK-CA	F	49	**+28.9**	271	<0.00001
	MHC-GAL4> AMPK-RNAi	F	28	-26.3	174	<0.00001
1	NP3084-GAL4>W^{1118}	F	43		447	
	NP3084-GAL4> mCh-AMPK	F	54	**+25.5**	378	<0.00001
	NP3084-GAL4> AMPK-CA	F	71	**+65.1**	351	<0.00001
	NP3084-GAL4> AMPK-RNAi	F	41	-4.65	319	<0.00001
2	NP3084-GAL4>W^{1118}	F	48		289	
	NP3084-GAL4> mCh-AMPK	F	55	**+14.5**	220	<0.00001
	NP3084-GAL4> AMPK-CA	F	66	**+37.5**	229	<0.00001
	NP3084-GAL4> AMPK-RNAi	F	38	-20.83	350	<0.00001
1	Esg-GAL4>W^{1118}	F	38		204	
	Esg-GAL4> mCh-AMPK	F	54	**+42.1**	243	<0.00001
	Esg-GAL4> AMPK-CA	F	52	**+36.8**	200	<0.00001
	Esg-GAL4> AMPK-RNAi	F	35	-7.89	158	<0.00001
2	Esg-GAL4>W^{1118}	F	65		278	
	Esg-GAL4> mCh-AMPK	F	73.5	**+13.07**	212	<0.00001
	Esg-GAL4> AMPK-CA	F	84	**+29.2**	216	<0.00001
	Esg-GAL4> AMPK-RNAi	F	58	-10.7	185	<0.00001

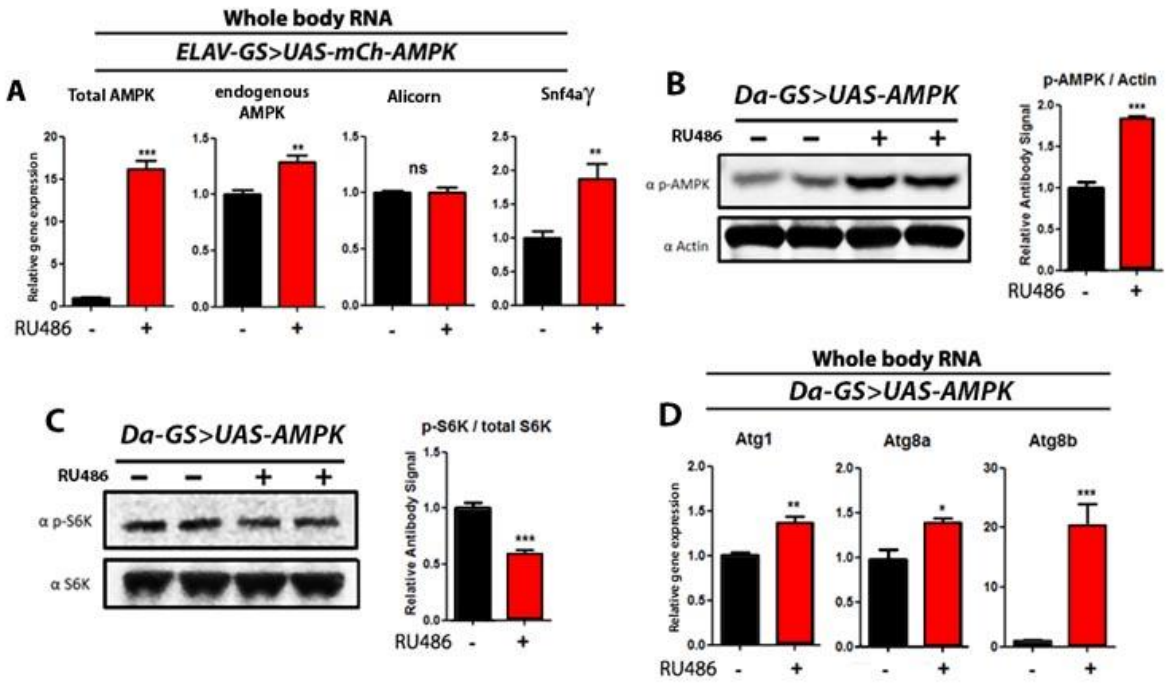

Figure A5. Ubiquitous expression of AMPK is sufficient to increase active phosphorylated AMPK, increase transcript levels of endogenous AMPK subunits, suppress TOR signaling, and induce expression of autophagy genes.

(A) Transcript levels of AMPK subunits, upon ubiquitous adult overexpression of AMPK. RNA was extracted from female flies at 10 days of age. Total levels of AMPK, endogenous AMPK, and Snf4aγ are significantly increased upon RU486 transgene induction (*p<0.01; t-test; n=3, of RNA extracted from 10 flies/replicate*).

(B) Western blot analysis of AMPK phosphorylated on T184 (p-AMPK) and loading control (actin) from whole body lysates of 10 day old female *Da-GS>UAS-AMPK* with or without RU486-mediated transgene induction. Overexpression of AMPK increased the amount of active phosphorylated AMPK. Densitometry quantification

(C) Western blot analysis of S6K phosphorylated at T398 and total S6K from whole body lysates of 10 day old *Da-GS>UAS-AMPK* females with or without RU486-mediated transgene induction. Overexpression of AMPK reduced the amount of phosphorylated S6K compared to vehicle controls. Densitometry quantification (right) (*p<0.0001; t-test; n=3 replicates; 10 flies/replicate*).

(D) Expression of autophagy genes in whole body of *Da-GS>UAS-AMPK* female flies at 10 days of adulthood. Upon AMPK induction we see significantly increased Atg1, Atg8a, and Atg8b RNA levels (*p<0.05*; *t-test; n=3 of RNA extracted from 10 flies/replicate*).

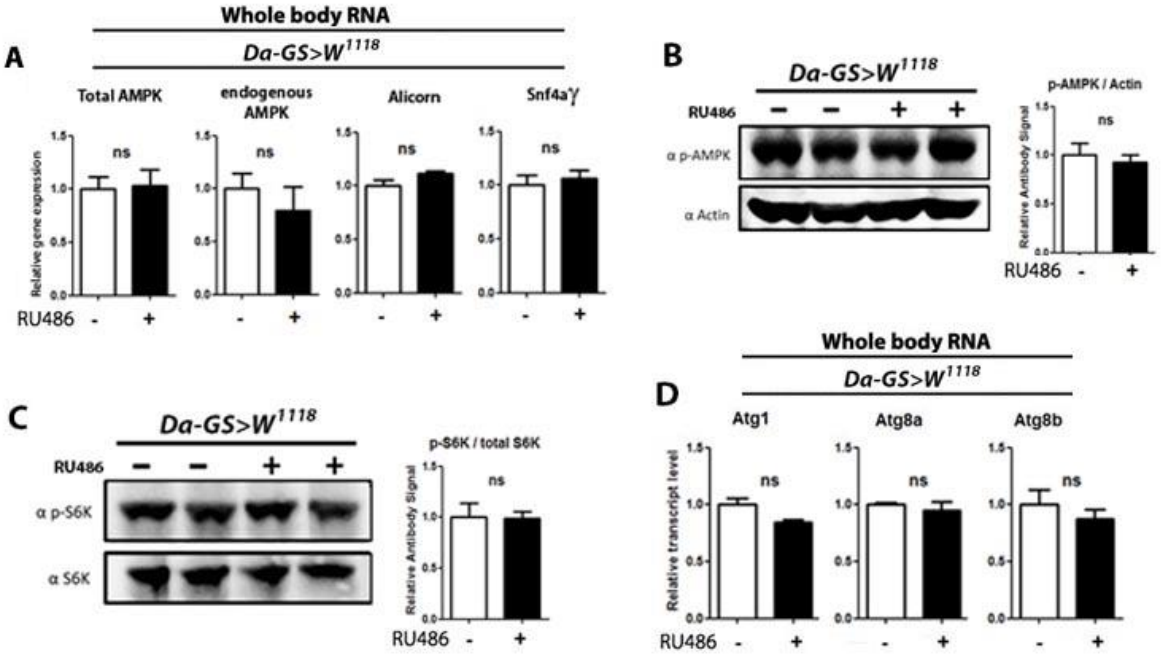

Figure A6. Feeding of RU486 to control *Da-GS>W^{1118}* control flies, does not influence transcript levels of AMPK subunits, AMPK phosphorylation, S6k phosphorylation, or expression of autophagy genes.

(A) Transcript levels of AMPK subunits, upon RU486 feeding to control flies. RNA was extracted from female flies at 10 days of age. Total levels of AMPK, endogenous AMPK, and Snf4aγ remain unchanged in response to RU486 feeding (*p>0.05; t-test; n=3, of RNA extracted from 10 flies/replicate*).

(B) Western blot analysis of AMPK phosphorylated on T184 (p-AMPK) and loading control (actin) from whole body lysates of 10 day old female control flies with or without RU486 feeding. RU486 treatment did not change the amount of active phosphorylated AMPK. Densitometry quantification (right) (*p>0.05; t-test; n=4 replicates; 10 flies/replicate*).

(C) Western blot analysis of S6K phosphorylated at T398 and total S6K from whole body lysates of 10 day old control females with or without RU486-mediated transgene induction. RU486 did not change the amount of phosphorylated S6K. Densitometry quantification (right) (*p>0.05; t-test; n=4 replicates; 10 flies/replicate*).

(D) Expression of autophagy genes in whole body of control female flies at 10 days of adulthood. RU486 feeding did not change the expression levels Atg1, Atg8a, and Atg8b (*p<0.05*; *t-test; n=3 of RNA extracted from 10 flies/replicate*).

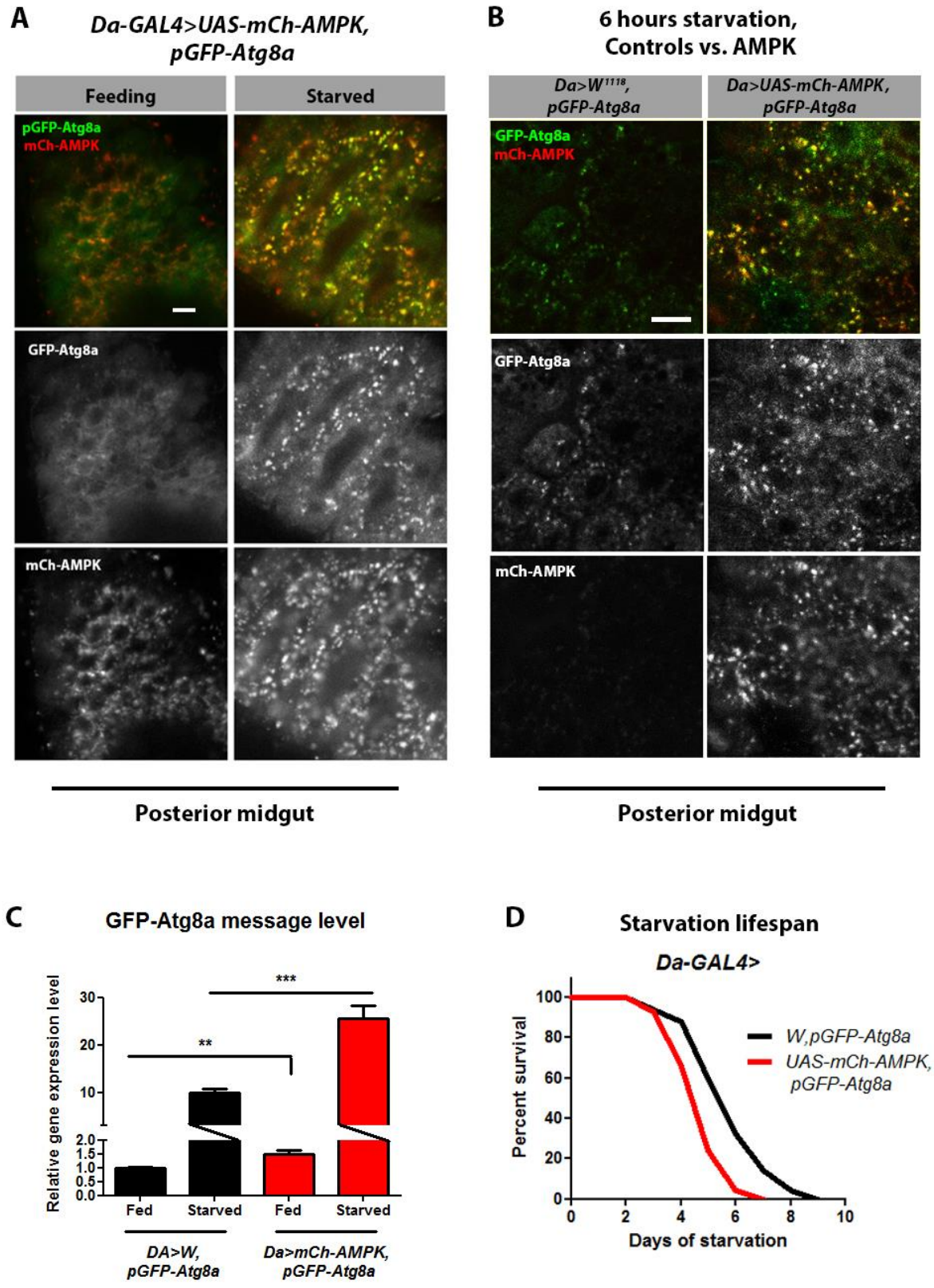

Figure A7. Ubiquitously overexpressed AMPK localizes to GFP-Atg8a foci under starvation conditions, and increases the autophagy response resulting in early lethality.

(A) AMPK localizes to GFP-Atg8a foci under starvation. Live imaging of pGFP-Atg8a reporter flies ubiquitously overexpressing mCherry-tagged AMPK via the Daughterless-Gal4 driver under feeding, and 6 hours of starvation. Upon starvation AMPK localizes to GFP-Atg8a puncta (*scale bar represents 10μm; experiment performed on dissected guts of 10 day old female flies*).

(B) Ubiquitous AMPK overexpression increases the number and fluorescent intensity of GFP-Atg8a puncta compared to control pGFP-Atg8a flies (*scale bar represents 10μm; experiment performed on dissected guts of 10 day old female flies*).

(C) Expression of autophagy genes in whole body of *Da-GAL4>UAS-AMPK, pGFP-Atg8a*, and control *Da-GAL4>W, pGFP-Atg8a* female flies at 10 days of adulthood under normal feeding and 24 hours of starvation. Upon AMPK induction we see significantly increased GFP-Atg8a reporter RNA in both feeding and starved conditions compared to controls ($p<0.01$; *t-test; n=3 of RNA extracted from 10 flies/replicate*).

(D) Starvation survival curves of 10 day old female flies ubiquitously overexpressing AMPK and controls. Systemic upregulation of AMPK decreases survival under starvation compared to control flies ($p<0.0001$; *log rank; n>120 flies/condition*).

APPENDIX II:

Appendix II contains modified partial figure reproductions from two publications.

Jae H. Hur, Sepehr Bahadorani, Jacqueline Graniel, Christopher L. Koehler, Matthew Ulgherait, Michael Rera, D. Leanne Jones, and David W. Walker. Increased longevity mediated by yeast NDI1 expression in *Drosophila* intestinal stem and progenitor cells. *Aging.* (Albany, NY) 2013

Michael Rera, Sepehr Bahadorani, Jaehyoung Cho, Christopher L. Koehler, Matthew Ulgherait, Jae H. Hur, William S. Ansari, Thomas Lo Jr., D. Leanne Jones, David W. Walker. Modulation of longevity and tissue homeostasis by the *Drosophila* PGC-1 homolog**.** *Cell Metabolism.* 2011

My specific contributions to (Hur et al. 2013) are found in **(Figure 2D)** and **(Figure S2A) (Combined as figure A2-1).**

My contributions to (Rera et al. 2011) are found in some of the longevity experiments presented in **(Fig 4)** Dihydroethidium (DHE) staining presented in **(Fig. 5E, F) (Fig. S5D, E) (combined as figure A2-2)** and initial characterization of smurf flies along with Michael Rera in **(Fig. 7).**

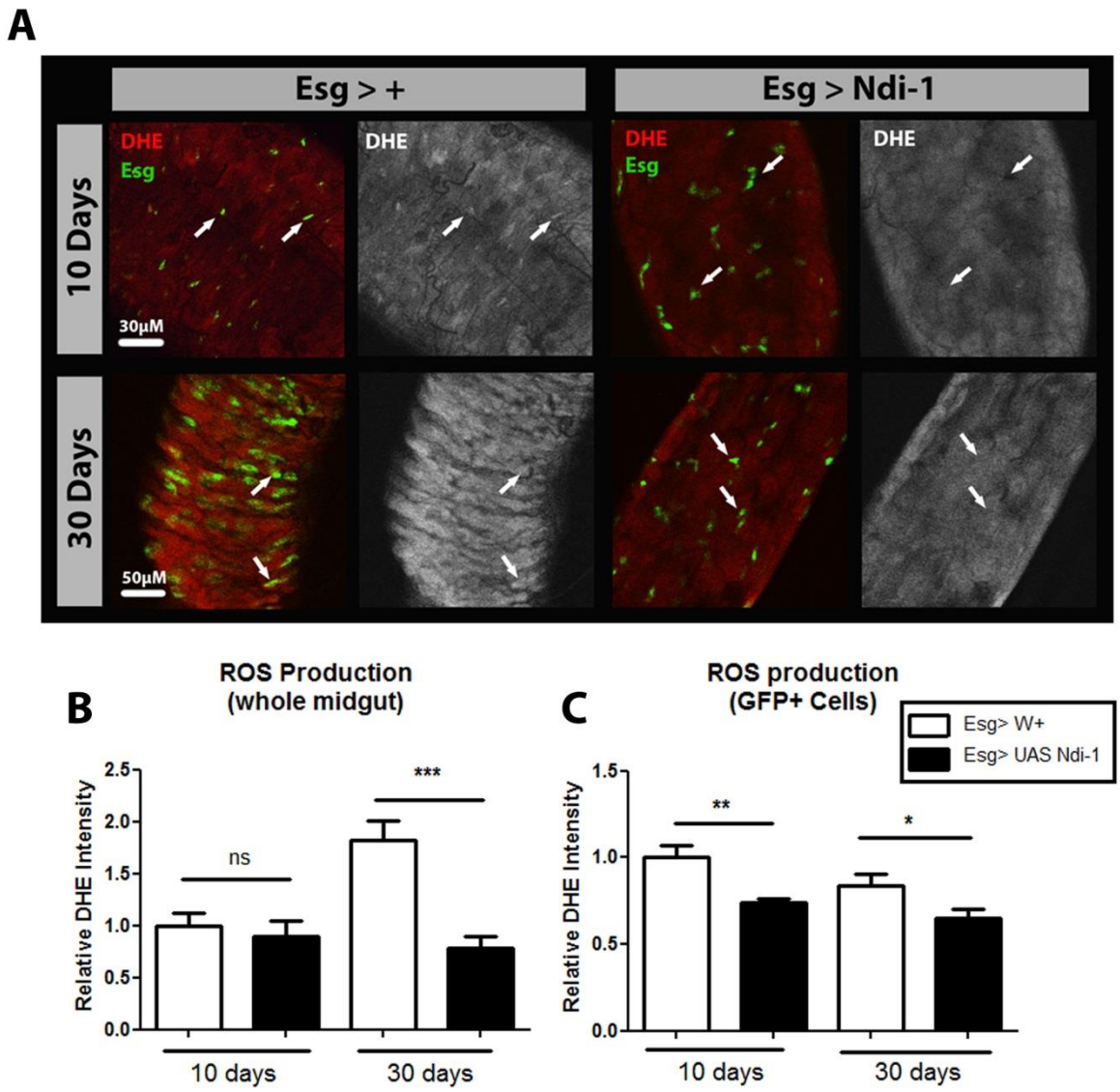

Figure A2-1. ISC-specific expression of NDI-1 suppresses ROS accumulation in ISCs, and whole intestine with age.

(A) Representative images of young (10day) and old (30day) intestines of female drosophila with or without ISC-specific NDI-1 expression (Green channel – esg>GFP, Red channel-dihydroethidium staining (ROS-specific stain).

(B) Overexpression of NDI-1 in ISCs and EBs delays age dependent accumulation of ROS in the whole intestine of female *Drosophila (T-test, $p<0.001$ at 30 days of age, $n>10$ intestines/condition).*

(C) Overexpression of NDI-1 in ISCs/EBs lowers ROS production in esg-positive cells at young and old age *(T-test, $p<0.05$ at 10 and 30 days of age, $n>10$ intestines/condition).*

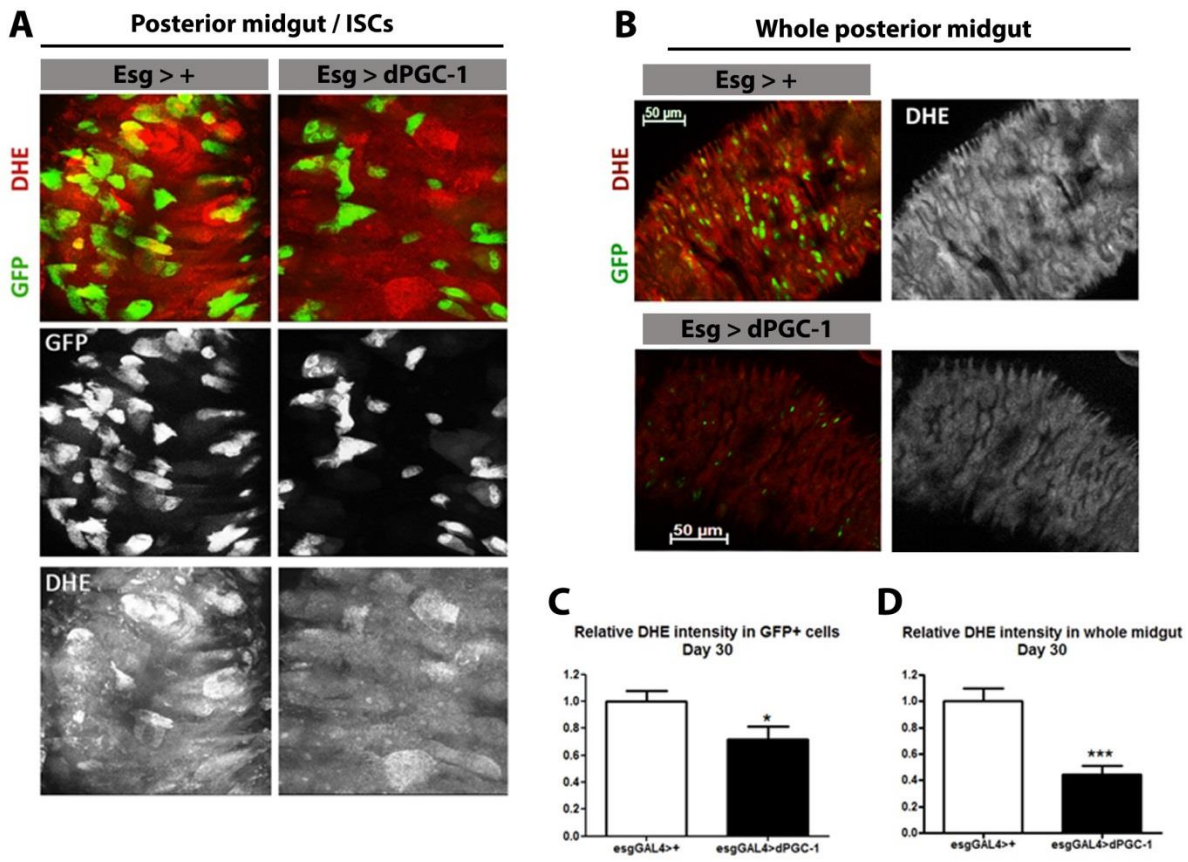

Figure A2-2. ISC-specific expression of PGC-1 suppresses ROS accumulation in ISCs, and whole intestine with age.

(A) Representative images of old (30day) ISCs of female drosophila with or without ISC-specific PGC-1 expression (Green channel – esg>GFP, Red channel-dihydroethidium staining (ROS-specific stain).

(B) Representative images of old (30day) whole posterior midguts of female drosophila with or without ISC-specific PGC-1 expression (Green channel – esg>GFP, Red channel-dihydroethidium staining (ROS-specific stain).

(C) Overexpression of PGC-1 in ISCs/EBs lowers ROS production in esg-positive cells at old age *(T-test, $p<0.05$ at 30 days of age, $n>10$ intestines/condition).*

(D) Overexpression of PGC-1 in ISCs and EBs delays age dependent accumulation of ROS in the whole intestine of female *Drosophila (T-test, $p<0.001$ at 30 days of age, $n>10$ intestines/condition).*

APPENDIX III:

Appendix III contains a modified partial reproduction of Fig 2 of the following article:

Ming Gong, Yanqiu Chen, Rachel Senturia, Matthew Ulgherait, Michael Faller & Feng Guo. Caspases cleave and inhibit the microRNA processing protein DGCR8. *Protein Science.* 2012.

My contribution to this paper is found in a small portion of the initial cloning and characterization of DGCR8 truncations. Additionally, I performed the analysis of DGCR8 cleavage upon apoptosis found in **(Figure 2) (presented as Figure A3).**

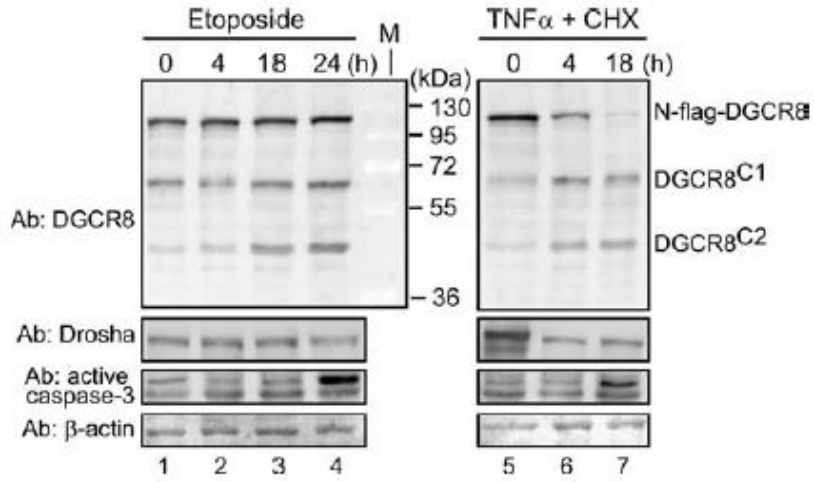

Figure A3. Induced extrinsic or intrinsic pathway-specific apoptosis causes proteolytic cleavage of full-length overexpressed DGCR8.

The DGCR8C2 fragment accumulates in apoptotic cells. Immunoblots of whole-cell extracts of HeLa cells that transiently expressed N-flag-DGCR8. Twenty-four hours post-transfection, cells were treated with either etoposide (100 μM) or the combination of TNFa (10 ng/mL) and cycloheximide (20 μg/mL) to induce apoptosis, and extracts were prepared at the indicated time of treatment.